University of Southampton

Human Development and Health

Faculty of Medicine

CDKN2A: A Predictive Marker for Bone Mineral Density or Direct Role in Osteoblast Function?

Eloïse Cook

PhD Thesis

July 2016

Supervisors: Prof Karen Lillycrop, Prof Nicholas Harvey and Dr Stuart Lanham

UNIVERSITY OF SOUTHAMPTON

ABSTRACT

FACULTY OF MEDICINE
ACADEMIC UNIT OF HUMAN DEVELOPMENT AND HEALTH

Doctor of Philosophy

CDKN2A: A Predictive Marker for Bone Mineral Density or Direct Role in Osteoblast Function?

By Eloïse Cook

As the population is becoming more aged, osteoporosis is becoming more prevalent and the number of fragility fractures that are occurring is increasing. One of the main predictors of developing osteoporosis in later life is a bone mineral density that is greater than 2.5 standard deviations below the young adult sex-matched mean, though studies have only been able to explain 5% of the variance seen in bone mineral densities between individuals. There is now increasing evidence that the development of osteoporosis can begin *in utero* and that epigenetic processes, such as DNA methylation, may be central to the mechanism by which early development influences bone mineral density and later bone health.

Previous work within the group has identified associations of a 300bp differentially methylated region within the *CDKN2A* locus with bone mineral content, bone area and areal bone mineral density in offspring from the Southampton Women's Survey (SWS) cohort. As methylation of *CDKN2A* increases, bone mineral content, bone area and areal bone mineral density all decrease at both 4 and 6 years of age. The two cell cycle regulators $p16^{INK4A}$ and $p14^{ARF}$ are transcribed from this gene as well as the lncRNA ANRIL.

Various techniques were used to determine whether this differentially methylated region has a functional role in osteoblasts or whether it is just a potential marker for predicting bone mineral density. It was shown that there was specific binding in the osteoblast-like SaOS-2 cell line to this region and that methylation of these CpGs led to a decrease in transcription factor binding. Treatment of both SaOS-2 cells and primary osteoblasts with siRNAs against ANRIL caused a decrease in cell number, a decrease in cell proliferation, an increase in cells in G_0/G_1 phase of the cell cycle and, in SaOS-2 cells, caused an increase in the expression of bone differentiation markers RUNX2 and ALP. Knock down of ANRIL expression also caused a change in genes that have roles in osteoblast specific pathways as well as genes that were involved in molecular functions such as nuclear regulation and acetylation. Associations were found between CpG methylation in *RXRA* and offspring bone outcomes at birth in both the SWS and MAVIDOS cohorts. Daily maternal cholecalciferol supplementation was also shown to decrease the methylation of CpG loci within *RXRA* in offspring umbilical cord and further investigation showed that this effect of maternal supplementation was only seen in children born during the winter months.

Together, these findings suggest that the association between *CDKN2A* methylation at birth and later bone health could indicate a potential role for *CDKN2A* in bone development and function and raises the possibility that differential methylation of *CDKN2A* may allow the identification of individuals at increased risk of osteoporosis in later life. Due to the effect of ANRIL knock down in primary osteoblasts, which could not be explained through normal cell cycle pathways, results suggest that ANRIL has potential *trans*-regulatory functions in these cells. These findings suggest that ANRIL could potentially play a role in bone differentiation, cell proliferation and metabolism and that dysregulation of the expression of this lncRNA could have adverse effects on bone health, potentially increasing the risk of individuals developing osteoporosis in later life.

Table of Contents

List of Figures

List of Tables

Academic Thesis: Declaration of Authorship

I, …… [please print name]

declare that this thesis and the work presented in it are my own and has been generated by me as the result of my own original research.

[title of thesis] ……..

……

I confirm that:

1. This work was done wholly or mainly while in candidature for a research degree at this University;
2. Where any part of this thesis has previously been submitted for a degree or any other qualification at this University or any other institution, this has been clearly stated;
3. Where I have consulted the published work of others, this is always clearly attributed;
4. Where I have quoted from the work of others, the source is always given. With the exception of such quotations, this thesis is entirely my own work;
5. I have acknowledged all main sources of help;
6. Where the thesis is based on work done by myself jointly with others, I have made clear exactly what was done by others and what I have contributed myself;
7. Either none of this work has been published before submission, or parts of this work have been published as: [please list references below]:

Signed: ……

Date: ……

Acknowledgements

Firstly, I would like to thank my supervisors Professor Karen Lillycrop and Professor Nick Harvey for their guidance and support throughout my PhD. I am truly grateful for the opportunity that you have provided me.

To the BioNerds – Paula, Emma, Rob, Chaz, Len, Becky, Sam and Jordan (whether you're still here or not). Thanks for all the help you've given me over the years, whether it be assessing the quality of endless DNA gels or testing out my latest cake creation. You've always been there offering good advice and I feel privileged to be able to call you my friends.

To Swim Team: for keeping me sane. There's nothing like dancing it out at Jesters with an absolutely fabulous bunch of people or completing a rather challenging training set to calm you down after a stressful day at work. Being around such an energetic group of people makes you realise that tomorrow's another day and things are as never as bad as they may seem.

To mum, dad and Liz: for always being there when I need you. I've had some good days and bad throughout these four years, but I've always known who I could turn to when I felt like it was getting too much. Thanks for putting up with all the science talk (I know it bores you half to death) and for always being on hand with words of encouragement.

To Rob: for everything you do. You've been with me from the beginning, through the ups and the downs, the good times and the bad and we're still going strong. Thank you for always being there when I've needed a sounding board, even though you have no clue about molecular biology, or for when I just need to take my mind off things and recharge. I couldn't have done it without you.

Abbreviations

Abbreviation	Full Term
%FM	Percentage Fat Mass
1,25VitD_3	1 Alpha, 25-Dihydroxyvitamin D_3
5-mC	5-MethylCytosine
aBMD	Areal Bone Mineral Density
ALP	Alkaline Phosphatase
ALSPAC	Avon Longitudinal Study of Parents and Children
ANRIL	Antisense Non-Coding RNA in the INK4A Locus
AP1	Activator Protein 1
APS	Ammonium Persulfate
ATF4	Activating Transcription Factor 4
BA	Bone Area
BATMAN	Bayesian Tool for Methylation Analysis
BGLAP	Bone Gamma-Carboxyglutamate Protein
BMC	Bone Mineral Content
BMD	Bone Mineral Density
BMI	Body Mass Index
BMP	Bone Morphogenic Protein
cAMP	Cyclic Ad*NOS3*ine Monophosphate
CDK	Cyclin Dependent Kinase
cDNA	Complementary Deoxyribose Nucleic Acid
CpG	Cytosine-Phosphate-Guanine
CREB	cAMP Responsive Element Binding Protein
CVD	Cardiovascular Disease
DMEM	Dulbecco's Modified Eagle's Medium
DMR	Differentially Methylated Region
DNA	Deoxyribose Nucleic Acid
DNMT	DNA Methyltransferase
dNTPs	Deoxynucleotide Triphosphates
DOHaD	Developmental Origins of Health and Disease
DXA	Dual-Energy X-ray Absorptiometry
EGR1	Early Growth Response Protein 1
EMSA	Electrophoretic Mobility Shift Assay
eNOS	Endothelial Nitric Oxide Synthase
EZH2	Enhancer of Zeste 2
FACS	Fluorescence-Activated Cell Sorting
FBS	Fetal Bovine Serum
FGF	Fibroblast Growth Factor
Fra1	FOS-Related Antigen 1
GR	Glucocorticoid Receptor
GWAS	Genome-Wide Association Study
HDAC	Histone Deacetylase
hBMSC	Human Bone Marrow Stromal Cell
HPA	Hypothalamic Pituitary-Adrenal
IGF1	Insulin-like Growth Factor 1
IGF2	Insulin-like Growth Factor 2
IHH	Indian Hedgehog
JAG1	Jagged 1
lncRNA	Long Non-Coding RNA

LRP	Low-Density Lipoprotein Receptor-Related Protein
MAPK	Mitogen Activated Protein Kinase
MAVIDOS	Maternal Vitamin D Osteoporosis Study
MBD	Methyl Binding Domain
MDM2	Murine Double Minute 2
MEG3	Maternally Expressed Gene 3
miRNA	microRNA
MSCs	Mesenchymal Stem Cells
OPG	Osteoprotegerin
OSX	Osterix
P-32	Phosphorous 32
PAH	Princess Ann Hospital
PBMC	Peripheral Blood Mononuclear Cell
PGC1α	Peroxisome Proliferator Gamma Coactivator 1 Alpha
PGE2	Prostaglandin E2
PI3K	Phosphoinositide 3-Kinase
PKCδ	Protein Kinase C Delta
PPARα	Peroxisome Proliferator Activated Receptor Alpha
PPARγ	Peroxisome Proliferator Activated Receptor Gamma
PRC	Polycomb Repressive Complexes
PTCH1	Patched Homologue 1
PTH	Parathyroid Hormone
RAINE	Western Australian Pregnancy Cohort Study
RANKL	Receptor Activator of Nuclear Factor Kappa-B Ligand
Rb	Retinoblastoma Protein
RBPJκ	Recombining Binding Protein Suppressor of Hairless Kappa
RISC	RNA-induced Silencing Complex
RNA	Ribose Nucleic Acid
RPL13A	60S Ribosomal Protein L13a
RT-qPCR	Real Time Quantitative Polymerase Chain Reaction
RUNX2	Runt-Related Transcription Factor 2
RXR	Retinoid X Receptor
RXRA	Retinoid X Receptor Alpha
RXRβ	Retinoid X Receptor Beta
RXRγ	Retinoid X Receptor Gamma
SAM	S-Ad*NOS3*ylMethionine
scBMC	Size Corrected Bone Mineral Density
Ser	Serine
siRNA	Small Interfering RNA
SNP	Single Nucleotide Polymorphism
SWS	Southampton Women's Survey
T2D	Type II Diabetes
TBP	TATA Box Binding Protein
TEMED	Tetramethylethylenediamine

TGF-β	Transforming Growth Factor Beta
Thr	Threonine
Tyr	Tyrosine
VDR	Vitamin D Receptor
VDRE	Vitamin D Responsive Element
VSMC	Vascular Smooth Muscle Cell

Chapter 1

Introduction

1. Introduction

1.1 Osteoporosis

Osteoporosis is a skeletal disease that is characterised by low bone mass and deterioration in the microarchitecture of bone which leads to an increased risk of fracture due to increased bone fragility (1). Clinically, osteoporosis has been hard to define, although the World Health Organisation has now defined osteoporosis in terms of BMD and fracture. Osteoporosis is diagnosed if bone mineral density (BMD) (measured by dual-energy X-ray absorptiometry (DXA)) is greater than 2.5 standard deviations below the young adult sex-matched mean, and if the patient also has a history of fragility fractures, the term 'established osteoporosis' is used (2). The three main outcomes of osteoporotic fracture are morbidity, mortality and economic cost (3,4), with the most common sites for fracture being the hip, spine and wrist. As people now live longer, the percentage of the population that is made up of older individuals has increased and as a result osteoporotic fragility fractures are becoming a major financial burden on the healthcare system, with the annual cost of these fractures in the UK being estimated at £1.7 billion (5).

1.1.1 Epidemiology of osteoporosis

1.1.1.1 Fracture

Osteoporotic fractures most commonly occur in areas that have high trabecular bone content after a low or moderate trauma and the frequency of which have been shown to increase with age in both males and females (6,7). Johnell *et al* have shown that lifetime risk of any osteoporotic fracture at 50 years of age is 40% in women and 13% in men (8). Fracture incidence has been shown to vary geographically, even within countries, which suggests that environmental factors, such as vitamin D and diet, may be important in the pathogenesis of osteoporotic fracture.

Out of the three most common osteoporotic fractures, hip fractures usually have the worst outcomes as they require hospital admittance and cause excessive mortality and significant morbidity. It has been estimated that around 90% of osteoporotic hip fractures occur after a fall from standing height (9) and their incidence increases exponentially with age. In Western countries, women over 50 years of age are twice as more likely to suffer from a hip fracture than men of the same age and, overall, 98% of hip fractures occur in individuals that are over 35 years of ages, 80% of which occur in women (10). Incidence rate appears to be seasonal, with a higher incidence occurring in winter, though this does not seem to be caused by slipping on icy pavements as most falls occur inside, suggesting that it could be due to an overall loss of balance or loss of neuromuscular function. As mentioned above, geographical area also seems to have an influence on fracture incidence. In Europe incidence rate varies seven-fold between countries

(11) and it seems to be those who live further away from the equator that have the higher incidence of hip fracture, with the highest rate being seen in Caucasians living in northern Europe, notably Scandinavia (12).

The epidemiology of vertebral fractures is less well established as many of these fractures do not get diagnosed. It has been estimated that after 60 years of age, women in the US and Europe are 3 times more likely to suffer from a vertebral fracture than men (13). In a study by Cooper *et al* on 341 residents of Rochester, Minnesota over a 5 year period, they showed that of all fractures, 14% occurred after severe trauma, 83% occurred following moderate or no trauma and 3% were caused by underlying pathological conditions, with those following moderate trauma occurring more frequently in women than men. There is also evidence of geographical location having an influence on vertebral fracture incidence as it has been demonstrated that there is greater incidence of fracture in Sweden over other countries in Europe (6).

1.1.1.2 Morbidity

All osteoporotic fractures have been shown to be associated with a significant increase in morbidity, which is defined as a loss in function. Different studies have tried to determine the true morbidity of osteoporotic fractures by analysing the outcome of these fractures. Johnell *et al* have demonstrated that the true morbidity caused by osteoporotic hip fracture is 6.07 times higher than that caused by hip fracture alone in women aged 50-54 years. In men of the same age, the disability caused is 4.48 times higher when compared to that of hip fracture alone (8).

Data in the US shows that a person's pre-morbid status also has an effect on the outcome of an osteoporotic fracture. Of those that were independent pre-fracture, 25% became partially dependent post-fracture, 50% of patients that were partially dependent before fracture were admitted into nursing homes after being released from hospital and those who were already in nursing homes remained there (10). Sernbo *et al* found that only 50% of patients who have suffered from an osteoporotic hip fracture returned to their pre-fracture level of ability (14). This was assessed by the ability of the patient to walk and the need for aids at home. Similar findings have been presented by Miller where it was shown that out of 360 patients that had sustained a hip fracture, only 51% returned to pre-fracture ambulatory function (15). This study also demonstrated that one year after injury 22% of these patients could no longer walk unaided.

Morbidity due to osteoporotic vertebral fracture can be quite low from one fracture; however multiple fractures have been shown to have adverse outcomes on everyday function as they can lead to loss of height, severe back pain and kyphosis (16). This can also exacerbate the underlying osteoporosis, which can lead to other fractures. Those who suffer from wrist fractures are not usually completely disabled post-fracture, though 50% of patients have not regained full

function 6 months post-fracture. Morbidity has also been shown to have psychological effects on patients due to loss-of-function, such as depression, anger, lowered self-esteem and anxiety (8).

1.1.1.3 Mortality

Another outcome of osteoporotic fracture is excess mortality, which has mainly been associated with hip and vertebral fractures; however there is also evidence to suggest that there is slight increase in mortality in patients that suffered from a wrist fracture. In a population-based study by Cooper *et* al of 335 patients from Rochester, Minnesota (79 men and 256 women), it was demonstrated that survival after hip or vertebral fracture differed significantly from what was expected (Figure 1.1) (17). The patients were observed for 809 person-years and survival was shown to decline and diverge from what was expected. For example, 5 years post vertebral fracture diagnosis the expected percentage survival was 76%, whereas the actual percentage survival was 61%. This was comparable to what was seen with patients that suffered from hip fractures; however the excess mortality was greatest during the first 6 months post-fracture.

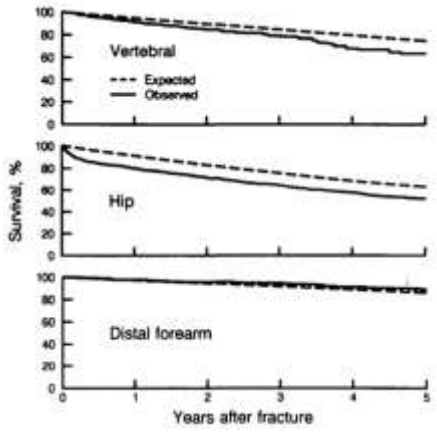

Figure 1.1: Survival rates after diagnosis of vertebral, hip and wrist fractures compared to expected rates of patients in Rochester, Minnesota. Reproduced from Cooper *et al* (17)

Similar results were shown by Johnell *et al* on a cohort of 2,847 patients in Sweden. Across a 5 year follow up period mortality increased in patients with hip fracture from 22% to 59%, though the highest percentage mortality was seen in patients who had suffered a vertebral fracture where mortality increased from 28% at 1 year post-fracture to 72% 5 years after fracture (18). However, in this study there was some increased mortality with wrist fractures across the 5 year follow-up period, though at 5 years this had only increased to 26%.

1.1.1.4 Economic cost

Many studies have looked into the economic burden of osteoporotic fractures on healthcare and it has been estimated that in the US osteoporotic fractures cost the US healthcare system $20 billion per annum, with hip fractures accounting for a third of this total (10). A study by Burge *et* al looked at predicting the incidence and cost of fracture in the US from 2005-2025. They estimated that in 2005 the number of total fractures in the US was more than 2 million with the total cost being close to $19 million. They then split the cost by sex, age group, race and fracture type. They found that women account for 75% of the costs and that the most costly fracture is that of the hip (72%) due to need for hospitalisation after and the fact that many patients end up needing assistance at home or are admitted into nursing homes (19). This study also predicted that the cost of fractures will increase by 50% by 2025 due to an increase in the aging population.

Research into prevention measures is ongoing and is now looking into ways of assessing patients for risk before a fracture occurs. Research is also focusing on intervention methods to prevent fractures; however some of the drugs that are used are expensive and are not available worldwide. There is now also evidence suggesting osteoporosis could have developmental origins depending on bone growth and formation *in utero*.

1.2 Bone formation

Bone formation is the process by which bone matrix replaces embryonic connective tissue to form the skeleton. This process begins during the second month in *in utero* and occurs through two mechanisms: intramembranous ossification and endochondral ossification. Intramembranous ossification is responsible for the formation of the skull and clavicles and bone is formed on or within fibrous connective tissue membranes, which are made up of mesenchyme and collagen fibres (20). Endochondral ossification occurs in all other bones of the skeleton and occurs through replacement of cartilage with bone matrix by osteoblasts (21). In the endochondral ossification method, mesenchymal stem cells (MSC) condense and differentiate into chondrocytes (22). The perichondrium is formed around the cartilage model and the chondrocytes then proliferate, which causes the cartilage model to grow. They then become hypertrophic and secrete a cartilaginous matrix that attracts blood vessels, before undergoing apoptosis (20). Osteogenic cells are then stimulated to differentiate into osteoblasts, which begin to deposit bone matrix and form the bone collar (a shell of compact bone around the cartilage model). This bone collar prevents nutrients from reaching the cartilage and it begins to disintegrate. Osteoblasts migrate to these areas through capillaries and use the cartilaginous matrix as a scaffold to deposit bone matrix (23). This forms the primary ossification centre (24)

and after a few days the osteoblasts become osteocytes that promote the deposition of calcium salts to form trabeculae. When these trabeculae fuse together they form trabecular bone, which then undergoes remodelling to form the medullary cavity. This cavity forms at the core of the cartilage model and becomes filled with capillaries and red bone marrow. Ossification then proceeds to form the diaphysis (the midsection of the bone), whilst the epiphyses (the ends of the bone) remain cartilaginous (20).

After birth blood vessels invade the cartilaginous epiphysis and a secondary ossification centre is formed (25). In this case no medullary cavity is formed and, instead, ossification progresses outwards leaving the core of the epiphysis as spongy trabecular bone. The last part of endochondral ossification involves the formation of articular cartilage and the formation of the epiphyseal plate. The articular cartilage is a thin layer of cartilage formed from the hyaline cartilage that covers the end of the epiphyses to reduce friction in joints. The epiphyseal plate is a layer of hyaline cartilage that remains between the diaphysis and the epiphyses that allows the long bones to length during growth in childhood (25).

1.2.1 Osteoblast differentiation

Osteoblasts are mononuclear cells that are responsible for the deposition of osteoid, which is an uncalcified bone matrix that becomes bone tissue once calcified. These bone forming cells secrete many different proteins that include alkaline phosphatase (ALP), type I collagen, proteoglycan, bone sialoprotein and osteopontin. There is also evidence that demonstrates that they have a role in osteoclast differentiation, in that they synthesise receptor activator of nuclear factor kappa-B ligand (RANKL), which activates osteoclast differentiation, and osteoprotegerin (OPG), which negatively regulates osteoclast function.

Osteoblast differentiation is controlled through the interplay of different signalling pathways and the activation of different transcription factors at certain times during the differentiation process. This process is shown in Figure 1.2.

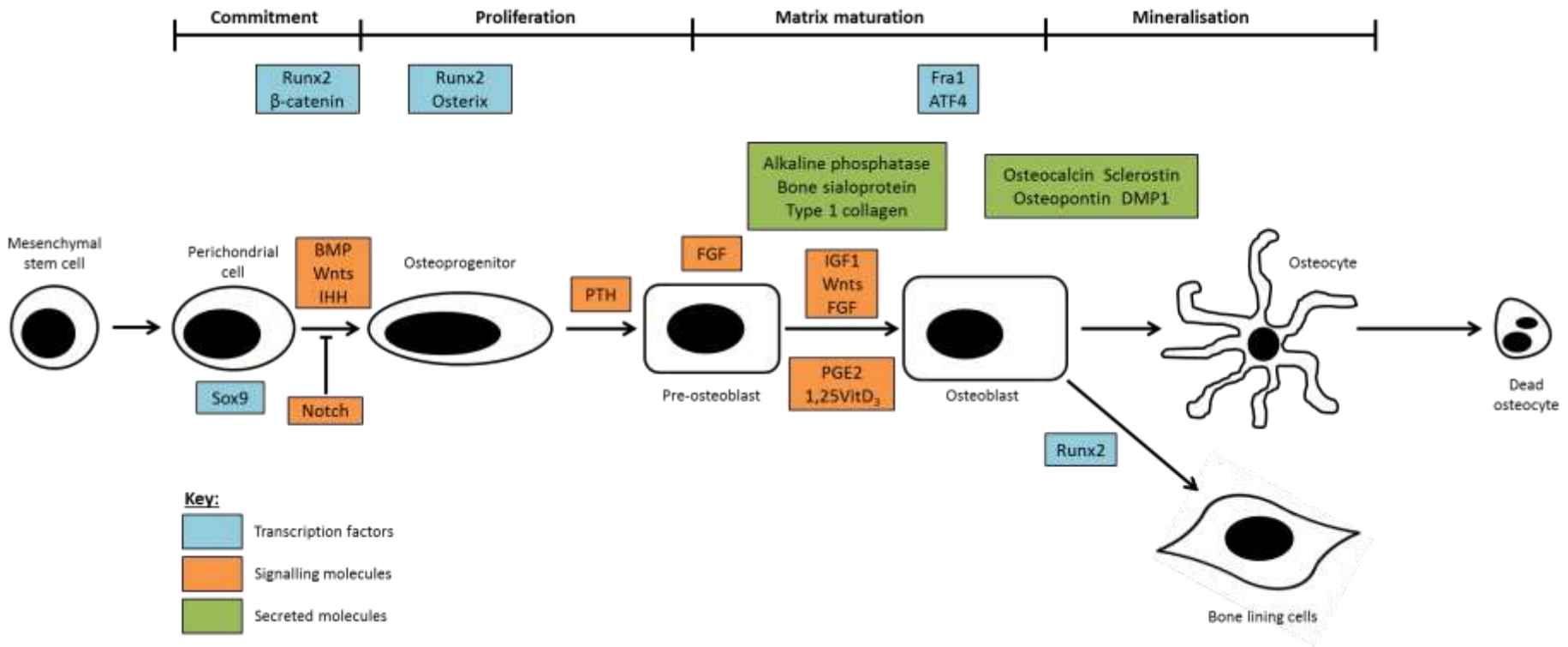

Figure 1.2: Stages of osteoblast differentiation from mesenchymal stem cells. Adapted from Crocket *et al* (26). Runx2 Runt-related transcription factor 2; Fra1 FOS-related antigen 1; ATF4 activating transcription factor 4; BMP bone morphogenic protein; IHH Indian hedgehog; PTH parathyroid hormone; FGF fibroblast growth factor; IGF1 insulin-like growth factor 1; PGE2 prostaglandin E2; 1,25VitD$_3$ 1α,25-dihydroxyvitamin D$_3$.

1.2.1.1 Transcription factors

Many different transcription factors are needed for the successful differentiation of osteoblasts and the formation of mineralised bone.

SOX9 is a transcription factor from the sex determining region Y (SRY)-related family of proteins that is expressed in chondrocytes and marks all mesenchymal progenitors that develop into osteoblasts (27); however its role in osteoblast differentiation is not fully understood. Akiyama *et al* demonstrated that when SOX9 is deleted in the mouse mesenchymal limb bud before MSC condensation, cartilage and bone are non-existent and Runx2 expression is eliminated (28). There was also some evidence to suggest that SOX9 is needed to prevent the transition of proliferating chondrocytes into hypertrophic chondrocytes, which would inhibit the progression of endochondral ossification. However, it is not clear that the lack of osteoblasts is due to the lack of cartilage or whether it has a direct role in the differentiation of osteoblasts.

Runt-related transcription factor 2 (RUNX2) is a member of the RUNX family of transcription factors and contains a Runt DNA binding domain. It is essential for the differentiation of osteoblasts in both intramembranous and endochondral ossification. Both Komori *et al* and Otto *et al* have shown that mice that are homozygous for a mutation in the Cbfa1 (equivalent of human RUNX2) locus have a complete lack of ossification and die of respiratory failure shortly after birth (29,30). Komori also found that there were some immature osteoblasts in the perichondral region that weakly expressed alkaline phosphatase but not osteopontin or osteocalcin, which are expressed later on in the differentiation pathway, and that there was not any vascular or mesenchymal stem cell invasion of the cartilage model (29). This transcription factor is also needed in the function of mature osteoblasts, which includes the synthesis of bone matrix (31). Other nuclear factors have been shown to interact with RUNX2 to promote osteoblast differentiation including MAF, Retinoblastoma protein (Rb), GLI2, DLX5 and MSX2.

Osterix (OSX) is a transcription factor that acts downstream of RUNX2 in the proliferation step of differentiation and is induced in response to BMP signalling. Nakashima *et al* demonstrated that bone formation does not occur in *Osx*$^{-/-}$ mice; however mesenchymal stem cells still condense and differentiate into chondrocytes (32). This indicates that *Osx*$^{-/-}$ MSCs in mice still possess the ability to differentiate down the chondrocyte lineage. They also showed that these cells did express *Runx2* but *Runx2*$^{-/-}$ mice did not express OSX, which suggests that this transcription factor works downstream of RUNX2. There is also evidence that OSX can be negatively regulated by the tumour suppressor transcription factor p53, as *p53*$^{-/-}$ mouse osteoblasts show a significant increase in the expression of Osx (33)

β-catenin is expressed via the activation of the Wnt signalling pathway and inactivation of this transcription factor in MSCs has been shown to completely block osteoblast differentiation, causing the MSCs to differentiate into chondrocytes instead (34,35). Day *et al* showed that when β-catenin is inactivated in mesenchymal progenitor cells, these cells will still differentiate into chondrocytes even when they are subjected to an osteogenic promoting environment (34). All three of these transcription factors work in conjunction with each other to cause the first stages of osteoblast differentiation. RUNX2 has been shown to be expressed in β-catenin$^{-/-}$ MSCs, but not OSX, this would suggest that β-catenin is important for progression of osteoprogenitors into pre-osteoblasts (35,36). Further to this, it has also been demonstrated by Gaur *et al* that β-catenin can enhance RUNX2 expression (37), which suggests that RUNX2 acts to supress the differentiation of MSCs into adipocytes and chondrocytes so that β-catenin and OSX can then direct the osteoprogenitors to pre-osteoblasts.

Other transcription factors are important for the proper function of mature osteoblasts, such as FOS-related antigen 1 (Fra1) and activating transcription factor 4 (ATF4). Fra1 is a member of the activator protein 1 (AP1) family of transcription factors. Its exact interactions with the previously described transcription factors are unknown, however when Fra1 was deleted in mouse embryos, Eferl *et al* found that the mice exhibited low bone mass, not unlike osteopenia in humans (38). The bones in these mice also showed reduced levels of bone matrix proteins. The reverse effect is seen in transgenic mice overexpressing Fra1, where there is an increase in bone mass which is due to an increase in the number of mature osteoblasts (39).

More is known about the basic Leu zipper transcription factor ATF4, which has a role in mature osteoblasts. It is believed that ATF4 exerts its function in osteoblasts by two potential mechanisms. The first is that it has direct regulation over the expression of osteocalcin (bone matrix protein) and RANKL, which promotes osteoclast differentiation, and the second is that it ensures the transport of proteins into cells for the production of proteins by osteoblasts (40).

1.2.1.2 Signalling pathways

There are five main signalling pathways that contribute to the differentiation of osteoblasts: Hedgehog signalling, Notch signalling, WNT signalling, BMP signalling and FGF signalling. These pathways lead to the expression of transcription factors at particular points through the course of differentiation. The BMP, Wnt and Hedgehog signalling pathways all work to cause mesenchymal stem cells to differentiate into osteoprogenitor cells, which is the first step of the differentiation pathway.

Bone morphogenic proteins (BMPs) are members of the transforming growth factor-β (TGF-β) superfamily of proteins that act by binding to heterotetramer membrane receptors made

up of type I and type II Ser/Thr kinase receptors. This causes the activation of SMAD1, 5 or 8 through site-specific phosphorylation and these phosphorylated SMADs then translocate to the nucleus, after forming a complex with SMAD4 (common to all SMADs), to regulate gene expression (Figure 1.3). Knockout of BMP2 and BMP4 expression in mice have shown that a threshold level of these two BMPs is needed in order to cause progression of differentiation from chondrocytes to osteoprogenitor cells, though the exact mechanism was not elucidated (41). This group also suggests that both BMP2 and BMP4 are needed to form mesenchymal condensations and that a loss of both these proteins causes osteogenesis to be severely impaired. It has also been demonstrated by the same group that although bone development during embryogenesis can occur when BMP2 expression is knocked out, these mice demonstrated limb fractures at birth due to a lower bone mineral density when compared to wild type mice, which were not able to heal (42). This suggests that BMP2 could be important in postnatal bone formation.

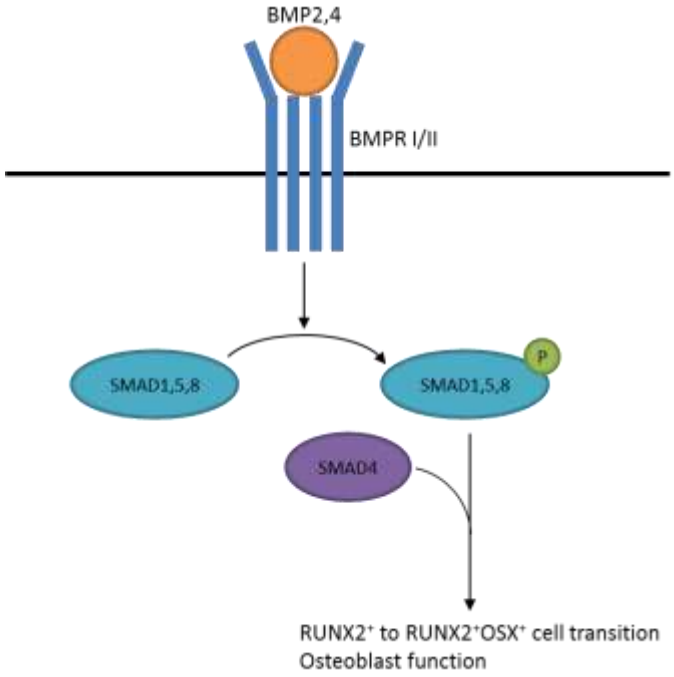

Figure 1.3: Bone morphogenic protein (BMP) signalling in osteoblast differentiation. BMP2 and 4 bind to bone morphogenic protein receptor (BMPR) I or II (type I and type II Ser/Thr kinase receptors) to cause the activation of SMAD1, 5 and 8 through phosphorylation. These bind to co-activator SMAD4 and translocate to the nucleus where they activate the transcription of genes to cause RUNX2+ to $RUNX2^{+}OSX^{+}$ cell transition

There is also evidence to show that BMP signalling has a role in the functioning of mature osteoblasts as well as differentiation. Devlin *et al* showed that when noggin, an inhibitor of BMP signalling, is overexpressed in mice there is an 23-29% decrease in bone mineral density, a decrease in the number of trabeculae and a decrease in bone formation rate; however number of osteoblasts was not significantly different from wild type mice (43). This implicates BMP signalling

as having a role in the correct functioning of osteoblasts. Tan *et al* also demonstrated that when Smad4 expression is disrupted in mature murine osteoblasts the proliferation and function of these cells were significantly decreased, with mice showing a decrease in bone mineral density, bone formation rate and numbers of osteoblasts (44).

Wnt signalling works through both β-catenin dependent and independent pathways to promote osteoblast differentiation from $RUNX2^{+}$ cells to $RUNX2^{+}OSX^{+}$ cells (Figure 1.4). The β-catenin dependent pathway is activated when WNT binds to Frizzled receptors and their co-receptors low-density lipoprotein receptor-related protein (LRP) 5 and 6. This leads to the stabilisation and translocation of cytosolic β-catenin to the nucleus where it interacts with various enhancers to regulate the expression of Wnt signalling target genes (45). It has been shown in both humans and mice that loss-of-function mutations or deletion of LRP5 can have adverse effects on bone development. In humans, a loss-of-function mutations in the LRP5 gene can lead to the onset of a form of juvenile osteoporosis called osteoporosis-pseudoglioma syndrome (46) and in mice, *Lrp5* deletion leads to a postnatal reduced bone mass phenotype, which was demonstrated to be because of a decrease in osteoblast proliferation (47). It has also been shown that β-catenin is required further down the differentiation pathway during the transition from pre-osteoblast to mature osteoblast, but convert to the chondrogenic lineage instead (48) and that deletion of this downstream signalling molecule in mesenchymal progenitors eliminates the generation of mature osteoblasts in mice (34). β-catenin independent signalling has been implicated in promoting osteoblast differentiation by stimulating the progression of cells from the prechondrial cell stage to the osteoprogenitor stage (49). This occurs when Wnt binds to a G-coupled receptor and leads to the activation of protein kinase C δ (PKCδ), which leads to the regulation of target genes. This group demonstrated that mice with homozygous mutant of PKCδ had decreased embryonic bone formation when compared to wild type mice. It also promotes osteoblast differentiation as it prevents the expression of peroxisome proliferator activated receptor-γ (PPARγ), which is necessary for adipocyte differentiation (50).

Indian hedgehog (IHH) signalling is stimulated by binding to Patched homologue 1 (PTCH1) receptor, which then causes a signal transduction through the 7 transmembrane protein Smoothened (Figure 1.5). This causes the activation of GLI2 and repression of GLI3 transcription factors to regulate gene expression that leads to the generation of osteoprogenitor cells (45). GLI3 acts to inhibit this transition, whereas GLI2 acts to promote it (51,52). St-Jacques *et al* have shown that, in IHH-null mice, there is a lack of osteoblast differentiation in endochondral bones as chondrocytes are unable to signal to cells to promote osteoblast differentiation (53) and Long *et*

al have demonstrated that IHH signalling is essential for RUNX2 expression in mice as knockout of Smoothened leads to Cbfa1 expression becoming completely abolished (54).

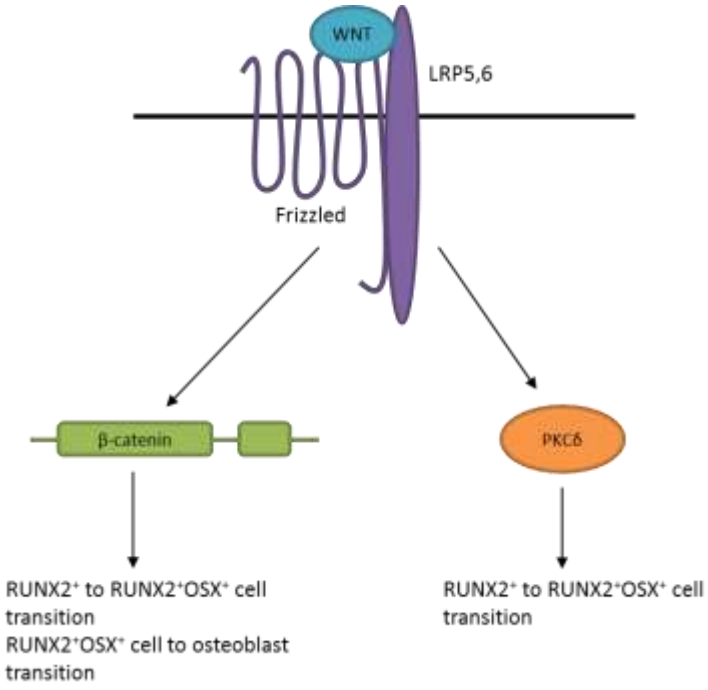

Figure 1.4: Wnt signalling in osteoblast differentiation. Wnt binds to Frizzled receptors and their co-receptors LRP5 and 6, which leads to the activation of either β-catenin dependent or independent pathways. In the dependent pathway, β-catenin is stabilised and translocates to the nucleus where it interacts with enhancers to regulate gene expression. In the independent pathway, PKCδ is activated and regulated Ant-activated genes. Both of these pathways are induce the transition of $RUNX2^{+}$ cells to $RUNX2^{+}OSX^{+}$ cells. B-catenin dependent pathways also regulate the $RUNX2^{+}OSX^{+}$ to osteoblast cell transition.

Figure 1.5: Indian Hedgehog signalling in osteoblast differentiation. Indian hedgehog (IHH) binds to its receptor Patched homologue 1 (PTCH1), which causes signal transduction through Smoothened (SMO), a seven transmembrane protein. This leads to the activation of transcription factor GLI2 and repression of transcription factor GLI3 to promote the generation of $RUNX2^{+}OSX^{+}$ cells.

Notch signalling functions at the same transition point as the previous signalling pathways; however it acts to suppress differentiation into osteoprogenitor cells rather than promote it (Figure 1.6). There are 4 Notch receptors in mammals to which a range of different ligands can bind. The main Notch receptor used to suppress osteoblast differentiation is Notch 1. After binding of a Jagged 1 (JAG1) to this receptor, its intracellular domain is cleaved and this interacts with recombining binding protein suppressor of hairless κ (RBPJκ) to translocate to the nucleus. Here it activates the expression of the HEY and HES families of transcription factors, which act to inhibit RUNX2 activity by directly binding to this transcription factor (55,56). Mouse studies have demonstrated that Notch signalling acts to suppress osteoblast differentiation. A study by Hilton *et al* where Notch1 was disrupted showed that adolescent mice had significantly increased trabecular bone mass compared to wild type mice, and these mice went on to develop osteopenia in later life. This increase in bone mass coincided with a decrease in the number of mesenchymal progenitors, suggesting that Notch signalling acts to suppress osteoblast lineage commitment and differentiation (56). Long *et al* have also elucidated that Notch suppression occurs before the induction of OSX activation as when Notch signalling is suppressed in osteoprogenitor cells there is no increase in trabecular bone mass (45).

Fibroblast growth factor (FGF) signalling is the final main signalling pathway that stimulates differentiation from pre-osteoblasts into mature osteoblasts (Figure 1.7). There are two main FGF receptors that are involved in bone formation, FGFR1 and FGFR2, which belong to the Tyr kinase family of receptors. When FGF proteins bind to these receptors, it causes the phosphorylation of signalling proteins that leads to the activation of signalling modules, which includes STAT1, PKC, mitogen activated protein kinase (MAPK) and phosphoinositide 3-kinase (PI3K) (45). It has been shown that FGF signalling has a role in both embryonic and postnatal stages of bone formation (57). In this study they found that $Fgf2^{-/-}$ mice had decreased trabecular bone volume, bone formation rate and mineralisation when compared to the wild type. FGFR1 signalling during the embryonic stages of bone formation stimulates osteoblast differentiation without affecting RUNX2 expression, whereas in mature osteoblasts, FGFR1 signalling acts to inhibit mineralisation activity (58). FGFR2 signalling on the other hand promotes both pre-osteoblast proliferation and mature osteoblast function, as shown by Yu *et al* (59). In this study, Fgfr2 inactivated mice showed a decrease in bone density, though the differentiation of mesenchymal stem cells into osteoblast was not affected. Instead, the proliferation of pre-osteoblasts and the ability to produce bone mineral matrix were severely decreased. This could have an adverse effect on bone formation, which could lead to a decreased peak bone mass and increased fracture risk in later life.

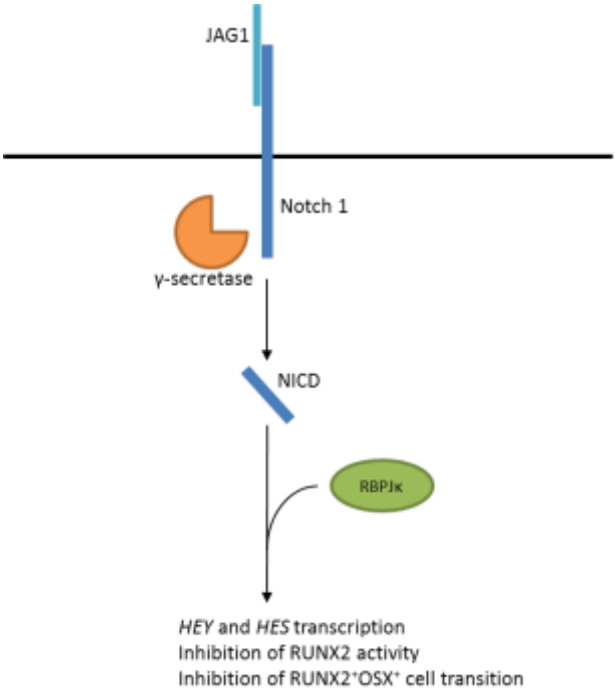

Figure 1.6: Notch signalling in osteoblast differentiation. When Jagged 1 (JAG1) binds to its receptor Notch 1, γ-secretase cleaves its intracellular domain (NICD), which interacts with recombining binding protein suppressor of hairless κ (RBPJκ). This complex then translocates to the nucleus where it leads to the activation of HEY and HES transcription factors, which act to suppress the osteoblast differentiation by directly interacting with RUNX2 to inhibit its activity.

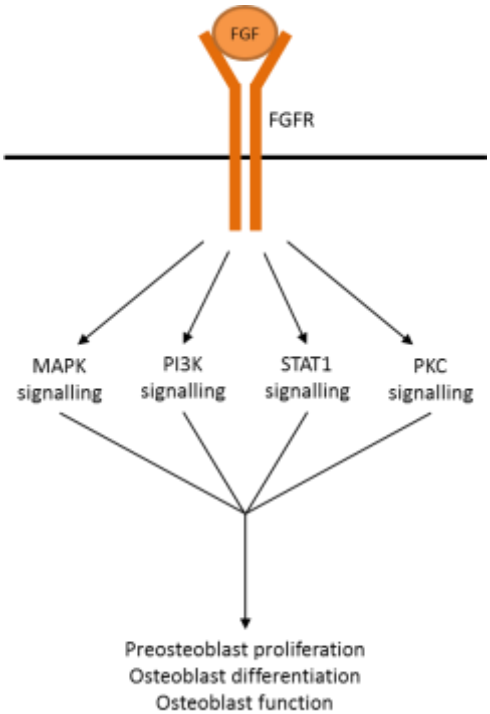

Figure 1.7: Fibroblast growth factor (FGF) signalling in osteoblast differentiation. The binding of FGF to the FGF receptor leads to the activation of various signalling pathways, which all have roles in regulating preosteoblast proliferation, osteoblast differentiation and osteoblast function.

1.2.1.3 Systemic regulation

As well as specific transcription factors and signalling pathways, bone formation is also regulated systemically. There are four main systemic regulators that contribute to osteoblast differentiation and function: parathyroid hormone (PTH), insulin-like growth factor 1 (IGF1), prostaglandin E2 (PGE2) and 1α,25-dihydroxyvitamin D_3.

PTH is crucial for the homeostasis of calcium in the body and has roles in regulating both bone formation and bone resorption. It has been shown that intermittent PTH exposure stimulates the anabolic function of PTH, whereas continuous exposure causes an increase in the catabolic role (60). PTH activates its signalling cascade by binding to the PTH receptor (a G-protein coupled receptor), which leads to the activation of cyclic adenosine monophosphate (cAMP) and cAMP responsive element binding protein (CREB). It has been shown by Isogai *et al* that PTH stimulates the progression of osteoprogenitor cells to pre-osteoblasts, whereas in mature osteoblasts it has an inhibitory effect on osteoblast function (61). This stimulation of differentiation progression has also been seen by Yang *et al*, where it was elucidated that this progression occurs due to the activation of PKCδ by PTH (62). At the pre-osteoblast stage, the main role of PTH is to increase pre-osteoblast proliferation rate through c-fos expression (63) and suppress apoptosis (64) in order to increase the number of bone matrix secreting cells. Mouse studies have demonstrated that PTH function needs both IGF1 and FGF2 to carry out its role (65,66), as when these genes were knocked out in mice PTH signalling was suppressed.

IGF1 is the most abundant growth factor in the bone matrix and it has been shown to have an indispensable role to play in the differentiation of pre-osteoblasts into mature osteoblasts as demonstrated by Xian *et al*. In this study, mice with knockout of Igf1 showed impaired osteoblast differentiation which resulted in lower bone mass and decreased mineral deposition when compared to wild type mice (67). When Igf1 receptor has been knocked out in mice osteoblasts, it has been shown that there is a significant decrease in osteocalcin expression, demonstrating the importance of IGF1 for correct bone matrix mineralisation (68).

Like PTH, PGE2 has been suggested to have roles in both bone resorption and formation (69). It has been demonstrated that PGE2 has a role in the growth and differentiation in rat osteoblast-like cells by Yoshida *et al*. When the PGE2 receptor is inhibited in these cells there is a significant decrease in the proliferation rate of the cells and a decrease in the number of mature osteoblasts (70), which both contribute to less bone formation as less bone forming cells are present. PGE2 has also been shown to increase alkaline phosphatase expression and osteocalcin synthesis in these cells, which are both expressed by mature osteoblasts during the final stages of differentiation and bone matrix maturation (71).

1α,25-dihydroxyvitamin D_3 is the active form of vitamin D_3 and is essential for the absorption and deposition of calcium in the bone mineral matrix (72). Vitamin D_3 is converted to its active form through the activity of 1α-hydroxylase, which is stimulated by the binding of PTH to the promoter of the gene that transcribes this enzyme (73,74). Once in its active form, 1α,25-dihydroxyvitamin D_3 binds to a heterodimer that is made up of the vitamin D receptor (VDR) and the retinoid X receptor (RXR) (26,75). This complex then translocates to the nucleus to bind to vitamin D responsive elements (VDREs) found in the promoters of various genes. One of these genes encodes a calcium binding protein, which allows for the increase of active transport of Ca^{2+} into cells allowing for bone calcification. The VDR has also been shown to stimulate the expression of osteocalcin (76,77) and osteopontin (78), which contribute to bone mineralisation. VDR overexpression studies in mature murine osteoblasts have shown an increase in bone formation and decrease in bone resorption (79), which could potentially be due to these osteoblasts having less of an ability to enhance osteoclast activity (80). In relation to earlier stages of differentiation, treatment of rats with high doses of 1α,25-dihydroxyvitamin D_3 has been shown to increase the proliferation rate of osteoprogenitors in bone marrow (81), which shows that vitamin D is important for the proper functioning of osteoblasts and proper bone formation.

If the expression of any of these systemic factors is altered, it could lead to an imbalance in bone formation and the development of a suboptimal peak bone mass. This could have a detrimental downstream effect on bone health in later life.

1.2.2 Osteoclasts

Unlike osteoblasts, osteoclasts are multinuclear cells that are derived from macrophages and are the cells that break down extracellular bone matrix in the process of bone resorption (26). The differentiation process for these cells is stimulated through the binding of macrophage colony stimulating factor (MCSF) to its receptor c-fms. This then causes an increase in the expression of RANK, which is the receptor for the osteoblast produced RANKL (82). Signalling through these two receptors are the key drivers for osteoclast differentiation. This leads to the expression of transcription factors such as nuclear factor κB (NF-κB) and AP1, which in turn bind to promoters and lead to the expression of osteoclast specific genes, such as cathespin K and matrix metalloproteinase 9 (MMP-9). These osteoclast specific genes are essential for the final differentiation of osteoclasts as well as the fusion of their precursors to form multinucleated cells and their function (26).

In mature osteoclasts, continued signalling from c-fms and RANK receptors are also needed for osteoclast survival. RANK signalling is also closely regulated by osteoblasts as they

produce OPG, which acts as a decoy to the RANK receptor, thus preventing osteoclast differentiation and survival. One of the hallmarks of osteoporosis is increased bone resorption through increased osteoclast activity. It has been shown that oestrogen deficiency can cause an increase in RANKL through the upregulation of IL-7 and the activation of T cells. This in turn leads to the production of cytokines and reactive oxygen species, which results in an increase in RANKL and therefore osteoclast differentiation (83)

1.2.3 Bone remodelling

Bone remodelling is the process through which mature bone tissue is resorbed from the skeleton and new bone tissue is formed through ossification (26) and occurs continuously throughout life. These processes control the replacement of bone after the injuries such as fractures and also microdamage caused by everyday life and is moderated by the creation of the bone multicellular unit. Bone lining cells form part of this unit and are quiescent cells formed from osteoblasts. Although their exact functions are not completely understood, it has been suggested that one of their functions is to transmit the activation signal that initiates bone remodelling (84). It has also been shown that bone lining cells can prevent direct interaction between osteoclasts and bone matrix when bone resorption should not be occurring (85). The first process that occurs in bone remodelling is the resorption of mature bone matrix by osteoclasts. When osteoclasts are activated to resorb bone matrix, they first become polarised and attach to the mineralised bone matrix, forming three distinct membrane domains: the sealing zone, the ruffled border and the functional secretory domain (86). The ruffled border is essential in bone matrix resorption as it delivers the proteins that are involved in the resorption process, which acidify the area under the ruffled border and cause the break down of the bone mineral matrix beneath. The resulting collagen fragments are then endocytosed by the osteoclast and transported through the cell to the functional secretory domain, where they are released into the bloodstream (87). Once resorption has taken place, osteoblasts migrate to the site and secrete osteoid, which is the unmineralised bone matrix consisting of type I collagen and other proteins such as osteocalcin, osteopontin and bone sialoprotein. Mineralisation then occurs through the localised release of phosphate from osteoblast derived vesicles containing phosphatases that are found within the osteoid. This reacts with the calcium within the extracellular fluid to form hydroxyapatite.

1.2.4 Genome-wide association studies (GWASs)

Bone mineral density has been shown to be influenced by hereditability (88,89) and is the most widely used predictor of fracture risk. GWASs have identified 62 loci that are associated with BMD of either the lumbar spine or the femoral neck (90). Richards *et al* identified two single nucleotide polymorphisms (SNPs) that were negatively associated with BMD and increased osteoporotic fracture risk using samples from the TwinsUK cohort. These results were then replicated in three independent cohorts (91). Another study by Rivadeneira *et al* identified twenty loci associated with bone mineral density through meta-analysis of GWASs. Thirteen of the identified loci were novel regions that included, for example, cytosine-phosphate-guanines (CpGs) associated with *LRP4, SOX6, HDAC5* and *FOXL1*. The meta-analysis confirmed that seven previously known BMD loci (including *ESR1*, *LRP5* and *SP7*) still had significant associations at a genome-wide level (92). By 2012 there had been 14 genome-wide analyses looking at the associations between SNPs and BMD, with the aim of trying to identify predictive markers of BMD and osteoporotic fracture risk, however most of the individuals who develop osteoporotic fractures have not been diagnosed with BMD-defined osteoporosis (90) and GWAS studies have only identified genes that account for 5% of the variance seen in BMD.

Osteoporotic fractures also have heritable features, some of which are independent of BMD (93). To date, the largest genome-wide meta-analysis looking at loci associated with fracture risk has been carried out by Estrada *et al*, with which they identified 56 loci associated with BMD by looking at associations in >80,000 subjects, 32 of which were novel associations. They then tested these loci for association with fracture in >130,000 cases and control, identifying 14 loci that reached genome-wide significance (94). Other groups have also shown significant association with fracture risk at a genome-wide level (92,95–97). Some of these associations were replicated in the meta-analysis by Estrada *et al*, whereas others were not.

1.2.5 Pathogenesis of osteoporosis

Osteoporosis is characterised by low bone mass and deterioration of bone microarchitecture. This leads to increased bone fragility, which increases the risk of bone fracture. Normal bone metabolism involves a balance between bone resorption and bone formation and it is when this system becomes unbalanced that bone deterioration occurs (98). Many factors are believed to contribute to the unbalancing of this system and development of osteoporosis (Figure 1.3).

Osteoporosis occurs most commonly in the older population, with aging being one of the factors that contributes to the pathogenesis of the disease. Studies have shown that the amount of bone produced with each remodelling cycle decreases with age in both men and women,

exhibited by the decrease in trabecular bone that occurs (99,100). Evidence from both mouse and human studies have shown that there is less osteoblastogenesis in older subjects, suggesting a possible mechanistic explanation for the decrease in bone formation (101,102). Both of these would lead to increased bone loss and a poorer bone quality.

Garnero *et al* have demonstrated that postmenopausal women have an increased rate of bone turnover that remains elevated for at least up to 40 years after menopause (103). They found that during menopause there was a 79-97% increase in bone resorption with only a 37-52% increase in bone formation being observed and where bone formation rate decreased again after menopause, bone resorption remained elevated. This leads to continuous bone loss which is a major determinant of osteoporosis. Loss of oestrogen during menopause has also been linked to the pathogenesis of osteoporosis as fracture risk increases as oestrogen levels decrease in postmenopausal women (104,105). It has been proposed that oestrogen may have three different sites of action in regulating bone turnover: (1) altering osteoblast production of RANKL and OPG, which upregulate osteoclast activity, (2) directly inhibiting osteoclast activity and (3) increasing osteoblast-mediated bone formation, which suggests that the action of oestrogen is both anti-catabolic and anabolic (106). Studies have also demonstrated that the treatment of postmenopausal women with oestrogen decreases the rate of bone resorption (107,108).

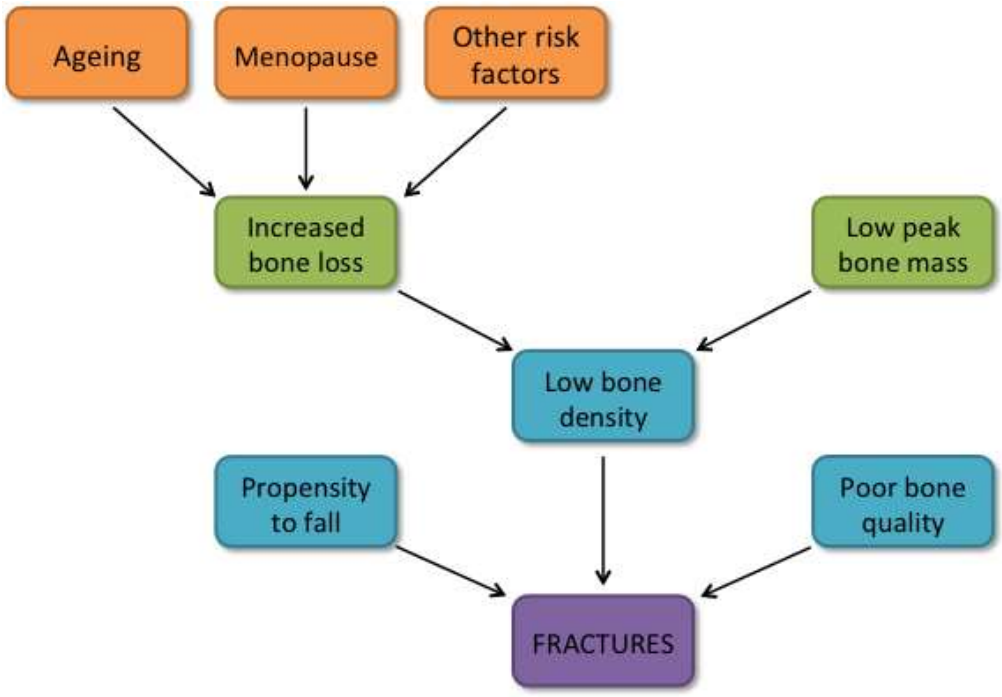

Figure 1.8: Pathogenesis of osteoporosis. Diagram adapted from Lane (109).

Other factors that contribute to increased bone loss are vitamin D and calcium deficiency, which in turn can lead to the development of secondary hyperparathyroidism as 1,25VitD_3 exerts

an inhibitory effect on the synthesis of PTH. Studies have demonstrated that, as well as contributing to increased bone loss in women, vitamin D deficiency and hyperparathyroidism is also associated with an increase in the rate of falls among the elderly (110,111). Sambrook *et al* also demonstrated associations between PTH levels in the elderly and time of first fall are independent of circulating 25-hydoxyvitamin D levels and that those patients with increased PTH levels are likely to have a fall sooner than those with lower circulating levels of PTH. Muscle biopsies from patients suffering with primary hyperparathyroidism have demonstrated atrophy of type II muscle fibres (112), which could suggest that increased levels of PTH are having a detrimental effect on the muscles of these patients, leading to decreased stability and increased likeliness to fall. Clinical trials where the elderly were supplemented with vitamin D and calcium have shown decreased serum PTH levels, decreased bone loss and increased bone mineral density in the supplemented group versus the control group (113), suggesting that supplementing the diets of at risk individuals with these factors could be advantageous in treating osteoporosis.

As well as increased bone loss, low peak bone mass also contributes to the pathogenesis of osteoporosis and is major determinant of bone density in later life: if an individual has less bone to begin with, then age-related bone loss is going to affect those with a lower peak bone mass more severely than those with a higher one. A person acquires most of their bone mass is attained by adolescence, even though the process starts *in utero* (109). A study by Hansen *et al* demonstrated that over a 12 year period of 154 women, those who had a lower peak bone mass had a greater reduction in bone mass and density than those that had a higher peak bone mass. They also showed that using baseline measurements and an estimation of bone loss rate, they can identify those women that are at greater risk of developing osteoporosis post-menopause (114).

All of the above contribute to the development of low bone density which, along with poor bone quality due to changes in microarchitecture brought about by unbalance of bone homeostasis and increased likeliness of a fall, participates in the pathogenesis of osteoporosis by leading to the occurrence of fractures.

1.3 Developmental origins of health and disease (DOHaD)

During the 19th century health professionals in Hertfordshire began to keep records relating to weight, childhood illnesses, development and feeding method of children from birth up until 1 years of age and these records have since been used by the Medical Research Council for epidemiological studies. Barker used this information to investigate the link between ischaemic heart disease in England and Wales and infant mortality. Ischaemic heart disease had been associated with increasing levels of prosperity in the UK, but the mortality rates were highest in the least prosperous areas. When the country was split into 212 regions, Barker *et al*

showed there was a strong correlation between ischaemic heart disease and both neonatal and postnatal mortality rates according to geographical location (115,116). He used these findings to postulate that a poor diet during childhood increased susceptibility of an individual to developing cardiovascular disease in later life due to the effects of an affluent diet.

1.3.1 Human studies

The research presented by Barker resulted in many other studies being undertaken to investigate the relationship between early life environment and its role in susceptibility to disease in later life (117–119). Good record keeping on mothers and infants at the beginning of the 20th century allowed for investigation into the relationships between maternal pelvic size, fetal growth and death from stroke and coronary heart disease in a sample of 13,249 men across Hertfordshire and Sheffield born between 1907 and 1930 (120). Mortality due to stroke was found to be associated with low birth weight and death from cardiovascular disease was shown to be associated with small head circumference, thinness and shortness of breath. In adults born in Preston during 1935-43, strong relationships were shown between placental weight, birth weight and both diastolic and systolic blood pressure during adulthood (121). An increase in birth weight was shown to be associated with an increase in blood pressure, though the relationships between placental weight and blood pressure and birth weight and blood pressure were independent of each other. This meant that those with the highest blood pressure at age 45-54 were individuals that had had a lower birth weight and greater placental weight for both men and women. These results showed for the first time that intrauterine growth has an important influence on blood pressure and hypertension in adults. The limiting factors in these studies is the number of confounding variables that are available to include in analysis, meaning that direct comparisons cannot be made. There is also a wide variety of differences in the environments across the studies, therefore the results cannot be generalised to the whole population. However, as these are observational studies, and due to ethical reasons, relationships between infant phenotypes and later disease cannot be explored when there are severe environmental circumstances.

During the winter of 1944-45, the Netherlands suffered a severe reduction in food supplies due to German actions in the Second World War. During this time calorific intake, which had been adequate before the war, fell below 1000kcal/day, which reduced even further to less than 500kcal/day by April 1945. Food supplies where then returned to normal immediately following liberation in May of that year. During this time it was ensured that children's daily intake did not fall below 1000kcal/day (122). Studies have gone on to characterise the effects of famine on birth weight and later disease risk, with focus on the effects of famine during different

stages of pregnancy (early, mid or late-gestation). It was shown that mean birth weight dropped by 300g for babies born to mothers that were exposed to famine during late-gestation and that in 296 individuals there was an increase in coronary heart disease in those that were exposed to famine during early gestation when compared to a non-exposed control group. Babies born to this group were also shown to have smaller head circumferences and lower birth weights when compared to the non-exposure group (123). Another study has shown that men and women exposed to famine during early gestation to have an increased BMI and low density lipoprotein-high density lipoprotein ratio at 50 years of age, which lead to an increased risk of coronary heart disease in these individuals (124). The findings from the Dutch Hunger Winter Famine emphasises the importance of timing of exposure to altered nutrition and that this can have an adverse effect on the offspring in later life, leading to increased risk for certain diseases.

Non-communicable disease such as osteoporosis, cardiovascular disease and type 2 diabetes, have also been linked to a poor early life environment. Investigation into the relationship between growth in infancy and bone mass in later life using 189 women and 224 men between 63-73 years of age from the Hertfordshire cohort showed significant associations between weight at 1 year and bone mineral content (125). Those individuals that weighed less at 1 year were also the ones who had a lower bone mineral content in later life, suggesting that skeletal growth may be programmed *in utero*. Using 297 women from the Hertfordshire cohort, relationships were revealed between birth weight and fasting plasma glucose concentrations, waist:hip ratio, systolic blood pressure and triglyceride concentrations in that increased birth weight led to a decrease in the above risk factors for cardiovascular disease in adulthood (126). This suggests that those babies that are small at birth are at greater risk of developing cardiovascular disease in later life, and those that become obese in adulthood are at greatest risk.

Cohort studies have been invaluable in demonstrating the developmental origins of adult disease. The Southampton Women's Survey was established to measure the pre-pregnant characteristics of women aged 20-34 living in Southampton and to follow-up those that became pregnant (117). This study focused on fetal development and post-natal growth and how they contributed to the child's risk of developing chronic disease in later life. Data has shown that babies who are smaller at birth have poorer lung function (127) and that poor maternal calcium and vitamin D status during pregnancy has been linked with impaired bone mineral accrual in the infant (128). The Western Australian Pregnancy Cohort (RAINE) Study was set up in 1989 and recruited 2900 pregnant women with the aim to investigate the hypothesis that pregnancy complications may be prevented with frequent ultrasound scans, as well as to set up a long-term cohort to study the effects of early life environment on later health (129). Data from this study

has revealed that maternal smoking during pregnancy and rapid childhood weight gain are associated with increased metabolic risk (130) and that infants with a smaller head circumference were at greater risk of neurodevelopment disorder (131).

Although human observational studies allow for identification of relationships between *in utero,* early life environment and the onset of disease in later life, they do not allow for the investigation of direct mechanisms that lead to the induction of certain phenotypes. There are too many uncontrollable variables, such as socio-economic status and maternal and paternal background, therefore animal studies in a controlled environment where variables can be removed were used to determine alterations to specific pathways that could increase risk of disease in later life.

1.3.2 Animal studies

Animal studies allow for the effect of altered nutrition on offspring phenotype to be investigated in a controlled setting and allows for the investigation of the mechanisms that may lead to an altered phenotype. A low protein model has been used extensively in animal studies to demonstrate how restricted protein intake during pregnancy can have an adverse effect on offspring phenotype. A study by Langley-Evans in 1994 showed that pups that were exposed to maternal low protein diet *in utero* were hypertensive at 4 weeks when compared to control pups (132). This was shown to be due to the exposure during gestation as pups that were fed a low protein diet for 14 days did not exhibit the same increase in blood pressure, thus highlighting the importance of maternal diet in the development of offspring phenotype. Langley-Evans *et al* also went on to show that maternal low protein diet altered the expression of maternally-derived glucocorticoids, which led to a loss in homeostatic control in the pups, and this in turn led to altered physiology and endocrine function (133). Other studies using a restricted maternal protein diet have shown reduced cellular proliferation in embryos, smaller birth size of pups and rapid decline in glucose tolerance, which have led to altered metabolism in the offspring (134).

Intrauterine growth restriction (IUGR) has also been used to investigate the developmental origins of disease by causing restricted fetal growth. This can be done via one of two methods, either by restricting maternal nutrition or by bilateral ligation of the uterine artery. Experiments have found that IUGR can cause obesity, type II diabetes and metabolic syndrome in the offspring. Ozanne *et al* have demonstrated that IUGR causes a change in liver morphology, and therefore metabolism, as well as changes to glucose metabolism and insulin response in skeletal muscle and adipose tissue (135). This demonstrates the influence that restricted fetal growth can have on the health the offspring from dams fed a nutrient restricted diet.

In a study by Guberman *et al*, pups born to mothers that had been on a high fat diet (60% of calories from fat) throughout pregnancy had increased adiposity and hypertension when compared to control offspring (136). This has also been demonstrated by Elahi *et al* where long-term maternal high fat diet also led to hypertension in the offspring as well as fatty liver (137). However, in this study mothers had been on a high fat diet from weaning, not just during pregnancy. Other studies have shown that a maternal high fat diet induces type II diabetes in offspring as well as increased birth weight and anxiety behaviours (138).

These various studies have demonstrated that both maternal undernutrition as well as over nutrition can both result in similar disease phenotypes; however, this is likely to be caused through different mechanisms. The data from these studies shows that the environment the offspring is exposed to *in utero* via maternal diet has adverse effects on the health outcomes of the offspring and highlights the importance of elucidating the mechanisms involved to help us better understand the developmental origins of disease.

1.3.3 Evidence for the developmental origins of osteoporosis

Fracture prevention has mainly been targeted at decreasing the rate of bone loss in the elderly through drug treatment, however it is now becoming evident that peak bone mass in adolescence is a major and important contributor to bone strength in later life. Even though there is evidence to suggest that peak bone mass is inherited, this only accounts for a small fraction of the variation that is seen in bone mass and fracture risk across individuals (93). Environmental factors such as gender, diet, physical activity and smoking, have been shown to affect the accumulation of bone mineral throughout childhood and adolescence, however as there is a rapid accrual of bone mineral at the later stages of pregnancy, paired with skeletal development having a high level of plasticity *in utero*, there is the possibility that environmental stimuli could have an effect on the genome at this stage of life.

Evidence for the developmental origins of osteoporosis comes from four main types of studies: 1) population studies, 2) physiological studies, 3) studies that characterised maternal nutrition and lifestyle and related these to bone mineral of their offspring and 4) studies that relate childhood growth to risk of hip fracture in later life (139).

1.3.3.1 Population studies

Using a cohort of 153 women who were born in Bath between 1968-1971, Cooper *et al* demonstrated that there was a significant association between weight at 1 year and bone mineral content (BMC), which was not replicated between weight at 1 year and BMD (140). This would suggest that there is some unbalance in the pathways that regulate skeletal growth and

mineralisation. These results were replicated by Dennison *et al* and Cooper *et al* in the Hertfordshire cohort, though the associations with BMC were weaker (118,125). These studies also demonstrated an association between weight at 1 year and bone area of the adult hip and spine. Another study by Dennison *et al* found a significant association between VDR genotype and birth weight as factors that influence BMD (141). Using 291 subjects from the Hertfordshire cohort (165 men, 126 women), they found that lumbar spinal BMD was higher in those that had the BB VDR genotype and were lighter at birth (p=0.01). These observations are not significantly altered by changes in adult weight, which suggest that modifications occur *in utero* rather than in post-natal life to cause changes in BMD and BMC.

Twin studies have also been undertaken to determine if genetic factors determine bone mineral content, density and mass. However, these studies have shown that only approximately 20% of variance seen in BMC can be explained through genetics. A study by Smith *et al* undertaken on 71 juvenile and 80 adult twin pairs showed that the variance in bone mass between juvenile monozygotic twins was 0.0013 g/cm^2 compared to 0.0069 g/cm^2 in adult monozygotic twins (88). This suggests that although genetic factors have a role in determining bone mass, environmental factors may also have a role as there is greater variance in bone mass between the adult twin pairs. Another study by Pocock *et al* has demonstrated that there is a higher level of correlation between BMD in monozygotic twins than dizygotic twins and that there is greater genetic contribution to BMD of the lumbar vertebrae and certain areas of the proximal femur (142). This suggests that environmental factors have a greater influence on BMD of different areas of the skeleton.

1.3.3.2 Physiological studies

In these types of studies groups have tried to identify the potential role of the hypothalamic-pituitary pathway osteoporosis but looking for associations between circulating growth hormone and cortisol levels with bone mineral density in both men and women. It was shown that birth weight was predictive of basal growth hormone and cortisol during adulthood (143,144) and it has been suggested that these two hormones can be factors in determining the rate of bone loss. Other studies have also shown that interactions between the genome and environmental stimuli can have an effect on the basal levels of growth hormone, which in turn can contribute to accelerated bone loss in later life (145). In this study, Dennison *et al* showed that a SNP in the promoter region of the growth hormone gene had a significant association with lower basal concentrations of growth hormone and increased bone loss in later life. This group also demonstrated significant associations between the SNP and weight at 1 year and rate of bone loss.

1.3.3.3 Maternal lifestyle

Many animal studies have also demonstrated that restriction in maternal diets or dietary excess have a negative effect on skeletal bone development. Fleeman *et al* showed that maternal nutrient restriction in pregnant rats caused a reduction in the levels of ossification in the offspring of dams on the lowest nutrient diet (146) and Lanham *et al* have demonstrated that low-protein maternal diet leads to reduced strength and increased porosity in micro-swine offspring (147). In contrast, Lanham *et al* have also shown that a maternal high fat diet can lead to the increase in deposition of fat in the distal femur of mouse offspring and female offspring also exhibited a change in trabecular structure (148). Both these results show that alterations to the maternal diet, whether it be restriction or excess can lead to alterations in the development and structure of the offspring's bones.

Godfrey *et al* investigated the influence of maternal diet and lifestyle on intrauterine growth of 154 babies and they found that there were positive correlations between offspring bone mass and birth weight, length and placental weight (149). They also demonstrated that maternal smoking and maternal energy intake at 18 weeks gestation had a negative association with BMC at birth as well as showing that the offspring of mothers who had a higher triceps skin fold thickness (a measure of fat stores) had higher BMC and BMD ($p=0.02$ and 0.007 respectively). This finding was replicated in a cohort of 216 9 year old children, where it was shown that lower fat stores at later stages of pregnancy was associated with lower BMC of children at 9 years of age (150). This study by Javaid *et al* also showed associations between reduced BMC at 9 years with shorter maternal height, history of maternal smoking and lower maternal social class. Of the subjects in this cohort, 77 of mothers also had below normal vitamin D status and both whole body and lumbar spine BMC of the offspring of these mothers was significantly reduced, ($p=0.0088$ and $p=0.03$ respectively). These data suggest that maternal lifestyle and diet might influence intrauterine skeletal growth and studies have shown that these children could be at greater risk of developing osteoporosis in later life as offspring childhood growth, birth weight and bone mineral content relates to later bone health and risk of hip fracture (151,152).

1.3.3.4 Childhood growth

7,000 men and women from a Finnish cohort were used to determine that childhood growth rate is directly linked to fracture risk (153). This Finnish cohort linked hospital discharge reports for hip fracture with birth and childhood growth data and found that tall maternal height ($p<0.001$) and reduced rate of growth in both childhood height and weight ($p=0.006$ and $p=0.01$ respectively) are factors that influence risk of hip fracture in later life. This study also showed a significant positive association between increased fracture risk and babies that are born short.

Javaid *et al* used 6,370 women from the same cohort to show that thinness in childhood is a risk factor for hip fracture in later life (151). Out of these women there were 49 hip fractures over an 187,238 person year period and Javaid *et al* found that women in the lowest quarter of changes in body mass index (BMI) scores through childhood had an 8.2-fold increase in hip fracture risk when compared to those women in the highest quarter. Data from both these studies show that poor growth in childhood has a direct effect on increasing hip fracture risk in later life.

1.3.4 Vitamin D

Vitamin D belongs to a group of fat-soluble secosteroids (a subclass of steroids) and has an important role in regulating calcium uptake and bone homeostasis. There are two forms of vitamin D: vitamin D_3, which is synthesised in the skin from 7-dehydrocholesterol after exposure to sunlight (ultraviolet B radiation), and vitamin D_2, which is acquired from food. Vitamin D_3 is hydrolysed into 25-hydroxyvitamin D_3 in the liver by 25-hydrolase, which is then subsequently hydrolysed in the kidney into 1α,25-dihydroxyvitamin D_3 (the biologically active metabolite of vitamin D_3) by 1α-hydrolase (76). In the circulatory system, the active metabolite of vitamin D_3 is bound to the vitamin D receptor (VDR), which transports it into the nucleus of cells where it forms a heterodimer with members of the retinoid receptor family, namely RXR (154). These complexes then bind to vitamin D responsive elements (VDREs) on target genes such as osteocalcin, calcium binding protein or 24-hydrolase. In intestinal cells, transcription of the calcium binding protein allows for the increased transport of calcium into the blood, which allows for bone mineralisation to occur. When there is a sufficient supply of 1α,25-dihydroxyvitamin D_3, it causes 25-hydroxyvitamin D_3 to be hydrolysed to 24,25-dihydroxyvitamin D_3 by 24-hydroxylase in the kidney. This then goes on to be catabolised further.

There have been many studies, in both humans and animals, which suggest that a deficiency in maternal vitamin D during pregnancy is a significant risk factor for severe adverse health outcomes in offspring during both fetal and childhood development. In humans, it has been shown by a number of different groups in a variety of cohorts that maternal serum 25-hydroxyvitamin D_3 concentrations are positively associated with childhood BMC, BA and BMD. Using the SWS cohort, Harvey and colleagues have shown that across 278 pregnancies (136 female offspring), female offspring of mothers that had a serum 25-hydroxyvitamin D_3 lower than 33 nmol/l had a mean whole body BA of 110cm^2 compared to 119cm^2 in offspring whose mothers had a serum 25-hydroxyvitamin D_3 concentration above 33nmol/l. This association reached significance, as did the positive association seen with whole body BMC (155).

Studies using the RAINE cohort and the Avon Longitudinal Study of Parents and Children (ALSPAC) have shown similar findings. Recently, Hart and colleagues demonstrated that in 901 mother-offspring pairs in the RAINE cohort, the offspring of the 37% of mothers which had a 25-hydroxyvitamin D_3 deficiency at 18 weeks of pregnancy (concentration less than 50nmol/l), had a lower peak bone mass at 20 years of age (156). Using the same cohort, Zhu *et al* showed maternal serum 25-hydroxyvitamin D_3 concentration to have a positive association with both offspring total body BMC and BMD at 20 years of age. The offspring of mothers who had a serum concentration of 25-hydroxyvitamin D_3 lower than 50nmol/l had a 2.7% lower total body BMC and 1.7% lower total body BMD when compared to those whose mothers had a serum 25-hydroxyvitamin D_3 concentration greater than 50nmol/l (157). A study by Sayers and colleagues using the ALSPAC cohort has also demonstrated that the exposure of a mother to UVB in the third trimester is also associated to the BMC of the child. A total of 6995 boys and girls were assessed whose mothers' exposure to UVB had been recorded and they found there to be a positive association between UVB exposure in the third trimester and childhood BMC, BA ad BMD, but not area adjusted BMC at 9 years of age (158). This would suggest that maternal UVB exposure has an effect on the bone size of the offspring.

There have also been some studies that have shown no associations between maternal serum 25-hydroxyvitamin D status and offspring BMC during childhood. For example, using the ALSPAC cohort, which had previously been used to show that there was an association between maternal UVB exposure and childhood bone outcomes, Lawlor *et al* did not find any association between childhood bone outcomes and maternal 25-hydroxyvitamin D status. Using 3960 mother-offspring pairs, they were split into three groups according to maternal serum 25-hydroxyvitamin D_3 concentration: sufficient (>50nmol/l), insufficient (49.99-27.5nmol/l) and deficient (<27.5nmol/l) and relationship to childhood BMC was assessed. This group did not find any differences in BMC at 9 years between the two lower concentrations and the sufficient group (159). However, further investigation into this cohort have demonstrated that whilst there are no associations between maternal 25-hydroxyvitamin D_2, there were positive relationships between child cortical bone density and thickness with maternal 25-hydroxyvitamin D_3 (160). This suggests that it is 25-hydroxyvitamin D_3, which exerts beneficial effect to offspring cortical bone development in contrast to 25-hydroxyvitamin D_2.

1.4 Epigenetics

As GWAS has only been able to explain 5% of variance seen in BMD, next generation sequencing should help to uncover much of the missing heritability, however, epigenetic

regulation may also have a role to play too. Epigenetics is the study of the regulation of gene expression through modifications that do not alter the underlying DNA sequence (161,162). These modifications can be influenced by a variety of environmental factors, such as diet and smoking, especially in early life.

1.4.1 Epigenetic mechanisms

1.4.1.1 DNA methylation

This is the process by which a methyl group is transferred from S-ad*NOS3*ylmethionine (SAM) to carbon 5 of cytosines of CpG dinucleotides to form 5-methylcytosine (5-mC) (163), as shown in Figure 1.9. Of all the CpG dinucleotides in the mammalian genome, it has been suggested that at least 80% of these are methylated (164). The remaining 20% are unmethylated and are located in constitutively active or inducible gene promoters. These clusters of CpGs are termed CpG islands and are defined as a region of <500 base pairs that has a CG content of more than 55% (165). It is methylation of these CpGs that leads to a decrease in gene expression either due to the inability of the transcription factor of the gene to bind to the methylated sequence (166) or through the recruitment of transcriptional repressor complexes, some of which possess histone deacetylase (HDAC) activity (164). Many CpG islands also have shores, which are slightly less dense regions of CpG dinucleotides near CpG islands and have been linked to tissue specific methylation (162).

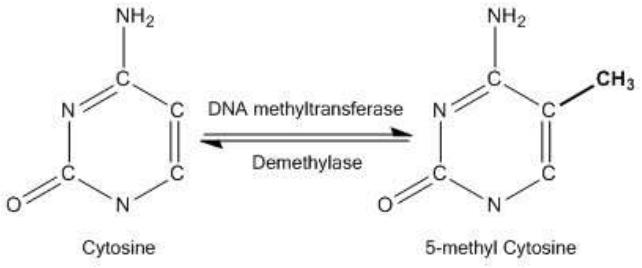

Figure 1.9: 5-methyl cytosine

DNA methylation is regulated by three DNA methyltransferases (DNMTs): DNMT1, -3A and -3B. DNMT1 is termed the 'maintenance' DNMT as it is specific for hemi-methylated DNA and is therefore responsible for passing on methylation patterns to the new strand of DNA. DNMT3A and-3B are *de novo* methyltransferases and are therefore the methyltransferases that respond to environmental stimuli to transfer a new pattern of methylation onto the DNA (162). Knockout studies have shown that deletion of any methyltransferase has a global effect on methylation (167). The demethylation mechanism is not yet fully understood, though data from Metivier *et al*

suggests that this could be carried out by DNMT3A and -3B (168), however it has also been suggested that demethylation is a passive event (169). There is now also increasing evidence to suggest that the TET family of enzymes can cause cytosine demethylation by converting 5-methylcytosine to 5-hydroxymethylcytosine (170).

1.4.1.2 Histone modifications

Chromatin is made up of nucleosomes, which consist of 146bp of DNA wrapped 1.65 times around a core of histone proteins. This core is formed from an octamer of two copies each of H2A, H2B, H3 and H4. A linker histone protein, H1, is also associated with the octamer core and binds at the entry and exit point of the DNA, thus locking it into place (164,171). The N-terminus tails of the histone proteins protrude past the DNA and make it ideal targets for post-translational modifications, such as acetylation, methylation and phosphorylation. Acetylation is a reversible modification where an acetyl group is transferred from acetyl CoA onto conserved lysine residues in H3 and H4 tails to form ε-N-acetyllysine. This modification is associated with inducible gene expression and was originally thought to increase gene transcription by reducing the electrostatic interactions between the histone proteins and the DNA, thus making it more accessible (164). This is now known not to be true, instead the acetyl group forms a bromodomain which allows for co-activators such as TATA box binding protein (TBP), TBP associated factors and RNA polymerase II to bind to DNA and promote gene expression (172). The removal of acetyl groups from lysine residues is associated with gene repression and gene silencing. This process is carried out by HDACs, which are classed into four groups: I, II, III and IV (164). It has been shown that the different classes of HDACs recognise different acetylation patterns and therefore repress different genes (173). Lysine residues can also undergo methylation at H3K4 and H3K36.

1.4.1.3 microRNAs (miRNAs)

The first type of non-coding RNA that has a role in genome regulation are microRNAs (miRNAs). These are small single stranded non-coding RNAs that are about 20 to 23 nucleotides in length that act as gene regulators in mammalian genomes (174). They are transcribed from one of two places: 1) from intergenic regions of promoters (175) or 2) from an intronic part of a gene (176). They are first formed into stem-loop structures, and are then exported out of the nucleus (177). The stem loop is then removed by the enzyme Dicer, an RNase III enzyme, to form a duplex of the arms of the loop, one of which is then incorporated into RNA-induced silencing complex (RISC) through association with members of the Argonaute protein family (178,179). The

RISC then either cleaves or suppresses translation of mRNA depending on the percentage of complementary base pairing between the miRNA and the target mRNA (180).

1.4.1.4 Long non-coding RNAs (lncRNAs)

There is now evidence to suggest that another class of non-coding RNAs, long non-coding RNAs (lncRNAs), may have a role to play in epigenetic regulation. lncRNAs are distinguished from short non-coding RNAs, such as miRNAs, as they are over 200bp in length. The expression of lncRNAs has been shown to be developmentally regulated and it can be tissue or cell-type specific (181), though a significant proportion has been shown to be exclusively located in the nucleus of the cells (182).

There are no biochemical features or structural motifs that can be exclusively assigned to lncRNAs. However, it is believed that the modifications that regulate and stabilise coding RNA structure may also regulate lncRNA function (183). It has been shown that lncRNAs can fold into stable secondary and higher order structures and studies have shown that it is these higher order structures that can determine the function of lncRNA. For example, Zhang *et al* have demonstrated that tumour suppressor function of *Maternally expressed gene* 3 (MEG3), a gene that causes growth suppression and the stabilisation of p53 when expressed in tumour cells, is determined by the secondary structure of the lncRNA transcribed from this gene, rather than the primary structure (184).

There are three different functional domains that have been described in lncRNAs: RNA- (185), protein- (186)and DNA-binding domains (187), although there is little evidence that there are direct RNA-DNA interactions, though has been suggested that folding of the RNA can create DNA binding pockets (187). The interactions of lncRNAs and their functions allow them to be separated into 3 groups: decoys, scaffolds and guides (188). lncRNAs can belong to one or more of these groups. The decoy class of lncRNAs are those that bind to regulatory proteins, such as transcription factors, and RNA that would otherwise bind to DNA and cause a change in gene expression (188). Scaffold lncRNAs act as adaptors that allow complexes to form by bringing two or more proteins together (189) and the final group of lncRNAs is the guide group which allow for specific localisation of RNA:protein complexes (190). There is also now evidence to suggest that some lncRNAs can act as transcriptional enhancers (191), though the mechanism for this is yet undiscovered.

1.4.1.5 Evidence epigenetic processes mediate developmental origins of adult disease using animal models

There are many animal studies that show that the epigenome can be affected by early life environment, both during gestation and immediately after birth. Agouti viable yellow mice are useful in these studies as a change in methylation of the promoter of the Agouti gene produces easily observed results, i.e. when the promoter of this gene is hypomethylated, gene expression is increased and the rats have a yellow coat and are obese, however when the promoter is hypermethylated, gene expression decreases and the rats have a brown coat and have a normal weight (192). Studies with these mice have shown that if the maternal diet is deficient of methyl donors and co-factors, the agouti promoter becomes hypomethylated and the resulting offspring have a high prevalence of obesity, cancer incidence and retain their yellow coats (193). Lillycrop *et al* were the first to show that feeding pregnant rats a protein restricted diet can cause specific epigenetic changes in genes involved in the metabolic pathways of the offspring. It was shown that protein restriction caused a decrease in methylation of the glucocorticoid receptor (GR) and peroxisomal proliferator-activated receptor alpha (PPARα) genes in the offspring that were persistent after weaning, however the methylation of PPARγ remain unaltered (194).

It has also been shown that maternal behaviour can alter the epigenome. A study on rats by Weaver *et al* has shown that methylation of the GR promoter can be altered in pups depending on the nursing behaviour of the mothers. Those offspring that were exposed to a greater amount of nursing had a greater level of methylation in the GR promoter, lower GR expression and a modest hypothalamic-pituitary-adrenal axis (HPA) stress response when compared to those who were exposed to a lower amount of nursing. These changes appeared within the first week of life and were persistent through adulthood, though the changes could be reversed through cross-fostering, showing that it is the maternal behaviour that has an effect (195).

1.4.1.6 Vitamin D and epigenetic mechanisms

There is evidence now suggesting that the active metabolite of vitamin D_3, 1α,25-dihydroxyvitamin D_3, can induce demethylation, however the exact mechanisms of how this occurs are not clear (196). In most cases it is believed to be a passive process that occurs over multiple cell divisions, but some cases it is believed to be an active process as demethylation occurs within 1-4 hours (197).

Various research groups have suggested that CpG methylation can be influenced by vitamin D status, in both cell lines and primary cells. Tapp and colleagues have demonstrated that serum 25-hydroxyvitamin D_3 concentrations are negatively associated with the methylation in the

promoter region of the tumour suppressor gene *APC* in human rectal mucosa (198) and a recent study on Canadian colorectal cancer patients demonstrated that high dietary intake of vitamin D is negatively associated with the promoter methylation of *DKK1* and *WNT5A*, both of which are WNT antagonists and their expression is usually silenced through hypermethylation during the early stages of colorectal cancer (199).

An EWAS comparing DNA methylation of 11 African American males aged 14-19 years with serum vitamin D levels $\leq$25nmol/l with age-matched controls revealed 79 novel CpGs that were differentially methylated between the two groups, only 2 of which remained significantly after multiple testing (200). These were CpGs found within *MAPRE2*, a gene believed to be involved with controlling proliferation of cells, and *DIO3*, which encodes the enzyme thyroxine 5-deiodinase. It also showed significant difference in methylation of CpGs that had previously been identified through GWAS: *DHCR7*, *CYP2R1* and *CYP24A1*, whose transcripts all have roles in the metabolism of vitamin D.

There is evidence in animal models that 1α,25-dihydroxyvitamin D_3 also influences histone acetylation. In murine osteoblastic MC3T3-E1 and primary osteoblasts, Kim and colleagues demonstrated that when these cells are treated with 1,25-dihydroxyvitamin D_3, it induces the rapid recruitment of co-activators, such as p300 and CREB binding protein (CBP), to the promoters of *Cyp24* and *Opn* (201). The recruitment of these co-regulators lead to the acetylation of histone 4 on *Cyp24*, but not *Opn*, suggesting a role for vitamin D in the regulation of histone acetylation. Kim and colleagues have also demonstrated that 1α,25-dihydroxyvitamin D_3 promotes the deacetylation of histones and the methylation of the *CYP27B1* promoter (202). This gene encodes for 1α-hydroxylase, which converts 25-hydroxvitamin D_3 into its biologically active metabolite 1α,25-dihydroxyvitamin D_3. Both of these epigenetic processes lead to the suppression of *CYP27B1* expression and is another example of how vitamin D can alter the epigenome.

1.4.2 Epigenetics and early life environment

The mechanism by which the fetus senses the environment and adapts its metabolism may involve the epigenetic regulation of genes. A change in this epigenetic pattern can lead to dysregulation of the genes that control placental transfer of nutrients, which in turn can lead to abnormal energy allocation in the developing fetus (161). However this is probably secondary to environmental stimuli the blastocyst receives during the pre-implantation stage. Watkins *et al* have shown that the offspring of mice fed on a low protein diet during pre-implantation stage of gestation are more susceptible to excess growth, cardiovascular and behavioural problems in

adulthood. This effect was found to be independent of maternal diet in later stages of pregnancy and was shown that some of these effects could be mediated by the visceral yolk sac endoderm (203).

Evidence from animal models has shown that epigenetic mechanisms are influenced by the environment the offspring is subjected to in early life and studies have now shown that similar mechanism may occur in humans. In a study by Heijmans *et al* they used the Dutch Hunger Winter cohort to determine if prenatal exposure to famine had an effect on the epigenome of the offspring. They investigated the methylation levels of 5 CpG sites within the promoter region of the insulin-like growth factor 2 (IGF-2) gene in 60 individuals who were exposed to famine compared to their same-sex non-exposed siblings. IGF-2 is a maternally imprinted gene that plays an important role in human growth and development. When comparing those individuals that had been exposed to famine *in utero* to those that had not, it was found that the methylation levels of all the CpGs but one was significantly lower in the siblings that had been exposed to famine ($p=5.9x10^{-5}$) (204). They also looked at methylation of these CpGs in adults who had been exposed to famine during late gestation and found no significant differences when compared to their non-exposed same-sex siblings.

In a similar study by Tobi *et al*, the methylation status of 15 imprinted and non-imprinted genes that have been implicated in growth and metabolic disease were characterised using the same cohort. Once again they looked at methylation levels of these 15 loci in 60 individuals that had been prenatally exposed to famine versus their non-exposed same-sex siblings and found that methylation of *INSIGF* was significantly lower in siblings that had been exposed to famine than those that had not ($p=2x10^{-5}$), which agrees with the results previously shown by Heijmans *et al*. However, they also showed that methylation of *IL10*, *LEP*, *ABCA1*, *GNASAS* and *MEG3* genes was significantly higher in exposed siblings than their non-exposed counterparts (all $p<0.01$). The study also demonstrated the importance of timing of famine exposure as there was a difference in methylation of *GNASAS* in a sample of 62 individuals that were exposed to famine during the late stages of gestation.

Maternal vitamin D status has also been shown to have an effect on offspring development (150) and recently Harvey *et al* have demonstrated that maternal free 25(OH)-vitamin D status is associated with the methylation of *RXRA*, the gene which encodes retinoid X receptor α (RXRα). Using 230 SWS participants, this study showed that free maternal 25(OH)-vitamin D index has a significant negative association with the methylation status of one CpG within the RXRα promoter ($p=0.03$) (205). This further supports that early life environment can

alter the epigenome of the offspring and can cause alterations to genes that have been shown to have roles in growth and development.

1.4.3 Epigenetics and bone

Studies have demonstrated that many epigenetic mechanisms regulate the differentiation of osteoblasts, which can have a downstream effect on bone development and homeostasis. Huang *et al* have demonstrated that miR-22 in human adipose derived MSCs can affect the balance between adipogenesis and osteogenesis by leading to an increase in osteogenic differentiation. When this miRNA is overexpressed in these cells, it causes an increase in ALP activity, matrix mineralisation and transcription of osteogenic specific genes whilst simultaneously causing repression of adipogenic transcription factors (206). Further experiments showed that this promotion of osteogenesis was due to direct repression of HDAC6 via miR-22. miR-17-5p and miR-106a have been shown to have to opposite effects by upregulating adipogenesis and suppressing osteogenesis. In this study, these miRNAs were shown to inhibit BMP2, which caused downregulation of genes such as TAZ2, MSX2 and RUNX2, which are essential for osteoblast differentiation (207).

Histone modifications have also been shown to have a role in regulating osteoblast differentiation. A study from Hassan and colleagues has demonstrated that HOXA10 promotes osteoblastogenesis by directly regulating the activation of RUNX2. It was also shown to upregulate other genes such as ALP, OCN and BGLAP, which are also essential for the progression of osteogenesis (208). HOXA10 mediates chromosome hyperacetylation and H3K4 trimethylation of these genes, which allows for binding of transcription factor complexes and the activation of transcription. Hemming *et al* have shown that EZH2 and KDMA6, a lysine demethylase, act as an epigenetic switch regulating H3K27 trimethylation to control lineage determination of MSCs. Overexpression of EZH2 caused an increase in adipogenesis and suppressed osteogenesis, whereas overexpression of KDMA6 had the opposite effect (209), demonstrating an important epigenetic switch centred around histone methylation that determines MSC differentiation.

In rats, reduced CpG methylation has been associated with the transcriptional activation of bone-specific osteocalcin. Villagra *et al*, using primary rat osteoblasts, demonstrated that during the differentiation process methylation levels of CpGs within the osteocalcin promoter was significantly reduced, which coincided with an increase in expression of bone-specific osteocalcin (210). Delgado-Calle *et al* have demonstrated that DNA methylation has a role in regulating the expression of ALP and the RANKL-OPG pathway in human bone. They found that across a variety of bone related cells the methylation of CpGs within the ALP promoter was inversely related to

the expression of alkaline phosphatase and when cells were treated with a demethylating agent, there was a 30-fold increase in the expression of this gene (211). This group have also demonstrated that the demethylation of CpGs within the promoter of RANKL and OPG genes, two osteoblast-derived factors that are important in osteoclastogenesis, caused an upregulation in the expression of these two genes. Treatment of HEK-293 cells with a demethylating agent led to a 170-fold increase in RANKL expression and a 20-fold increase in OPG expression (212). However, when looking at methylation across patients with osteoporotic fracture and those with osteoarthritis, there was no difference in methylation levels even though RANKL:OPG ratio was significantly higher in those patients with osteoporotic fracture. This suggests that other mechanisms other than methylation could be at play to cause the increased ratios seen in patients with osteoporotic fractures.

Research from independent groups has now demonstrated roles for specific lncRNAs in the osteogenic differentiation process. A recent expression profile by Zuo *et al* has shown that there is differential expression of lncRNAs during the early differentiation of C3H10T1/2 mesenchymal stem cells (murine mesenchymal stem cell line obtained from embryos) into osteoblasts (213). Zuo and colleagues used an Arraystar lncRNA array to look at the expression of lncRNAs between control MSCs and those that had been treated with BMP2 to initiate osteoblast differentiation. This expression array identified 116 lncRNAs that were differentially expressed between the two treatment groups – 59 upregulated and 57 downregulated in the BMP2 treated group. Through bioinformatics analysis, this group also found potential regulatory mechanisms that allow lncRNAs to control osteoblast differentiation and identified 24 lncRNAs with nearby protein-coding gene pairs. Zhu and colleagues have demonstrated that the lncRNA ANCR interacts with enhancer of zeste homolog 2 (EZH2), a subunit of PCR2, to repress RUNX2 expression (214). This was done through quantitative PCR and ChIP analyses, which demonstrated that it was the association of ANCR with EZH2 and their translocation to the promoter of the RUNX2 gene that caused this suppression. When ANCR expression is knocked down via a siRNA in hFOB1.19 cells, a human fetal osteoblastic cell line, there is an increase in alkaline phosphatase and osteocalcin expression, differentiation and mineralisation markers respectively. van de Peppel *et al* have shown that lncRNA H19 expression increases during osteogenic differentiation (215). When expression of this lncRNA is knocked down by short hairpin RNAs (shRNAs) in human mesenchymal stromal cells, results showed a 70-90% decrease in ALP expression and an 80-95% decrease in matrix mineralisation. This coincided with a decrease in the expression of RUNX2 and collagen type I, an extracellular matrix protein, which suggests that H19 may have a direct role in regulating osteoblastic differentiation. This research does

suggest that there may be a role for lncRNAs in regulating the differentiation process of mesenchymal stem cells into osteoblasts.

1.5 Identification of potential predictive markers of offspring bone outcomes

1.5.1 Epigenetic biomarkers of later health

A biomarker is defined as 'a characteristic that is objectively measured and evaluated as an indicator of normal biological processes or pharmacological responses to a therapeutic intervention' (216). If early life environment alters the epigenome as suggested from animal studies and if these marks are largely stably maintained, it may be possible to detect such marks in early life and use these to predict later metabolic capacity and future disease risk. This would also allow for preventative therapies to be given to these individuals to increase the chances of a better health outcome.

Both animal and human studies suggest that early life environment may alter the epigenome and that these altered marks then persist into adulthood (193), contributing to future metabolic health and risk. It should be possible to detect such marks in early life and use these to predict later metabolic health; however, DNA methylation is tissue specific. This suggests that it may not be possible to use methylation patterns in proxy tissue to predict methylation patterns in other, metabolically relevant cell types across the body. However, rat studies have shown that the percentage methylation of the promoter of PPAR-α in umbilical cord is comparable to that in hepatic cells (217).

Studies in humans also suggest that, at least for some CpG loci, methylation is correlated between different tissues, which strengthens the argument that methylation in one tissue can be representative of methylation in another tissue. Woodfine *et al* demonstrated, through pyrosequencing assays, that methylation levels were stable in all germ-line differentially methylated regions (DMRs) associated with imprinted genes across all somatic tissues that were investigated (218). Lu *et al* have identified five genes (*N4BP2*, *EGFL8*, *CTRB1*, *TSPAN3* and *ZNF690*) that have consistent methylation levels across 13 different tissue types, which include brain, lung and colon cell lines (219).

Supportive of epigenetic marks, even in proxy tissues, being used as biomarkers are various studies on human cohorts that shown associations between methylation in umbilical cord collected at birth and later childhood adiposity. Godfrey *et al* showed that methylation of the RXRα promoter region had a strong positive association with a child's adiposity at 9 years in two independent cohorts. The results from the first cohort (Princess Ann Hospital (PAH) study, n=64) demonstrated that as percentage methylation of the *RXRA* promoter increased, so did the

percentage of whole body fat (p=0.009) and fat mass (p=0.023). These associations were then replicated with both percentage whole body fat and fat mass (both p=0.002) using subjects from the Southampton Women's Survey (SWS) cohort (n=239) (220). These marks explain 25% of the variance in fat mass, and so supports the hypothesis that developmentally induced epigenetic markers significantly contribute to later phenotype.

Potential biomarkers could also come from other tissues such as blood. For example, Clarke-Harris *et al* have demonstrated that methylation levels in peroxisome proliferator-γ-co-activator-1α (PGC1α) in blood at 5-7 years predicts adiposity in the child at 9 to 14 years of age (221). Using 40 subjects from the EarlyBird cohort (20 boys and 20 girls) Clarke-Harris *et al* showed that the methylation levels of all 7 CpG loci of interest within the promoter region of PGC1α are stable from 5-7 years up to 14 years of age and that methylation of 4 of these CpGs was significantly associated with future adiposity, where 10% difference in methylation led to a 12.5% change in body fat (p=0.002-0.03). This demonstrates that stable methylation marks can be used to predict future risk.

1.5.2 Epigenetic markers of later bone health

1.5.2.1 RXRα

RXRα, along with RXRβ and RXRγ form the retinoid X receptor family, which belongs to a superfamily of steroid hormone receptors (222). RXRs were first shown to form heterodimers with retinoic acid receptors (RARs), but were subsequently shown to form dimers with other steroid hormone receptors, such as VDR, thyroid hormone receptor (223) and PPARs (224). This demonstrates the versatile nature of RXRs as they mediate several different signalling pathways, exhibiting the potential of these receptors to influence different areas of development.

In bone, RXRα has been shown to have a role in osteoclast differentiation and in postnatal bone remodelling as when RXR function is lost there is an increase in bone mass and the formation of non-resorbing osteoclasts. Menéndez-Gutiérrez and colleagues discovered that this was because RXR forms a homodimer and binds to *Mafbp* promoter, which is a key regulator in osteoclast differentiation, proliferation and activity (225). Through its formation of a heterodimer with VDR, RXRα also functions in osteoblasts by stimulating the expression of osteocalcin, an important protein in bone mineralisation (226) and by regulating osteoblast differentiation and proliferation (227).

Godfrey and colleagues have previously identified significant positive associations between the methylation of a CpG within the promoter region of the *RXRA* gene and adiposity during childhood (220). Methylation levels of 15 umbilical cord tissue DNA samples from the PAH cohort were examined using a NimbleGen promoter array. This array identified 78 potential

differentially methylated genes, of which 5 were shown to have correlations with CpG methylation and adiposity at 9 years of age: *RXRA*, *NOS3*, *SOD1*, *IL8* and *PI3KCD*. Of the 14 CpGs within the DMR of *RXRA*, only 1 (chr9: 136355885) showed any associations with childhood adiposity. This CpG showed a significant positive correlation with both fat mass (FM) and percentage fat mass (%FM) in both the PAH and SWS cohorts.

As adipocytes and osteoblasts share a common lineage, it was reasoned that epigenetic marks associated with umbilical cord tissue DNA and fat mass might also be related to bone development. To this end, using the PAH and SWS cohorts, Harvey *et al* demonstrated associations between *RXRA* promoter methylation and size corrected bone mineral content. Using 230 children from the SWS cohort, they showed that an increase in the percentage methylation of the CpGs within the RXRα promoter at birth was significantly associated with a decrease in size corrected bone mineral content at 4 years (205).

1.5.2.2 Endothelial nitric oxide synthase (eNOS)

eNOS is an enzyme that is encoded by the *NOS3* gene found on chromosome 7 and is one of three isoforms that synthesise nitric oxide (NO), which is a small lipophilic molecule that has a role in a number of biological processes (228). It is most well known for having a role in regulating vascular tone in the cardiovascular system by promoting vascular relaxation through its activation of guanylate cyclase and the subsequent production of cyclic guanosine monophosphate (229,230).

eNOS has also been shown to have mechanistic roles in osteoclasts, osteoblasts and osteocytes. In osteoclasts NO has been shown to increase osteoclastogenesis, possibly through enhancing cellular fusion (231), whereas in osteoblasts, when the eNOS system is disrupted in mice, there is an increase in bone formation markers, such as serum alkaline phosphatase concentration and mineral deposition rate, as well as an increase in BMD (232). In osteocytes Zaman and colleagues have demonstrated that increased mechanical strain on primary osteoclast cell culture leads to an increase in the expression of eNOS and in the production of NO (233). However, the other two isoforms of NOS were not expressed in osteoclasts or any other cells derived from the osteoblast/osteocyte lineage, suggesting that eNOS has a key role in osteocyte function.

Godfrey and colleagues also found associations between a CpG (chr7: 150315553) within the *NOS3* promoter and childhood adiposity. In the PAH cohort, *NOS3* methylation showed significant positive associations with childhood FM, %FM and ratio of truck to limb fat ratio at 9 years of age. However, unlike *RXRA*, these findings were not replicated in the larger SWS cohort.

Harvey and colleagues have since gone on to demonstrate that in a cohort of 66 SWS children that there is a strong positive correlation between the methylation of a CpG within the *NOS3* promoter and the child's bone area (BA), BMC and areal bone mineral density (aBMD) at 9 years of age (234).

1.5.2.3 *CDKN2A*

CDKN2A is found on chromosome 9 and encodes for two cell cycle inhibitors, $p16^{INK4A}$ and $p14^{ARF}$. Both of these transcripts have been shown to have roles in senescence and mutations and deletions in this gene have been found in a wide variety of tumours (235). In osteosarcoma it has been found that deletions in the *CDKN2A* gene and loss of $p16^{INK4A}$ expression occur in the types of osteosarcoma that also had retinoblastoma (Rb) protein inactivation. This protein is involved in the downstream processes of the pathway that $p16^{INK4A}$ regulates.

To identify potential perinatal epigenetic markers associated with later adiposity and bone outcomes, a methyl binding domain (MBD)-ChIP array (Agilent) was carried out on DNA from a 21 umbilical cord samples from the SWS cohort looking for differentially methylated regions across the samples in relation to offspring %FM, BA, BMC and aBMD. Using the BATMAN algorithm, this identified 93 DMRs associated with %FM, one of which was a 300bp region within the *CDKN2A* gene locus that contains 9 CpGs. Upon further analysis, Dr R Murray found that the methylation of this DMR has a negative association with fat mass, BA, BMC and aBMD (unpublished data).

Preliminary analysis was carried out on a larger sample size of SWS subjects (n=292) that had DXA measurements at 4 and 6 years of age and this revealed that there were significant negative associations in offspring between all three and methylation with relation to CpG 9 at both 4 years and 6 years of age (Figure 1.10). For every 1% change in methylation, bone mass decreased by 1.0g (p=0.005) and 1.8g (p=0.008) at 4 and 6 years respectively and it was determined that further investigation was warranted. These relationships remained the same even after adjustments were made for maternal smoking, maternal parity and physical activity in later pregnancy, which have all previously been associated with childhood bone mass. Negative associations were also seen with CpG 5 (data not shown).

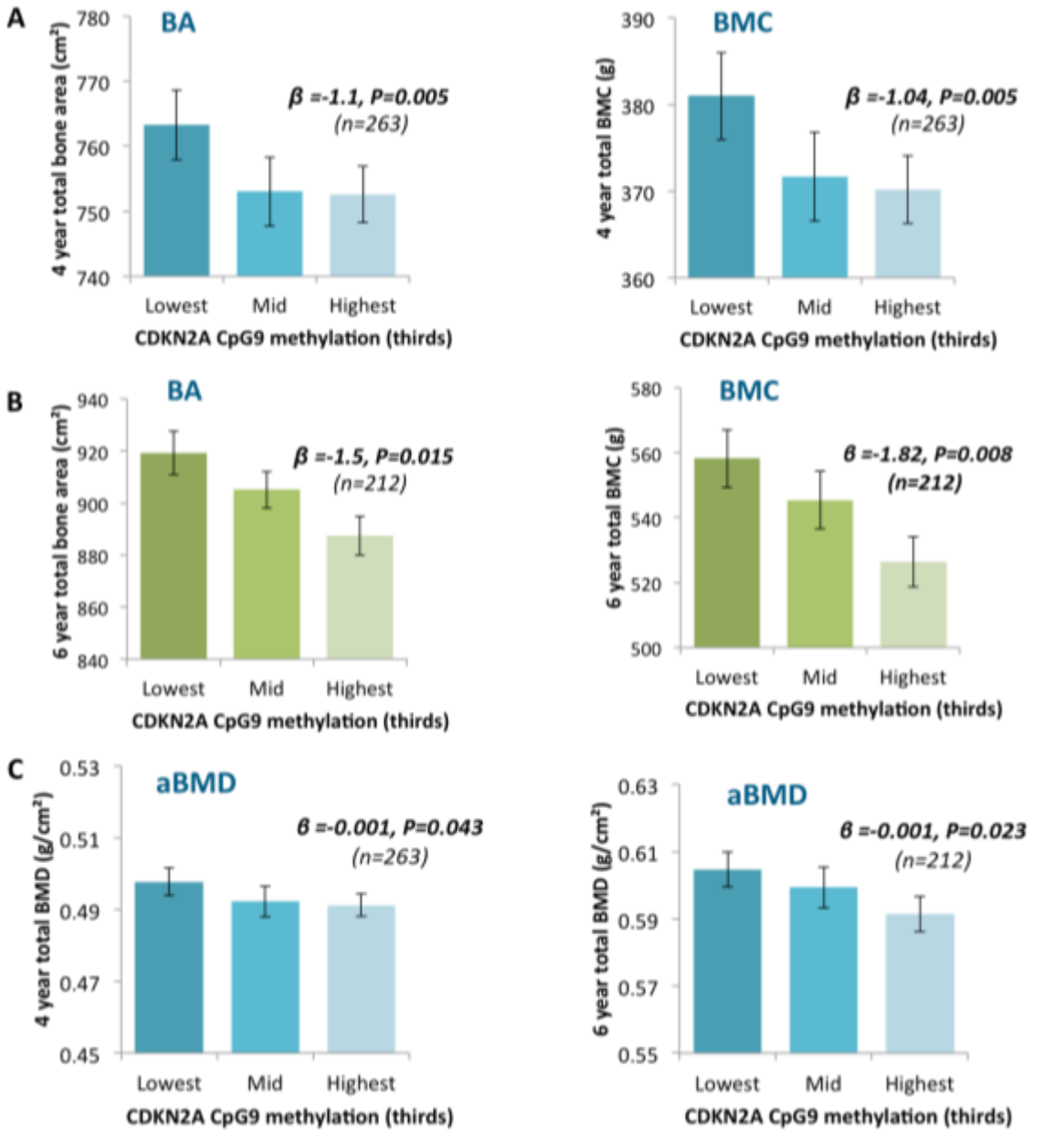

Figure 1.10: Association between CpG 9 methylation and (A) bone area and bone mineral content at 4 years, (B) bone area and bone mineral content at 6 years and (C) areal bone mineral density at 4 and 6 years. For both ages, methylation has a negative association with bone area, bone mineral content and areal bone mineral density. Graphs reproduced with permission from Prof NC Harvey.

1.6 Aims and hypotheses

Osteoporosis is becoming a major burden on the healthcare system as the population is becoming more aged and fragility fractures are becoming more frequent. One of the main contributors to the pathogenesis of the disease seems to be low bone mineral density brought about by increased bone loss, aging, menopause and other factors such as vitamin D deficiency and secondary hyperparathyroidism (109), though there is also evidence that early life environment can alter skeletal development, and therefore can also contribute to the pathogenesis of osteoporosis (118,149,153,236). Bone homeostasis is maintained through the synergy brought about by the various signalling pathways and transcription factors that contribute to the regulation of bone formation. It is when these systems become unbalanced that increased bone loss occurs and results in a lower bone density than is desirable for preventing fragility fractures in later life.

Population studies, physiological studies, mother-offspring cohort studies and studies looking at childhood growth have all provided evidence for the developmental origins of osteoporosis through the affects environmental factors have on bone mineral accrual *in utero*, during childhood and during adolescence. They have highlighted the importance of diet and lifestyle, both of the mother and the offspring in acquiring an optimal peak bone mass and density. However, these studies do not explain all the variance seen in BMD between individuals and genetic studies have only explained 5% of this variance.

Epigenetic studies has provided some evidence in humans to suggest that DNA methylation of various genes associates with future BMD (205,234); however more evidence is needed to determine whether the relationship between regions of altered methylation in cord tissue and bone are simply markers or whether the differentially methylated genes are part of the causal pathway that leads to low bone mass and low bone mineral density. Understanding which of the latter these marks represent is critically important for our understanding of bone development and the utility of such marks as biomarkers for later disease risk. Both *RXRA* and *CDKN2A* are the markers most strongly associated with later bone health and there is evidence that they may have roles in bone development, but whether these regions of differential methylation influence their function is unknown.

The aims of my project are to:

- Identify whether the differentially methylated CpGs associated with later BMC are functionally important in the regulation of *CDKN2A* transcription.

- Determine whether perturbation in expression of the long non-coding RNA ANRIL, a product of the *CDKN2A* locus gene, affects bone cell proliferation, apoptosis or differentiation markers.
- Determine whether ANRIL has any *trans*-functional effects in primary osteoblasts.
- Determine whether a randomised controlled trial, which has seen changes in offspring BMC with maternal vitamin D treatment, causes changes in the methylation status of specific regions within *CDKN2A*, *RXRA* and *NOS3*.

Chapter 2

Materials and Methods

2. Materials and Methods

2.1 Materials

Chemical/Reagent	Details
Ethanol 99%+	Fisher Scientific, #E/0600/05
DNase and RNase free water, DEPC treated	Fisher Scientific, #BPE561-1
Human Liposarcoma SW-872 Cell Line	Cell Lines Service, #SW 872
Human Osteosarcoma SaOS-2 Cell Line	Cell Lines Service, #36025
Dulbecco's Modified Eagle Medium (DMEM)/ Ham's F-12	Gibco, #11320-074
Penicillin-Streptomycin	Sigma-Aldrich, #P4333
Fetal Bovine Serum	PAA, #A15-151
L-Glutamine	Sigma-Aldrich, #G7513
Trypsin EDTA	PAA, #L11-004
Phosphate Buffered Saline (PBS) Tablets	Fisher Scientific, #12821680
Trypan Blue Solution (0.4%)	Sigma-Aldrich, #T8154
FastRead Counting Slides	Immune Systems Ltd, #BVS100
4-(2-Hydroxyethyl)-1-Piperazineethanesulfonic Acid (HEPES)	Sigma-Aldrich, #H4034
Potassium Chloride (KCl)	Sigma-Aldrich, #P9541
Ethylenediaminotetraacetic Acid Disodium Salt (EDTA)	Sigma-Aldrich, #03690
Dithiothreitol (DTT)	Melford, #MB1015
Sodium Chloride (NaCl)	Sigma-Aldrich, #S3014
Phenylmethanesulfonyl Fluoride (PMSF)	Sigma-Aldrich, #P7626
Leupeptin Hemisulfate Salt	Sigma-Aldrich, #L5793
Igepal CA-630	Sigma-Aldrich, #I8896
BCA Protein Assay Kit	Fisher Scientific, #23227
Osteosarcoma SaOS-2 Nuclear Extract	Active Motif, #36025
40% Acrylamide Solution	Fisher Scientific, # BPE1402-1
10X Tris-Borate-EDTA Buffer (TBE)	Fisher Scientific, # T/P050/15
Ammonium Persulfate (APS)	Fisher Scientific, #BPE179-25
Tetramethylethylenediamine (TEMED)	Sigma-Aldrich, #T7024
ATP, [γ-^{32}P]	Perkin Elmer, #BLU002A250UC
T4 Polynucleotide Kinase (100u)	Promega UK, #M4101
illustra™ MicroSpin™ G-50 Columns	GE Healthcare, #27-5330-01
Ficoll 400	Sigma-Aldrich, #F9378
Tris(hydroxymethyl)aminomethane	Sigma-Aldrich, #252859
Poly(deoxyinosinic-deoxycytidylic) Acid Sodium Salt (Poly DIDC)	Sigma-Aldrich, #P4929
Primers for electromobility shift assays	Sigma-Aldrich
Carestream® Kodak® autoradiography GBX developer/replenisher	Sigma-Aldrich, #P7042
Carestream® Kodak® processing chemicals for autoradiography films GBX fixer/replenisher	Sigma-Aldrich, #P7167

CL-XPosure™ Film	Thermo Scientific, #34088
FuGENE 6 Transfection Reagent	Promega, #E2691
Dual-Luciferase® Reporter Assay System	Promega, #E1910
TRI Reagent	Sigma-Aldrich, #T9424
Chloroform, 99.8+%, Certified AR for analysis, stabilised with amylene	Fisher Scientific, #10090120
Lipofectamine® RNAiMAX Transfection Reagent	Invitrogen, #13778
Opti-MEM® I Reduced Serum Medium	Invitrogen, #31985062
Silencer Select siRNA against CDKN2B-AS (n272158)	Ambion, #4390771
Silencer® Negative Control #1 siRNA	Ambion, #AM4611
AllStars Hs Cell Death Control siRNA (5nmol)	Qiagen, #1027298
Custom Silencer Select siRNA against CDKN2B-AS	Life Technologies
DNase I Amplification Grade	Sigma-Aldrich, #AMPD1-1KT
Random nonamers	Sigma-Aldrich, #R7647
Deoxynucleotide Triphosphates (dNTPs)	Promega, #U1420
M-MLV Reverse Transcriptase kit	Promega, #M1701
GeNorm 12 Kit (Human)	Primer Design, #ge-SY-12
TaqMan® Gene Expression Master Mix	Applied Biosystems, #4369016
RPL13A TaqMan® Gene Expression Assay Assay (Hs04194366_g1)	Applied Biosciences, #4331182
TaqMan® Non-Coding RNA Assay (Hs04259476_m1)	Applied Biosciences, #4426961
TaqMan® Non-Coding RNA Assay (Hs01390879_m1)	Applied Biosciences, #4426961
Dual hydrolysis RT-PCR primers and probes	Eurofins
CDKN2B TaqMan® Gene Expression Assay (Hs00793225_m1)	Applied Biosciences, #4331182
CDKN2A TaqMan® Gene Expression Assay (Hs02902543_mH)	Applied Biosciences, #4331182
CDKN2A TaqMan® Gene Expression Assay (Hs99999189_m1)	Applied Biosciences, #4331182
RUNX2 TaqMan® Gene Expression Assay (Hs00231692_m1)	Applied Biosciences, #4331182
Alkaline phosphatase, liver/bone/kidney TaqMan® assay (Hs01029144_m1)	Applied Biosciences, #4331182
BGLAP TaqMan® Gene Expression Assay (Hs01587814_g1)	Applied Biosciences, #4331182
HIF1A TaqMan® Gene Expression Assay (Hs00153153_m1)	Applied Biosciences, #4453320
IGF2 TaqMan® Gene Expression Assay (Hs04188276_m1)	Applied Biosciences, #4448892
MAPK3 TaqMan® Gene Expression Assay (Hs00385075_m1)	Applied Biosciences, #4453320

ETS1 TaqMan® Gene Expression Assay (Hs00428293_m1)	Applied Biosciences, #4448892
CYR61 TaqMan® Gene Expression Assay (Hs00998500_g1)	Applied Biosciences, #4448892
TWSG1 TaqMan® Gene Expression Assay (Hs00221028_m1)	Applied Biosciences, #4448892
Propidium iodide	Sigma-Aldrich, #P4170
Ribonuclease A from bovine pancreas	Sigma-Aldrich, #R6513

2.2 Methods

2.2.1 Cell culture

2.2.1.1 Osteosarcoma SaOS-2 cell line

Human osteosarcoma cells, SaOS-2 (Cell Lines Service) were grown to 70-80% confluence in 75cm^2 tissue culture flasks in Dulbecco's Modified Eagle's Medium (DMEM)/Ham's F-12 supplemented with 5% fetal bovine serum (FBS), 2mM L-glutamine and 1% penicillin/streptomycin in a humidified atmosphere at 37^{o}C with 5% CO_2 in air. Cells were sub-cultured twice a week using 0.05% trypsin/EDTA and used to re-seed flasks with a 1:3 split ratio or spun down to create a cell pellet for total RNA extraction.

2.2.1.2 Human bone marrow stromal cells (hBMSCs)

hBMSCs were isolated from human bone marrow by adding 5mL plain MEMα to a 50mL falcon tube containing bone marrow, after which it was shaken. The bone marrow is obtained from patients undergoing hip replacement surgery at Southampton General Hospital who have given consent for the bone marrow to be used for research purposes. The shaking process was repeated three times, with MEMα being transferred into separate 50mL falcon tube after each wash, to ensure maximum cell retrieval. The cells were then pelleted at 1100rpm for 4 minutes, after which they are passed through a cell strainer and then transferred into a 175cm^2 cell culture flask with complete MEMα (MEMα supplemented 10% FBS and 1% Penicillin/Streptomycin). The hBMSCs were left to attach for a week in a humidified atmosphere (5% CO_2; 37^{o}C) before media removed and replaced with fresh complete MEMα. Sub-culturing occurred when cells reached 70% confluence using 0.05% trypsin/EDTA, when they were split in a 1:2 ratio, with one flask of cells being differentiated into osteoblasts using osteogenic differentiation medium that consisted of complete MEMα supplemented with 2µL/mL ascorbic-2-phosphate and 1µL/mL dexamethasone. Differentiation was detected through a positive alkaline phosphatase staining result (Figure 2.1).

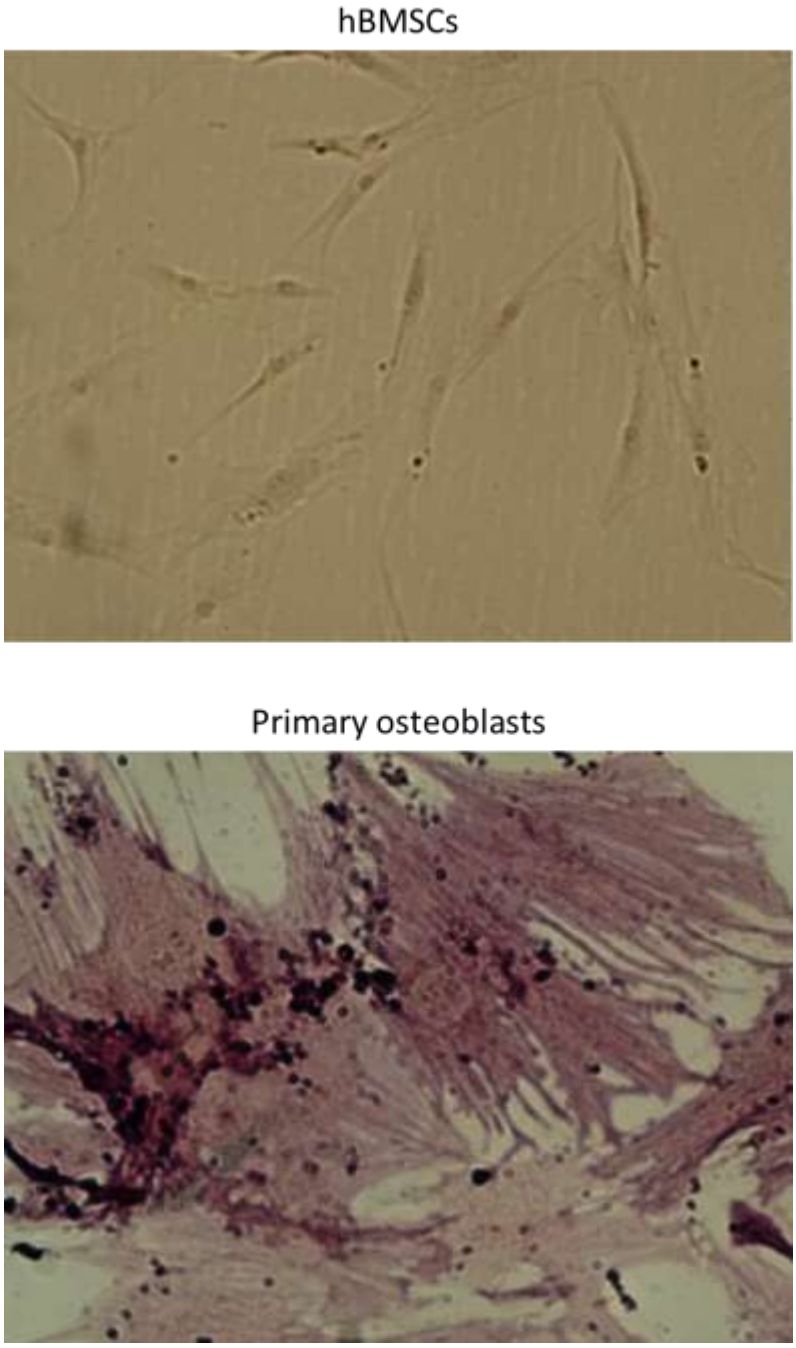

Figure 2.1: Alkaline phosphatase staining of hBMSCs (top) and primary osteoblasts (bottom). Alkaline phosphatase staining shows that there is no alkaline phosphatase activity in the hBMSCs, whereas the primary osteoblasts show a positive result for alkaline phosphatase activity (indicated by the red colour). This confirms that the hBMSCs have been successfully differentiated into osteoblasts.

2.2.2 Transfection of SaOS-2 cells with luciferase reporter constructs

2.2.2.1 ANRIL/p14^{ARF} luciferase reporter constructs

Luciferase reporter constructs contained the promoter region of ANRIL (-1281bp to +20bp relative to TSS) (Figure 2.2A) and the 5' region of the p14^{ARF} gene (-500bp to +1125bp relative to TSS) (Figure 2.2B), which were fused to the firefly luciferase reporter gene in the pGL3-Basic vector and were provided by Dr R Murray. Ten copies of the construct were produced each for ANRIL and p14^{ARF} through mutagenesis PCR - nine with one individual CpG mutated within the DMR and one where none of the CpGs were mutated within 300bp DMR to use as a control. Each of these separate constructs were then transformed into JM109 cells.

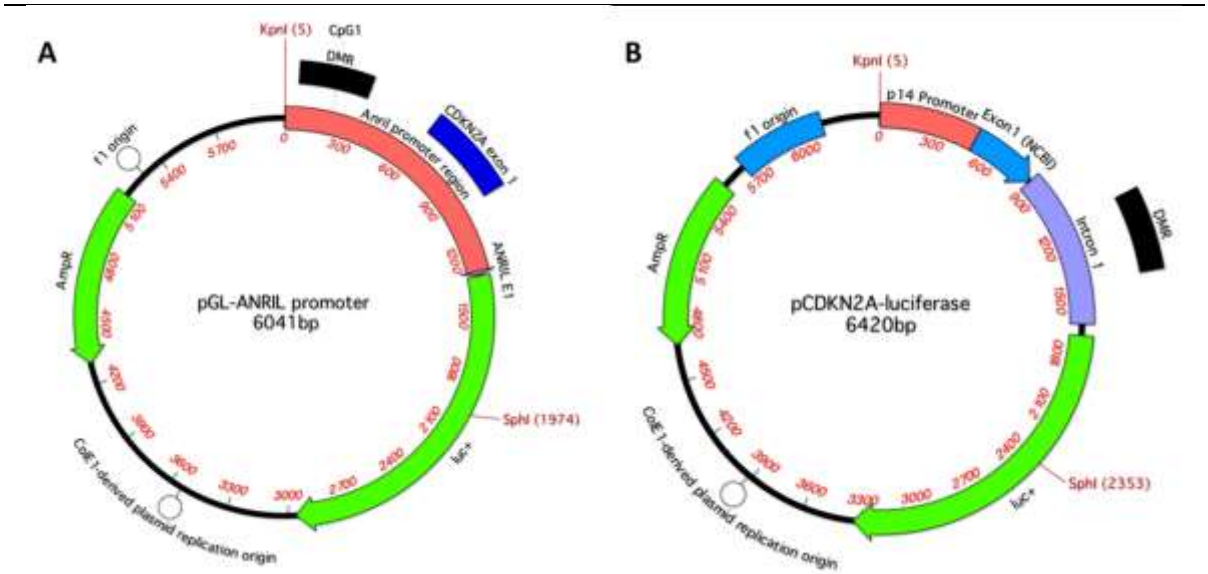

Figure 2.2: ANRIL **(A)** and p14^{ARF} **(B)** pGL Basic plasmid constructs used for Dual-Luciferase® Reporter Assays

2.2.2.2 Inoculation and minipreparation of plasmid DNA

A sterile inoculation loop was used to distribute previously transformed JM109 cells over pre-warmed luria broth (LB) agar plates, containing 100µg/mL ampicillin, to allow for single colonies to be picked. Plates were then incubated upside down for 16 hours at 37^{o}C, after which they were stored at 4^{o}C until colonies were picked.

Using a sterile tip, a single colony was picked from each plate and was added to 10mL of LB media that contained ampicillin (100µg/mL). The bacterial cultures were then incubated for 16 hours at 37^{o}C with shaking (225rpm). A negative culture that contained 10mL of LB medium but no cells was also incubated.

Plasmid DNA was extracted from cells using the GeneJET Plasmid Miniprep Kit (Thermo Scientific) according to manufacturer's instructions. In brief, 1mL bacterial culture was centrifuged at 8000rpm for 2 minutes, after which supernatant was aspirated and any remaining

media removed. Cells were then resuspended in 250µL Resuspension Solution and vortexed, after which 250µL Lysis solution added and samples mixed thoroughly by inverting 4-6 times. 350µL Neutralisation Solution then added and samples inverted 4-6 times immediately after addition. Samples then centrifuged for 5 minutes at 12,000rpm to pellet cell debris, after which supernatant was transferred to GeneJET spin column and spun at 12,000rpm for 1 minute to bind plasmid DNA to column. Flow-through was discarded and 500µL Wash Solution added to the column. Samples centrifuged at 12,000rpm for 30seconds and wash step repeated. After an additional spin for 1 minute to ensure the removal of any remaining Wash Solution, DNA was eluted using 50µL RNase-free water by incubating for 2 minutes at room temperature and then spinning for 2 minutes at 12,000rpm.

2.2.2.3 Preparing plasmid DNA for transfection

Plasmid DNA was sterilised by addition of $1/10^{th}$ of the volume of sodium acetate (pH 5.2), 2 volumes of ice cold 100% ethanol and incubating at -20^{o}C overnight. Plasmid DNA was the pelleted by centrifugation at 13,000rpm for 15 minutes, after which the supernatant was removed and the DNA was washed with 1mL 70% ethanol. After the samples were centrifuged at 13,000rpm for 5 minutes, the supernatant was carefully aspirated and the pellets were air dried for 5 minutes. DNA was then resuspended in 200µL of sterile water and quantity and quality determined using the Nanodrop.

2.2.2.4 Transfection of plasmid DNA

SaOS-2 cells were seeded at $1x10^5$ cells per well in a 24-well plate. Six wells were plated for each separate transfection and cells then grown overnight in 1mL DMEM/Ham's F-12 media supplemented with 5% FBS, 2mM L-glutamine and 1% penicillin/streptomycin at 37^{o}C in a humidified atmosphere containing 5% CO_2. After 24 hours, cells were transfected with plasmid DNA using FuGENE 6 transfection reagent (Promega) as per manufacturer's instructions. FuGENE 6 and Opti-MEM were left to reach room temperature before use and FuGENE 6 was vortexed immediately prior to use. The Opti-MEM was added to each eppendorf to make the total volume up to 25µL per well, and 3µL FuGENE 6 added directly to media, before eppendorfs were vortexed, pulse spun and incubated for 5 minutes at room temperature. After the incubation, 3201ng of the reporter plasmids and 39ng Renilla CMV control plasmid DNA were added to the eppendorfs. Samples were vortexed, pulse spun and then left to incubate at room temperature for 15 minutes, after which 25µL of transfection mix was added to the appropriate wells. Media was carefully mixed by pipetting up and down, before incubating for another 48 hours at 37^{o}C in a humidified atmosphere with 5% CO_2.

2.2.2.5 Preparation of cells for Dual-Luciferase assay

Media was removed 48 hours after transfection and SaOS-2 cells were rinsed with 100µL of 1x PBS. All traces of liquid was removed before the addition of 150µL 1x Passive Lysis Buffer (Promega) to each well and mixed by pipetting up and down before transferring plates to -80^{o}C overnight. Plates were then thawed and 30µL of the lysed cells from each well was transferred into an opaque 96-well plate in order to read the luciferase activity on the VarioSkan Flash Luminometer (Thermo Scientific).

The luminometer was primed with 1500µL Luciferase Assay Reagent II and 1500µL Stop and Glo reagent (Promega). 100µL Luciferase Assay Reagent II was added to each well, followed by 100µL Stop and Glo reagent, with luciferase activity being read after each addition. The level of firefly luciferase was then normalised to renilla luciferase.

2.2.3 Isolation of nuclear extract

Cell pellets from the liposarcoma cell line SW-872 were resuspended in 800µL of hypertonic buffer (10mM HEPES, 10mM KCl, 1mM EDTA, 1mM DTT, 0.5mM PMSF and 10ng/mL leupeptin) and incubated on ice for 10 minutes. 50µL of 10% NP-40 was added to the cell suspension, which was then vortexed and centrifuged at 12,000 rpm for 30 seconds. Supernatant was discarded and pellet resuspended in 50µL of high salt buffer (0.4M NaCl, 20mM HEPES, 10mM EDTA, 1mM DTT and 1mM PMSF). Samples were incubated on ice for 30 minutes then centrifuged at 13,000 rpm for 5 minutes at 4^{o}C. The concentration of the nuclear extract (the supernatant) was determined using BCA protein assay kit (Pierce) according to manufacturer's instructions and stored at -80^{o}C. SaOS-2 cell nuclear extract was purchased from ActiveMotif at 2.5µg/µL.

2.2.4 Analysis of transcription factor binding by electrophoretic mobility shift assay

2.2.4.1 Annealing oligonucleotides

Complementary single stranded oligonucleotides (100µM) were mixed together in a 1:1 ratio and were diluted down to the correct concentration in 1mL of annealing buffer (10mM Tris, 1mM EDTA, 50mM NaCl) (pH 8.0). Each of the unmethylated and methylated oligonucleotides shown in Table 2.3 were diluted down to 1pmol/µL and 5pmol/µL to be used as 100x and 500x competitor respectively in experiments. Oligonucleotides were annealed by heating to 95^{o}C for 5 minutes and were then slowly cooled to room temperature overnight. Annealed oligonucleotides were then stored at -20^{o}C for use as competitors in electrophoretic mobility shift assays or to be end-labelled with phosphorous-32 (P-32).

2.2.4.2 Electrophoretic mobility shift assay (EMSA)

All unmethylated oligonucleotides shown in Table 2.3 were end-labelled with P-32 using T4 polynucleotide kinase. The probe was prepared by mixing 2µL of 1pmol/µL competitor stock, 5µL 5x Polynucleotide kinase buffer (Promega), 1µL polynucleotide kinase, 2µL P-32 and 40µL water in and eppendorf tube. Reaction mixture was then incubated for 30 minutes at 37°C, after which another 50µL of water was added to tube and all of reaction mixture was spun through illustra™ MicroSpin™ G-50 Columns (GE Healthcare) for 5 minutes. 2µL of probe (theoretical final concentration of 20fmol/µL) was then checked using Geiger counter to ensure oligonucleotide had been successfully labelled and that labelled oligonucleotide was at 200 counts or above.

5% polyacrylamide gels were prepared using the components shown in Table 2.2 and allowed to set in glass plates cleaned with 70% ethanol for 30 minutes. Gels were pre-run with 1x Tris-Borate-EDTA (TBE) buffer for 1 hour on ice. This allows the temperature to equalise across the gel. Whilst the gels were pre-running, the binding reactions were set up. For each binding reaction, 5µg of liposarcoma or osteosarcoma nuclear extract, 10µL of 10x Parker buffer and 1µL of Poly dIdC were incubated at 4°C for 10 minutes before the addition of 2µL of labelled probe (final concentration of 2fmol/µL). Samples were then incubated for a further 10 minutes at room temperature before being loaded into a pre-run 5% polyacrylamide gel. Gel was run for 45 minutes at 100V, when the gels were removed from the gel tank and dried down using a gel dryer for 45 minutes. Two CL-XPosure™ films were then exposed to the gels in light tight cassettes at -80°C overnight. The films were then developed using Carestream® Kodak® GBX developer and then fixed using Carestream® Kodak® GBX fixer.

Component	Volume (mL)
40% acrylamide	3.125
10x Tris-Borate-EDTA (TBE)	1.250
Ultrapure water	20.600
MIX	
10% ammonium persulfate (APS)	0.250
MIX	
TEMED	0.025
TOTAL	**25.00**

Table 2.2: Components for 5% polyacrylamide gels used in electrophoretic mobility shift assays.

	Forward (5'→3')	Reverse (3'→5')
Unmethylated CpG -769	TTTCTGGAGGCGGCCTTTTTTC	GGCCGCCTCCAGAAA
Unmethylated CpGs -793 and -796	CCCCAGCCTCCCGGCGGGGTCACCC	GGGTGACCCCGCCGGGAGGCTGGGG
Unmethylated CpGs -836 to -861	GAGTGGAGGACCCGTGAGATACGGGGCACGCAGGCAGCGACTTC CTGAA	TTCAGGAAGTCGCTGCCTGCGTGCCCCGTATCTCACGGGTCCTCCA CTC
Unmethylated CpGs -887 and -907	CTAACAAGGATCGTAGGATCAGTTACTGCTGCGAG	CTCGCAGCAGTAACTGATCCTACGATCCTTGTTAG
Methylated CpGs -887 and -907	CTAACAAGGAT^{me}CGTAGGATCAGTTACTGCTG^{me}CGAG	CT^{me}CGCAGCAGTAACTGATCCTA^{me}CGATCCTTGTTAG
Unmethylated CpG -907	ATCAGTTACTGCTGCGAGGAGCAAGCACTTGCT	AGCAAGTGCTTGCTCCTCGCAGCAGTAACTGAT
Methylated CpG -907	ATCAGTTACTGCTG^{me}CGAGGAGCAAGCACTTGCT	AGCAAGTGCTTGCTCCT^{me}CGCAGCAGTAACTGAT

Table 2.3: EMSA oligonucleotide sequences

2.2.5 Transfection with siRNA against ANRIL

2.2.5.1 SaOS-2

SaOS-2 cells were plated out at 50,000 cells per well in 24-well culture plates, left for 24hrs and then transfected with siRNA using Lipofectamine RNAiMax (Life Technologies) according to manufacturer's instructions. In brief, 23.5µL Opti-MEM and 1.5µL Lipofectamine RNAiMAX per well were added to an eppendorf and mixed by pipetting up and down. Then 23.5µL Opti-MEM and 0.5µL of 20µM siRNA per well were added (final concentration 10µM in well) and samples mixed by pipetting (master mix volumes shown in Table 2.4). Eppendorfs were pulse spun to collect liquid and left to incubate at room temperature for 5 minutes. 50µL of transfection mixture then added to appropriate wells and cells left to incubate at 37^{o}C in a humidified atmosphere with 5% CO_2 for a further 72hrs.

Cells were transfected with three siRNAs against different exons of ANRIL (n=12 for each siRNA; Table 2.5), a negative 'scrambled' control (n=12) and a positive cell death control (n=6) at 10nM. Some wells were also left untreated as a control (n=12). After 72hrs untreated cells and cells treated with negative 'scrambled' control, positive control and ANRIL siRNAs were trypsinised and counted (n=6 for each treatment). The remaining untreated, negative control and ANRIL siRNA wells (n=6 for each) were treated with TRI Reagent (Sigma-Aldrich) and RNA was extracted for RT-qPCR.

Component	Volume (µL)
Opti-MEM	23.50
Lipofectamine RNAiMAX	1.50
siRNA (10nM)	0.50
Opti-MEM (10nM)	24.50
TOTAL	**50.00**

Table 2.4: Transfection master mix volumes for 24-well plate with 50,000 SaOS-2 cells seeding density. Volumes of siRNA added to master mix based on 20µM stock concentration.

	Sequence (5'-3')	Target exon	Designation
Silencer Select against CDKN2B-AS (n272158; #4390771)	GAAAACAAGCGAAAUUAAAtt	ANRIL exon 1	Ambion E1
Custom Silencer Select designed by Congrains *et al* (237)	GAAUGUCAGUUUUGAACUAtt	ANRIL exon 1	Congrains E1
Custom Silencer Select designed by Congrains *et al* (237)	GAACCAGGACUGGAACCUAtt	ANRIL exon 19	Congrains E19

Table 2.5: siRNAs used in SaOS-2 transfections

2.2.5.2 hBMSCs and primary osteoblasts

The siRNA transfection protocol was re-optimised in primary cells to ensure a high level of efficiency of transfection as both seeding density and treatment time have been shown to affect this. These experiments determined that 30,000 seeding density for both hBMSCs and primary osteoblasts with a 6 hour treatment of siRNA were the optimal conditions to use (see Appendix, Section 9.1.1 for full summary of optimisation experiments).

Before plating, media was removed from flasks and primary cells treated with 2% Collagenase Type IV (100mg Collagenase Type IV dissolved in 5mL plain MEMα supplemented with 25µL 1M $CaCl_2$) for 30 minutes before trypsinisation with 0.05% trypsin/EDTA. Primary cells then plated out in 24-well plates at 30,000 cells/well in either basal or osteogenic medium, incubated for 24hrs and then transfected with siRNA using Lipofectamine RNAiMAX as described in section 2.2.3.1). Cells were treated with two siRNAs against ANRIL (Congrains E1 and Congrains E19; shown in Table 2.2; n=6 for each siRNA) as well as a negative 'scrambled' control (n=6) and a positive cell death control (n=2) at 10nM. As with SaOS-2 transfections, some wells were also left untreated (n=2). Master mix volumes were the same as shown in Table 2.4.

Plates were incubated with siRNAs for 6hrs, after which media was replaced with fresh basal or osteogenic medium and then left to incubate for a further 66hrs in a humidified atmosphere at 37^{o}C with 5% CO_2. Two wells of each treatment were then trypsinised, cells counted and then fixed for FACS analysis (described in Section 2.2.8), whereas the remaining 4 wells for 'scrambled' control, Congrains E1 and Congrains E19 were treated with TRI Reagent and RNA extracted for RT-qPCR.

2.2.6 Isolation of total RNA

2.2.6.1 TRI Reagent

Cells were trypsinised and pelleted before being homogenised with TRI Reagent (Sigma-Aldrich) and incubated at room temperature for 5 minutes. The homogenate was collected and 200µL of chloroform added to each sample per 1mL of TRI Reagent used. The samples were shaken for 15 seconds and incubated at room temperature for a further 10 minutes before centrifugation at 11,200 rpm for 15 minutes at 4^{o}C. This separated out the RNA from the DNA and protein fractions, and the top aqueous layer (containing RNA) was transferred to a clean tube. 500µL of isopropanol per 1 mL TRI Reagent used was added to each sample and vortexed for 10 seconds to precipitate out RNA before being transferred to -80^{o}C overnight. Samples were then incubated at room temperature for 10 minutes and then centrifuged at 11,200 rpm for 8 minutes at 4^{o}C after which supernatant was removed and 1mL of 75% ethanol added per mL of TRI

Reagent. Samples were centrifuged again for 5 minutes, then the ethanol removed and RNA pellets left to air dry for 10 minutes. Pellets were then resuspended in 30-50µL of RNase-free water and heated to 55^{o}C for 10 minutes.

2.2.6.2 RNeasy kit

RNA was extracted from primary cells using RNeasy Micro Kit (Qiagen) as per manufacturer's instructions. In brief, media was aspirated from cells and cells lysed directly with 350µL Buffer RLT (lysis buffer). Lysate then homogenised by vortexing for 1 minute, after which an equal volume of 70% ethanol was added and samples mixed by pipetting. Samples were transferred to RNeasy MinElute spin column and centrifuged for 15 seconds at 10,000rpm. Flow-through was discarded and 700µL of Buffer RW1 added to column to bind total RNA. Column centrifuged for 15 seconds at 10,000rpm and flow-through discarded. 500µL Buffer RPE (wash buffer) added to the samples and then centrifuged once again for 15 seconds at 10,000rpm. Samples then centrifuged for 2 minutes at 10,000rpm after the addition of 500µL of 80% ethanol, after which, samples were dried by centrifuging for a further 5 minutes at 13,000rpm with lids open. RNA was then eluted into 14µL of RNase-free water at 13,000rpm for 1 minute and quantified using the Nanodrop.

2.2.7 Illumina Human H12 Gene Expression Array

Osteoblast cRNA was normalised and hybridised onto Illumnia Human H12v4 expression beadChip arrays by a service provider Genome Centre, Barts and the London School of Medicine and Dentistry. Signal extraction was performed by the Genome Centre within GenomeStudioTM and AVG_Signal and Detection_Pvalue values were obtained for each of the 47,229 protests on the array. Only the 14,757 probes that achieved detection p_value <0.05 in all ten samples were retained for analysis. Paired *t*-tests were performed on AVG_Signal values to determine the probes varying by treatment within each cell line pair. 274 probes (mapping to 260 unique genes) were significantly differentially expressed with respect to treatment after multiple testing correction (FDR corrected pvalue < 0.05). HT12 arrays do not contain probes specific to ANRIL expression but do include probes within the CDKN2B locus, which also are predicted to hybridise to ANRIL (ILMN_1723198 and ILMN_2376723). Signal at these probes decreased in all cell lines after treatment.

2.2.8 DNase I treatment

DNase treatment was performed using a kit as per manufacturer's instructions (Sigma-Aldrich). In brief, 1µg of RNA in 8µL of water is incubated with 1 µL of 10x Reaction buffer and

1µL of Amplification grade DNase I at room temperature for 15 minutes. After this 1µL of Stop Solution was added to bind calcium ions and the solution then heated to 70°C for 10 minutes to denature the DNase I. The RNA samples were then chilled on ice before reverse transcription.

2.2.9 cDNA synthesis

After DNase I treatment, 1µg RNA was incubated with 1µL 10mM dNTP mix and 1µL random nonamers (5µM), briefly centrifuged and incubated at 70°C for 10 minutes. Eppendorfs were then placed on ice and 4µL 10x M-MLV Reverse Transcription buffer, 1µL M-MLV Reverse Transcriptase and 5µL RNase-free water (Promega) are then added to each sample. After this, samples were incubated at room temperature for 10 minutes, then at 37°C for 50 minutes. Samples were then incubated at 95°C for 10 minutes to denature the enzyme. cDNA was then diluted to 25ng/µL and stored at -20°C.

2.2.10 Real time quantitative polymerase chain reaction (RT-qPCR)

2.2.10.1 GeNorm assay

To determine the best housekeeping gene to use for RT-qPCR analysis we used a GeNorm assay kit (Primer Design). In brief, RT-qPCR assays for 13 of the most commonly used housekeeping genes were run on 10 samples each of SaOS-2, hBMSC and primary osteoblast cDNA. The housekeeping genes that were analysed were 18S, ACTB, ATP5B, B2M, CYC1, EIF4A2, GAPDH, RPL13A, SDHA, TOP1, UBC, YWHAZ and PPIA. For each 10µL reaction, 0.5µL primers (working concentration of 300µM), 5µL SYBR Green master mix, 0.5µL RNase free water and 25ng cDNA were added to 384-well plates and went through 50 cycles of 95°C for 10 minutes, 95°C for 15 seconds and 60°C for 60 seconds, at which point data was collected. Melt curve was also run to determine if any primer dimers were present. Analysis of RT-qPCR results identified 60S ribosomal protein L13a (RPL13A) as the best candidate to use as a housekeeping gene for each of the three different cell types.

2.2.10.2 TaqMan assays

Expression levels of ANRIL were determined through use of TaqMan assays from Applied Biosystems (Life Technologies Ltd). The two assays contained primers for ANRIL transcripts containing exons 1 and 2 (Hs04259476_m1) and exons 5 and 6 (Hs01390879_m1). Primers and probe for exons 18 and 19 were taken from Burd *et* al (238) and were supplied by Eurofins. The primers and probe for exons 18 and 19 were diluted to 100µM upon arrival and stored at -20°C. Positions for each RT-qPCR assay relative to ANRIL transcript exons are shown in Figure 2.3 and

RT-qPCR primer and probe information for custom exon 18-19 assay is shown in Table 2.6. Remainder of TaqMan assays used are shown in Materials.

Figure 2.3: Diagram of positions of (A) exon 1-2 RT-qPCR assay, (B) exon 5-6 RT-qPCR assay and (C) exon 18-19 RT-qPCR assay in relation to exons of ANRIL transcript. Diagram not to scale.

For each sample 100ng cDNA, 1µL 20x TaqMan Gene Expression Assay, 10µL 2x TaqMan Gene Expression Master Mix and 5µL RNase-free water was used, giving a reaction volume of 20µL for each set up. Primers and probes from Eurofins were diluted to 18µM and 5µM respectively and 1µL used per reaction. Each sample was measured in triplicate on a 96-well plate using the Step One Plus PCR machine (Applied Biosystems), with three negative template controls (NTCs) on each plate, where the cDNA was replaced with RNase free water.

Cycling conditions were: UNG incubation step of 50^{o}C for 2 minutes, polymerase activation step of 95^{o}C for 10 mins then 40 cycles of 95^{o}C for 15 seconds and annealing/extension at 60^{o}C for 1 minute. For each assay the standard curve method (100ng-0.78ng) was used to measure gene expression. All assays were normalised to RPL13A. All real time assays had previously been optimised either experimentally or commercially.

Primer Name	Primer Sequence (5' → 3')	Location
ANRIL 18F	AATGAGGCTGAGAGCATGGGAGATAC	ANRIL Exon 18 (238)
ANRIL 19R	GAGATATAGGTTCCAGTCCTGGTTCTG	ANRIL Exon 19 (238)
ANRIL 18/19 probe	/5HEX/TGTGTGTTTCCTTGTGAGCTACTGCA/ 3BHQ_2/	ANRIL 18/19 exon boundary (238)

Table 2.6: Custom real-time PCR primer and probe sequences

2.2.11 Fluorescence-activated cell sorting (FACS)

At 72hrs after transfection SaOS-2 cells were harvested for FACS analysis. Medium was aspirated into a FACS tube and cells were washed once with 1x PBS. This was then also aspirated in to the FACS tube and 0.25% trypsin EDTA added to each well. SaOS-2 cells were incubated at 37^{o}C until cells had detached from plate when FBS added to each well to inactive the trypsin EDTA. Cells were collected into the FACS tube and all tubes spun at 1000rpm for 5 minutes. Media then poured off, cells resuspended in 1mL 1x PBS and pelleted again at 1000rpm for 5

minutes. After 1x PBS poured off the SaOS-2 cells were resuspended in 300µL ice cold 1x PBS and then fixed by drop pipetting 700µL 100% ice cold ethanol into the FACS tube whilst vortexing. Cells were then stored at 4^{o}C for at least 2hrs, after which they were resuspended and spun for 5 minutes at 1000rpm. Ethanol was then aspirated and cell pellet resuspended in 1mL 1x PBS before being spun at 1000rpm for 5 minutes. 200µL propidium iodide staining mixture was made up for each sample containing 189µL 1x PBS, 10µL 20x propidium iodide and 1µL 200x RNase A. Once the PBS wash has been aspirated, cells were resuspended in 200µL of the propidium staining mixture and incubated at 37^{o}C in the dark for 30 minutes. After the incubation, tubes were placed on ice and then analysed on the flow cytometer.

5000 events were measured for forward and side scatter on FACScalibur® flow cytometer (Applied Biosystems) with the FL2 channel (258nm λ) and analysed using Cellquest™ software (Applied Biosystems). The number of cells in each stage of the cell cycle was analysed by selecting for live and dead cells and by setting markers to outline each stage of the cell cycle. The percentage of gated cells in each phase was then plotted on a graph. Figure 2.4 shows the different areas that were measured for each phase of the cell cycle.

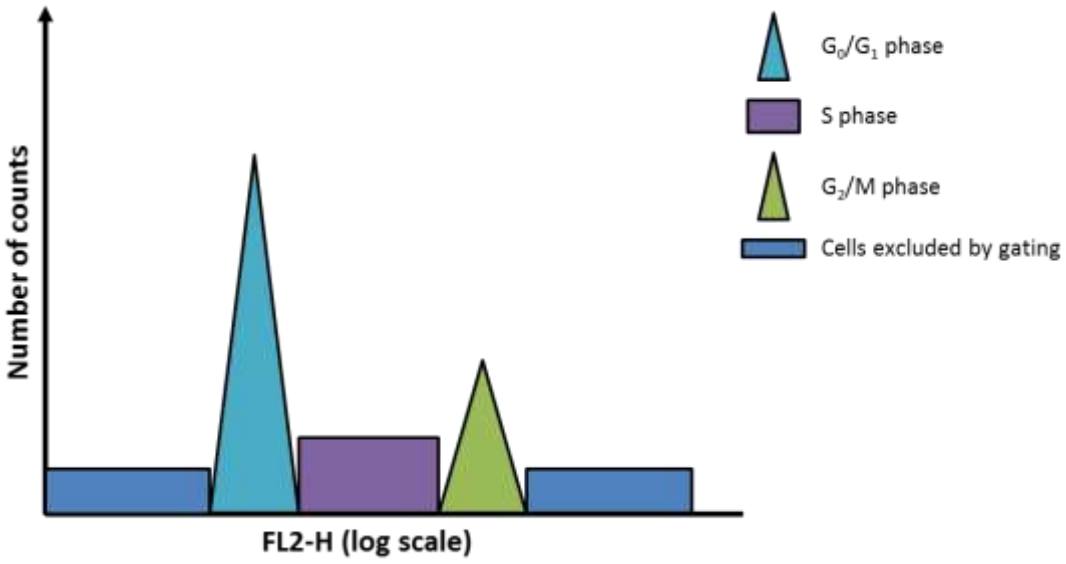

Figure 2.4: Scheme of flow cytometry scan showing the different areas measured for each phase of the cell cycle, which are then converted into graph form

2.2.12 Measuring methylation levels of MAVIDOS umbilical cord

2.2.12.2 Isolation of genomic DNA from umbilical cord tissue

DNA was isolated from umbilical cords which were collected as part of the MAVIDOS study. Umbilical cords were frozen within 24hrs of collection and stored at -80^{o}C long term. Samples were crushed, in the presence of liquid nitrogen, using metal pestle and mortar that had been cooled, and were not allowed to thaw during the crushing process.

500mg of crushed umbilical was measured into a gentleMACS™ homogenisation tube (Miltenyi Biotec) and 500µL of hyaluronidase solution (0.0125mg/mL) was added to the sample. Samples were centrifuged to 1000 rpm to ensure all tissue was fully immersed in hyaluronidase solution and then incubated for 30 minutes at 37°C with shaking (150rpm). After incubation, 500µL of TNES (50mM Tris, 400mM NaCl, 100mM EDTA, 0.5% SDS) was added to each sample and tapped to ensure mixing before homogenisation for 30 seconds on Xiril Dispomix Homogeniser. Samples were then pulse spun before the addition of 5µL of Proteinase K (20mg/mL), after which the umbilical cord was incubated overnight at 55°C.

After complete digestion of umbilical cord tissue, lysate was transferred into tubes, 500µL of 2.6M NaCl was added and samples were shaken vigorously for 15 seconds before being spun at 12,000 rpm for 20 minutes at room temperature. After centrifugation, the supernatant was transferred to a new tube and equal volume of ice cold 100% ethanol then added to each sample. Tubes were inverted to precipitate out DNA, which was then spooled, using a glass pipette, into 500µL of sterile water containing 5µL RNase A (10mg/mL). Care was taken to ensure excess ethanol was not transferred with the DNA. Samples were incubated at 37°C for at least 1 hour to ensure DNA had gone into solution, after which 500µL phenol/chloroform (50:50) was added to each sample. Samples were shaken and then centrifuged at 12,000 rpm for 5 minutes at room temperature. Supernatant (~400µL) was then transferred into a new tube and 400µL phenol/chloroform was added. Tubes were once again shaken and spun for 5 minutes at 12,000 rpm, after which supernatant (~300µL) was transferred into a fresh tube. Two volumes of ice cold 100% ethanol (600µL) and 30µL NaAc (3M, pH5.2) were then added to supernatant, tubes inverted to precipitate DNA and DNA then spooled into DNAse and RNAse free water. DNA was then quantified on Nanodrop 1000 and 250ng of DNA run on 0.8% agarose gel to check quality of extracted genomic DNA (Figure 2.5). All samples had a 260/280 ratio between 1.4 and 1.8 and all samples had yields between 10µg and 124µg. Any samples less than 40ng/µL were concentrated to allow for 1µg of DNA to be bisulphite converted. All samples were stored at -20°C.

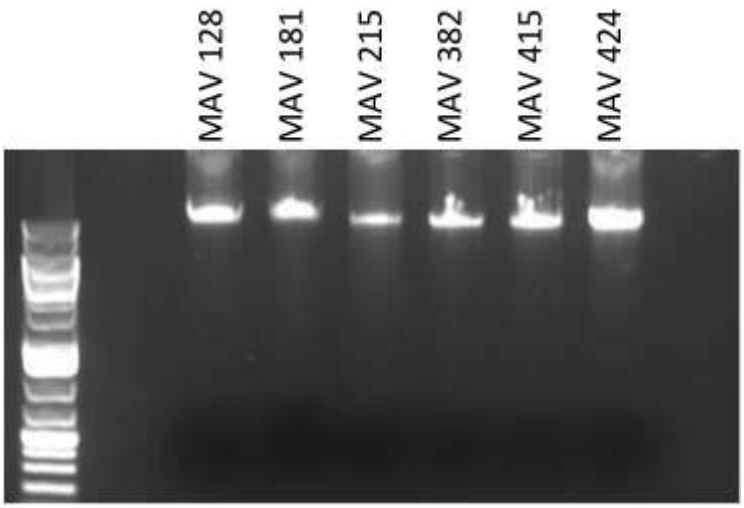

Figure 2.5: Example of MAVIDOS umbilical cord DNA run out on an agarose gel. 250ng of seven random MAVIDOS umbilical cord DNA samples run on a 0.8% agarose gel at 120V for 30 minutes. Samples were run to determine if DNA was of a good enough quality for bisulphite conversion.

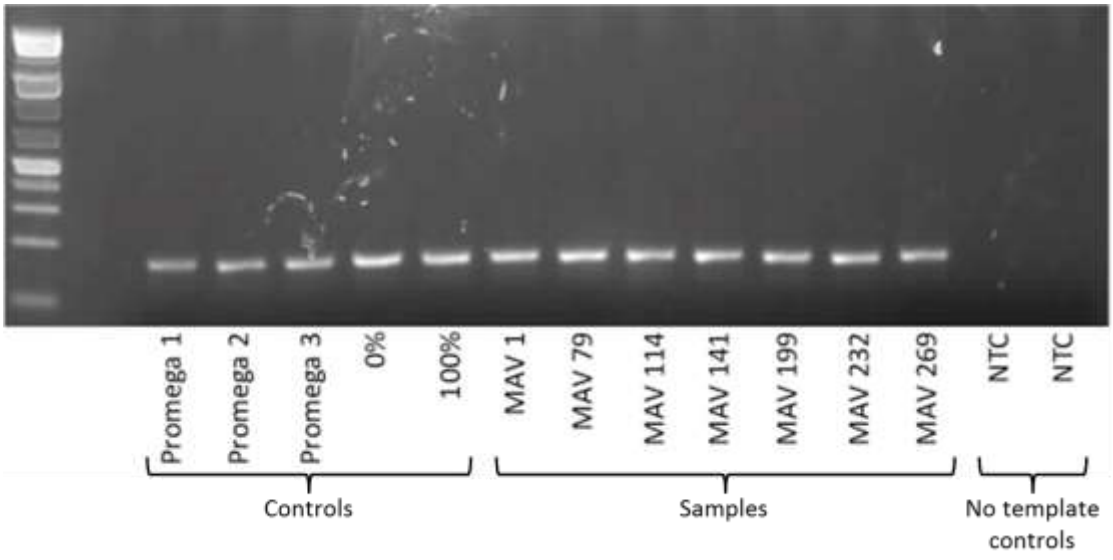

Figure 2.6: Example of pyrosequencing PCR product run on a 1.5% agarose gel at 120V for 20 minutes. 5µL of each sample was run on the gel. Seven random MAVIDOS umbilical cord PCR samples were run alongside the five control samples (Promega 1-3, 0% methylated DNA and 100% methylated DNA). Both NTCs were run to confirm that they hadn't been contaminated with DNA, and therefore the bands that are seen in the sample lanes are due to the amplification of the samples of interest, not foreign DNA.

2.2.12.3 Bisulphite conversion of genomic DNA

1µg of genomic DNA was bisulphite converted using the EZ DNA Methylation-Gold™ kit (Cambridge Biosciences) according to manufacturer's instructions. In brief, Each sample was eluted in 30µL of DNase and RNase free water. Each plate of MAVIDOS samples also contained controls to allow for inter and intra plate validation. Controls included unmethylated DNA (Qiagen), 100% methylated DNA (Merck Millipore), human genomic DNA (Promega) that was run in triplicate and no template controls run in duplicate, where DNA was replaced with 20µL water.

2.2.12.4 Polymerase chain reaction (PCR)

Polymerase chain reaction was used to amplify MAVIDOS bisulphite converted DNA for each of the regions of interest within different genes. The forward and reverse primers used for each PCR are shown in Table 2.7. 4µL of bisulphite converted DNA was added to a master mix containing the components shown in Table 2.6 to make up a 50µL reaction. Samples were then amplified using the conditions detailed in Table 2.7. The specific temperatures used for the PCR reaction for each gene are shown in Table 2.8. To confirm the product size and DNA amplification, 5µL of each of the controls and a random selection of seven MAVIDOS samples were run on a 1.5% agarose gel at 120V for 20 minutes (Figure 2.6).

Component	Volume (µL)
10x Qiagen Buffer	5.00
dNTPs (10mM)	1.00
Forward Primer (10µM)	1.00
Reverse Primer (10µM)	1.00
Qiagen HotStar Taq (5ng/µL)	0.25
RNase-free water	37.75
DNA (50ng total)	4.00
TOTAL	**50.00**

95°C 5 minutes
95°C 30 seconds
45-60°C 30 seconds } 45 cycles
72°C 1 minute
72°C 10 minutes
4°C ∞

Table 2.7: Components and conditions used for pyrosequencing PCR

Assay Name	Forward Primer (5'-3')	Reverse Primer (3'-5')	Biotin tag?	Annealing Temperature °C	Product size (bp)
CDKN2A **CpG -769 to -796**	AGTAGGAAAGGTGTATTTTAAGTATATTT	TATCTCACCAATCCTCCACTCTCCTAAA	Reverse	57.6	154
CDKN2A **CpG -836 to -907**	TGGGGAGAATTATTGTTAATTATTTAAGTT	AAAAACCCATTTCCCTATTAACTACA	Reverse	57.6	236
RXRA **CpG -2686 to -2642**	TGGGAAGGTTGAAGGTTTTAGAA	AACACAAAAACTAAATATAAACCCAAATCT	Reverse	60.0	139
RXRA **CpG -2406 to -2357**	TGGGATTATTGGTTTTTGAGTTAGGT	CCCACTATTAAAAAATAACCTCAAACACTT	Forward	60.0	194
RXRA **CpG -2357 to -2346**	TTTTAGGGATAAGGAGTGAGATGG	CCAACCAAAAAACTCAAACAACTT	Reverse	60.0	274
NOS3 **CpG -3434**	GGGAGTTTTTTAGTTGGGGAGTAG	ACAAACCCCTACCACTACCAAAAT	Forward	60.0	176

Table 2.8: PCR forward and reverse primers for pyrosequencing

2.2.12.5 Pyrosequencing

The methylation of individual CpG sites was determined by pyrosequencing. 10µL of each PCR product was aliquoted into a fresh 96-well plate and immobilised using a binding master mix containing 38µL binding buffer (Qiagen), 2µL sepharose streptavidin beads (Fisher Scientific) and 30µL ultrapure water per sample. Plates were sealed and after 5 minutes on a plate shaker, samples were washed, denatured and released into annealing buffer (Qiagen) containing the appropriate sequencing primer at 10µM (Table 2.9). Pyrosequencing was carried out using PyroMark Gold Q96 Reagents (Qiagen) on a PyroMark Q96 MD Pyrosequencer (Qiagen). The percentage methylation was calculated using PyroMark CpG software 1.0.11 (Qiagen).

Assay Name	Sequencing Primer (5'-3')	Direction	Sample Pass Rate
CDKN2A **CpG -769 to -796**	AGAATTATTGTTAATTATTTAAGTT	Forward	87%
CDKN2A **CpG -836 to -861**	TAGGAGAGTGGAGGA	Forward	81%
CDKN2A **CpG -887 to -907**	GTAGGTAGAGATTTTTTGAAATGT	Forward	92%
RXRA **CpG -2686 to -2673**	GTTATTTTTTGTTTTAGAGAT	Forward	81%
RXRA **CpG -2649 and -2642**	AGAAGGGTTTTTTGTTTTTAA	Forward	99%
RXRA **CpG -2406 to -2385**	CCCAACCTTCCCACC	Reverse	99%
RXRA **CpG -2357**	CCTACTACTCCTTCTCT	Reverse	99%
RXRA **CpG -2357 to -2346**	GTTGTTTTTTTTTTTTGTAG	Forward	65%
NOS3 **CpG -3434**	ATCTTAAATTTCCAAATCAC	Reverse	99%

Table 2.9: Sequencing primers for pyrosequencing

2.2.13 Statistical analysis

2.2.13.1 Statistical analysis of siRNA transfected cells

Statistical analyses were performed using IBM SPSS Statistics version 22.0. An independent *t*-test was used to determine if there were statistically significant differences between the means of each of the siRNA transfected cells and the 'scrambled' control.

2.2.13.2 Statistical analysis of MAVIDOS cohort

Statistical analyses were performed using IBM SPSS Statistics version 22.0. Where appropriate, the data was transformed when the methylation or phenotypic outcomes were not normally distributed. The methylation of each CpG loci was the independent variable and the

phenotypic outcome was the dependent variable when determining the association between methylation of each CpG and total BMC, total BA, total BMD and total prentice BMC at birth. The statistical model was corrected for gestational age, sex and age at time of DXA when using linear regression.

When determining if there were statistically significant differences between the mean methylation of the placebo and vitamin D supplemented groups, a Mann-Whitney U test was used in the case of *CDKN2A* as all methylation measurements were not normally distributed. In the case of *RXRA*, where appropriate, methylation data was transformed so that it was normally distributed and an in independent *t*-test was used to determine if there were statistical differences between the mean methylation across the two groups.

Chapter 3

Identification of *CDKN2A* as a Predictive Marker of Bone Mineral Density

3.1 Introduction

Recent methylation association studies by Harvey *et al* (205,234) have shown that methylation of specific CpG loci in umbilical cord DNA at birth is predictive of BMC outcomes in later childhood. They found that percentage methylation of 2 CpGs in the *NOS3* promoter in umbilical cord had a significant positive association with offspring whole-body BA, BMC and aBMD at nine years of age (234), while there was a significant negative association between the methylation of 4 CpG sites within the promoter of *RXRA* in umbilical cord and bone mineral content at 4 years of age (205).

To identify further methylation differences at birth which are associated with bone outcomes in childhood, a discovery MDB-array was performed on umbilical cord DNA samples from 21 subjects from the SWS cohort, who were selected as they represented a range of bone mineral contents at 6 years of age (Garratt, unpublished data). This identified a significant association between the methylation of a 300bp region within the *CDKN2A* gene locus at birth and offspring bone outcomes at 6 years (Section 1.5). These associations were then validated by pyrosequencing in a larger subset of SWS subjects (n=292), where a significant negative association was observed between the methylation of the nine CpG loci within the 300bp differentially methylated region (DMR) of *CDKN2A* at birth and offspring BA, BMC and aBMD at both 4 and 6 years of age, consistent with the findings from the MBD array.

3.1.1 *CDKN2A* gene locus

This *CDKN2A* gene locus, which covers 35kb, is found on chromosome 9p21 and encodes for two cell cycle inhibitors – $p16^{INK4A}$ and $p14^{ARF}$, both of which have been shown to have a role in cellular senescence (239). *CDKN2A* also produces an anti-sense transcript, a long non-coding RNA called ANRIL (antisense non-coding RNA in the INK4 locus), the function of which has not been fully elucidated. $p16^{INK4A}$ binds to CDK4 and 6 and blocks cell cycle progression by preventing the phosphorylation of Rb, causing G_1 arrest (240). $p14^{ARF}$, which shares the same exon 3 as $p16^{INK4A}$, binds to murine double minute-2 (MDM2) protein to inactivate it (241). MDM2 is a p53 negative regulator encoded by p53-responsive gene and this inactivation triggers a p53-dependent programme that can lead to either G_1 phase arrest or apoptosis. Inactivation of this protein also prevents p53 turnover as E3 ubiquitinase activity of MDM2 is also inhibited. Downstream to the *CDKN2A* locus is *CDKN2B*, which encodes for $p15^{INK4B}$, a cyclin dependent kinase (CDK) inhibitor that prevents cell cycle progression by binding to CDK 4 and 6. ANRIL has been shown to suppress both $p16^{INK4A}$ and $p15^{INK4B}$ expression by either acting as a scaffold for the recruitment of Polycomb repressive complexes (PRC) 1 and 2 (242,243) or by functioning as an antisense transcript repressing $p15^{INK2B}$ expression. Figure 3.1 shows a diagrammatic representation of the

CDKN2A/B locus and the 300bp DMR containing the 9 CpGs in yellow, with Table 3.1 showing the position of each CpG relative to the *CDKN2A* transcription start site (TSS).

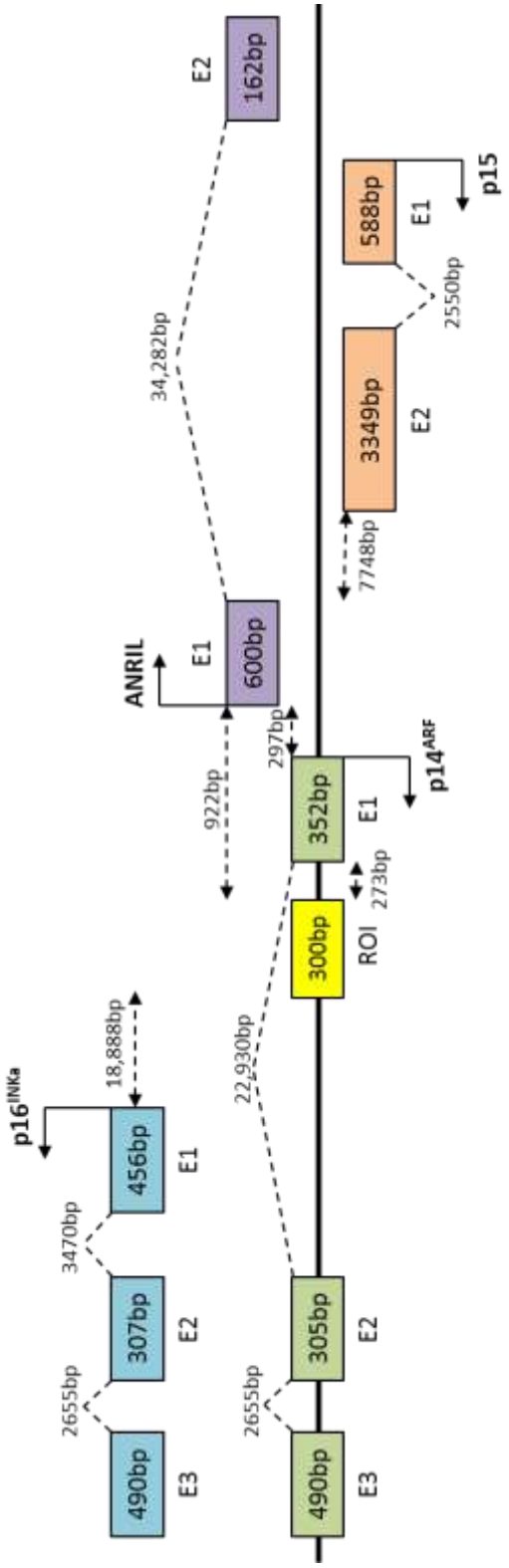

Figure 3.1: Layout of *CDKN2A/B* locus with position of the DMR within the locus highlighted in yellow. *CDKN2A/B* gene locus encodes for four transcripts: $p16^{INK4A}$ and $p14^{ARF}$ from the *CDKN2A* gene and $p15^{INK4B}$ and ANRIL, a long non-coding RNA, from the CDKN2B gene. $P16^{INK4A}$, $p14^{ARF}$ and $p15^{INK4B}$ are all cyclin dependent kinase inhibitors and have a role in regulating cell cycle. The DMR highlighted in yellow is located within intron 1 of $p14^{ARF}$ and 922bp upstream of the ANRIL transcription start site. Note that diagram is not to scale.

CpG in DMR	Base pairs from CDKN2A TSS
1	-769
2	-793
3	-796
4	-836
5	-845
6	-852
7	-861
8	-887
9	-907

Table 3.1: The 9 CpGs in the differentially methylated region (DMR) of the *CDKN2A* locus and their positions relative to the *ANRIL* transcription start site (TSS).

The *CDKN2A* locus, and its products $p16^{INK4A}$ and $p14^{ARF}$, play a key role in cellular senescence and aging (244). $p16^{INK4A}$ expression significantly increases in many tissues with aging. This observation was first noted by Sherr and colleagues in 1997 (245) and was later confirmed by several independent groups (245–247). It has since led to the proposal by Krishnamurthy *et al* that expression of $p16^{INK4A}$ could be used as a biomarker for aging (239). There have been various animal studies looking at the decline in replicative potential of self-renewing cells that show both an age-related increase in $p16^{INK4A}$ expression and that cell proliferation seems to be CDK4/6 dependent (246,248,249). These studies suggest that $p16^{INK4A}$ promotes aging by decreasing proliferation potential and self-renewal, causing the cells to become senescent. However, $p16^{INK4A}$ deficiency only partially diminished the age-induced decrease in proliferation but did not completely remove the effects of aging suggesting that other proteins may also have a role in cellular aging and senescence.

Recent GWAS have demonstrated that the *CDKN2A*/*B* locus is a hotspot for disease-associated polymorphisms, with the majority of the SNPs locating to the gene that encodes ANRIL, *CDKN2B-AS*. SNPs within this gene have been linked to frailty (250), T2D (251), Alzheimer's disease (252) and CVD, with the SNP associated with CVD being highlighted as the strongest susceptibility locus for this disease (251).

3.2 Aims

Given the associations between *CDKN2A* DMR methylation at birth and measures of bone mineral content and density in later childhood, the aim of this chapter was to investigate the functional relevance of differential DMR methylation within the *CDKN2A* locus by i) determining the effect of mutagenesis of each of the CpG sites within the DMR on ANRIL and $p14^{ARF}$ expression through luciferase reporter constructs, ii) determining, through the use of electrophoretic mobility shift assays, if proteins bind to this region within an osteoblast-like cell line, iii) establishing whether CpG methylation alters protein binding to specific loci within the DMR and iv) elucidating what proteins bind to this region.

3.3 Results

3.3.1 Does the DMR control *CDKN2A* expression?

As the DMR identified within the *CDKN2A* gene is located 922bp upstream of the ANRIL transcription start site and within the first intron of $p14^{ARF}$, the role that the CpG sequences within the DMR play in the regulation of ANRIL and $p14^{ARF}$ expression was investigated. The role of these CpGs on $p16^{INK2A}$ was not investigated, as the *CDKN2A* DMR is located >16,000bp upstream from the transcription start site of this trasnscript. To test this, the promoter region of ANRIL (-1281bp to +20bp relative to TSS) and the 5' region of the $p14^{ARF}$ gene (-500bp to +1125bp relative to TSS) were fused to the firefly luciferase reporter gene in the pGL3-Basic vector, and each of the individual CpG sites within the DMR were mutated, before co-transfection into the human osteosarcoma cell line, SaOS-2 cells. Mutated plasmids were transfected along with a control pGL CMV Renilla plasmid. The level of firefly luciferase activity was normalised to the Renilla luciferase activity to remove any variability between samples caused by pipetting error, differences in transfection efficiencies and difference in cell number.

The mutation of the individual CpG sites led to a decrease in ANRIL promoter activity ($p<0.022$ for all CpGs), apart from CpGs -769 and -907, where no significant change in the ANRIL promoter activity was seen (Figure 3.2A). With regards to $p14^{ARF}$ promoter activity, mutation of CpGs -793, -796 and -845 caused a significant decrease in activity ($p<0.0072$ for all) when compared to the control, whereas mutation of CpG sites -852, -861, -887 and -907 led to increase in promoter activity ($p<0.035$ for all) (Figure 3.2B). The mutation of CpGs -769 and -836 did not cause a significant change in $p14^{ARF}$ promoter activity when compared to control.

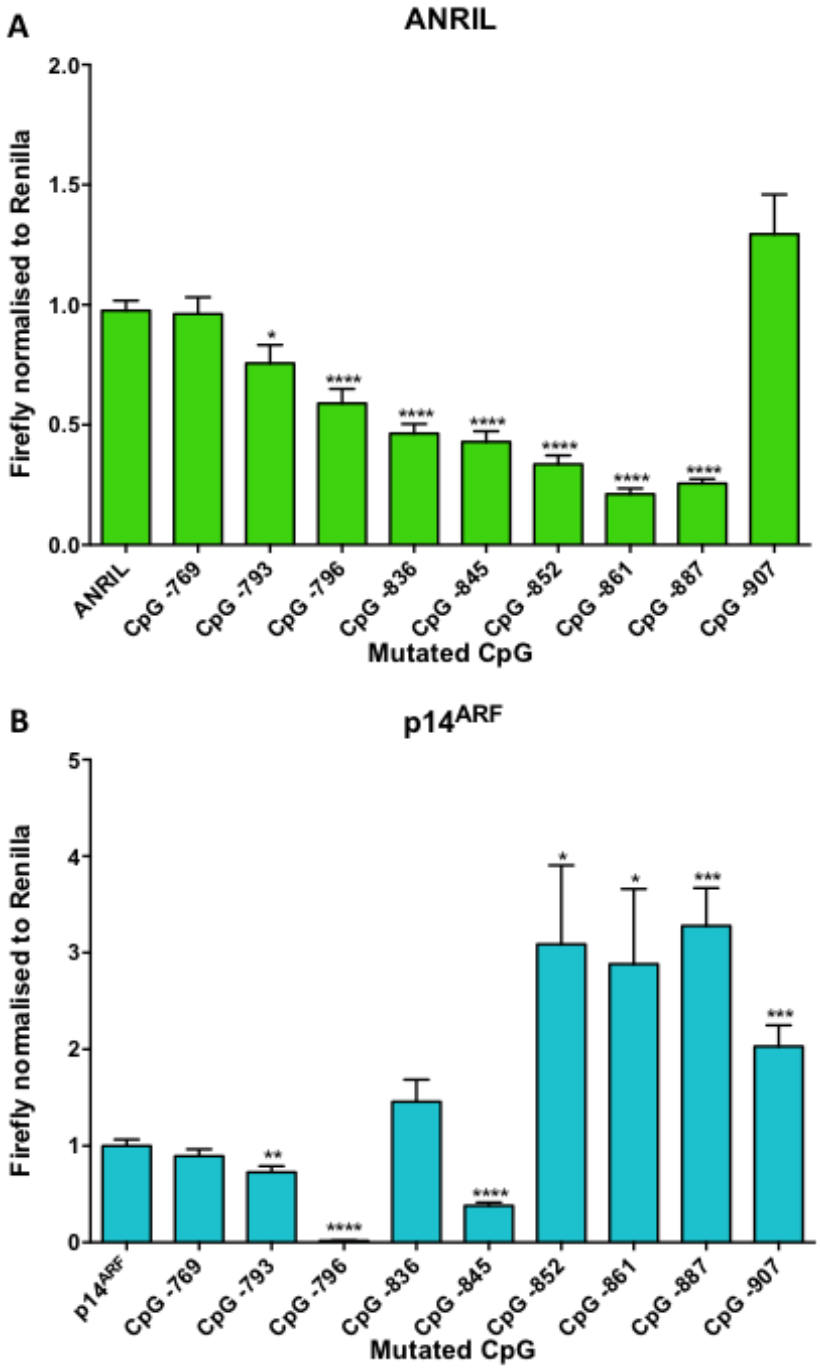

Figure 3.2: Promoter activity of ANRIL (A) and p14^{ARF} (B) relative to normal promoter activity when individual CpG sites within the DMR are mutated. (A) Mutation of all CpG sites, apart from CpGs -769 and -907 cause a significant decrease in ANRIL promoter activity when compared to control. (B) p14^{ARF} promoter activity significantly decreases when CpGs -793, -796 and -845 are mutated and increases when CpGs -852 to -907 are mutated within the DMR. Mutation of CpGs -769 and -836 do not cause a significant change in p14^{ARF} promoter activity. (****p≤0.0001; ***p≤0.001; **p≤0.01; *p≤0.05) (n=2)

3.3.2 Is there specific binding to the CpGs within the *CDKN2A* DMR in bone cells?

Having shown that a number of the CpG sites within the DMR are important in the regulation of ANRIL and/or $p14^{ARF}$ promoter activity, electrophoretic mobility shift assays (EMSAs) were then used to determine what transcription factors bound to this sequence in SaOS-2 cells and whether this binding was affected by methylation. Moreover, in order to look at tissue specific differences in binding across the DMR, we also compared protein binding in the liposarcoma cell line SW-872, an adipose derived cell line. Nuclear extracts from SaOS-2 cells were incubated with five P^{-32} radiolabelled double-stranded oligonucleotide probes. The five probes, approximately 40bp in length, covered CpG -769, CpGs -793 and -796, CpGs -836 to -861, CpGs -887 and -907 and CpG -907 respectively (see Figure 3.3 for sequences covered by individual probes). Binding to this region was analysed across five probes as binding to larger DNA fragments makes the identification of individual protein complexes much harder to detect and distinguish. Results described below were consistent across three independent experiments.

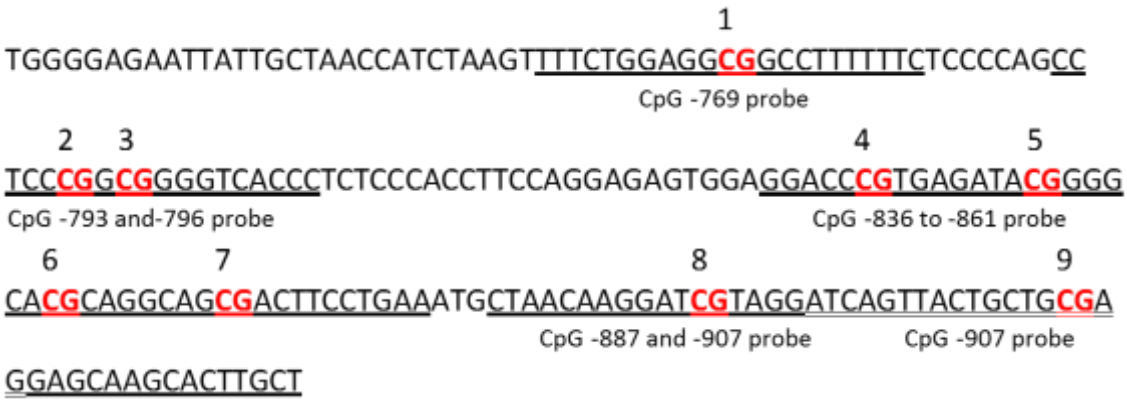

Figure 3.3: Location of EMSA probes on DMR sequence within *CDKN2A* locus. Probe sequences are underlined. Sequence that has a double underline is where the probes containing CpGs -887 and -907 and CpG -907 only overlap.

Specific protein binding was observed to two of the five of the oligonucleotide probes in SaOS-2 cells. There were three protein complexes bound to the oligonucleotide probe containing CpG -769 (Figure 3.3A), which were bound out by the addition of a 500-fold excess of an unlabelled specific competitor probe. Complex 1 and 4 bound very strongly, while complex 3 showed much weaker binding. One protein complex was also observed binding to the oligonucleotide probe containing CpGs -887 and -907 (Figure 3.3D), which was competed out by the addition of an excess of specific competitor. Protein binding to the oligonucleotide probes containing CpGs -793 to -796 (Figure 3.3B), CpGs -836 to -861 (Figure 3.3C) and CpG -907 (Figure 3.3E) was also observed, although this binding was not competed out by a 500-fold excess of specific competitor, suggesting that the binding is non-specific.

There were also cell type specific differences in the binding across the different probes in the osteosarcoma cell line compared to SW872, a liposarcoma cell line. Three protein complexes were seen binding to the probe containing CpG -769 in both SaOS-2 and SW-872 cells, however although the 2 fastest migrating complexes were common to SaOS-2 and SW-872 cells, the slowest migrating complexes were unique to the specific cell type (Figure 3.3A).

One protein complex specific to liposarcoma cells was seen binding across CpGs -793 to -796, which was competed out by an excess of specific competitor. A faster migrating protein complex was seen in both SaOS-2 and SW-872 cells but this was not competed out by the addition of a specific competitor in either cell type (Figure 3.3B). Three specific protein complexes bound to the probe containing CpGs -836 to -861 in liposarcoma cells (Figure 3.3C), whereas no bands of equivalent mobility were seen in SaOS-2 cells. A lower band was observed in both SaOS-2 and SW-872 cells but a specific competitor in either cell line did not compete this band out. In contrast, a similar size complex was seen binding to the probes containing CpGs -887 and -907, or CpG -907 alone (Figures 3.3D and E respectively), in both liposarcoma and osteosarcoma cells, although binding to the probe containing just CpG -907 was extremely weak suggesting a weaker interaction between the probe and the protein complex when the CpG site -887 is absent.

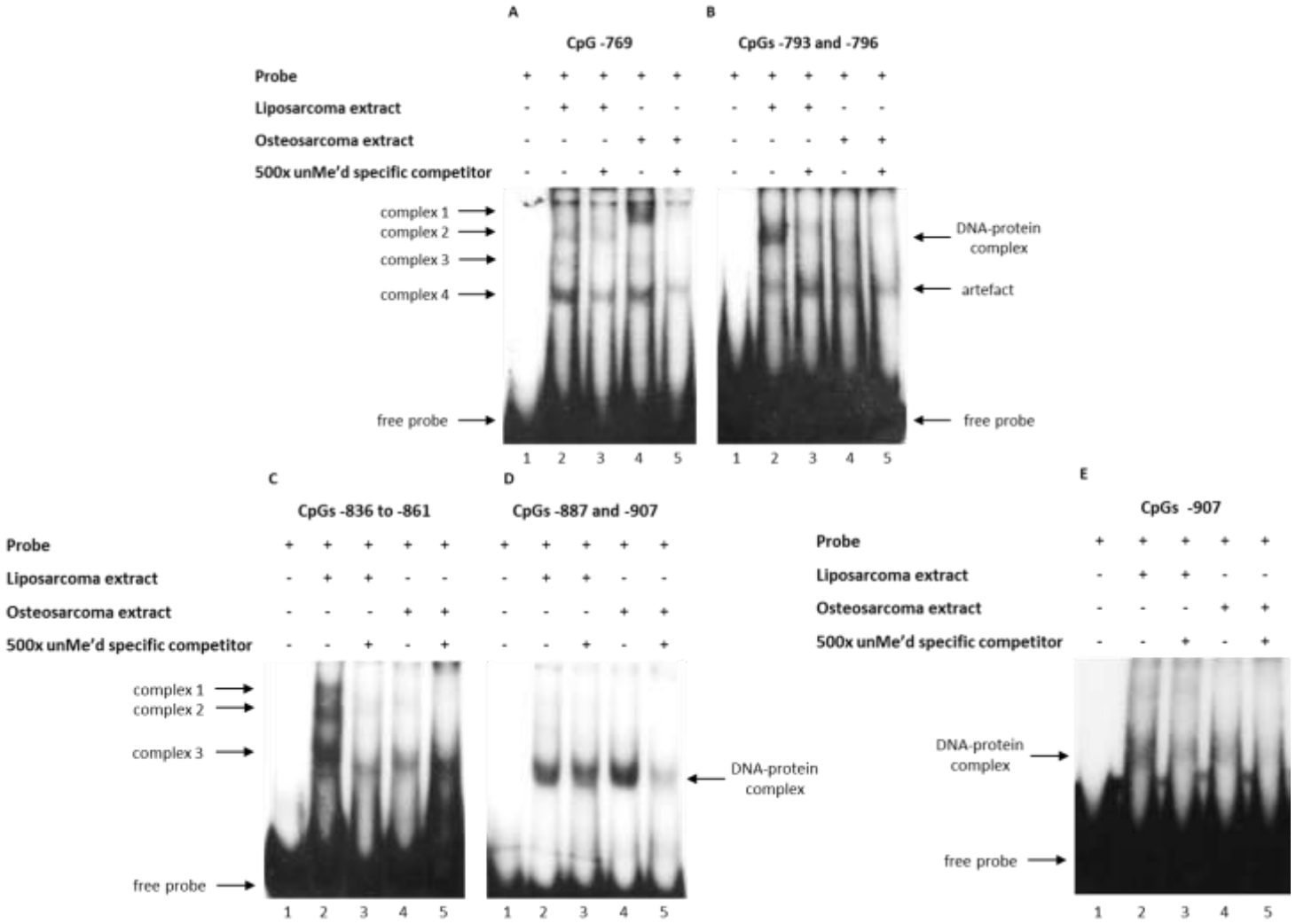

Figure 3.4: Testing the specificity of protein binding of liposarcoma and osteosarcoma cell lines to **(A)** CpG -769, **(B)** CpGs -793 and -796, **(C)** CpGs -836 to -861, **(D)** CpGs -887 and -907 and **(E)** CpG -907 probes (n=3). Liposarcoma (lane 2) and osteosarcoma (lane 4) nuclear extract were incubated with a radiolabelled probe specific for the CpGs within the DMR. The retarded DNA-protein complexes and the remaining free probe are indicated by the arrows. These complexes were then competed out by unlabelled probe at 500x excess (lanes 3 and 5). Radiolabelled probe was also run on its own to confirm probe was not contaminated with protein, i.e. no band present (lane 1).

3.3.3 Does the methylation of CpGs -887 and -907 in the *CDKN2A* DMR alter the binding of transcription factors?

As strong binding to CpGs -887 and -907 was observed and these CpGs were previously shown to be strongly associated with bone mineral content (unpublished data), EMSAs were then used to determine whether differential methylation of these CpGs altered transcription factor binding to this sequence within SaOS-2 cells.

Firstly, the unmethylated radiolabelled probe was incubated with osteosarcoma nuclear extract along with 100-, 250- or 500-fold excess of either the unmethylated or methylated unlabelled specific competitor, where both cytosines within the CpGs at -887 and -907 were methylated. Binding to the unmethylated radiolabelled probe was reduced in the presence of both 250-fold and 500-fold excess of unlabelled unmethylated specific competitor (Figure 3.4A) but not in the presence of 100-fold excess unmethylated specific competitor. In contrast, binding to the radiolabelled probe was not reduced in the presence of 100- or 250-fold excess of unlabelled methylated specific competitor, binding was only effectively competed out with a 500-fold excess of unlabelled methylated competitor.

Reciprocal EMSAs were also run using radiolabelled methylated probe to confirm whether there is preferential binding to unmethylated DNA over methylated DNA. Consistent with the previous results, binding to the methylated sequence was effectively competed out in the presence of 250- and 500-fold excess of unmethylated specific competitor, however, with methylated specific competitor, only 500-fold excess of unlabelled probe was able to reduce binding (Figure 3.4B).

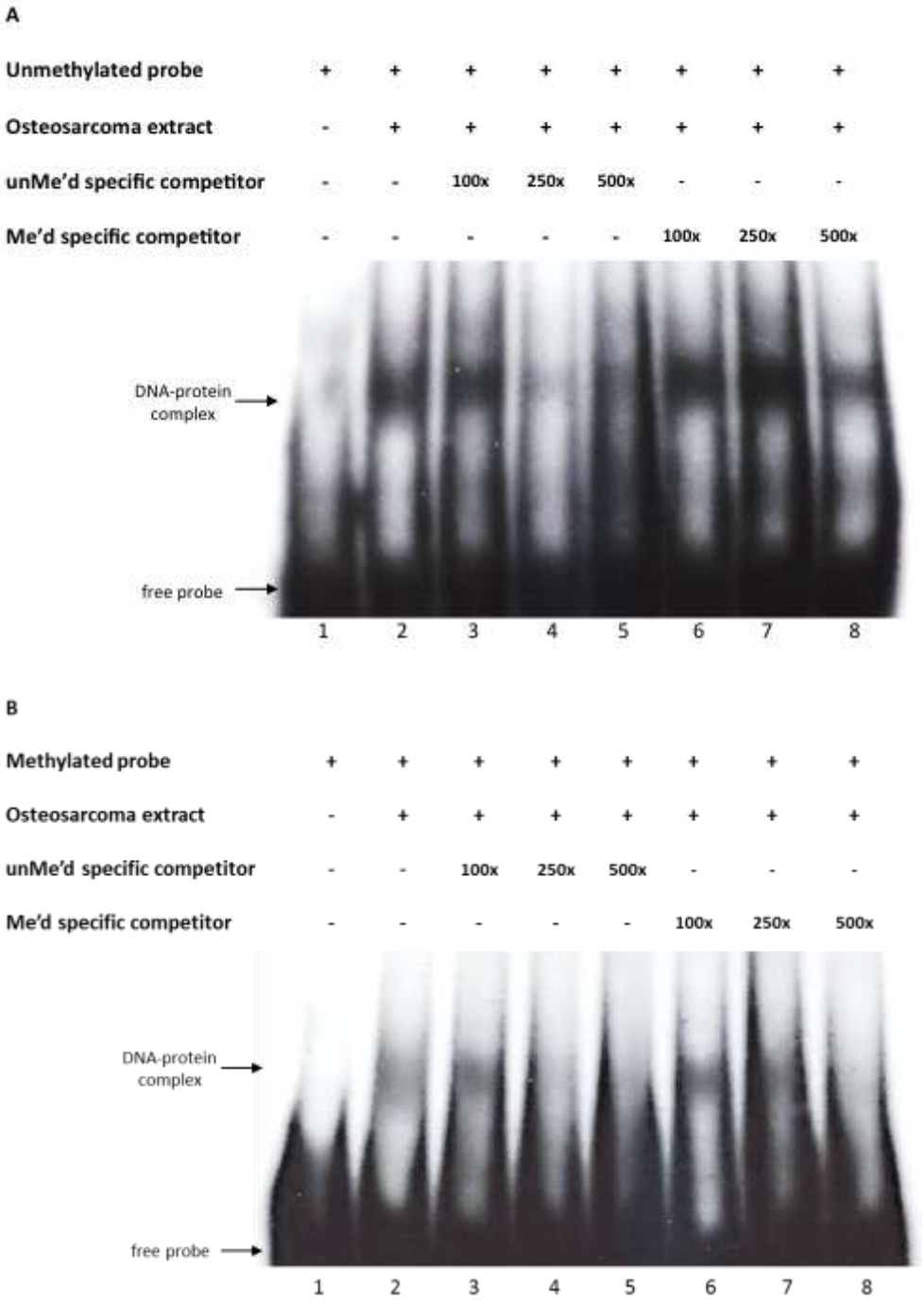

Figure 3.5: Testing the preference of protein binding to unmethylated and methylated radiolabelled CpG -887 and -907 (n=3). Osteosarcoma nuclear extract was incubated with unmethylated **(A)** or methylated **(B)** radiolabelled probe specific for CpGs -887 and -907 and three different concentrations of unmethylated and methylated specific competitor. The retarded DNA-protein complexes and the remaining free probe are indicated by the arrows. This complex (lane 2) was then competed out by unlabelled unmethylated probe at 100x (lane 3), 250x (lane 4) and 500x excess (lane 5) and methylated competitor also at 100x (lane 6), 250x (lane 7) and 500x excess (lane 8). Radiolabelled probe was also run on its own to confirm probe was not contaminated with protein, i.e. no band present (lane 1).

To confirm that both unmethylated and methylated sequences were binding the same protein complex, EMSAs containing the methylated and unmethylated probes were run alongside each other. Results demonstrate that upon incubation of osteosarcoma extract with methylated and unmethylated radiolabelled probe (Figure 3.5) a retarded DNA-protein complex of similar mobility was seen.

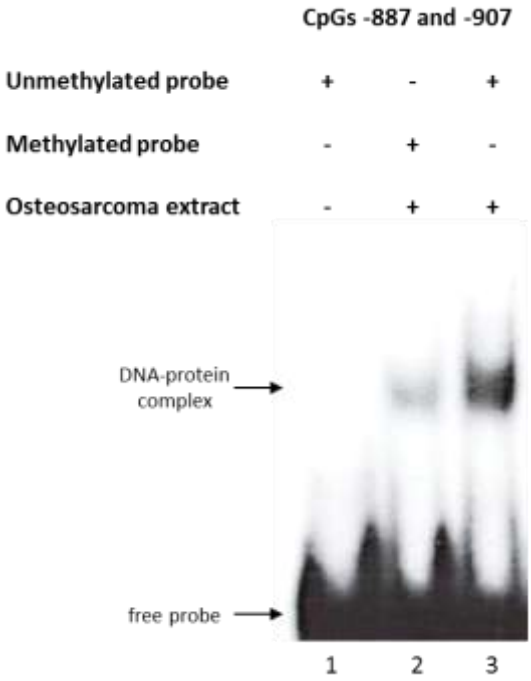

Figure 3.6: Both the unmethylated and the methylated radiolabelled CpGs -887 and -907 probes bind to the same protein complex (n=3). Osteosarcoma nuclear extract was incubated with an unmethylated (lane 2) or a methylated (lane 3) radiolabelled probe specific for CpGs -887 and -907. The retarded DNA-protein complexes and the remaining free probe are indicated by the arrows. Radiolabelled probe was also run on its own to confirm probe was not contaminated with protein (lane 1).

3.3.4 What transcription factors bind to CpGs -887 and -907?

Multiplexed competitor EMSAs (253) were used to investigate what transcription factors bind across CpGs -887 and -907 within the *CDKN2A* DMR in the osteosarcoma cell line SaOS-2. SaOS-2 nuclear extract was incubated with the unmethylated probe containing CpGs -887 and -907 along with a 500-fold excess of eight 'cocktails', each of which contained ten or eleven unlabelled oligonucleotides for different transcription factor binding site consensus sequences.

Figure 3.6 shows that binding to the unmethylated radiolabelled probe containing CpGs -887 and -907 is reduced in the presence of three of the transcription factor cocktails, namely cocktails 2, 5 and 8. This was consistent across three independent experiments.

Table 3.2 lists the transcription factor consensus sequences in each of these three cocktails.

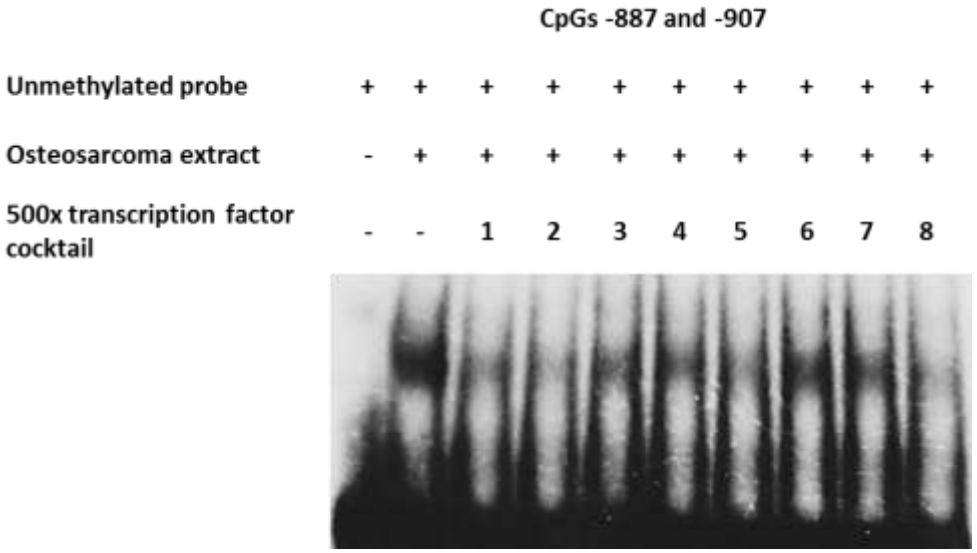

Figure 3.7: Transcription factor competition with radiolabelled unmethylated CpGs -887 and -907 probe (n=3). Cocktails containing 500-fold excess of different transcription factor consensus sequences were incubated with CpG -887 and -907 probe and SaOS-2 extract.

TRANSCRIPTION FACTOR COCKTAILS			
Cocktail 1	**Cocktail 2**	**Cocktail 3**	**Cocktail 4**
AP1	E2F1	HIF1a	NFATc
AP2a	Egr	Sox2	NFkB
AR	ER	HNF4	NR5A2
Brn3	Ets	IRF1	OCT1
CBP	Ets1	MEF1	p53
CDP	FAST1	MEF2	Pax5
CEBP	GAS	MIBP1	Pbx1
cMyb	GATA	MycMax	Pit1
CREB	Gfi1	NF1	PPAR
CTCF	GR	NFE2	PR
Cocktail 5	**Cocktail 6**	**Cocktail 7**	**Cocktail 8**
RAR	Stat4	VDR	NRF1
RXR	Stat5	YY1	PAX3
SIE	Stat5/6	ZEB	Mash1
Smad	Tbet	HNF1	Maf
Smad3/4	TFE3	ARP1	MyoD
Smuc	TFEB	NFY	Oct4
Sp1	TFIID	HNF3	GABPA
SRE	TGIF	BARP	NR4a2
Stat1	TR	SREBP1	TCF4
Stat3	USF1	HSF1	Zic
			Sox2

Table 3.2: List of transcription factor consensus sequences that are present in their respective cocktail.

To determine which specific transcription factor may be binding to the CpG -887 and -907 unmethylated probe, osteosarcoma extract was incubated with 500-fold excess of each of the individual transcription factor consensus sequences from cocktails 2, 5 and 8. As shown in Figure 3.7 addition of a 500-fold excess of the gamma activated site (GAS) and Smad3/4 consensus binding sequence effectively reduced binding to this sequence.

Consensus sequences for the gamma activated site (GAS) and the binding site of the Smad3/4 complex are shown in Table 3.3. There are some similarities between the CpG -887 and -907 containing probe and both the consensus sequences.

Sequence	5'-3'
CpG -887 and -907 probe	CTAACAAGGATCGTAGGATCAGTTACTGCTGCGAG
GAS	AAGTACTTTCAGTTTCATATTACTCTA
CpG -887 and -907 probe	CTAACAAGGATCGTAGGATCAGTTACTGCTGCGAG
Smad3/4	TCGAGAGCCAGACAAAAAGCCAGACATTTAGCCAGACAC

Table 3.3: CpG -887 and -907 probe, GAS and Smad3/4 consensus sequences. CpG sites are highlighted in red and bold. Core binding sequences for GAS and Smad3/4 complex are underlined. The sequence similarities between the CpG -887 and -907 probe and GAS consensus sequence are highlighted in blue and the sequence similarities between the CpG -887 and -907 probe and Smad3/4 consensus sequence are highlighted in purple.

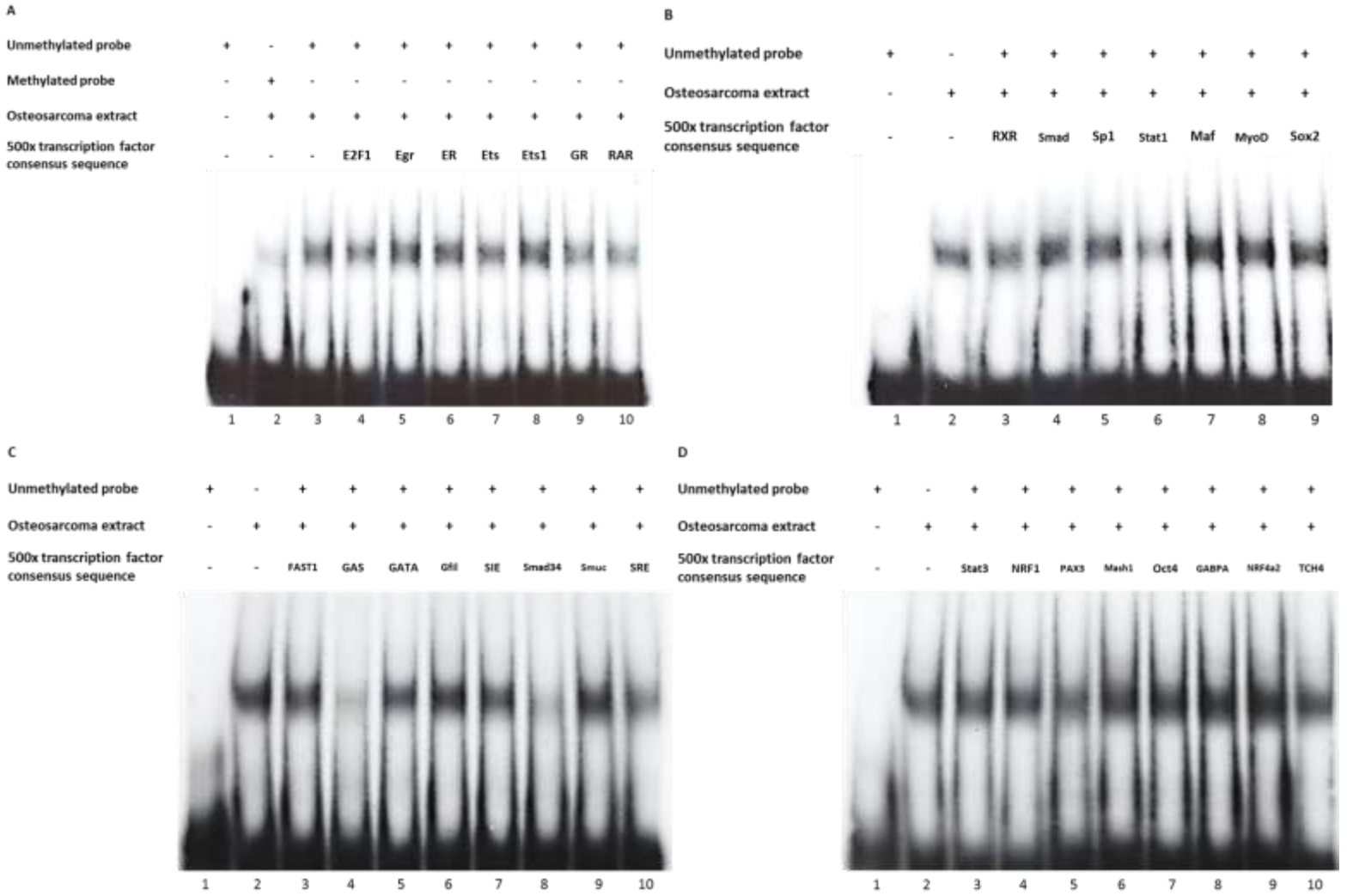

Figure 3.8: Transcription factor consensus sequence competition with CpG -887 and -907 probe (n=3). 500-fold excess of each transcription factor consensus sequence found in each transcription factor cocktail was incubated with radiolabelled unmethylated CpG -887 and -907 probe and SaOS-2 extract. Transcription factor consensus sequences shown above are the ones that were found to have a relationship to bone homeostasis from a literature search **(A-B)** and those that have not previously been shown to have a role in bone homeostasis **(C-D)**.

3.4 Discussion

As the DMR associated with the *CDKN2A* gene locus was found within intron 1 of $p14^{ARF}$ and 922bp upstream of the ANRIL transcription start site, we investigated whether the CpGs within this 300bp region were important for the regulation of $p14^{ARF}$ and/or ANRIL expression in the osteosarcoma cell line SaOS-2. Interestingly mutagenesis of the individual CpGs within the DMR had different effects on ANRIL and $p14^{ARF}$ promoter activity. Mutation of CpGs -793 to -887 within the ANRIL construct led to a decrease in promoter activity, however, mutation of CpG -763 and -907 had no effect, suggesting that the CpG sites within the DMR may be differentially regulated but that seven of the nine CpG sites within the DMR are important in regulating the level of ANRIL promoter activity. Mutation of the CpGs within the $p14^{ARF}$ construct had a range of effects; when CpGs -793, -796 and -845 are mutated within this region this caused a decrease in $p14^{ARF}$ promoter activity, whereas the mutation of CpGs -852, -861, -887 and -907 caused a significant increase is promoter activity. The different effect of CpG mutagenesis on $p14^{ARF}$ and ANRIL promoter activity might reflect the different genomic context of the DMR with regards to the TSS of ANRIL and $p14^{ARF}$, as the DMR lies within the promoter of ANRIL but within the first intron of $p14^{ARF}$. The finding that CpG mutagenesis within the DMR which lies downstream of the TSS of $p14^{ARF}$ affects the level of $p14^{ARF}$ promoter activity suggests that this region may be part of a downstream enhancer or part of an alternative promoter, however to date no functional role of this region has been described.

Although it should be noted that mutagenesis of the CpG sites does not test whether differential methylation of these sequences would affect ANRIL or $p14^{ARF}$ expression, but does show that these sequences are potentially important for ANRIL and $p14^{ARF}$ expression. Unfortunately, methods to directly test whether specific CpG sites are methylated *in vivo* are technically difficult (254) and limited studies have reported the use of patch promoter methylation to measure the effect of the methylation of a single CpG site within a promoter on gene activity (255–257). However, the ligation of the modified DNA into plasmids is not always 100% efficient (258) and this makes comparison between the unmethylated and methylated plasmids difficult. An alternative approach would be to clone the promoter region of ANRIL and $p14^{ARF}$ into a CpG free luciferase vector and then methylate the promoter region *in vitro*; however, this would induce methylation across the whole promoter region, making it impossible to determine the contribution of the CpGs in question.

To determine whether transcription factors bind across the DMR and whether methylation of the CpGs had an effect on this binding, EMSAs were carried out. This revealed strong protein binding across CpGs -769 and CpGs -887 and -907 in SaOS-2 cells. Interestingly, binding was cell type specific and differences in the protein complexes bound across the CpGs

were seen between SaOS-2 and SW-872. This may suggest that this region is subject to tissue specific regulation. There are many putative transcription binding sites across this region, one of which belongs to PPARγ that spans CpGs -793 and -796 and this gene has a well-documented role as an activator of adipogenesis (259–261). Using MATInspector, we determined that there are potential putative binding sites that span CpGs -887 and -907, which has shown preferential binding in osteosarcoma cells over liposarcoma cells, for transcription factors that have been shown to have a role in bone metabolism (Figure 3.9).

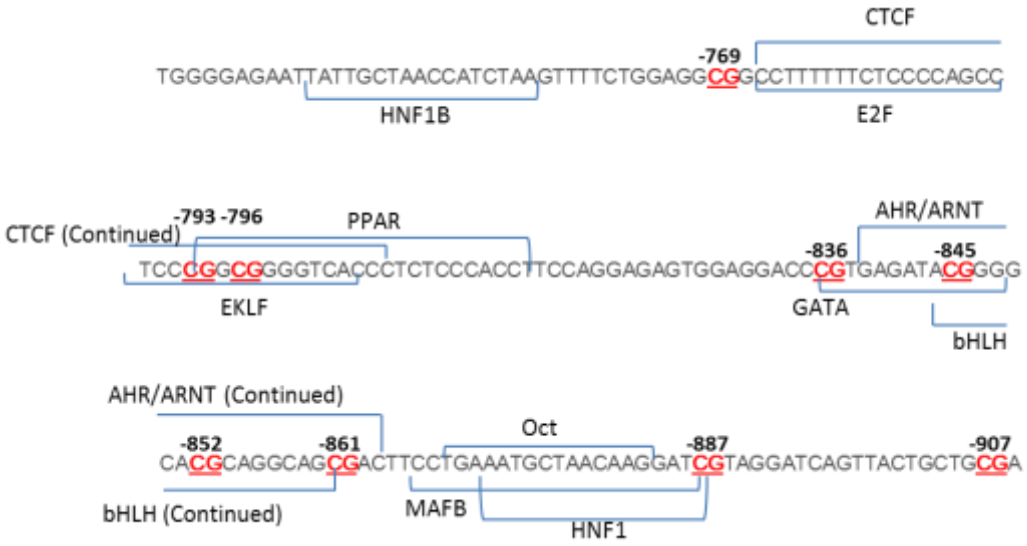

Figure 3.9: THE CDKN2A DMR with putative regulatory transcription factor binding sites. Putative transcription factor binding sites were determined using MATInspector and are shown by blue brackets. Each CpG site is numbered according to the distance from the TSS of ANRIL and shown in red. HNF1B Hepatocyte Nuclear Factor-1-Beta; CTCF CCCTC-binding Factor; EKLF Erythroid Kruppel-Like Factor; PPAR Peroxisome Proliferator-Activated Receptor; AHR/ARNT Aryl Hydrocarbon Receptor/AHR Nuclear Translocator; bHLH Basic Helix-Loop-Helix; MAFB V-maf Musculoaponeurotic Fibrosarcoma Oncogene Homolog B; Oct Octamer Binding Transcription Factor

To determine whether methylation affects binding to this region, the effect of methylation of CpGs -887 and -907 on transcription factor binding was investigated. The findings show that in osteosarcoma cells, there was specific binding of a complex to CpGs -887 and -907, but when the cytosine of CpGs -887 and -907 were methylated, protein binding was reduced. This is consistent with the findings from many studies which show that transcription factor binding is generally reduced by methylation (262). EMSAs showed that a protein of similar molecular weight binding to both the unmethylated and methylated CpG -887 and -907 containing probes, with the protein binding more strongly to the unmethylated probe, suggesting that proteins forming this complex preferentially bind to unmethylated DNA. This further suggests that the binding between the unmethylated CpG -887 and -907 containing probe and proteins in SaOS-2 cells is stronger than the binding of protein to the methylated probe and that

transcription factors in the osteosarcoma extract preferentially bind to this particular region of the *CDKN2A* DMR when it is unmethylated. As methylation of CpGs -887 and -907 within this region have a negative association with offspring bone outcomes during childhood, this could be due to reduced transcription factor binding due to increased methylation. This could prevent correct regulation of bone development and could put the child at risk for adverse bone outcomes during later life.

Identification of the complexes that signal through this region will be important in understanding factors that regulate ANRIL/p14^{ARF} and how perhaps perturbation in early life environment may influence methylation at this locus. To identify transcription factors that may bind to this region, multiplexed competitor EMSAs were carried out. The excess addition of the consensus binding sequences for both GAS and Smad3/4 effectively competed out binding across CpGs -887 and -907.

Interferon (IFN) gamma-activated site (GAS) elements are found in the promoters of IFNγ inducible genes as they were originally defined as a requirement for the induction of IFNγ signalling, however they have now been shown to be present in IL-6, growth factor, hematopoietic growth factor and growth hormone inducible genes in various species (263). The most common core binding sequence of these short stretches of DNA consists of AAG(N_{2-4})CTT, where 'N' is any base. There is almost an exact match between the core consensus sequence and the CpG -887 and -907 containing probe, in that the only part that does not match is the first T in the GAS consensus sequence is replaced by a G in the probe sequence, though in some cases, this T has been replaced by other bases (263). This binding site would then lie directly over CpG -887. Various transcription factors that have a role in IFNγ signalling have been shown to bind to these sequences but the most common is STAT1 (263). IFNγ has been shown to have a role in both osteoblastogenesis and osteoclastogenesis. Using microarray expression analysis, Duque and colleagues demonstrated that various IFNγ-inducible genes were upregulated during the early phases of hMSC differentiation into osteoblasts and when IFNγ expression was knocked down by siRNA, RUNX2 expression also decreased, suggesting IFNγ is important for this process (264). The same group also went on to show that IFNγ knock out mice display a reduction in bone mineral density when compared to their wild-type littermates and that treatment of ovariectomised mice with doses of IFNγ can rescue them from osteoporosis by causing an increase in bone mass and a improves the balance between bone formation and resorption (265). There are conflicting reports on the role of IFNγ in osteoclastogenesis as there is evidence to support that IFNγ both inhibits and promotes osteoclastogenesis. Takayanagi *et al* demonstrated that IFNγ inhibits osteoclastogenesis by interfering with the RANK-RANKL signalling pathway (266), which is the

major pathway regulating this process, whereas Gao *et al* have shown that IFNγ stimulates the production of RANKL, promoting osteoclast activation and bone resorption (267).

Binding to CpGs -887 and -907 was also competed out by the addition of the consensus sequence for the SMAD3/4 complex. The SMAD3/4 complex is part of the SMAD family of proteins, which are important in the signal transduction pathway by which BMPs on binding to their receptors activate gene expression, as well as signal transduction in the TGF-β pathway, also for the activation of gene transcription. SMAD proteins are separated into three subgroups: receptor-regulated SMADS (SMAD1, 2, 3, 5 and 8), common-mediator SMAD (SMAD4) and inhibitory SMADs (SMAD 6 and 7) (268). There is much research that demonstrates the importance of the SMAD3/4 complex in the transduction of TGF-β signalling to allow for correct osteoblast differentiation and function. Feng *et al* have demonstrated that this complex can cooperate with Sp1, a zinc finger transcription factor where SNPs within the recognition site of this protein have been associated with reduced bone density and increased risk of osteoporotic fracture, to induce $p15^{INK4B}$ expression, causing cell cycle arrest (269). The SMAD3/4 complex has also been shown to repress the expression of osteoblast differentiation transcription factors. Kang *et al* demonstrated that Runx2 function was repressed in murine osteoblasts, leading to the decrease in expression of osteocalcin (270). Furthermore, they showed that SMAD3/4 formed a complex with Runx2 at its DNA binding sites to recruit HDACs to these areas, thereby repressing the expression of Runx2 activated genes. Alliston *et al* have also independently demonstrated that Smad3 can repress the expression and function of CBFA1 (murine RUNX2), which leads to the inhibition of Cbfa1 and osteocalcin genes (271). There is no evidence in the literature to suggest that these transcription factors work in synergy. Altering the binding potential transcription factors to either of these two sites through methylation could have consequences on bone structure and risk of fracture in later life by altering bone mineral content and bone mineral density.

STAT1 is a transducer of IFNγ pathway whereas the SMAD3/4 complex is a signal transducer for the TGF-β pathway and there is evidence to suggest that there is a mechanism for transmodulation between these two signal transduction pathways (272). Given that in osteoblasts these two pathways have been shown to regulate RUNX2 function but in opposite directions, this could suggest that the signal received from the environment determines which of these two transcription factors bind to these CpGs in *CDKN2A* to regulate ANRIL expression and whether this leads to an upregulation or downregulation of downstream effector molecules.

However, MATInspector and PROMO searches did not reveal any known putative binding sites for these transcription factor complexes across the probe containing CpGs -887 and -907,

though this could be because the probe sequence is not an exact match for either transcription factor binding consensus sequence, though there are similarities between the both the consensus sequences and the CpG -887 and -907 probe sequence. This could suggest that the CpG -887 and -907 containing probe includes previously unknown binding sites for the Smad3/4 complex and that there are potentially many transcription factors that could be binding to the GAS consensus sequence, or the highly similar sequence within the CpG -887 and -907 containing probe.

3.5 Summary

We sought to establish whether the differentially methylated region identified in the *CDKN2A* gene locus may have a causal role in the pathway that could lead to differences in bone mineral content or whether it is simply a marker of bone development. These data suggest that the DMR region may have a role in regulating the expression of the lncRNA ANRIL and $p14^{ARF}$. Although, because of the difficulty in obtaining tissues from infants, the relevance of altered methylation of this region in cord tissue or its relation to the methylation patterns seen in bone is unknown, as methylation patterns have been shown to be tissue specific, though others have been shown to be consistent across different tissue types (219,273) .

We also sought to demonstrate that differential methylation of CpGs -887 and -907 alters transcription factor binding to this region of the CDKNA gene, a DMR negatively associated with total bone mineral content and density. These data show that methylation decreases protein binding and that this region is bound by SMAD and STAT transcription factors, which have been shown to have effects on osteogenesis and bone metabolism. Together these data suggests that differential methylation of this region may influence the transcription of both ANRIL and $p14^{ARF}$ though further work will be required to determine what factors bind and how this impacts ANRIL or $p14^{ARF}$ expression. However, even if methylation does affect ANRIL, and/or $p14^{ARF}$ expression, whether differential methylation of this region is causally involved in the adverse bone development remains to be determined. Perturbations in ANRIL or $p14^{ARF}$ expression however could address, at least in cell lines, whether ANRIL in particular is important for bone function and development.

3.6 Future work

In order to determine whether members of the GAS family of transcription factors and the SMAD3/4 complex are binding to this region within the DMR, EMSAs would be repeated using antibodies against the GAS transcription factors and the SMAD3/4 complex. If these proteins are binding to the unmethylated CpG -887 and -907 probe, the antibody would bind to the protein and retard the complex, causing a super shift on the EMSA. EMSAs using the methylated CpG -887

and -907 probe could also determine whether the binding of these two consensus sequences is affected by methylation of this region in the *CDKN2A* DMR.

If it is indeed SMAD3/4 that is binding to this region and the GAS element has transcription factors binding to it, we could co-transfect expression vectors containing this transcription factor or this consensus sequence and the ANRIL/$p14^{ARF}$ promoter constructs to determine whether overexpression of these proteins leads to a change in activity of the ANRIL and/or $p14^{ARF}$ promoters.

Chapter 4

Functional Significance of ANRIL in SaOS-2, an Osteoblast-like Cell Line

4.1 Introduction

Previous research has demonstrated that *CDKN2A* methylation at birth is associated with BMC, BA and aBMD at 4 and 6 years of age, suggesting that altered *CDKN2A* methylation maybe a valuable marker of later bone health but whether it is directly involved in bone development or simply a marker of later bone outcomes is unknown. Methylation patterns have been shown to be tissue specific; however, there is now also research demonstrating inter tissue correlation of methylation patterns. Byun *et al* have demonstrated inter tissue correlation of methylation patterns between 11 different tissues (274) and Lokk and colleagues have shown that methylation patterns were well conserved across 17 different somatic tissues (275), whether the methylation pattern observed in cord tissue reflects methylation changes in bone cells in these individuals is unknown. The *CDKN2A* locus encodes for $p16^{INK4A}$, $p14^{ARF}$ and the lncRNA ANRIL and in the previous chapter, we found that site directed mutagenesis of the CpG sequences within the DMR of CDKN2A are important for ANRIL and $p14^{ARF}$ expression. $P14^{ARF}$ has a well-defined role in cell cycle progression and this has been characterised in a wide range of cell types. Such studies would suggest that perturbation of $p14^{ARF}$ expression during development might impact on osteoblast cell number, differentiation potential or turnover. We have also shown that the DMR can influence ANRIL expression, however the function of this lncRNA is relatively poorly defined with no research to date as to its role in bone cell development or function although SNPs within ANRIL have been associated with frailty. Much of the previous research on ANRIL has investigated its role in vasculature because of the link between SNPs within ANRIL and CVD risk (237,276). Here siRNAs directed against ANRIL have been shown to cause a decrease in vascular smooth muscle cells (VSMCs) number and rate of proliferation. However, there are conflicting reports as to whether ANRIL acts through $p16^{INK4A}$ and/or $p15^{INK4B}$, which is encoded for by *CDKN2B*, a gene that is upstream of *CDKN2A*, or through a *trans* mechanism independent of $p16^{INK4A}$/$p15^{INK4B}$ (237,276,277).

ANRIL is a long non-coding RNA (lncRNA), which are a group of RNAs that are defined and distinguished from short non-coding RNAs as those which have a length of more than 200 base pairs (278). Very little is known about the function of lncRNAs, though there is evidence to suggest that they can act as scaffolds, where they act as platforms for the assembly of molecular complexes (279,280), either in *cis* or in *trans*. The first ANRIL transcript was discovered by Pasmant *et al* in 2007 (281) and the gene encoding this RNA contained 19 exons spanning a region of 126.3kb; a more recent study however by Holdt *et al* have also now shown the existence of transcripts that contain a novel exon 20 (282). ANRIL is transcribed by RNA polymerase II (283) into 3834bp mRNA in the antisense direction of the CDKN2B gene locus. The first exon of this

ANRIL transcript is approximately 14,850bp downstream from $p15^{INK4B}$ TSS and approximately 300bp upstream of the TSS for $p14^{ARF}$ (277).

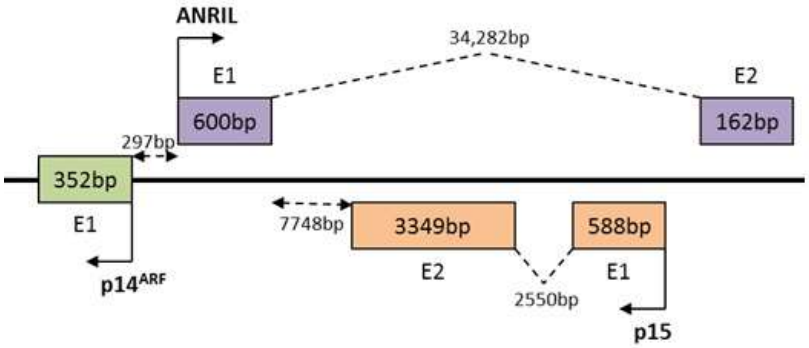

Figure 4.1: Position of ANRIL in relation to $p14^{ARF}$ and $p15^{INK4B}$. The TSS of ANRIL is located approximately 14,850bp downstream of the $p15^{INK4B}$ TSS, encoded for by the *CDKN2B* gene, and 300bp upstream of the $p14^{ARF}$ TSS, encoded for by the *CDKN2A* gene. ANRIL is transcribed from the *CDKN2A* gene locus in the antisense direction to $p15^{INK4B}$.

Since 2007 it has been shown that there are many different linear isoforms of ANRIL created from alternate splicing (238,284), Burd *et al* have also shown that circular isoforms also exist, and these are predominantly formed from the less abundant central exons 4-12 (238). The expression of the circular isoforms has been shown to be associated with CVD-risk alleles; however their functions have yet to be clarified. It has been shown that some splice variants are tissue specific, which further suggests that ANRIL has a physiological relevance, though the characterisation of the isoforms in different tissues and cell lines are still incomplete (285). Various isoforms have been shown to have a range of diverse functions that include gene regulation, epigenetic regulation, cell cycle control and cell differentiation, which are mediated by RNA-RNA, RNA-DNA or RNA-protein interactions (reviewed by Lee (286)).

Recent GWAS have demonstrated that the *CDKN2A*/*B* locus is a hotspot for disease-associated polymorphisms. Two SNPs within this gene locus have been linked to frailty (250). In this study Melzer *et al* showed that the rare allele (G) of two SNPs located 3.5kb proximally to the *CDKN2A*/*B* locus (rs2811712 and rs3218005) are associated with increased physical function in older people. Of the 2673 subjects that were common homozygous, 15% of them had severely impaired physical function compared to the 7% of subjects that were genotyped as rare homozygous (250), suggesting that those with the rare homozygous genotype are less at risk of suffering from severe physical impairment later in life. Other SNPs within this gene locus have been linked to T2D (251), Alzheimer's disease (252) and CVD (251). Studies have also shown that these disease-associated SNPs are frequently located within exons of ANRIL and, in most cases, associated with a change in ANRIL expression. ANRIL exons 1-2 expression seems to be the most

commonly affected (285), though some SNPs have been shown to alter the expression of exons 15-16 and 17-18 as well (276,287). Some of the SNPs within ANRIL are associated with a specific disease while others are associated with a range of ageing associated diseases, demonstrating the potential of different ANRIL splice variants having roles in different tissues.

Studies have shown that a knockdown in ANRIL expression leads to a decrease in cellular proliferation, characterised by significant decreases in both VSMCs and peripheral blood mononuclear cell (PBMC) number (276,282), which is potentially due to the *cis* functional effects of ANRIL. This lncRNA has been shown to act in *cis* by down regulating the expression of $p15^{INK4B}$ and $p16^{INK4A}$ (both cell cycle inhibitors) from the *CDKN2A*/*B* locus by recruiting PRCs to the promoters of both these genes and causing trimethylation of lysine 27 of histone 3 (243,283). This prevents the binding of transcriptional machinery and so suppresses $p16^{INK4A}$ and $p15^{INK4B}$ expression, thus preventing cell cycle progression. ANRIL also regulates $p15^{INK4B}$ through an antisense mechanism where it binds directing to its complementary sequence in the CDKN2B locus and prevents the transcription of this gene (288).

Recent studies have however also suggested that ANRIL may act in *trans* by binding to Alu elements (277,282,289). Using a genome-wide mRNA expression array carried out on cell lines overexpressing ANRIL transcripts, Holdt *et al* found that there were significant changes in gene expression distributed across the genome. They then went on to show that these *trans* functional effects were due to binding of PRC proteins, recruited by ANRIL binding, to Alu binding elements in the promoters of ANRIL regulated genes (282). Sato *et al* have demonstrated the role of a novel splice form of ANRIL to be involved in the regulation of the nucleus (277). They overexpressed this isoform in HeLa cells and found, using gene ontology enrichment analysis, that expression of 38 genes involved in nucleus regulation were altered – 36 genes were down regulated and 2 genes were upregulated. However, what role, if any, ANRIL plays in the function of bone-derived cells is unknown.

4.2 Aims

To determine whether i) the long non-coding RNA ANRIL is expressed in bone-related cells, such as primary osteoblasts and human mesenchymal stem cells, ii) to explore the role of ANRIL in osteoblast cell proliferation, differentiation and mineralisation and iii) to determine whether these effects are dependent or independent of $p16^{INK4A}$ expression.

4.3 Results

4.3.1 Is ANRIL expressed in bone-related cells?

The expression of ANRIL in different tissue types has not been well documented, therefore to determine whether ANRIL is expressed in bone-related cells, RT-qPCR was used. Three RT-qPCR assays were used that spanned the exon 1-2, exon 5-6 and exon 18-19 boundaries of ANRIL. These exons were chosen as the major ANRIL isoforms in other cell types (some of which are shown in Figure 4.2) have been shown to contain these exons more frequently than others.

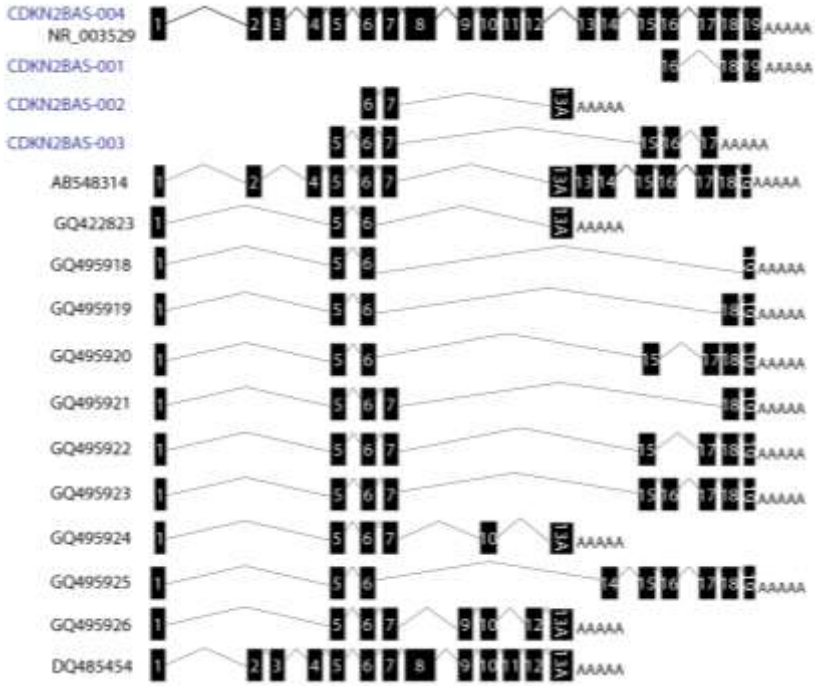

Figure 4.2: Figure showing the exons present in previously reported ANRIL isoforms. Figure taken from Burd *et al* (238).

Using these assays ANRIL expression was investigated in bone-related cells, which included: primary osteoblasts, human bone marrow stromal cells (hBMSCs) and SaOS-2, an osteoblast-like osteosarcoma cell line. As very little is known about ANRIL expression in other cell types, cDNA from different cells and tissues were run alongside the bone-related cells, which included SW-872 (an adipocyte derived cell line), HepG2 (liver cancer cell line), Hs578T (breast cancer cell line) and HMT-3522 (breast epithelial cell line).

RT-PCR analysis showed that ANRIL expression was detectable across a wide range of tissues and cell types, although there were differences in the relative expression of the amplicons across the different tissues (Figure 4.3). The pattern of expression was very similar for assays measuring transcripts containing exons 1-2 and exons 5-6, with transcripts containing exons 18-19

being quite distinct. ANRIL expression in all three RT-PCR assays was highest in the bone-related cells (hBMSCs, primary osteoblasts and SaOS-2 cells). hBMSCs had the highest expression of transcripts containing exon 1-2 and 5-6. Interestingly expression of ANRIL transcripts containing exons 1-2 or 5-6 is lower in primary osteoblasts and osteoblast-like SaOS-2 cells when compared to the expression of these exons in hBMSCs, however there was no significant change in expression of ANRIL transcripts containing exon 18-19 between hBMSCs and primary osteoblasts or SaOS-2 cells. Relatively high expression was also observed in the liposarcoma cell line SW-872 and breast cancer cell lines. HepG2 cells showed the lowest expression of ANRIL exons 1-2 and exons 5-6.

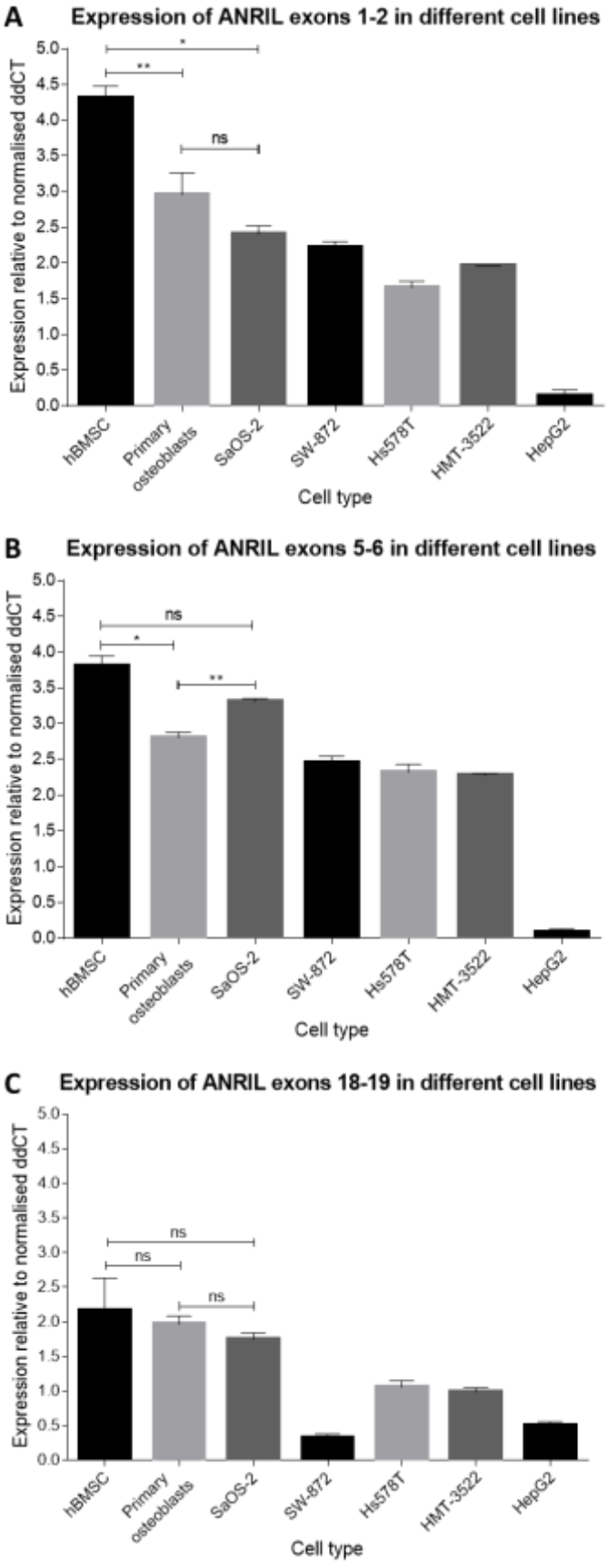

Figure 4.3: Expression ANRIL exons 1-2 (A), exons 5-6 (B) and exons 18-19 (C) in different cell lines relative to normalised ddCT. Comparisons were made between each of the bone-related cell types

4.3.2 Does ANRIL knock down affect SaOS-2 cell number?

Having shown that ANRIL is expressed in hBMSCs, primary osteoblasts and the osteoblast-like cell line SaOS-2, the function of ANRIL in the osteosarcoma cell line SaOS-2 was then examined. SaOS-2 cells were transfected with 10nM of 3 siRNAs directed against different exons of ANRIL using Lipofectamine RNAiMAX. Of the three siRNAs used, one siRNA targeted exon 1 of ANRIL (Ambion E1 siRNA), while the other two matched the ANRIL siRNAs used successfully by Congrains *et al* to knock down expression of ANRIL in VSMCs (237). Of the latter two siRNAs, one targeted exon 1 of ANRIL (Congrains E1 siRNA), but a different sequence to the siRNA from Ambion, and the other siRNA targeted exon 19 (Congrains E19 siRNA). All three of these siRNAs have been commercially or experimentally shown to successfully knock down ANRIL expression. After optimisation of transfection conditions with a control 'cell death' siRNA, cells were transfected with the three ANRIL siRNAs, and cells incubated at 37^{o}C for 72hrs, after which they were either, trypsinised and counted, or RNA extracted for expression analysis.

To confirm that the siRNAs effectively knocked down ANRIL expression in SaOS-2, RT-qPCR assays were run using primers across ANRIL exons 1-2, 5-6 and 18-19. Results showed that each of the three ANRIL siRNAs significantly knocked down ANRIL exon 1-2, 5-6 and 18-19 expression (Figure 4.4). However, there were significant differences in the effectiveness of the siRNAs in knocking down ANRIL expression. ANRIL exon 1-2 transcripts were knocked down 2.4-fold by Ambion E1 siRNA, 5.9-fold by Congrains E1 and 1.4-fold by Congrains E19. ANRIL exon 5-6 transcript expression was knocked down 2.2-fold by Ambion E1 siRNA, 6.4-fold by Congrains E1 siRNA and 1.5-fold by Congrains E19 siRNA. ANRIL exon 18-19 transcripts were knocked down 1.4-fold by Ambion E1 siRNA, 2.7-fold by Congrains E1 siRNA and by 2.9-fold by Congrains E19 siRNA.

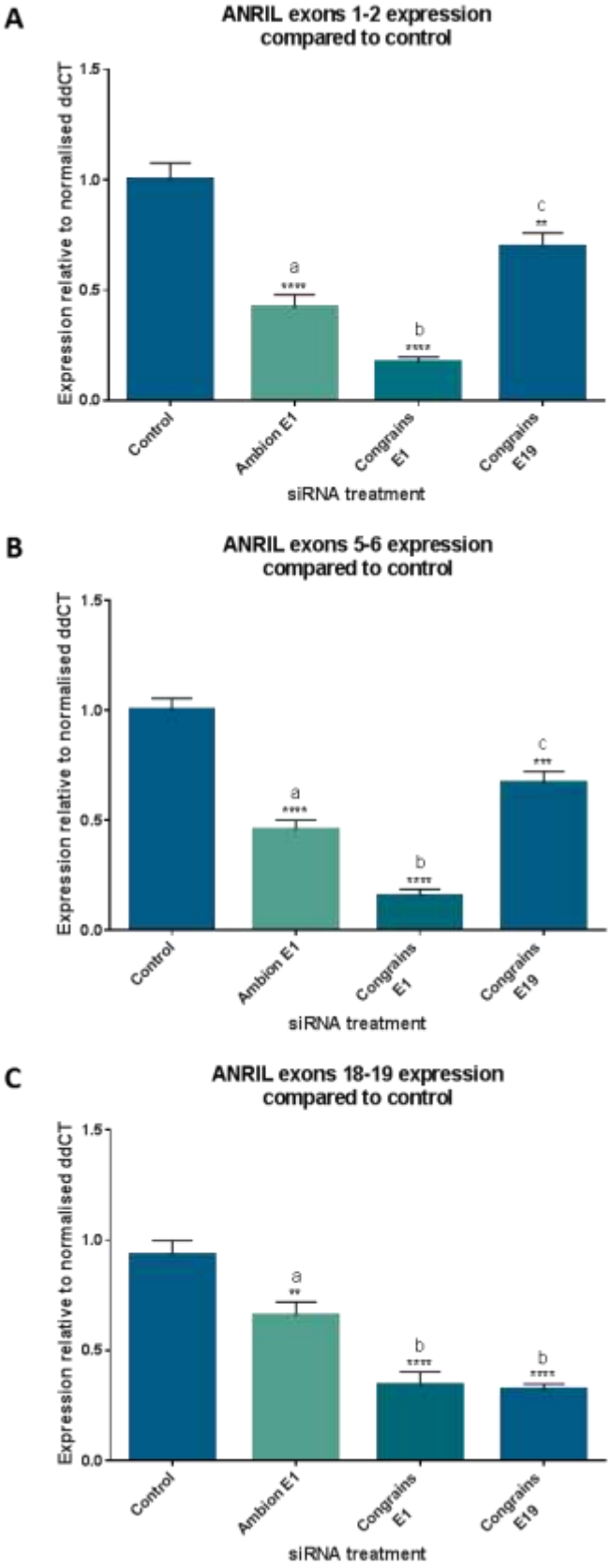

Figure 4.4: Results from RT-qPCR confirming knockdown of ANRIL exons 1-2 (A), exons 5-6 (B) and exons 18-19 (C) in transfected SaOS-2 cells. Graphs represent results from three independent transfections (n=3). Results shown as mean ±SEM * denote comparisons to control (****p<0.0001; ***p≤ 0.001; **p≤0.01). Letters denote comparisons between the three ANRIL siRNAs.

To determine the effect of a reduction in ANRIL expression, cell number was assessed in the SaOS-2 cells transfected with each of the three ANRIL siRNAs, a positive cell death siRNA and a negative scrambled siRNA. Results from three independent experiments (Figure 4.5) showed that there was a significant decrease in the number of live cells in cells treated with the positive 'cell death' siRNA control when compared to the 'scrambled' control. There was also a significant decrease in cell number upon treatment with the three ANRIL siRNAs ($p<0.0001$ for each siRNA treatment). The decrease in cell number induced in SaOS-2 cells transfected with the ANRIL siRNAs was similar for all three siRNAs used. These results suggest that ANRIL knock down leads to a decrease in cell number.

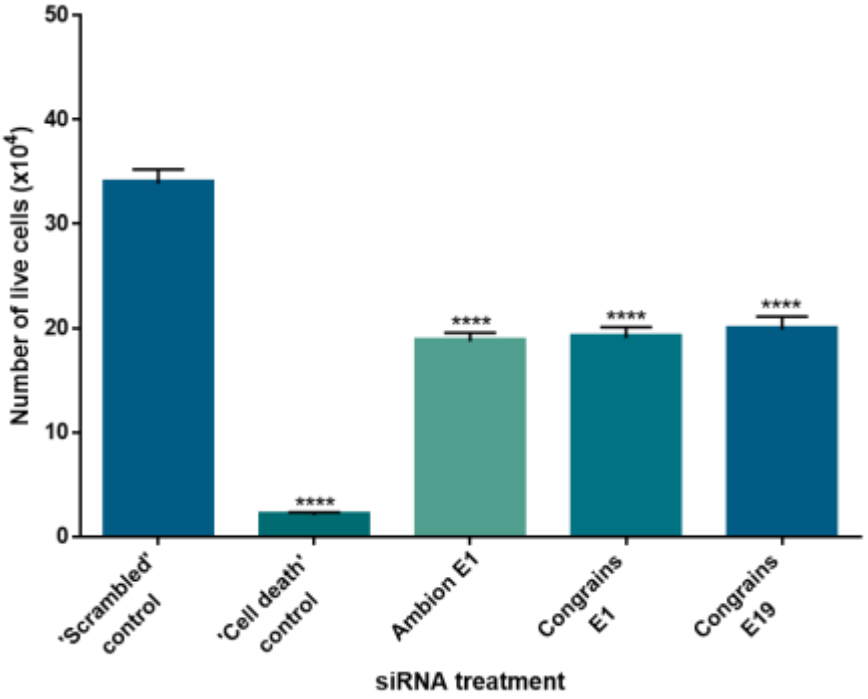

Figure 4.5: Number of live SaOS-2 cells after 72hr incubation with 10nM 'scrambled', 'cell death' and three siRNAs against ANRIL. Graph summarises data from three independent transfections (n=3). Results shown as mean ±SEM ****p<0.0001

4.3.3 Does knock down of ANRIL expression cause cell cycle arrest?

A decrease in cell number may be due to either a decrease in cell proliferation or an increase in cell death, therefore to determine what process a decrease in ANRIL expression may perturb, FACS analysis was used. ANRIL siRNA treated SaOS-2 cells, together with SaOS-2 cells transfected with the scrambled siRNA control were fixed in 70% ethanol and then stained with propidium iodide and analysed by FACS to assess cell cycle progression by measuring the amount of DNA within 5000 cells.

In cells transfected with the ANRIL siRNAs, there were significant changes in the percentage of cells undergoing apoptosis and those held in G_0/G_1 phase. However, the different ANRIL siRNAs cause different effects. Ambion E1 siRNA caused a significant increase ($p<0.0001$) in the percentage of cells being held in G_0/G_1, whereas there was no significant change seen with the Congrains E1 or Congrains E19 siRNAs (Figure 4.6A). However, significant increases in the percentage of cells undergoing apoptosis were seen when the cells were treated with Congrains E1 and Congrains E19 siRNAs ($p=0.0006$ and $p<0.0001$ respectively) (Figure 4.6B) but not with cells treated with Ambion E1 siRNA. These results suggest that a reduction in ANRIL transcripts can affect cell cycle progression and apoptosis of the osteosarcoma cells.

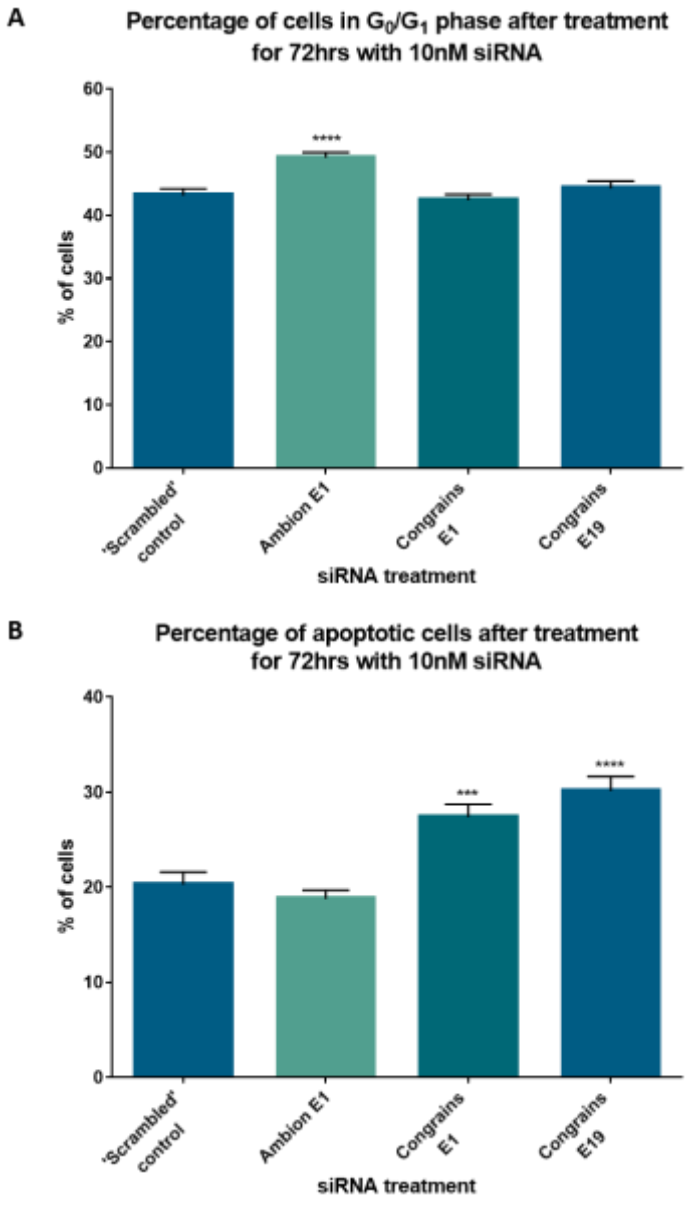

Figure 4.6: Percentage of SaOS-2 cells in G_0/G_1 phase (A) and apoptotic cells (B) after treatment with 10nM siRNA for 72hrs. Graphs represent results of three independent transfections (n=3). Results shown as mean ±SEM ****p≤0.0001; ***p≤0.001

4.3.4 Does ANRIL knock down have an effect on RUNX2 and ALP expression?

To determine whether knock down of ANRIL expression caused a change in the differentiation potential of SaOS-2 cells, cells were transfected with the three ANRIL siRNAs, as previously described, and RT-qPCR used to look at the expression of two differentiation markers: RUNX2 and ALP. RUNX2 is expressed during the early stages of differentiation, whereas ALP is expressed at the later stages of differentiation. Both of these genes have been shown to be expressed by SaOS-2 cells (290)

When ANRIL expression was knocked down in SaOS-2 cells, there was a significant increase in RUNX2 expression, though Ambion E1 and Congrains E19 caused a greater increase (2.5-fold and 1.9-fold respectively; $p<0.0001$ for both) in RUNX2 expression than Congrains E1 siRNA (1.4-fold increase; $p=0.0018$) (Figure 4.7A). A significant increase in ALP expression was seen compared to control when SaOS-2 cells were treated with the Ambion E1 and Congrains E19 siRNAs ($p=0.0059$ and $p=0.012$ respectively; Figure 4.7B), whereas there was no statistical difference in ALP expression when cells were treated with Congrains E1 siRNA.

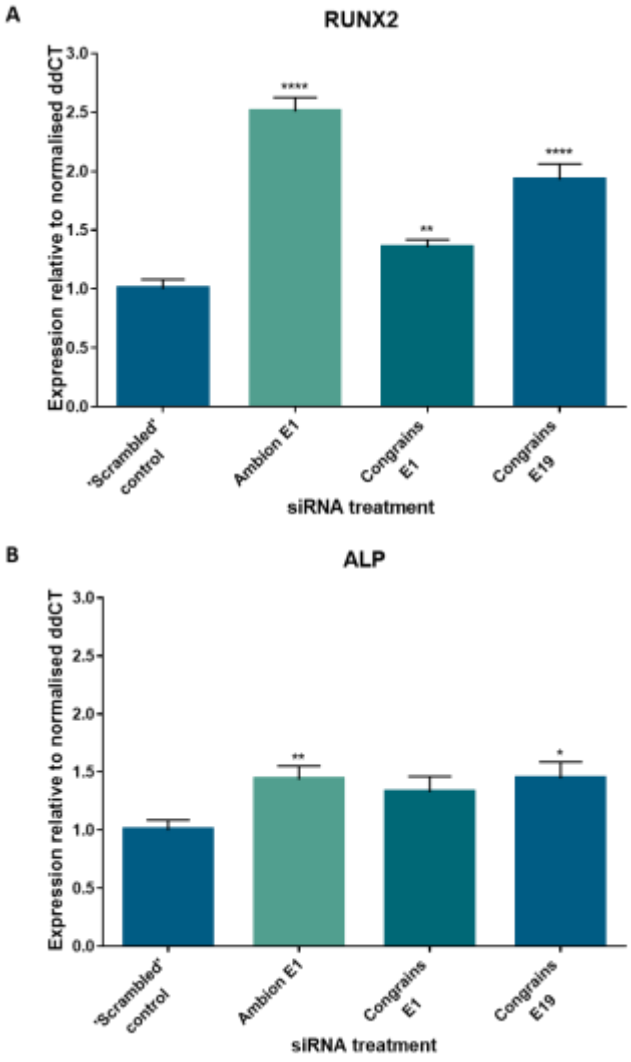

Figure 4.7: Expression of (A) RUNX2 and (B) ALP in SaOS-2 cells compared to control when ANRIL expression has been knocked down. All three siRNAs cause a significant increase in RUNX2 expression but only Ambion E1 and Congrains E19 siRNAs cause an increase in ALP expression. Graphs represent three independent transfections (n=3). Results shown as mean ±SEM ****p≤0.0001; ***p≤0.001; **p≤0.01; *p≤0.05

4.3.5 Does ANRIL knock down have an effect on expression of BGLAP?

To determine whether knock down in ANRIL expression leads to a change in the ability of the SaOS-2 cells to mineralise extracellular matrix, RT-qPCR was used to determine the expression levels of bone gamma-carboxyglutamate protein (BGLAP). BGLAP, also known as osteocalcin, is a marker for bone mineralisation and its expression has been characterised in the SaOS-2 cell line (290). ANRIL knock down had no significant effect on osteocalcin expression (Figure 4.8).

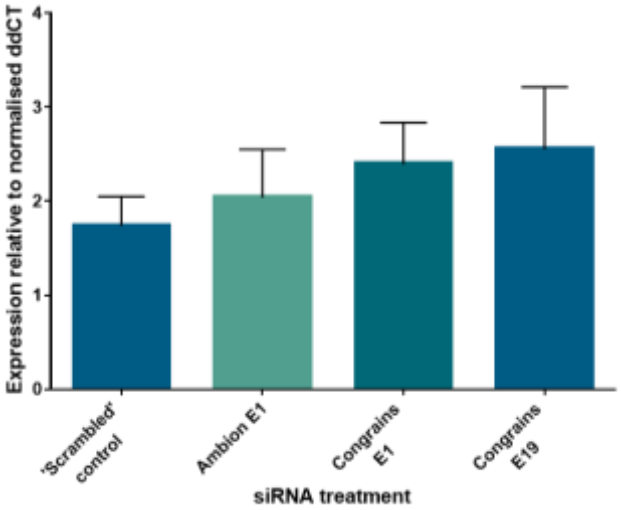

Figure 4.8: Expression of BGLAP in SaOS-2 cells compared to control when ANRIL expression has been knocked down. ANRIL knockdown by any of the three siRNAs does not cause a significant change in BGLAP expression. Graphs represent three independent transfections (n=3). Results shown as mean ±SEM

4.3.6 Does ANRIL mediate its effect through altered expression of the *CDKN2A/B* locus?

As ANRIL has been shown to negatively regulate $p16^{INK4A}$ and $p15^{INK4B}$, RT-qPCR was used to determine if the knockdown of ANRIL expression also induced a change in expression of these transcripts. Following transfection of cells with Ambion E1 siRNA, there was a significant increase in $p16^{INK4A}$ expression ($p=0.0018$), however there was no change in $p16^{INK4A}$ expression in cells transfected with either Congrains E1 or E19 siRNAs (Figure 4.9A). Interestingly, $p15^{INK4B}$ expression was significantly decreased in cells transfected with each of the three ANRIL siRNAs ($p=0.0045$, $p<0.0001$ and $p<0.0001$), though Ambion E1 siRNA caused a smaller decrease in expression compared to either Congrains E1 and Congrains E19 siRNAs (statistical differences in expression between the three siRNAs denoted by letters in Figure 4.9B).

Expression of $p14^{ARF}$, a third product of the *CDKN2A*/*B* locus was also investigated, though there is no evidence to suggest that this transcript is regulated by ANRIL. Results showed that when ANRIL expression is knocked down, there was a significant decrease in $p14^{ARF}$ expression when SaOS-2 cells were treated with the Congrains E1 and Congrains E19 siRNAs ($p=0.0029$ and $p<0.0001$ respectively) (Figure 4.9C).

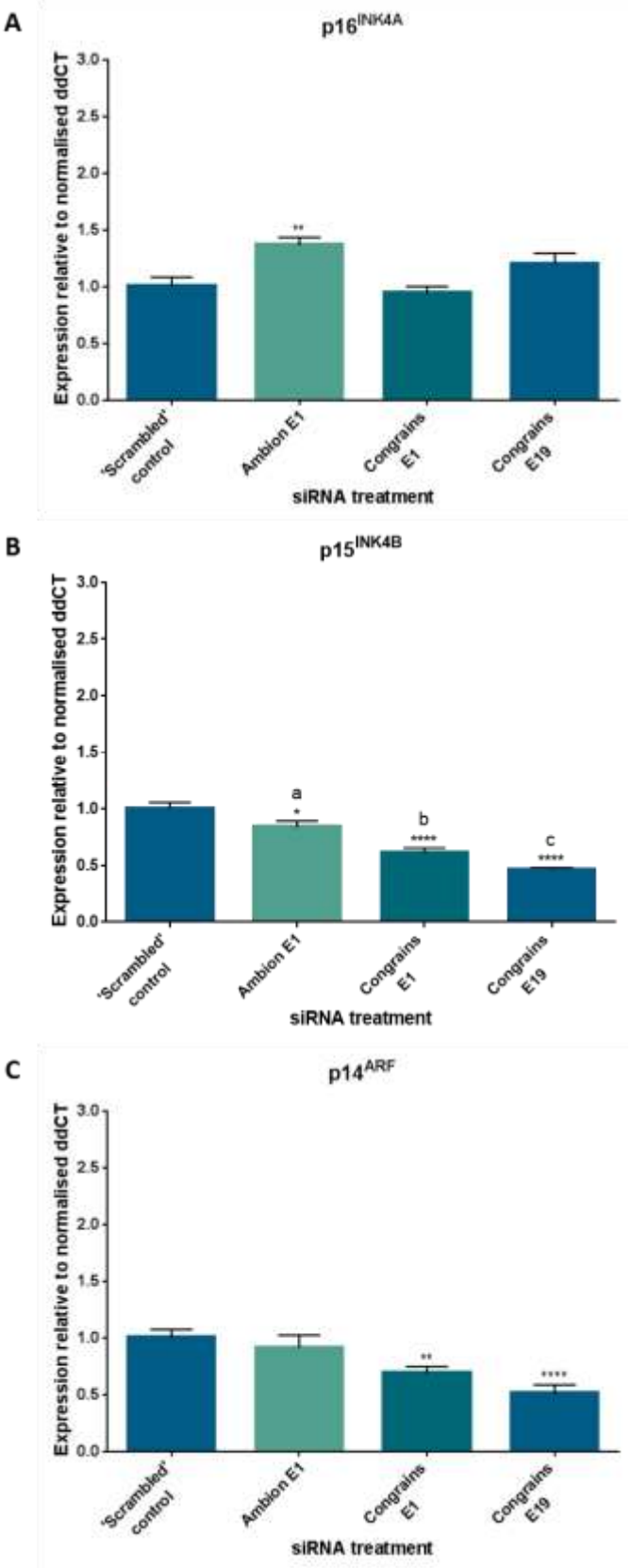

Figure 4.9: Expression of $p16^{INK4A}$ (A), $p15^{INK4B}$ (B) and $p14^{ARF}$ (C) in SaOS-2 cells compared to control when ANRIL expression has been knocked down. Graphs represent three independent transfections (n=3). Results shown as mean ±SEM * denote comparisons to control (****p≤0.0001; ***p≤0.001; **p≤0.01; *p≤0.05) Letters denote comparisons between the three siRNA treatments.

4.4 Discussion

In this chapter the role of ANRIL was investigated in the osteoblast derived cell line SaOS-2 cells. Previously, very little was known about the expression of ANRIL, which cell types it is expressed in and what its precise function is. The results in this chapter show that ANRIL is highly expressed in the osteoblast-like derived cell line SaOS-2 and primary osteoblasts, as well as human bone marrow stromal cells (hBMSCs). Transcripts containing exon 1-2, 5-6 and 18-19 were all detected. Moreover, ANRIL expression was also detected in a liposarcoma cell line (SW-872), breast cancer cell line (Hs578T) and liver cell line (HepG2), suggesting tissue wide expression patterns. Although interestingly, the relative abundance of the transcripts containing exons 1-2 and 5-6 in SW-872 cells compared to SaOS-2 cells was similar, whereas transcripts containing exons 18-19 were relatively low.

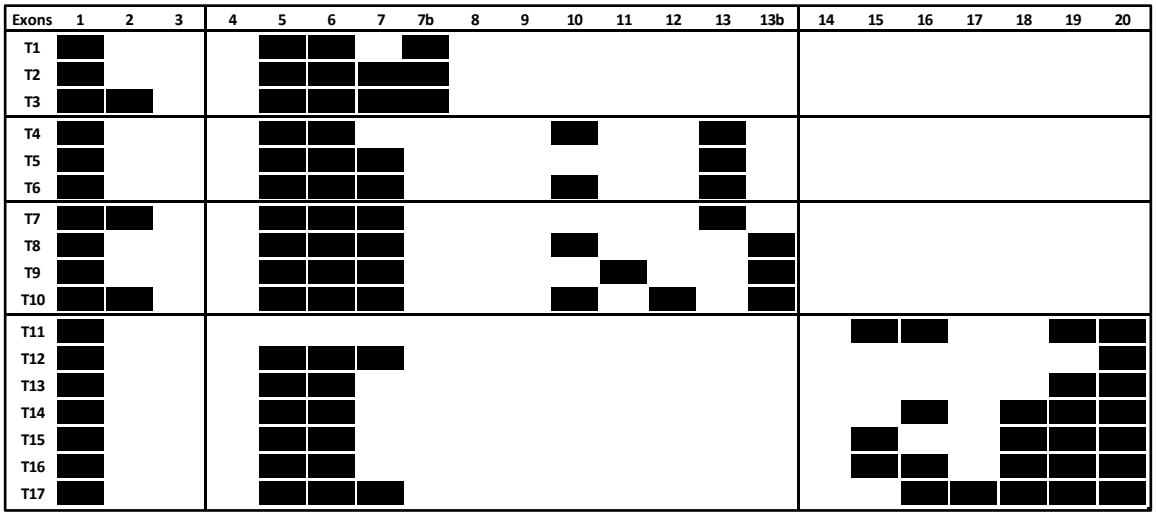

Figure 4.10: Exons present in 17 different ANRIL transcripts in PBMCs. Transcripts identified using RACE and PCR amplification. Figure replicated from Holdt *et al* (282).

Our results show that expression of ANRIL transcripts containing exons 1-2 or 5-6 is higher in hBMSCs than those that have been differentiated into primary osteoblasts, whereas there was no significant difference in exons 18-19 expression. As ANRIL has been shown to repress $p16^{INK4A}$ and $p15^{INK4B}$, cell cycle inhibitors, high levels of ANRIL expression in hBMSCs would be consistent with the higher self-renewal capacity of these stem cells. It has been shown across different cell types that differentiation is co-ordinated with cell cycle exit (291). In the case of ANRIL, you would potentially expect to see decreased expression in cells that are undergoing differentiation as cells exit the cell cycle in order to differentiate, which would allow for an increase in $p16^{INK4A}$ levels. These results do suggest that different cell types express different levels of ANRIL, which agrees with results from other research groups (238,281,284,292). Figure 4.10 shows exons present in different known ANRIL transcripts and this figure shows that exons 5 and 6 are more abundant in

ANRIL transcripts when compared to exons 18 and 19. Even though exon 1 is present in the majority of the transcripts shown in these figures, exon 2 is present in only a few of the transcripts shown. This agrees with our RT-qPCR results as we found that transcripts containing exons 5-6 were the most highly expressed and transcripts containing exons 18-19 had the lowest expression. However, even though different isoforms have been shown to be expressed in VSMCs, HeLa and PBMCs, the specific isoforms that are expressed in bone are not known.

Further work would need to be done in order to determine which specific ANRIL transcripts are expressed in bone. This could be done by rapid amplification of cDNA ends (RACE), where reverse transcription of RNA and PCR amplification are used to determine the sequence of unknown transcripts, which can then be mapped back to its unique genomic region. An alternative method would be to use PCR, with forward and reverse primers mapping to sequences within the exons of known ANRIL transcripts.

To determine what phenotypic and functional effects ANRIL has on bone development, siRNAs were used to knock down ANRIL expression in the osteoblast-like cell line SaOS-2. Three siRNAs were used to knock down ANRIL expression, and the results show that ANRIL was successfully knocked down by all three siRNAs. The effectiveness of knockdown was different for the three siRNAs depending on the transcript examined. For example, as Congrains E19 siRNA is less effective in knocking down transcripts containing exons 1-2 compared to Congrains E1 or Ambion E1, this suggests that not every ANRIL transcript that contains exon 1 also contains exon 19. Although, as exons 18-19 expression is knocked down to the same level when cells are treated with both Congrains E1 and Congrains E19, this may additionally suggest that the majority of ANRIL transcripts that do contain exon 19 also contain exon 1. To fully understand the significance of these results, the next step would be to map the ANRIL isoforms present in these cells. Interestingly the Ambion E1 siRNA did not knock down ANRIL expression to the same extent as Congrains E1 siRNA, which suggests there is a difference between the effectiveness of the siRNAs directed against exon 1 of ANRIL, potentially due to the different sequence that is targeted within exon 1 or a difference in secondary structure of the region.

The results show that when ANRIL expression is successfully knocked down by all three siRNAs, SaOS-2 cell number decreases. This decrease could be due to different mechanisms which include cell cycle arrest, an increase in apoptosis or potentially both of these mechanisms working together. To determine if the cells were being held in G_0/G_1 phase or whether an increase in cell death is the cause of the decrease in cell number, samples were stained using propidium iodide and analysed using FACS. Ambion E1 siRNA induced a significant increase in the number of cells in the G_0/G_1 phase of the cell cycle, but no effect on G_0/G_1 cell number was seen

with the other ANRIL siRNAs. Congrains E1 and E19 transfection lead to a significantly higher number of cells undergoing apoptosis compared to the 'scrambled control'. This difference is interesting especially between the two siRNAs directed against exon 1. Ambion E1 siRNA was less effective at knocking down exons 1-2 and exons 5-6 expression than Congrains E1 siRNA and less effective at knocking down ANRIL exons 18-19 expression than either Congrains E1 or E19 siRNAs. Even though there are 6 known variants of exon 1 across the 17 sequenced ANRIL transcripts, both Ambion E1 and Congrains E1 siRNAs map to all 6 different exon 1 sequences, so this does not explain the difference seen in knock down efficiency. Whether this difference in response is then due to the severity of the knock down is not clear, however it could probably be tested by transfecting SaOS-2 cells with an increasing concentration range of ANRIL Ambion E1 siRNA. However, another possibility is that the secondary structure of the sequence of mRNA maybe be different, therefore this could affect the effectiveness of siRNA binding and its knock down efficiency.

As the Ambion E1 siRNA from Life Technologies caused an increase in the number of cells being held in G_0/G_1 phase, this points to ANRIL working in *cis* to prevent cell cycle arrest. Consistent with this, treatment with Ambion E1 siRNA did lead to an increase in $p16^{INK4A}$ expression, while the others did not. As ANRIL negatively regulates $p16^{INK4A}$, expression of this transcript should increase when ANRIL expression decreases. This would lead to cell cycle arrest and prevention of cell cycle progression into S phase. The results shown here agree with what have previously been demonstrated in other cell types (237,243,293) and agrees with all the theories that low expression of ANRIL leads to an increase in the expression of $p16^{INK4A}$ and, consequently, an increase in the number of cells held in the G_o/G_1 phase of the cell cycle.

A decrease in ANRIL expression and increase in $p16^{INK4A}$ expression, in relation to bone development, could lead to premature cell cycle exit and differentiation. This could lead to an imbalance in bone formation as it has been shown in mice that premature osteoblast differentiation can lead to deregulated bone formation (294) and there is also evidence to suggest that premature cell cycle exit and early differentiation can lead to mislocalised transcription factors (295). An increase in $p16^{INK4A}$ expression has also been linked to replicative senescence (239), which is when cells no longer undergo proliferation (296), and this could potentially be another 'state' that the cells adopt upon ANRIL knockdown.

There is now also evidence from mouse models demonstrating that premature senescence can lead to impaired osteogenic differentiation potential, with bone marrow stromal cells from 3 different mouse strains favouring adipogenic differentiation (297–299). These mice showed lower trabeculae number, decreased bone strength and reduced bone mineral density

from a young age, further highlighting the need for proper regulation of osteogenesis. If osteoblasts became prematurely senescent, this could cause an imbalance in bone cell turnover which favoured osteoclasts and bone degradation. This would potentially lead to a lower peak bone mass and greater risk of fracture and osteoporosis in later life (114).

ANRIL siRNAs Congrains E1 and E19 induced apoptosis in the SaOS-2 cells, though no effect was seen upon treatment with Ambion E1 siRNA. There is evidence to suggest that ANRIL has a role in apoptosis pathways, though the evidence is contradictory. Holdt *et al* have demonstrated a pro-apoptotic effect of ANRIL knockdown in PBMCs and MonoMac cells (a monocytic cell line), shown by a significant increase in Annexin V^+ cells (282), whereas Congrains *et al* have demonstrated an anti-apoptotic effect when VSMC are treated with an siRNA against exon 19 of ANRIL (237). This demonstrates the potential of ANRIL having cell type specific *trans* functions and if, as my results suggest, ANRIL has an anti-apoptotic function in osteoblasts, this could have adverse effects on bone development by decreasing bone formation and potentially leading to a lower peak bone mass (64,300,301).

Interestingly, our results show that $p16^{INK4A}$ expression is not changed upon knock down of ANRIL with Congrains E1 and E19 siRNAs, which suggests that the cells are not undergoing premature senescence or cell cycle arrest via $p16^{INK4A}$. This agrees with results previously shown by other groups (282), though others have shown that when ANRIL expression is knocked down $p16^{INK4A}$ expression increases and cells become senescent (243). In this study ANRIL knock down did induce a decrease in $p15^{INK4B}$ expression when ANRIL expression is knocked down. As ANRIL is the antisense RNA to the *CDKN2B* gene, one would expect an increase in $p15^{INK4B}$ expression as previously demonstrated by independent groups (276,289). However, these experiments were not carried out in bone cells; therefore this may not be the case for SaOS-2 cells. As ANRIL acts as a scaffold lncRNA to recruit PRC complexes to the $p15^{INK4B}$ gene locus, if ANRIL expression is knocked down, this could allow for other repressive complexes to bind to this region instead, potentially acting as a compensatory mechanism due to the importance of the cell cycle pathway. Dysregulation of cell cycle control regulators may induce apoptosis or ANRIL may do this through an independent mechanism, through which it could alter other regulatory factors that would otherwise cause the upregulation of $p15^{INK4B}$.

The Ambion E1 siRNA also induced a decrease in $p14^{ARF}$ expression. Though there is evidence to suggest that $p14^{ARF}$ can induce apoptosis in cells by stabilising p53, which leads to the induction of Bax expression (302), this is unlikely to be the case with SaOS-2 cells as this cell line is p53-null. However, there is evidence to suggest that a p53 homologue, p73, can induce apoptosis independently of $p14^{ARF}$ expression (303), and its expression has been demonstrated in SaOS-2

cells (304). Interestingly, our results show that upon knock down of ANRIL expression with Congrains E1 and E19 siRNAs there is a decrease in the expression of $p14^{ARF}$, though there is no evidence in the literature to suggest that ANRIL directly regulates the expression of this transcript. However, the first exon of the ANRIL transcript does cover the promoter region of $p14^{ARF}$; therefore a decrease in ANRIL expression could allow for potential repressor complexes to bind to the promoter of this transcript and cause the decrease in expression that is observed.

To see whether ANRIL has any osteoblast specific functions that affect phenotype, we looked at the expression of differentiation and mineralisation markers in SaOS-2 cells where ANRIL expression had been knocked down. Our results show that upon ANRIL knock down differentiation markers significantly increase, as shown by increases in both RUNX2 expression (an early stage differentiation marker) and ALP expression (a late stage differentiation marker). No significant changes were seen with regards to the mineralisation maker osteocalcin (BGLAP). These results suggest that knock down of ANRIL enhances differentiation down the osteogenic lineage, regardless of the effect on $p16^{INK4A}$, all siRNAs also effected the expression of these osteogenic markers, which suggests that this change in expression could be $p16^{INK4A}$ independent. There is evidence to show that lncRNAs and other epigenetic mechanisms have a role to play in osteogenic differentiation. A recent paper by Zhu *et al* has demonstrated that the downregulation of lncRNA-ANCR (anti-differentiation ncRNA) promotes osteogenic differentiation by regulating RUNX2 expression through associations with enchancer of zeste 2 (EZH2) (214), thus demonstrating the potential of ANRIL as a mediator of osteoblast differentiation. lncRNA expression assays are also identifying new lncRNAs that have roles to play in the early differentiation of MSCs (213). However, as there was a change in $p15^{INK4B}$ and $p14^{ARF}$ expression, this could suggest that the effects seen on RUNX2 expression and ALP expression could be $p15^{INK4B}$ and $p14^{ARF}$ dependent, rather than through direct regulation by ANRIL. Though there is evidence to suggest that RUNX2 can regulate the osteoblast cell cycle.

In cells from wild type and Runx2 deficient mice, osteoblasts from Runx2 deficient mice proliferated at a higher rate than those from wild type mice. When Runx2 was reintroduced to the cells, it caused a decrease in cell proliferation, suggesting that stringent cell cycle control had been restored (305). This could explain the decrease in $p14^{ARF}$ and $p15^{INK4B}$ expression seen upon ANRIL knock down, with RUNX2 potentially acting as a compensatory mechanism in order to maintain cell cycle control, or that the increase in RUNX2 expression causes the decrease in the expression of these two inhibitors.

There is evidence demonstrating that RUNX2 can have an anti-proliferative effect in osteoblasts by causing cell cycle arrest at the G_0/G_1 phase of the cycle. Galindo *et al* have

demonstrated that an increase in RUNX2 expression in MC3T3 cells (a murine osteoblast cell line) suppresses proliferation and causes an increase in the number of cells being held in G_1 phase (306). This effect was also seen in primary murine calvarial cells. Pratap *et al* have also shown that MC3T3 and primary calvarial cells that do not express Runx2 ($Runx2^{-/-}$) or express a protein that lacks the Runx2 COOH terminus ($Runx2^{\Delta C/\Delta C}$), which is essential for the interaction of this protein with several different pathways, exhibit an increase rate of cell growth. When Runx2 was then reintroduced to the cells through use of an adenovirus, the rate of cell growth reduced to a rate that was comparable to the control cells (305).

RUNX2 has been shown to have a role in pathways that regulate cell proliferation, such as Smad and MAPK pathways (305) as well as G protein-coupled signalling pathways (307). However, it is also known to be regulated by cell signalling pathways that are involved in bone homeostasis (308), such as the BMP, Wnt and IHH pathways. If ANRIL has a role in regulating one of these pathways, when it's expression is knocked down it could lead to an increase in RUNX2 expression, which could, in turn, lead to a reduction in cell growth and proliferation. Either of these scenarios could potentially explain the increase in RUNX2 that is seen in SaOS-2 cells that have been treated with siRNAs against ANRIL.

4.5 Summary

We sought to demonstrate that ANRIL expression is cell type and tissue type specific by looking at the expression of three different ANRIL exons across a range of cell types. Our results show that ANRIL expression does differ across cell types, with ANRIL expression being lower in cells that have undergone osteogenic differentiation when compared to undifferentiated hBMSCs.

We sought to establish the functional effects of ANRIL in the osteoblast-like cell line SaOS-2 by transfecting these cells with siRNA against ANRIL and knocking down its expression. We showed that ANRIL knock down caused a decrease in cell number, which is most likely due to an increase in pro-apoptotic pathways as $p16^{INK4A}$ and $p15^{INK4B}$ expression did not increase upon ANRIL knock down. This suggests that the cells were not becoming senescent or undergoing cell cycle arrest. Our results show that RUNX2 and ALP expression, both markers of osteogenic differentiation, significantly increase when ANRIL expression is knocked down. This suggests that ANRIL may have a role in the regulation of these two proteins.

In order to confirm our findings experiments need to be repeated in primary osteoblasts as there are limitations to using cell lines. SaOS-2 cells do not have Rb, which is a downstream repressor of E2F and is indirectly regulated by $p16^{INK4A}$, or p53, both of which have roles in the cell

cycle pathway, which is why we may have seen a decrease in $p15^{INK4B}$ expression and no change in $p16^{INK4A}$ expression.

Chapter 5
Characterisation of ANRIL in Human Bone Marrow Stromal Cells and Primary Osteoblasts

5.1 Introduction

lncRNAs are non-coding RNA transcripts that are over 200bp in length which are often developmentally regulated (181). To date, very little is known about the specific functions of lncRNAs, however they are known to contain RNA-, DNA- and protein-binding domains, which allows them to be classed into three main groups: scaffolds, decoys and guides (188). Though there is no direct evidence of a role for ANRIL in the regulation of osteoblast differentiation, there are studies linking the *CDKN2A* locus and ANRIL to replicative senescence, which could have an adverse effect on osteoblast differentiation, bone homeostasis and frailty. Studies have demonstrated that replicative senescence can alter the differentiation abilities of mesenchymal stem cells into osteoblasts. Banfi *et al* (309) and Kretlow *et al* (310) have both demonstrated, in human and mice respectively, that as stem cells undergo replicative senescence their ability to differentiate into osteoblasts decreases.

The *CDKN2A* locus has been linked with cellular senescence (244) and it has been suggested that an increase in $p16^{INK4A}$ expression can be used as a biomarker for aging (239). ANRIL is known to negatively regulate the expression of the *CDKN2A* locus transcripts via the recruitment of the Polycomb repressive complexes (PRC) 1 and 2 (283), which consequently leads to the trimethylation of lysine 27 on histone 3. Yap *et al* have demonstrated a role for ANRIL in the regulation of senescence in a variety of cell lines as well as cancerous prostate epithelial cells (283). This study showed that chromobox 7 (CBX7), a subunit of PRC1 that binds to chromatin, binds to ANRIL and that this interaction allows CBX7 to carry out its function, as well as allowing for correct recognition of H3K27 methylation. When the interaction between ANRIL and CBX7 was disrupted, it affected the ability of CBX7 to negatively regulate the *CDKN2A* locus and control senescence, suggesting that ANRIL could have a senescence-dependent role in proliferation. If ANRIL expression becomes deregulated it could lead to premature cellular senescence, which, in terms of osteoblast differentiation and bone homeostasis, could have adverse consequences.

5.2 Aims

Having shown that ANRIL is important for the growth and survival of SaOS-2 cells, the aim of this chapter was to determine whether ANRIL played a similar role in human primary bone marrow stromal cells (hBMSCs) and primary osteoblast and whether ANRIL acts via $p16^{INK4A}$ or $p15^{INK4B}$ or independently of the pathways as has been reported recently in other cell types.

5.3 Results

5.3.1 ANRIL knock down causes a decrease in hBMSC and primary osteoblast cell number

To determine whether ANRIL has an effect on bone cell growth and cell proliferation, primary hBMSCs and osteoblasts were transfected with 10nM of the ANRIL siRNAs, Congrains E1 and Congrains E19, which are designed against different exons of ANRIL using Lipofectamine RNAiMAX, using a similar protocol to that used with SaOS-2 cells. Cells were also transfected with 'scrambled' and a cell death siRNAs as negative and positive controls respectively. Cells were treated with the siRNAs, and incubated for 6hrs at 37^{o}C, when the media was removed and replaced with either fresh complete MEMα or osteogenic supplemented medium for another 66hrs, after which they were either trypsinised and counted or treated with TRI Reagent for RNA extraction and expression analysis using RT-qPCR.

To confirm that there was successful knock down of ANRIL expression at the transcriptional level in both hBMSCs and osteoblasts, RT-qPCR assays were run using primers for exons 1-2, 5-6 and 18-19, as described in previous chapter. Results show that there was significant knock down of ANRIL expression with both siRNA treatments, however this level of reduction in ANRIL expression was exon dependent (Figures 5.1 and 5.2).

In hBMSCs, exon 1-2 expression was significantly reduced after transfection with Congrains E1 siRNA (p=0.016; Figure 5.1A) when compared to control by 1.9-fold but is unchanged when cells are treated with Congrains E19 siRNA, which targets exon 19. Exon 5-6 expression was unchanged in comparison to the control when hBMSCs are treated with either siRNA (Figure 5.1B), suggesting that ANRIL transcripts in these cells which contain the exon 5-6 boundary do not also contain exon 1 or exon 19. Expression of the exon 18-19 was significantly decreased in hBMSCs treated with both Congrains E1 siRNA (p=0.042) and Congrains E19 siRNA (p=0.0001) by 1.9-fold and 2.2-fold respectively (Figure 5.1C).

In primary osteoblasts, there was a similar effect of the siRNAs on ANRIL as seen in hBMSCs though there are slight differences (Figure 5.2). Exon 1-2 and exon 18-19 expression were significantly knocked down upon treatment with Congrains E1 siRNA (p=0.035) by 1.8-fold and 1.3-fold respectively. Treatment with Congrains E19 siRNA also caused a significant decrease in exon 1-2 expression when compared to the control by 1.3-fold (p=0.048; Figure 5.2A) and exon 18-19 by 2-fold (p=0.0014; Figure 5.2C). As with hBMSCs, there was no change in exon 5-6 expression with either Congrains E1 siRNA or Congrains E19 siRNA treatment (Figure 5.2B).

To determine whether a reduction in ANRIL expression affected cell growth, live cells were counted after a 72hr period. There were significant decreases in the number of live cells in wells treated with the positive cell death control when compared to the negative 'scrambled'

control for both hBMSCs (Figure 5.3A) and osteoblasts (Figure 5.3B). There was also a significant decrease in the numbers of hBMSCs when they were treated with each of the ANRIL siRNAs ($p<0.0001$ for both; Figure 5.3A). This was also seen in the primary osteoblasts, when treatment with Congrains E1 siRNA and Congrains E19 siRNA once again caused a significant decrease in the number of live cells ($p<0.0001$ for both; Figure 5.3B).

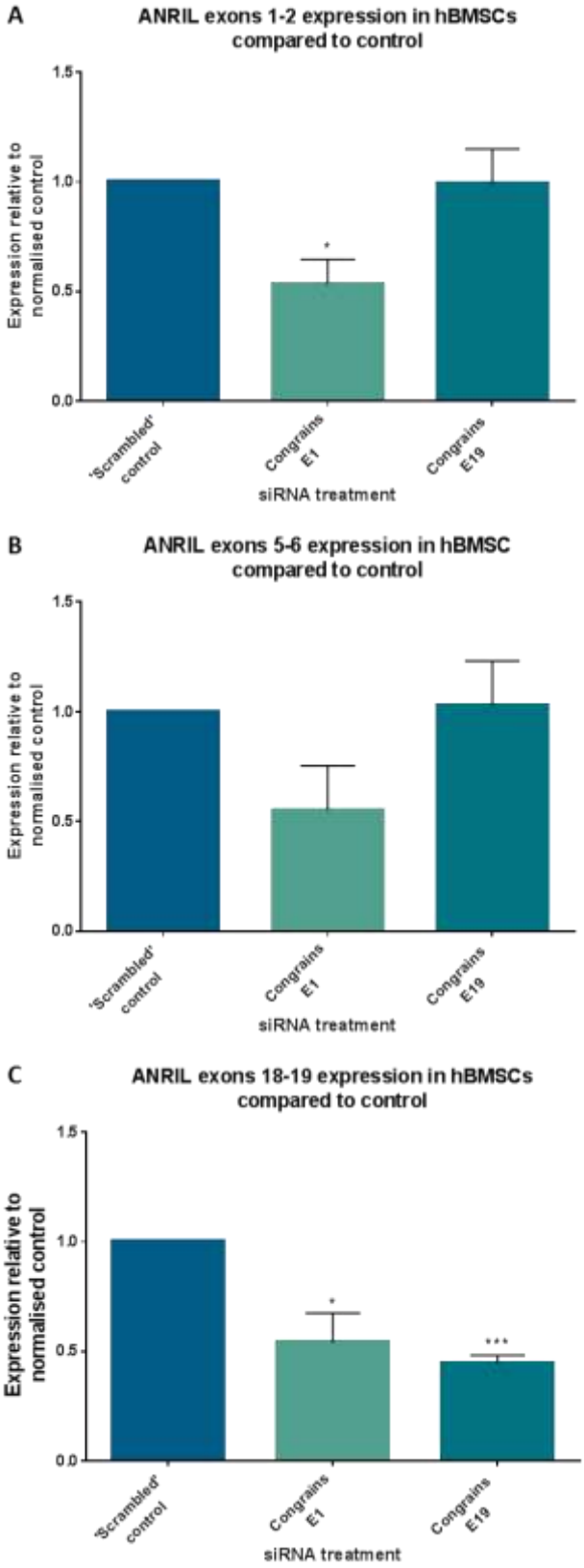

Figure 5.1: Results from RT-qPCR confirming knockdown of (A) ANRIL exons 1-2, (B) exons 5-6 and (C) exons 18-19 in transfected hBMSCs (n=5). Results shown as mean ±SEM *p≤0.05; ***p≤0.001

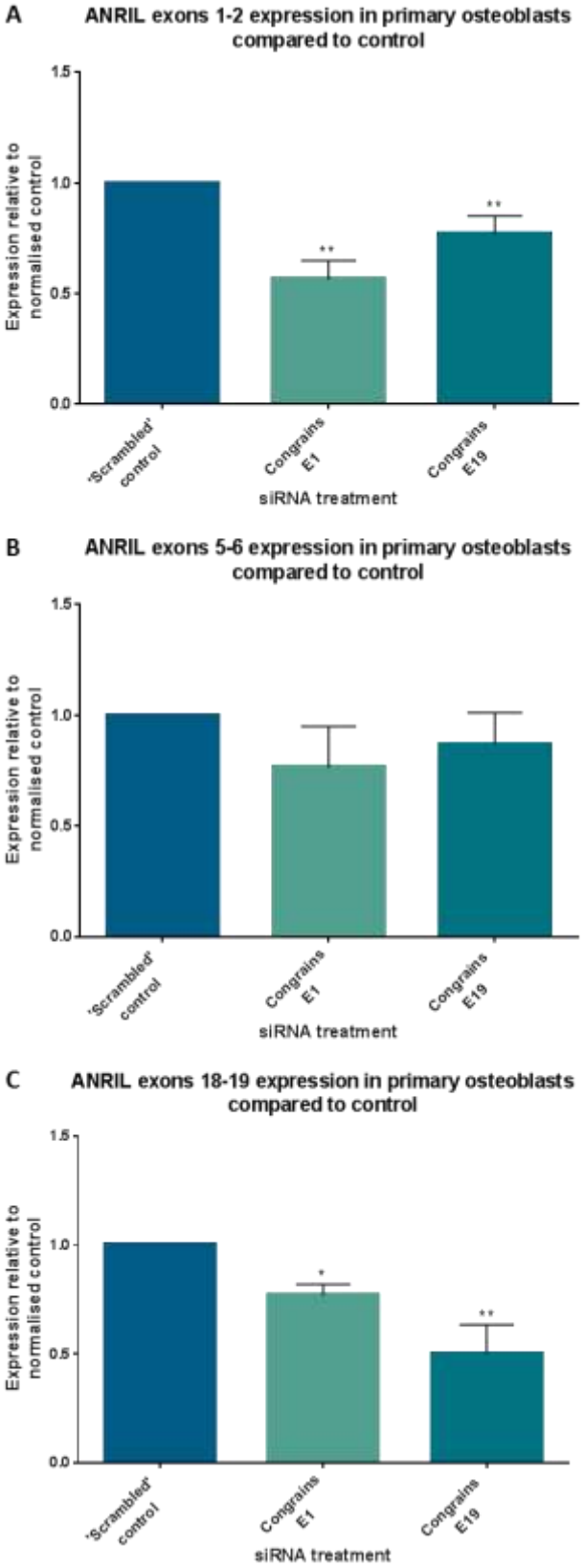

Figure 5.2: Results from RT-qPCR confirming knockdown of (A) ANRIL exons 1-2, (B) exons 5-6 and (C) exons 18-19 in transfected primary osteoblasts (n=6). Results shown as mean ±SEM *p≤0.05; **p≤0.01

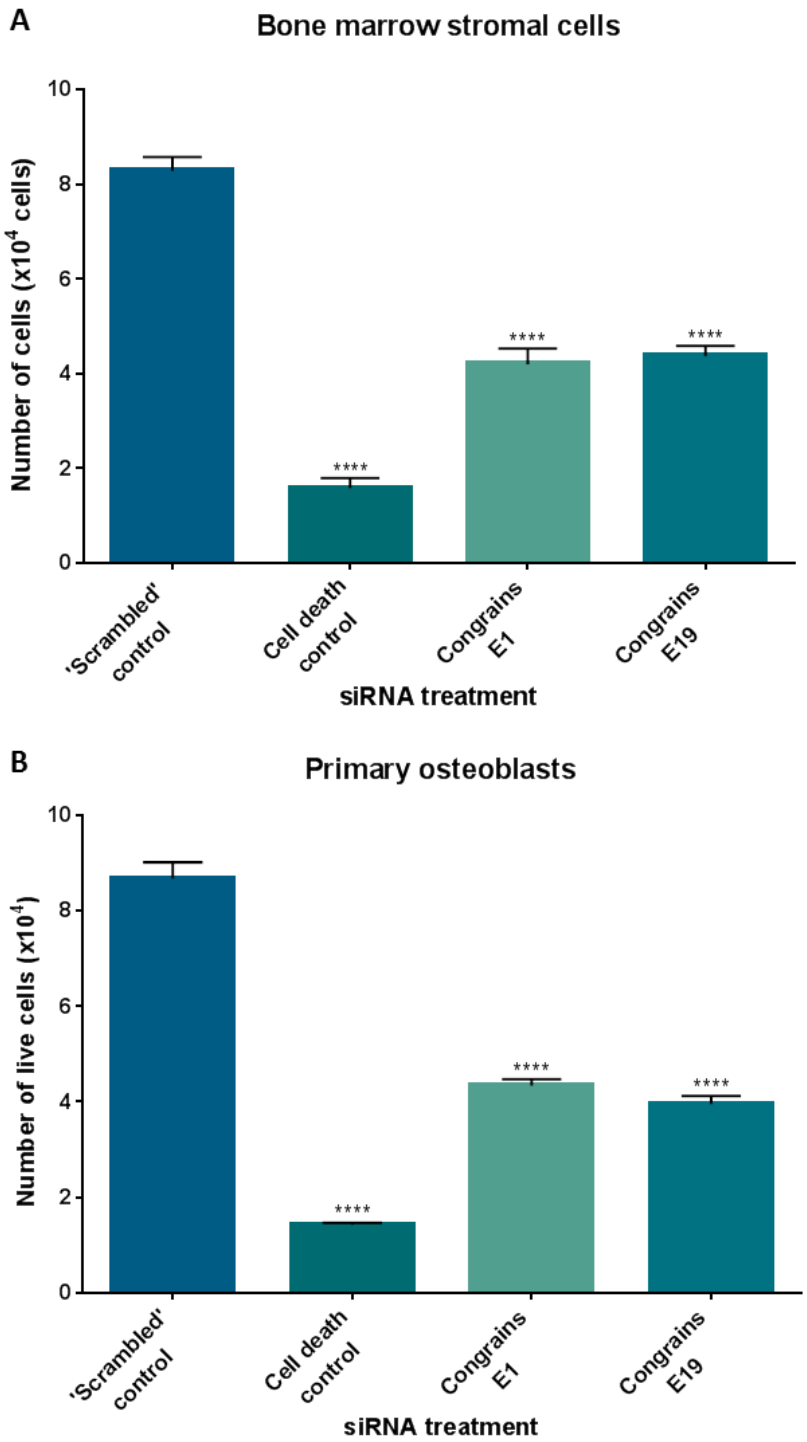

Figure 5.3: Number of live (A) human bone marrow stromal cells (n=5) and (B) human primary osteoblasts (n=6) after 72hr transfection. Cells were plated at 30,000 cells/well and were incubated with 10nM 'scrambled', cell death, Congrains E1 and Congrains E19 siRNAs for 6hrs, after which media was changed to fresh basal or osteogenic medium for the remainder of the 72hrs. Results shown as mean ±SEM ****p<0.0001

5.3.2 ANRIL knock down does not have an effect on the viability of primary cells

To investigate whether there was a decrease in cell viability, as seen in SaOS-2 cells, hBMSCs and osteoblasts were plated in 96-well plates at 5,000 cell/well and treated with 'scrambled' control, cell death control and both Congrains E1 and E19 siRNAs to determine if the knock down of ANRIL expression causes a change in cell viability. To determine the viability of the cells, each of the wells were treated with CellTiter-Glo 2.0 luciferase assay (Promega) according to manufacturer's instructions. The ATP produced by the viable metabolically active cells reacts with the luciferase to produce a luminescent signal, which was then measured using a VarioSkan Flash Luminometer to determine the number of viable cells in each well as the ATP produced is directly proportional to the number of viable cells.

hBMSCs showed a significant decrease in luminescent signal in the cells treated with the cell death control siRNA ($p=0.0005$; Figure 5.4A); however, cells treated with either Congrains E1 or Congrains E19 siRNAs did not show any significant change in luminescent signal when compared to the 'scrambled' control. The results were the same for primary osteoblasts with cells treated with the cell death siRNA also caused a significant decrease in the luminescent signal ($p<0.0001$; Figure 5.4B). As with the hBMSCs, primary osteoblasts did not show any significant change in luminescence, and therefore viability, when compared to cells treated with the 'scrambled' control. This would suggest that knock down of ANRIL does not have an effect on cell viability and that the decrease seen in cell number is not due to an increase in cell death.

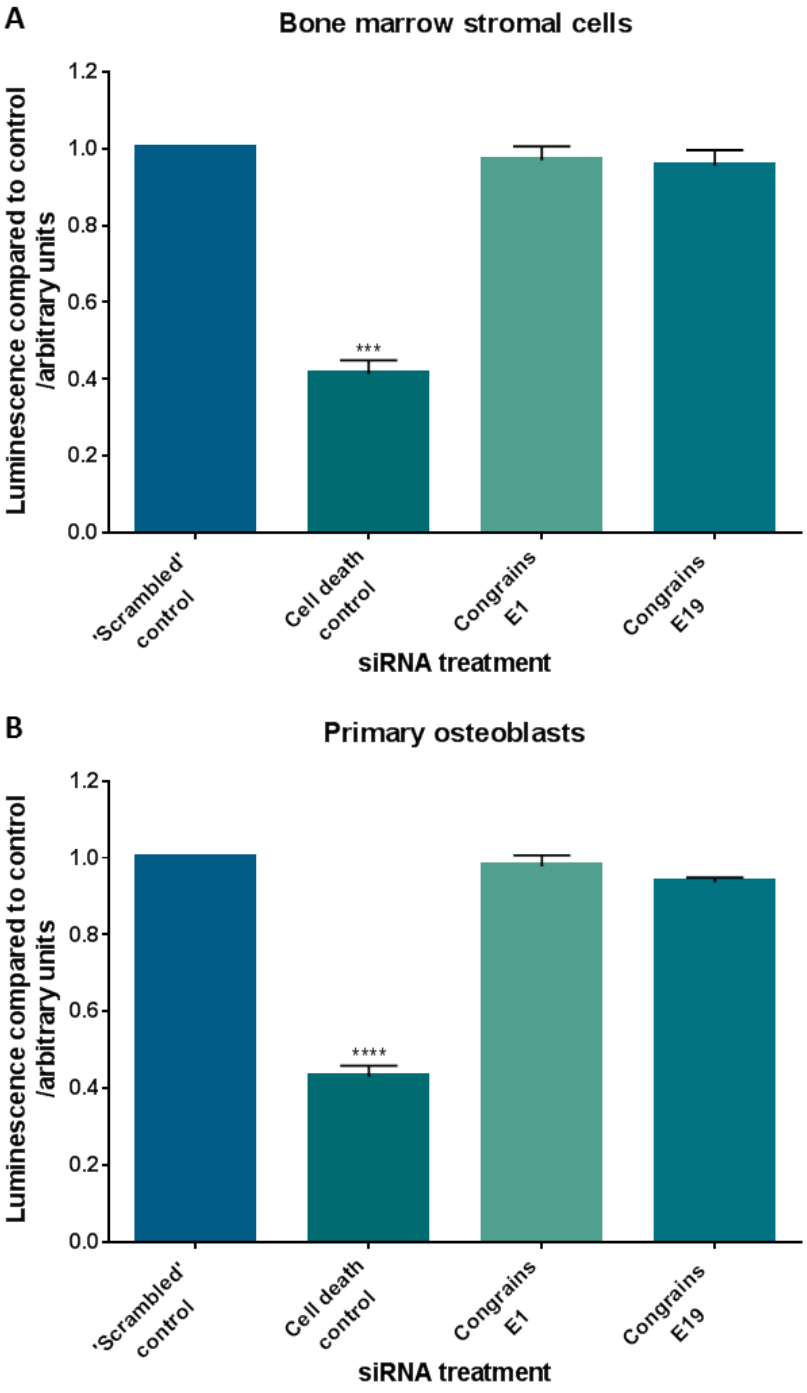

Figure 5.4: Relative luminescent signal from (A) viable hBMSC (n=5) and (B) viable primary osteoblasts (n=6) compared to control. Cells were plated in a 96-well plate at 5000 cells/well and treated with 10nM 'scrambled', cell death, Congrains E1 and Congrains E19 siRNAs for 6hrs, after which media was replaced with either fresh basal or osteogenic medium for the remainder of the 72hrs. CellTitre-Glo 2.0 luciferase assay determined the amount of viable cells via the luminescent signal detected produced by ATP metabolism. Results shown as mean ±SEM ****p≤0.0001

5.3.3 Knock down of ANRIL expression causes a decrease in the proliferation of primary cells

ANRIL knock down could be affecting the proliferation pathway, by modulating levels of the cell cycle inhibitor $p16^{INK4A}$. To determine if there is a change in the proliferation of both hBMSCs and osteoblasts upon treatment with ANRIL siRNAs, cells were plated in 96-well plates at 5,000 cells/well and treated with 10nM 'scrambled' control, cell death control, Congrains E1 or Congrains E19 siRNAs for 6hrs, after which media was replaced and cells incubated at 37^{o}C for another 66hrs. 24hrs before the end of the transfection, cells were treated with 1x BrdU reagent to allow incorporation into the DNA of proliferating cells. Cells were then analysed using the BrdU Cell Proliferation ELISA Kit (Abcam) according to manufacturer's instructions. Absorbance was determined using a plate reader at λ450nm and analysed relative to 'scrambled' control absorbance.

There is a significant decrease in the proliferation of hBMSCs treated with the cell death control siRNA ($p=0.0041$; Figure 5.5A) when compared to cells treated with 'scrambled' control. There is also a significant decrease in the proliferation of hBMSCs treated with both Congrains E1 and Congrains E19 siRNAs ($p=0.018$ and $p=0.035$ respectively). A similar effect is seen with primary osteoblasts (Figure 5.5B). Once again, the proliferation of the osteoblasts is significantly decreased in the wells treated with the cell death control siRNA ($p=0.023$). Primary osteoblasts treated with 10nM of Congrains or Congrains E19 siRNA showed a significant decrease in proliferation ($p=0.046$ and $p=0.043$ respectively).

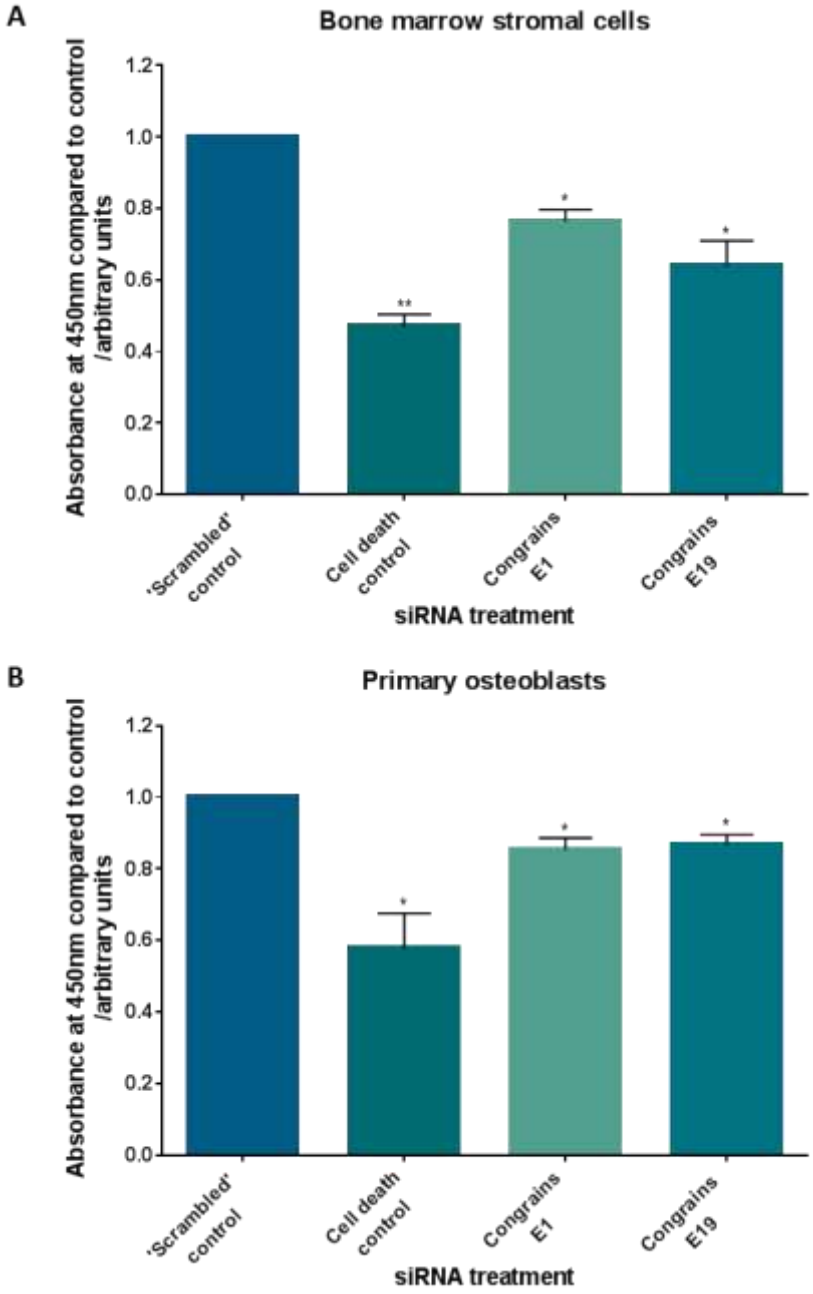

Figure 5.5: Relative absorbance of (A) viable hBMSC (n=5) and (B) viable primary osteoblasts (n=6) compared to control at λ450nm. Cells were plated in a 96-well plate at 5000 cells/well and treated with 10nM 'scrambled', cell death, Congrains E1 and Congrains E19 siRNAs for 6hrs, after which media was replaced with either fresh basal or osteogenic medium for the remainder of the 72hrs. Cells were treated with 2x BrdU 24hrs before end of transfection and incorporation of BrdU into DNA was determined through an ELISA. The amount of BrdU incorporation is used as a measure of cellular proliferation. Results shown as mean ±SEM *p≤0.05; **p≤0.01

5.3.4 Knock down of ANRIL expression causes cell cycle arrest in hBMSCs and primary osteoblasts

To determine whether this decrease in cell number was due to cell cycle arrest, FACS analysis was carried out. hBMSCs and osteoblasts were transfected with either the 'scrambled' siRNA or the two ANRIL siRNAs. After transfection cells were fixed with 70% ethanol and stained with propidium iodide. The DNA content of 5000 cells was then analysed using FACS to determine which phases of the cell cycle the cells were in.

Upon treatment with Congrains E1 and Congrains E19 siRNAs, there was a significant increase in the percentage of hBMSCs being held in G_0/G_1 phase when compared to 'scrambled' control ($p=0.045$ and $p=0.022$ respectively; Figure 5.6A). However, in transfected osteoblasts, only Congrains E19 siRNA caused an increase in the percentage of cells being held in G_0/G_1 phase compared to control ($p=0.016$; Figure 5.6B).

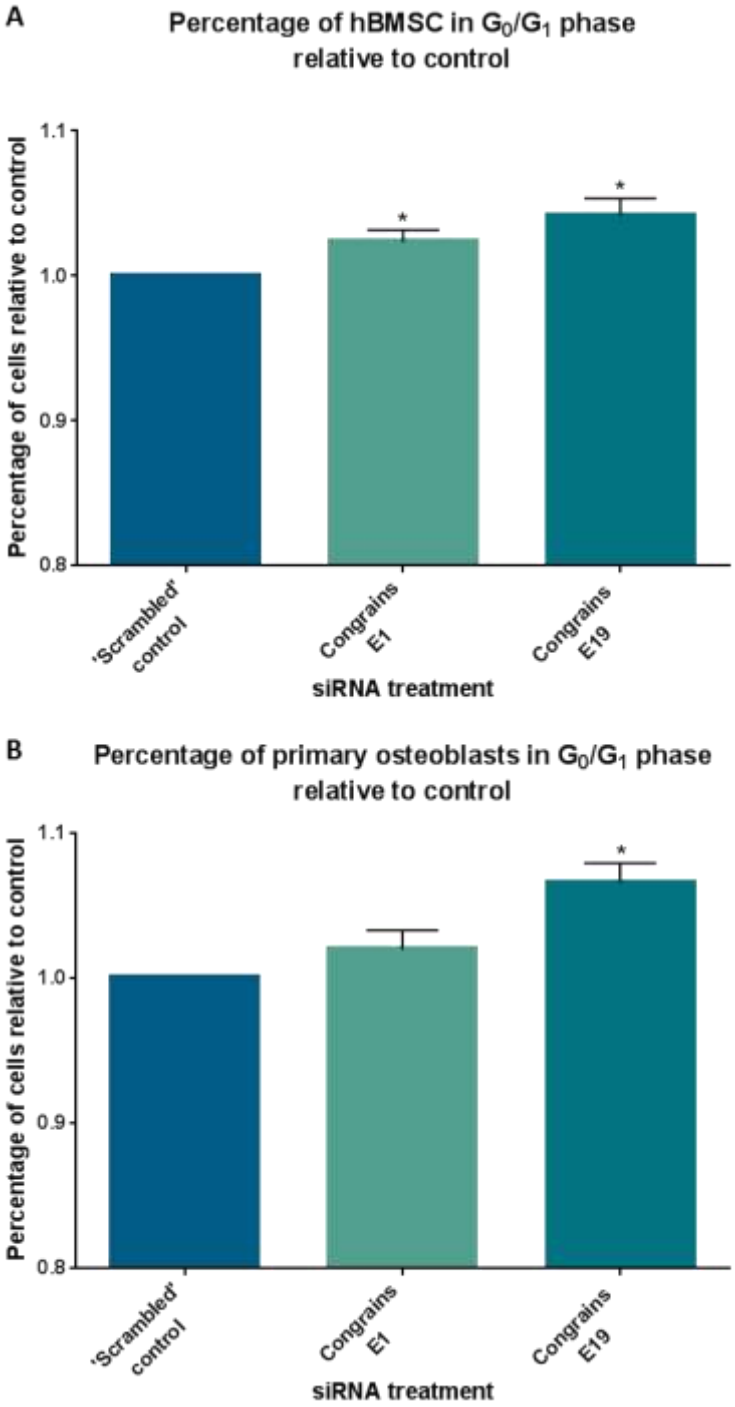

Figure 5.6: Percentage of (A) hBMSCs (n=5) and (B) primary osteoblasts (n=6) in G_0/G_1 phase relative to control determined through FACS analysis. Cells were treated with 10nM of 'scrambled', Congrains E1 and Congrains E19 siRNAs for 6hrs, after which media was changed to fresh basal or osteogenic medium for the remainder of the 72hrs. Cells were collected, lysed and DNA was stained with propidium iodide. The DNA content of 5000 cells was then analysed using FACS to determine which stage of the cell cycle the cells were in. Results shown as mean ±SEM. *p≤0.05

5.3.5 Does ANRIL mediate its affect through altered expression of the *CDKN2A/B* locus in primary cells?

To determine whether the decrease in proliferation rate seen in primary cells is due to an increase in the expression of the cell cycle inhibitors $p16^{INK4A}$ and $p15^{INK4B}$, RT-qPCR was used to see what affect ANRIL knockdown had on the expression of these transcripts.

Knock down of ANRIL expression in hBMSCs had no effect on $p16^{INK4A}$ when cells are treated with either siRNA (Figure 5.7A), however transfection of hBMSCs with Congrains E1 siRNA, caused a significant decrease in $p15^{INK4B}$ expression ($p=0.039$; Figure 5.7B). In primary osteoblasts, neither Congrains E1 siRNA nor Congrains E19 siRNA mediated knockdown of ANRIL expression lead to a change in $p16^{INK4A}$ (Figure 5.8A) or $p15^{INK4B}$ expression (Figure 5.8B).

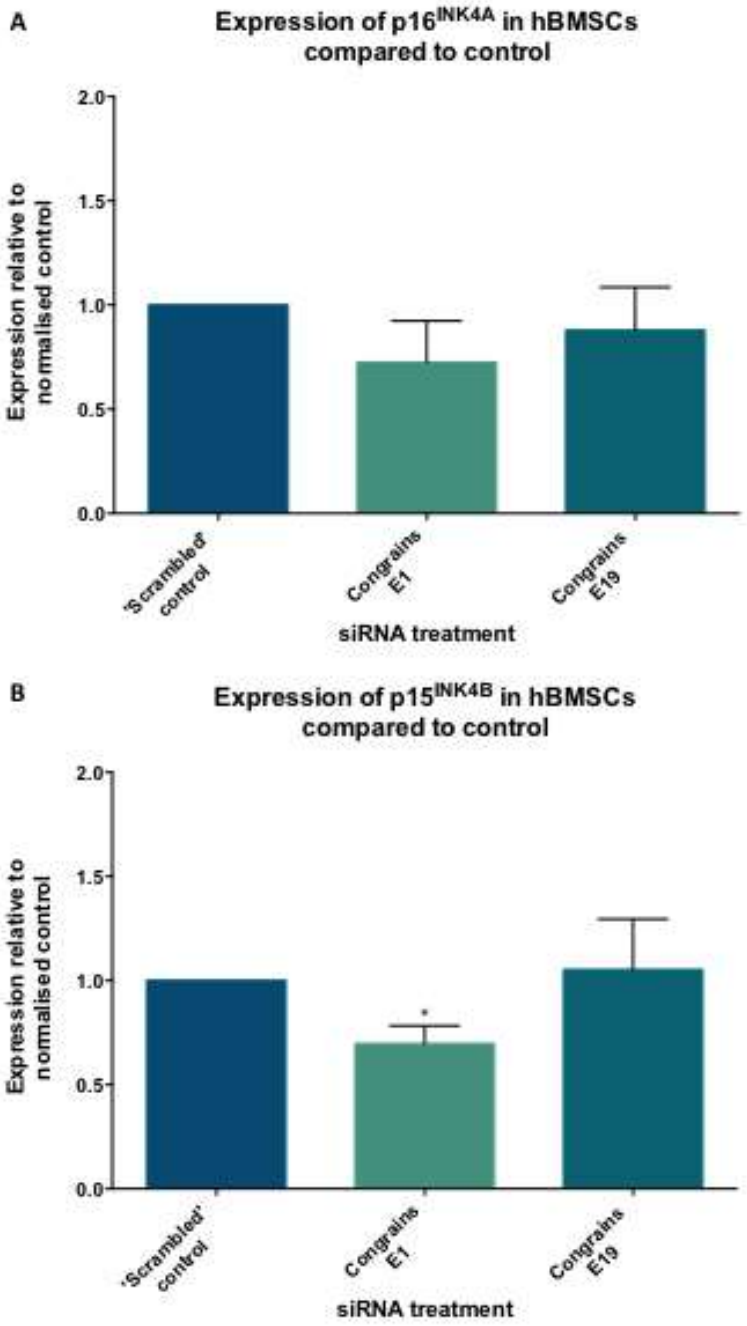

Figure 5.7: Expression of $p16^{INK4A}$ (A) and $p15^{INK4B}$ (B) in hBMSCs after knock down of ANRIL expression (n=5). Cells were plated in a 96-well plate at 5000 cells/well and treated with 10nM 'scrambled', cell death, Congrains E1 and Congrains E19 siRNAs for 6hrs, after which media was replaced with either fresh basal or osteogenic medium for the remainder of the 72hrs. There is no change in $p16^{INK4A}$ expression with either siRNA treatment, but there is a decrease in $p15^{INK4B}$ expression only with Congrains E1 siRNA treatment (p=0.039).

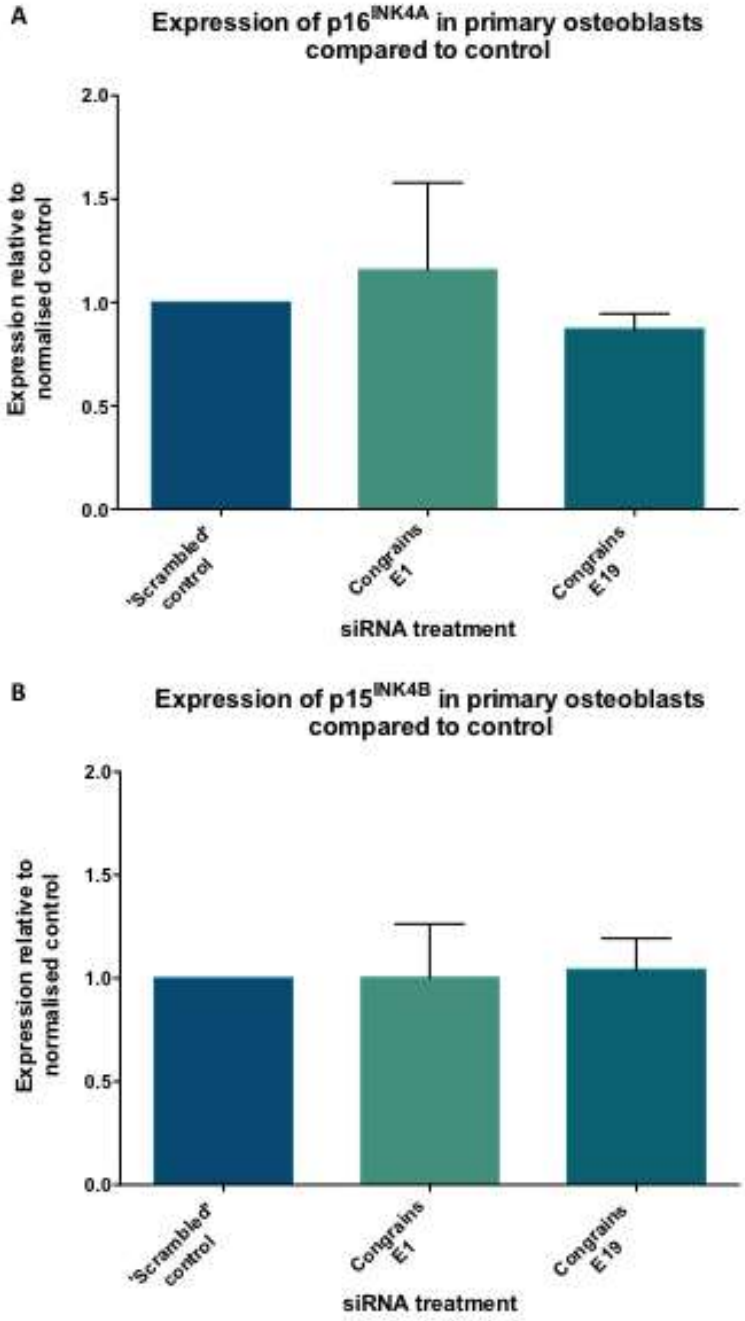

Figure 5.8: Expression of $p16^{INK4A}$ (A) and $p15^{INK4B}$ (B) in human primary osteoblasts after knock down of ANRIL expression (n=6). Cells were plated in a 96-well plate at 5000 cells/well and treated with 10nM 'scrambled', cell death, Congrains E1 and Congrains E19 siRNAs for 6hrs, after which media was replaced with either fresh basal or osteogenic medium for the remainder of the 72hrs. There is no change in either $p16^{INK4A}$ or $p15^{INK4B}$ expression with either of the siRNA treatments

5.3.6 hBMSCs and primary osteoblasts treated with siRNAs against ANRIL are not undergoing replicative senescence

To confirm whether hBMSCs (n=5) and primary osteoblasts (n=6) were becoming senescent or not, cells were stained for senescence-associated β-galactosidase (SA β-galactosidase). After primary cells had been treated with 'scrambled', Congrains E1 and Congrains E19 siRNAs, cells were incubated overnight with X-gal (20mg/mL) after 72hrs. Cells were then examined under the microscope for the presence of a blue precipitate that results from the cleavage of X-gal, signalling that there is SA β-galactosidase activity. As the assay is carried out at pH6, only the cells that have become senescent will stain blue, any immortal, quiescent or presenescent cells will remain unstained.

When both hBMSCs and primary osteoblasts are stained for senescence-associated β-galactosidase activity after treatment with 10nm 'scrambled', Congrains E1 and Congrains E19 siRNAs, there is no visible difference in β-galactosidase activity between the different treatments in either of the primary cell types (Figure 5.9), though there is visibly less staining when compared to positive control cells. This would suggest that neither the hBMSCs nor the primary osteoblasts are undergoing senescence when ANRIL expression is knocked down.

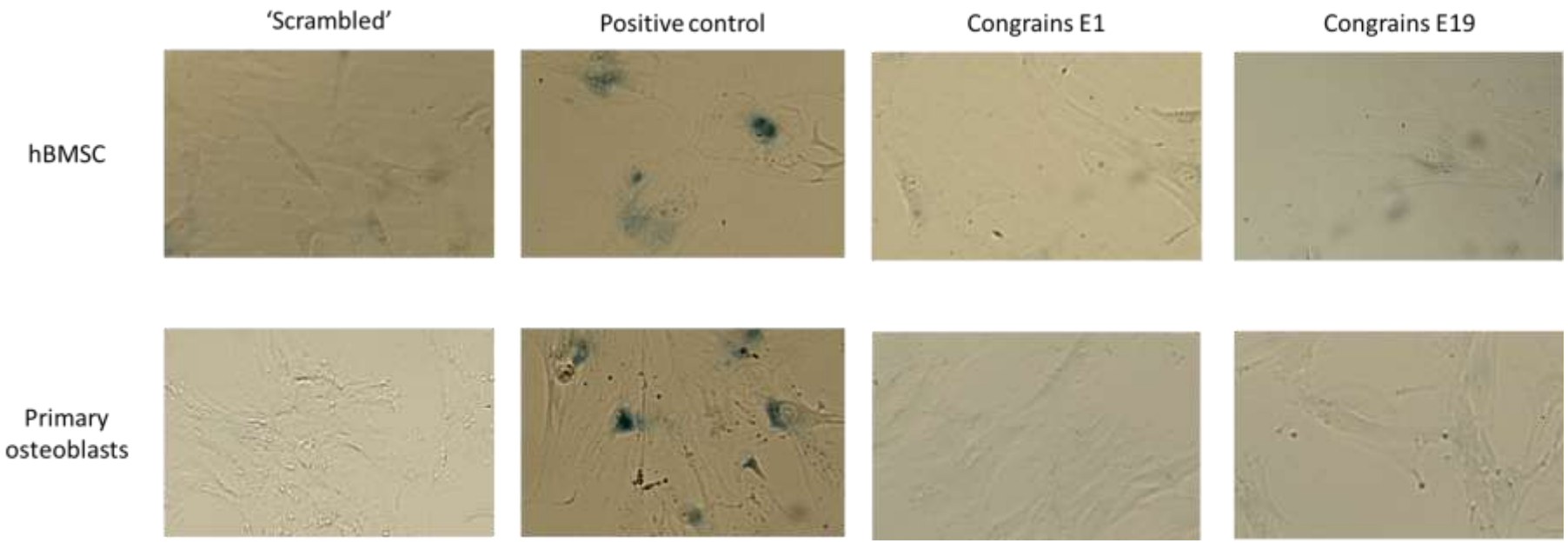

Figure 5.9: Senescence-associated β-galactosidase activity of hBMSCs and primary osteoblasts treated with 'scrambled', Congrains E1 and Congrains E19 siRNAs for 6 hours. Cells were stained at 72hrs according to manufacturer's instructions. There is no obvious visible increase in β-galactosidase activity indicated by presence of a blue precipitate between the different cell types across the three treatments. hBMSCs and primary osteoblasts at passage 10 were used as a positive control. 'n' is 5 for hBMSCs and 6 for primary osteoblasts.

5.4 Discussion

To determine the effect of reducing ANRIL expression in primary human bone marrow stromal cells and primary human osteoblasts, cells were transfected with two siRNAs against ANRIL (Congrains E1 and Congrains E19) and the effect on cell number, cell cycle stage, viability and proliferation assessed. Congrains E1 and E19 siRNAs were used in the primary cells, as these were shown to have the strongest effects in previous experiments. The Ambion E1 siRNA, used in SaOS-2 cells, was not used in these experiments due to the constraints in growing large numbers of primary cells and keeping the passage number low. Although hBMSCs were used, which represent a heterogeneous population of cells comprising of stem cells, osteoprogenitors, chondroprogenitors, osteoblasts, fibroblasts, etc, these cells did not show any positive alkaline phosphatase staining (as shown in Chapter 2; Figure 2.1) and preliminary testing showed that results between hBMSCs and STRO1+ selected stem cells were not different between the two cell populations.

Transfection with siRNAs directed against exons 1 and 19 of ANRIL induced a decrease in ANRIL expression in both hBMSCs and primary osteoblasts. Only Congrains E1 effectively reduced ANRIL exon 1-2 expression in hBMSCs, however in primary osteoblasts both the Congrains E1 and E19 induced a decrease in exon 1-2 expression. This would suggest that different transcripts might be expressed in the different cell types and that in hBMSCs those transcripts, which contain exon 1, do not contain exon 19, whereas in primary osteoblasts those that contain exon 1 also contain exon 19. Transfection of SaOS-2 cells with the siRNAs induced a similar pattern, with both siRNAs inducing a decrease in exon 1 and exon 19 expression, which is consistent with report that SaOS-2 expression analysis shows a similar profile to that of primary osteoblasts (290). Both Congrains E1 and Congrains E19 siRNAs were found to also reduce expression of ANRIL exons 18-19 containing transcripts in both primary cell types, which is consistent with the earlier findings.

Interestingly, neither Congrains E1 nor E19 affected the expression of ANRIL exon 5-6 transcripts in either hBMSCs or primary osteoblasts suggesting that those transcripts containing exons 1 and exon 19 do not contain the exons 5/6. Previous studies have shown that some ANRIL transcripts do not contain exon 5/6 (238) and Holdt *et al* have discovered a novel ANRIL transcript in PBMCs that does not contain either exon 5 or 6 but does contain exons 1 and 19 (282). However, results of cell line assay from Chapter 3 do show that some of the ANRIL transcripts in hBMSCs and primary osteoblasts do express the exon 5-6 boundary, but these may be a minor proportion of the transcripts containing exon 5-6.

Treatment with Congrains E1 and E19 caused a significant decrease in ANRIL expression in hBMSCs and primary osteoblasts; however, the expression levels of the exon 18-19 boundary was not reduced by the same fold across the two siRNA treatments. In hBMSCs, Congrains E1 reduced

expression by 1.9-fold and Congrains E19 by 2.2-fold and in primary osteoblasts Congrains E1 caused a 1.3-fold decrease in expression and Congrains E19 a 2-fold decrease; however, in both cases, there is no significant difference between the knock down in expression cause by both ANRIL siRNAs. In hBMSCs as exon1-2 expression was only knocked down by Congrains E1 treatment, whereas exon 18-19 expression was knocked down by both, this would suggest that some transcripts which exon 19 also contain exon 1, whereas others do not. Though the majority of ANRIL transcripts do contain exon 1, there are a few that are known to lack this exon (238). However, in primary osteoblasts, as exon 1-2 and exon 18-19 expression is reduced in the presence of both Congrains E1 and E19 siRNAs, it would suggest that the majority of ANRIL transcripts in this cell type contain both exon 1 and exon 19.

A reduction in ANRIL expression induced a significant decrease in both hBMSC and osteoblast cell number when treated with either Congrains E1 or E19 ANRIL siRNAs against ANRIL; however, this does not seem to be caused by an increase in cell death, as the cell viability assay did not show an increase in the number of cells undergoing apoptosis. The FACS data for both cell types showed a significant increase in the number of cells being held in the G_0/G_1 phase of the cell cycle, except for primary osteoblasts treated with the Congrains E1 siRNA, which would suggest that the cell are exiting the cell cycle or that they could be undergoing premature senescence. The BrdU incorporation assay confirmed that the proliferation rate of the cells was decreased in both primary cell types with both siRNA treatments, which we would expect when ANRIL expression is knocked down as this lncRNA, as stated previously, negatively regulates cell cycle inhibitors and would be caused by cell cycle exit or when cells become senescent. However, $p16^{INK4A}$ expression, a marker for senescence and cell cycle arrest, is not increased in either of the primary cell types upon ANRIL knockdown and when cells are stained for senescence-associated β-galactosidase activity, there is no visible difference between control and ANRIL siRNA treated cells.

A gene expression profile carried out by Jia *et al* has revealed the top 30 transcripts that are expressed in hBMSCs. Out of these 30 genes, 13 have a role in cell structure/motility, 13 a role in cell signalling and communication, 2 that are related to gene/protein expression and 2 whose roles are unknown (311). These genes include transforming growth factor β-induced (TGFBI), fibronectin, osteonectin and many members of the collagen family. Certain proteins on this list have been shown to have a role in regulating cell cycle or proliferation such as fibronectin and TGFBI. TGFBI has been shown in mice to have an effect on cell proliferation by Zhang *et al*. When mice are deficient in *TGFBI* it leads to an increased rate of proliferation, which is caused by unregulated activation of the CREB-Cyclin D1 pathway (312). However, when TGFBI protein is

reintroduced to the cells, the activation of the CREB cycle becomes suppressed, as does cyclin D1 expression. Fibronectin has also been shown to inhibit the terminal differentiation of human keratinocytes (313), which could potentially suggest a role for fibronectin in preventing the differentiation of hBMSCs. If ANRIL has a role in regulating either of these pathways, it could explain why there is a decrease in cell number and proliferation rate with the knock down of ANRIL expression.

Unexpectedly, $p15^{INK4B}$ expression does not increase when ANRIL expression is knocked down and, as ANRIL is the antisense sequence to this gene, we would expect an increase in expression. Similarly to what was seen with SaOS-2 cells, there is a decrease in $p15^{INK4B}$ expression when hBMSCs are treated with the Congrains E1 siRNA. This could be because the decrease in ANRIL expression allows for the recruitment of other repressive complexes to the $p15^{INK4B}$ locus. Both Basu *et al* and Staller *et al* have demonstrated that $p15^{INK4B}$ expression is suppressed through interactions of two different proteins with Myc-interacting zinc finger protein-1 (Miz-1): Gfi-1 and Myc (314,315). Both of these groups showed that, when these proteins are recruited to the *CDKN2B* gene locus and form a complex with Miz-1, there is a decrease in $p15^{INK4B}$ expression.

It is clear that the effects we see on cell number, cell proliferation and cell cycle phase due to the knock down of ANRIL do not primarily occur through the *cis*-function of regulating the *CDKN2A/B* gene locus. This would suggest that ANRIL could be having some *trans*-functional effects in both hBMSCs and primary osteoblasts.

5.5 Summary

We sought to demonstrate that knock down of ANRIL expression in hBMSCs and primary osteoblasts had similar effects to those observed in SaOS-2 cells. Our results show that when ANRIL expression is knocked down in both hBMSCs and primary osteoblasts there is a decrease in cell number and proliferation rate with both siRNA treatments; however in primary osteoblasts only the Congrains E19 siRNA caused an increase in the number of cells being held in the G_0/G_1 phase of the cell cycle, whereas both Congrains E1 and Congrains E19 cause this effect in hBMSCs. Cell viability was unaffected, which informs us that a decrease in ANRIL expression does not lead to an increase in apoptosis in these two cell types.

We determined through RT-qPCR and senescence-associated β-galactosidase staining that the cells were not becoming senescent as there was no increase in either $p16^{INK4A}$ or $p15^{INK4B}$, both markers of senescence, and cells did not stain positive for β-galactosidase activity. However, $p15^{INK4B}$ expression did decrease in hBMSCs treated with Congrains E1, which suggests that with

ANRIL expression knocked down, this could allow for other repressive complexes to be recruited to CDKN2B and suppress $p15^{INK4B}$ expression.

These results suggest ANRIL could have a potential *trans*-functional role in these two cell types, as knock down of ANRIL expression does not seem to have an effect on *CDKN2A/B* gene expression. In order to determine whether ANRIL has any effects elsewhere in the genome, RNA samples from cells treated with siRNAs against ANRIL can be analysed with a gene expression array to see if this knock down causes a change in the expression of any other genes.

5.6 Further work

A way to continue this work further would be to stably transfect hBMSCs with an ANRIL siRNA and then try to differentiate these cells in primary osteoblasts to determine whether ANRIL has a potential role during this process. We could also introduce an ANRIL construct into both cell types to see what effect ANRIL overexpression would have on the cells, if any.

The results presented in this chapter hint that there may potentially be different ANRIL transcripts expressed in the different cell types. It could be interesting to determine what the sequences of these transcripts actually are as ANRIL expression has not previously been investigated in hBMSCs or bone cells thoroughly. This could potentially be done through rapid amplification of cDNA ends (RACE), which would allow for the transcripts to be amplified so that they could be sent off for sequencing. Another way of looking at currently known ANRIL transcript expression would be through a literature search for ANRIL PCR primers and running them with DNA from hBMSCs and primary osteoblasts. This would allow us to determine what transcripts are being expressed in these bone-related cells.

It would also be interesting to determine the effect that ANRIL has on MSC differentiation into osteoblasts, if any. To do this, ANRIL siRNA would be transfected into hBMSCs using a lentiviral vector, which would allow for a stable transfection. A transient transfection could not be used for this experiment, as the differentiation process takes longer than three days, which is the maximum time that a transient transfection has an effect. This would allow us to determine if a reduction in ANRIL expression has an adverse effect on the development of osteoprogenitors and mature osteoblasts.

Chapter 6
Effects of ANRIL knock down on gene expression in primary human osteoblasts

6.1 Introduction

The down regulation of ANRIL expression in both SaOS-2 cells and primary human osteoblasts leads to a decrease in cell number and a decrease in proliferation; however this was not accompanied by an increase in $p16^{INK4A}$ expression. ANRIL has been reported to function both in *cis* and in *trans*. In *cis*, ANRIL can act by down regulating the expression of $p15^{INK4B}$ and $p16^{INK4A}$ by recruiting PRCs to the promoters of the *CDKN2A/B* gene locus and causing trimethylation of lysine 27 of histone 3 (243,283). This prevents the binding of transcriptional machinery and so suppresses $p16^{INK4A}$ and $p15^{INK4B}$ expression, thus preventing cell cycle progression. ANRIL also regulates $p15^{INK4B}$ through an antisense mechanism where it binds directing to its complementary sequence in the *CDKN2B* locus and prevents the transcription of this gene (288). In *trans*, ANRIL has been shown to regulate genes that are involved in atherogenic pathways and are not found on the chromosome as *CDKN2A*.

Trans-regulation is defined as intermolecular interactions where gene products regulate the expression of distant genes, for example, genes that encode transcription factors, as opposed to *cis*-regulation, where the gene acts in an intramolecular fashion to regulate the action of the same molecule or the same gene (316,317). It has been suggested that a potential function of lncRNAs is to act as *trans*-regulators of transcription. One well characterised lncRNA that acts in this way is HOX transcript antisense RNA (HOTAIR). This lncRNA is transcribed from the *HOXC* gene located on chromosome 12 and was the first lncRNA to be shown to influence transcription on another chromosome (190). Rinn *et al* found that, through interactions with PCR2, HOTAIR repressed the expression of *HOXD* found 40 kilobases away from *HOXC* on chromosome 2 via chromatin remodelling (279).

Although there are not any studies looking at a potential *trans*-function of the lncRNA ANRIL specifically in bone differentiation or homeostasis, there have been studies suggesting that ANRIL may have a *trans*-regulatory role in other tissues. In HeLa cells, Sato *et al* have suggested that a novel isoform of ANRIL may be involved in the regulation of the nucleus (277). When this isoform was overexpressed in these cells, using gene ontology enrichment analysis, it was found that the expression of 38 genes involved in nucleus regulation were altered – 36 genes were down regulated and 2 genes were upregulated. However, it was not definitively shown that ANRIL was specifically binding to the promoters of the genes that showed differential expression. This could mean that the changes observed could be $p16^{INK4A}$ and $p15^{INK4B}$ dependent. Holdt *et al* have also demonstrated through overexpression of certain ANRIL transcripts, that ANRIL *trans*-regulates genes that are involved in cellular adhesion, cellular proliferation and apoptosis. Through ChIP assays they also revealed that these *trans*-regulatory effects were dependent on Alu motifs in the promoters of target genes (282). This group postulated that ANRIL acts as a scaffold for PRC1 and

2 through binding to CBX7 and SUZ12 respectively and that ANRIL then directs epigenetic changes to chromatin by binding to Alu elements found in the promoters of target genes. These data suggest that Alu elements could be essential for ANRIL binding to *trans*-regulated target genes.

6.2 Aims

In primary osteoblasts, although ANRIL induced a decrease in cell proliferation and cell number, there was no effect on $p16^{INK4A}$ expression, suggesting that these effects may be induced via ANRIL acting in *trans*. To determine, therefore, what genes and pathways were affected by a decrease in ANRIL expression, RNA was extracted from osteoblasts that had been treated with 'scrambled' and Congrains E1 siRNAs and mRNA expression in these samples was analysed using the Illumina Human HT12 Gene Expression Array.

6.3 Results

6.3.1 Validation of Illumina Human H12 Gene Expression Array results

To determine whether knock down of ANRIL had an effect on gene expression in human primary osteoblasts, RNA from primary osteoblasts treated with 'scrambled' and Congrains E1 siRNAs (n=5) was analysed using Illumina Human H12 Gene Expression Array (Genome Centre, Barts and the London Medical School). After QC and normalisation, the Genome Centre performed signal extraction, and AVG_Signal and Detection_Pvalue values were obtained for each of the 47,229 probes on the array. Only the 14,757 probes that achieved detection p-value <0.05 in all ten samples were retained for analysis. Paired *t*-tests were performed by Prof Joanna Holbrook on AVG_Signal values to determine the probes varying by treatment within each cell line pair. 274 probes (mapping to 260 unique genes) were significantly differentially expressed with respect to treatment after multiple testing correction (FDR corrected p-value<0.05), of these 128 were upregulated and 132 were down regulated. The top twenty upregulated and down regulated genes that showed the greatest fold change are shown in Table 6.1. All genes that were shown to have significant differential expression after multiple testing correction are shown in Appendix, Table 9.1.

UPREGULATED GENES				DOWNREGULATED GENES			
Gene	Fold Change	p-value	False Discovery Rate	Gene	Fold Change	p-value	False Discovery Rate
BCYRN1	2.14	0.000828	0.0496	ETS1	-2.30	0.000375	0.0440
PTGES	2.05	3.49E-05	0.0395	CAV2	-2.03	7.71E-05	0.0408
LSM14A	1.91	0.000414	0.0440	CPD	-1.97	0.000801	0.0496
OLFML3	1.89	0.000742	0.0496	PLEKHB2	-1.92	0.000272	0.0416
HIF1A	1.83	0.000864	0.0496	GALC	-1.78	0.000103	0.0408
IL10RB	1.81	0.000653	0.0496	ATP2B1	-1.74	0.000432	0.0440
NT5DC2	1.79	0.00027	0.0416	HOXA9	-1.72	0.000381	0.0440
TOP1MT	1.75	0.000138	0.0408	HDDC2	-1.71	0.000105	0.0408
CHPF	1.74	0.000132	0.0408	NIN	-1.67	1.35E-05	0.0395
LAMP2	1.73	0.000801	0.0496	GMFB	-1.67	1.46E-05	0.0395
ROD1	1.71	5.11E-05	0.0395	TFPI	-1.66	0.000179	0.0408
POLR3E	1.68	0.000155	0.0408	NQO1	-1.63	0.000378	0.0440
SCAMP1	1.67	0.000692	0.0496	EIF4EBP2	-1.63	0.000852	0.0496
GAMT	1.65	0.000704	0.0496	C2ORF28	-1.59	0.000652	0.0496
ATP11C	1.64	0.00039	0.0440	EAF1	-1.57	0.000289	0.0425
MAPK3	1.62	0.000798	0.0496	ARL8B	-1.57	0.000792	0.0496
SAR1B	1.62	0.000612	0.0494	PIGA	-1.54	0.000904	0.0496
IGF2	1.62	0.000466	0.0458	ZFYVE26	-1.53	0.00014	0.0408
IPO11	1.58	0.000254	0.0416	TWSG1	-1.49	0.000203	0.0408
TLN1	1.58	0.000151	0.0408	CYR61	-1.46	0.000614	0.0494

Table 6.1: Twenty upregulated and twenty down regulated genes with the highest fold changes. Of the 136 upregulated genes and the 138 downregulated genes, the ones listed above showed the greatest fold change with an FDR corrected p-value ≤0.05.

In order to validate the results from the array, RT-qPCR was used to determine whether the changes in expression between the treatment and control group seen in the array can be replicated using a different platform. Interestingly, the array did show that the expression of both $p16^{INK4A}$ and $p15^{INK4B}$, were unaffected by a decrease in ANRIL expression. This agreed with what has been shown in the previous chapter using RT-PCR in that $p16^{INK4A}$ and $p15^{INK4B}$ expression was unchanged in osteoblasts upon treatment with siRNA against ANRIL (Section 5.3.5).

Six genes were selected for validation based on their known associations with osteoblast regulation or bone homeostasis and the level of differential gene expression. The upregulated gene chosen for validation were HIF1A, MAPK3 and IGF2 and the down regulated genes were ETS1, TWSG1 and CYR61 from the list of down regulated genes were chosen to validate the array data. RT-qPCR analysis showed that treatment with Congrains E1 siRNA caused an increase in the expression HIF1A (Figure 6.1A), IGF2 ($p=0.043$; Figure 6.1B) and MAPK3 ($p=0.032$; Figure 6.1C), although HIF1A only showed a trend towards significance ($p=0.09$). The change in expression was in the same direction as that shown on the array, though the fold differences were not replicated. On the array both IGF2 and MAPK3 showed a 1.62-fold increase in gene expression when cells were treated with Congrains E1 siRNA, whereas using RT-qPCR demonstrated a 3.6-fold increase in IGF2 expression and a 2.8-fold increase in MAPK3 expression. When the change in gene expression was examined in the down regulated genes, only ETS1 expression was significantly decreased between the Congrains E1 siRNA treated cells and the control cells (Figure 6.1D), whereas both CYR61 and TWSG1 did not reach significance (Figure 6.1E and 6.1F respectively), although CYR61 showed a trend towards significance in the same direction as shown on the array ($p=0.066$). The fold changes of ETS1 gene expression between the array and RT-qPCR did not replicate as the fold expression for this gene on the array was -2.3-fold decrease, whereas the fold change determined by RT-qPCR was -1.3-fold decrease.

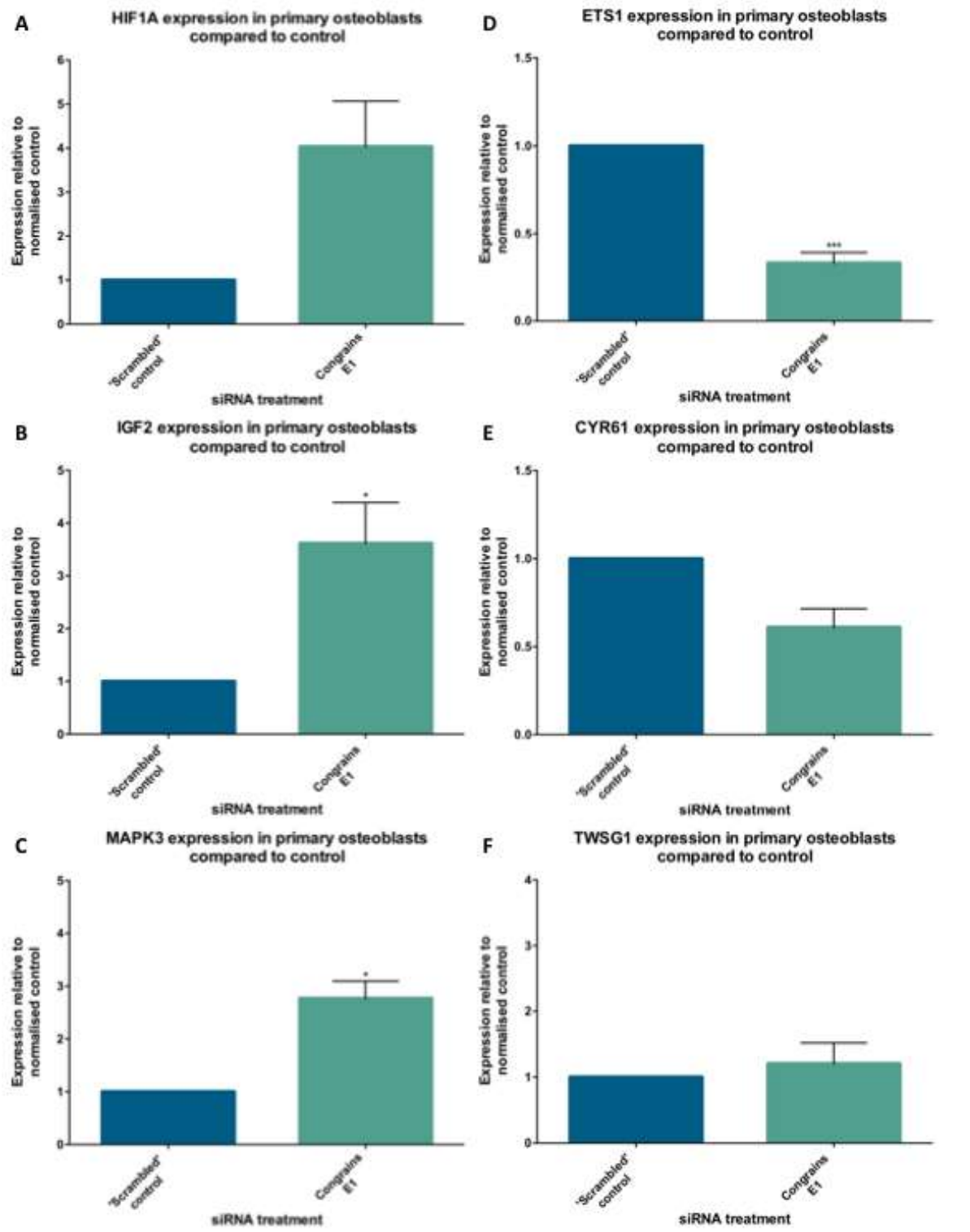

Figure 6.1: Gene expression levels of (A) HIF1A, (B) IGF2, (C) MAPK3, (D) ETS1, (E) CYR61 and (F) TWSG1 in primary osteoblasts compared to control when cells have been treated with a siRNA against exon 1 of ANRIL. Treatment with Congrains E1 siRNA caused an increase in IGF2 and MAPK3 expression and caused a decrease in ETS1 expression. This agrees with what was shown on the Illumina Human H12 array. Results shown as mean ±SEM **p≤0.01; *p≤0.05. n=5

Expression of these genes were also examined in primary osteoblasts that had been treated with Congrains E19 siRNA, which targets exon 19 of ANRIL, as treatment with this siRNA had also been shown to have an effect on primary osteoblast cell proliferation and cell number. Treatment with this siRNA caused a significant increase in both HIF1A ($p=0.0015$; 2.1-fold increase) and IGF2 expression ($p=0.044$; 2.7-fold increase), but MAPK3 expression was unchanged. In the genes that demonstrated down regulation on the array, there was a significant decrease in ETS1 ($p=0.013$; -2.1-fold decrease) and CYR61 expression ($p=0.041$; -2.4-fold decrease) and a significant increase in TWSG1 expression ($p=0.0085$; 3.3-fold increase), when cells were treated with Congrains E19 siRNA.

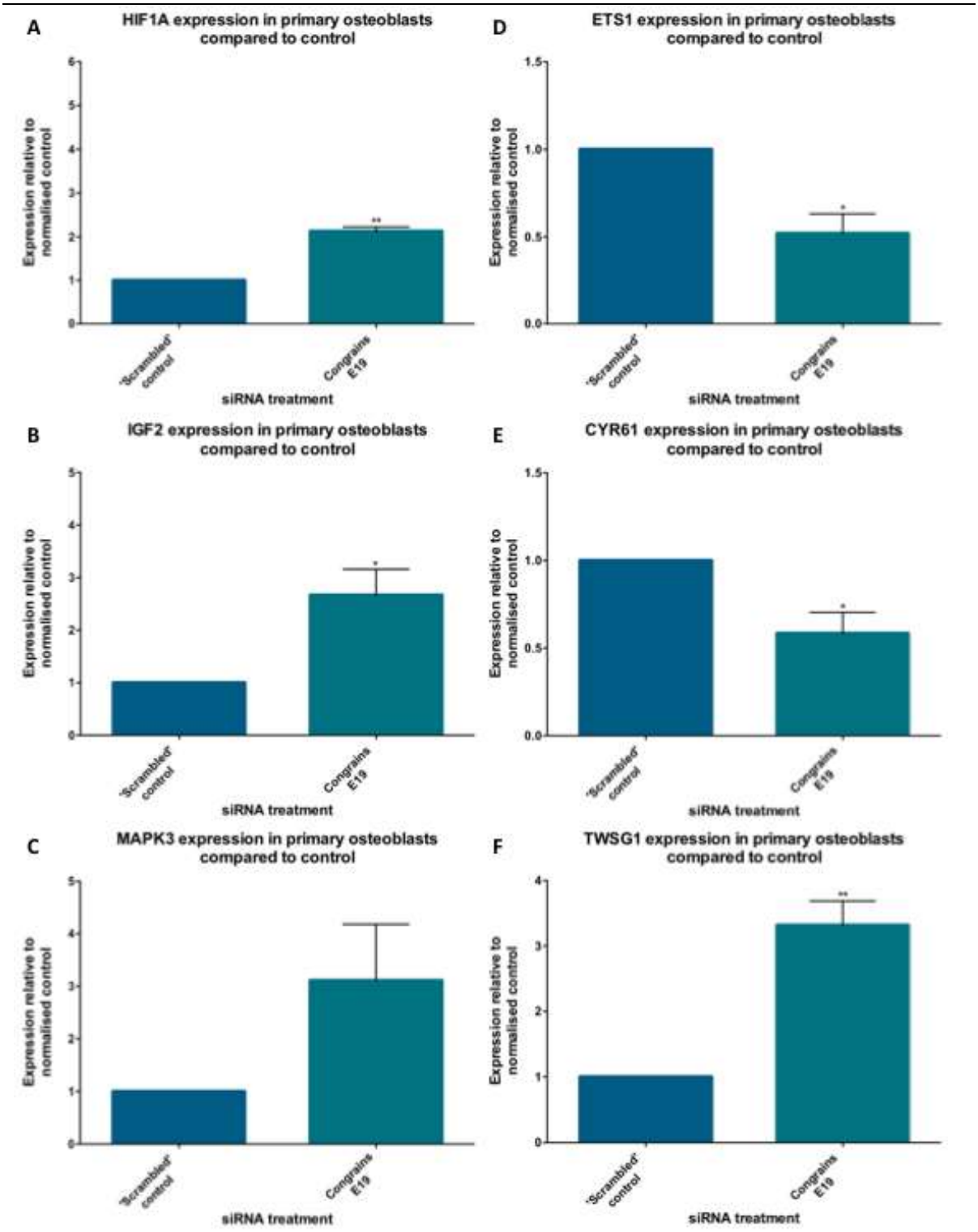

Figure 6.2: Gene expression levels of (A) HIF1A, (B) IGF2, (C) MAPK3, (D) ETS1, (E) CYR61 and (F) TWSG1 in primary osteoblasts compared to control when cells have been treated with a siRNA against exon 19 of ANRIL. Treatment with Congrains E19 siRNA caused an increase in HIF1A, IGF2 and TWSG1 expression and caused a decrease in ETS1 and CYR61 expression. Results shown as mean ±SEM ***p≤0.001; **p≤0.01; *p≤0.05. n=5

6.3.2 ANRIL knock down in primary osteoblasts alters osteoblast-specific pathways.

In order to determine whether particular pathways were altered between the ANRIL siRNA treated osteoblasts and the control group, Ingenuity Pathway Analysis (IPA) software (Qiagen, California) was used to determine how the 274 genes that showed differential expression relate to pathways with biological function. Genes were divided into two main subcategories: molecular and cellular functions and physiological system development and function. These categories are further subdivided into functionally related pathways.

Within molecular and cellular functions, the top two most altered pathways were those related with cellular development, growth and proliferation, showing a total of 75 altered genes, which is more than 50% of the altered genes associated with this subcategory (Figure 6.3A). Within the physiological system development and function subcategory, the top pathway with the most altered genes is tissue development, showing 19 altered genes (Figure 6.3B). The second most altered pathway is skeletal and muscular system development and function, which contains 12 altered genes.

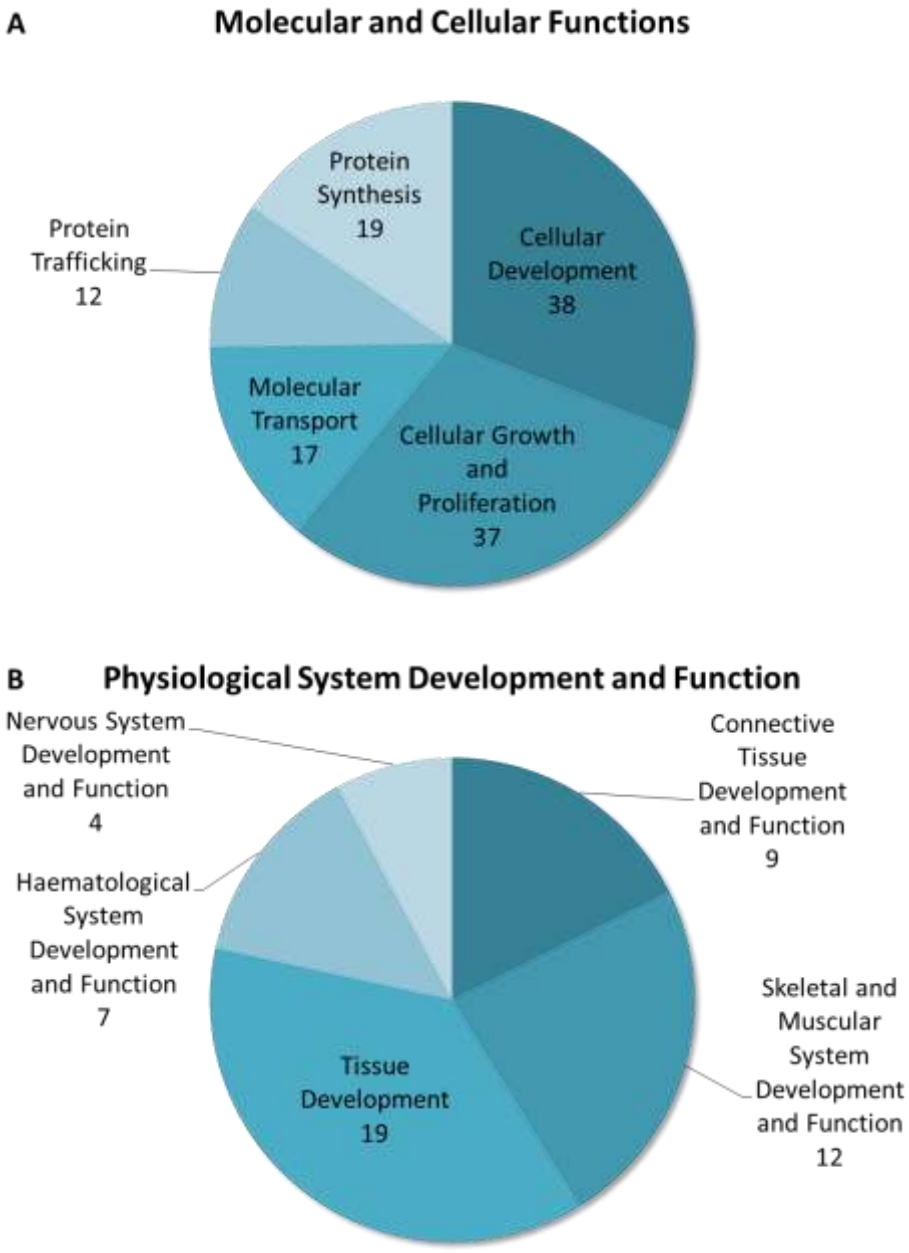

Figure 6.3: Break down of biological functions and the number of genes with changed expression associated with those functions. (A) Molecular and cellular functions and (B) Physiological system development and function.

Pathways within these main categories were investigated further and altered genes within these pathways were found to have specific functions in osteoblast-related pathways. Genes that were altered in the cellular development pathway were shown to have roles in osteoblast differentiation, differentiation of bone cell lines, osteoblast proliferation and the differentiation of stem cells (Figure 6.4A). In the cellular growth and proliferation pathways, the genes that were altered were shown to have roles in the proliferation of osteoblasts, development of bone marrow cells and the colony formation of cells (Figure 6.4B).

In the tissue development pathways, genes that were altered fell under two categories, ones that were involved in osteoblast regulation and ones that were involved with connective tissue development. Those that were involved in osteoblast regulation were shown to have roles in osteoblast cell viability, the development of bone marrow cells and the proliferation, adhesion, differentiation and migration of osteoblasts (Figure 6.5A). Those that were involved with connective tissue development had roles in pathways that regulated the differentiation, proliferation and growth of connective tissue cells, as well as the deposition of fibrous tissue, S phase entry of fibroblasts and the senescence of fibroblasts (Figure 6.5B).

In the skeletal and muscular system development and function pathways, the genes that were altered by ANRIL knock down were once again involved in adhesion, cell viability, proliferation, differentiation and migration of osteoblasts as well the differentiation of bone cell lines (Figure 6.6). These were also the pathways shown to contain altered genes in the tissue development pathways and involve many of the same genes.

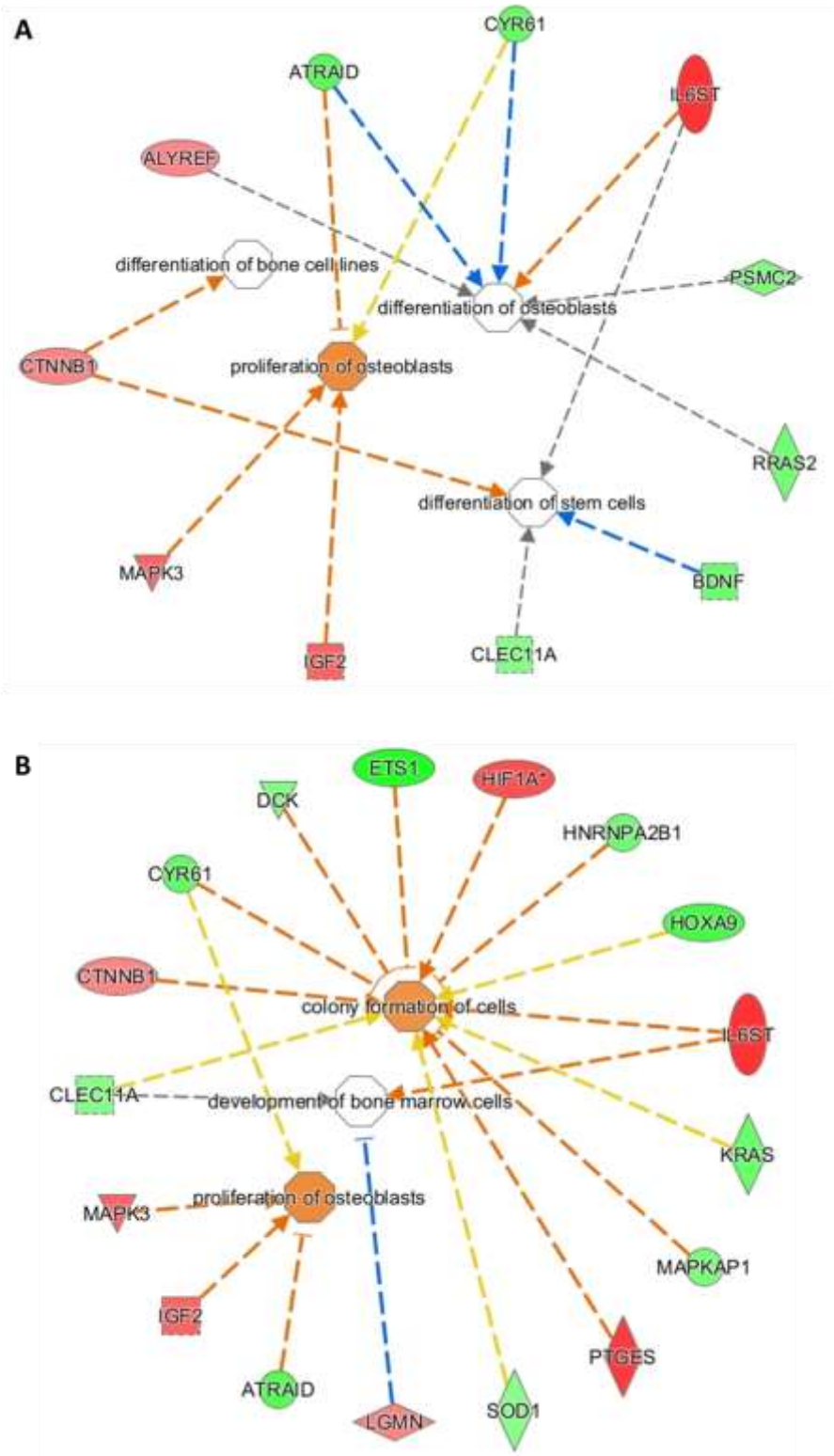

Figure 6.4: The top two altered pathways under the molecular and cellular function subcategory that showed relation to osteoblast function. (A) Altered genes that are involved in cellular development pathways and (B) altered genes that are involved in cellular growth and proliferation pathways. Red symbols denote upregulated genes and green symbols denote downregulated genes. The intensity of the colour denotes the magnitude of the change in expression.

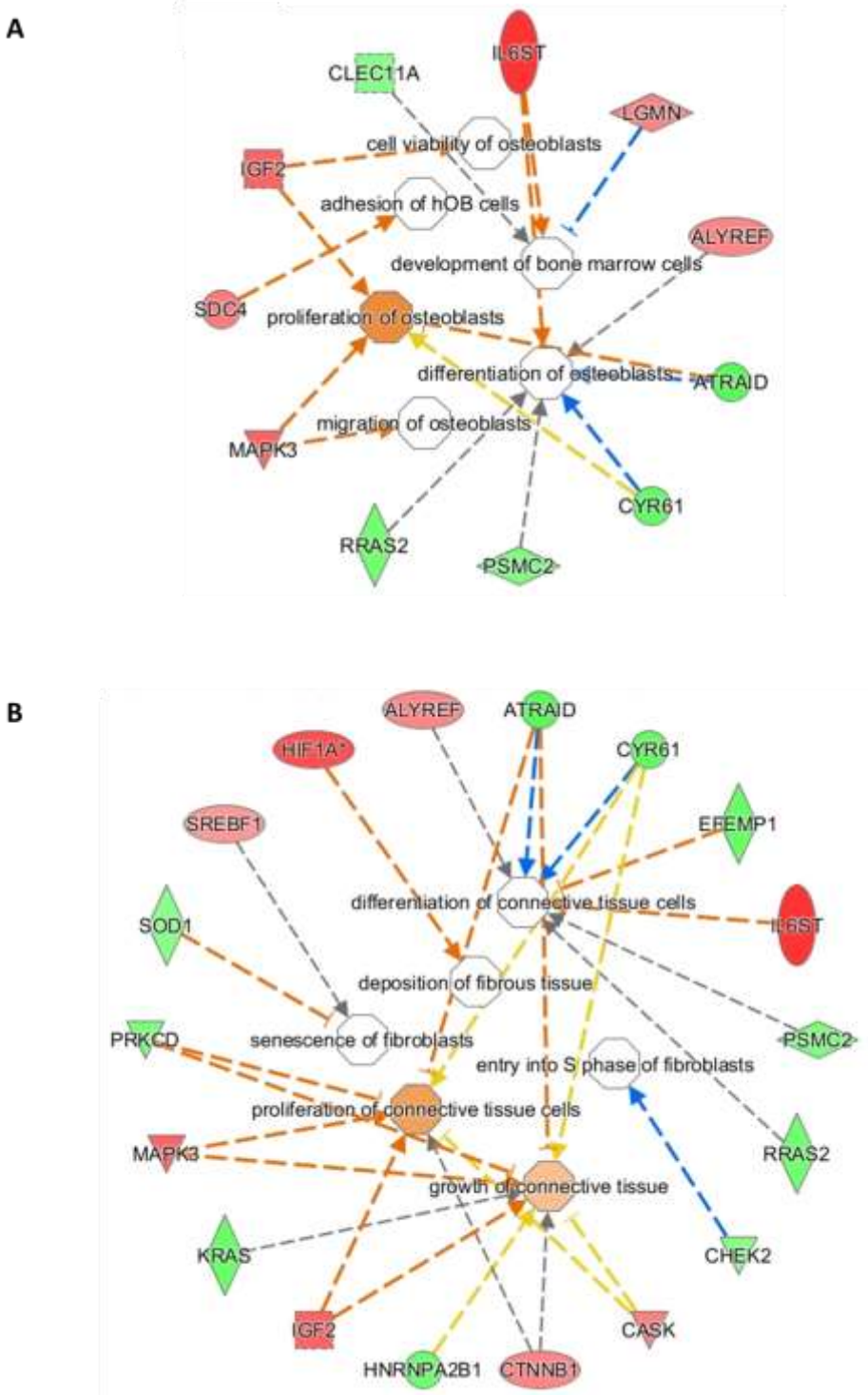

Figure 6.5: Tissue development pathways that involve genes altered by ANRIL knock down. (A) Altered genes involved in pathways that regulate osteoblasts and (B) altered genes involved in pathways that regulate the growth of fibroblasts and connective tissue. Red symbols denote upregulated genes and green symbols denote downregulated genes. The intensity of the colour denotes the magnitude of the change in expression.

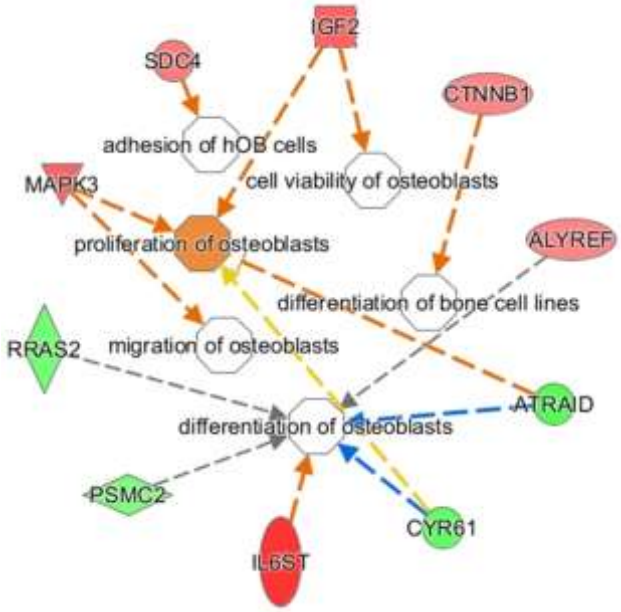

Figure 6.6: Skeletal and muscular system development and function pathways that involve genes altered upon ANRIL knock down. Network shows those genes involved with osteoblast and bone specific pathways. Red symbols denote upregulated genes and green symbols denote downregulated genes. The intensity of the colour denotes the magnitude of the change in expression.

To gain further insight into the pathways changed upon decrease in ANRIL expression, the Gene Ontology Consortium (http://geneontology.org/page/go-enrichment-analysis) and the Database for Annotation, Visualisation and Integrated Discovery (DAVID) (https://david.ncifcrf.gov/) analysis packages were used to determine what biological processes, molecular function and functional categories the differently expressed genes were involved in gene ontology enrichment analysis was used. The two biological processes that were enriched were protein transport and cellular processes. Of the 260 genes that showed altered gene expression, only 218 were able to be mapped to the database, which could be explained by the fact that some of the genes included on the Illumina array map to predicted gene locations. Of the genes that were differentially expressed, 69 genes were involved in protein transport, with 37 being upregulated and 32 being down regulated (Figure 6.7A). 183 of these genes were shown to be involved with cellular processes, with 89 being upregulated and 94 being down regulated (Figure 6.7B). The only molecular function that was shown to be significantly enriched was protein binding, of which 152 of the genes were involved, with 67 being upregulated and 85 being down regulated (Figure 6.8).

The top five functional categories that were enriched were phosphoprotein, alternate splicing, nucleus, cytoplasm and acetylation. 123 genes of the 218 that mapped to the database came under the phosphoprotein category, with 48 being upregulated and 75 being downregulated (Figure 6.9A) and 104 genes are involved in alternate splicing, of these 39 are upregulated and 65 are down regulated (Figure 6.9B). More of the differentially expressed genes had roles in the nucleus than in the cytoplasm (62 and 60 respectively). Of the genes involved in nuclear processes, 28 were upregulated and 34 were down regulated (Figure 6.9C), whereas 23 genes involved in cytoplasmic processes were upregulated and 37 were downregulated (Figure 6.9D). The final category that was enriched was acetylation, which involved 57 genes of the 218 that mapped to the database. 28 of these genes were upregulated and 29 of these genes were downregulated (Figure 6.9E).

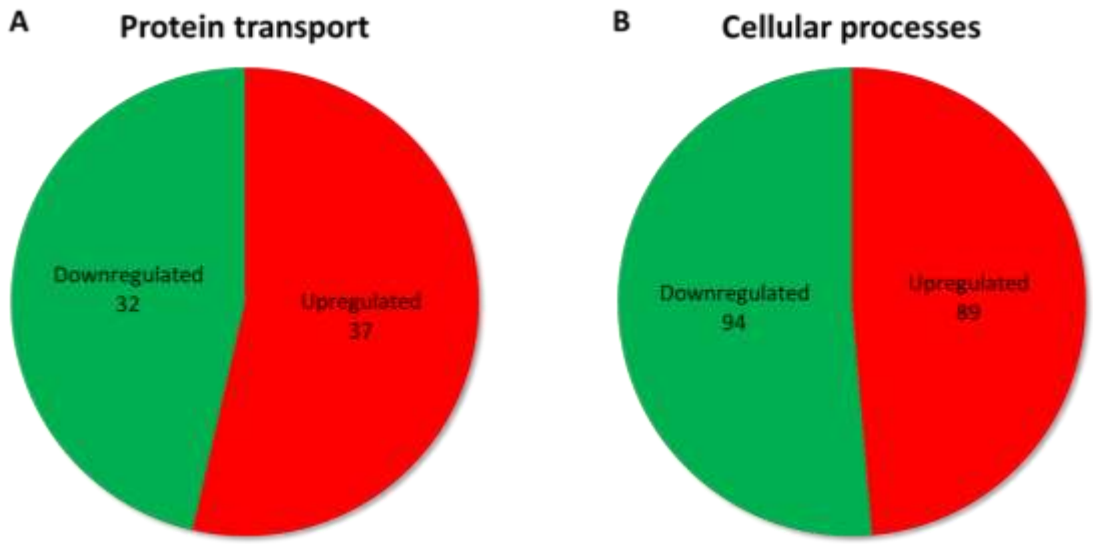

Figure 6.7: The number of up and downregulated genes involved in (A) protein transport and (B) cellular processes in osteoblasts upon ANRIL knock down. Gene ontology enrichment analysis revealed that the genes which showed altered expression upon ANRIL knock down were mainly involved in two biological processes.

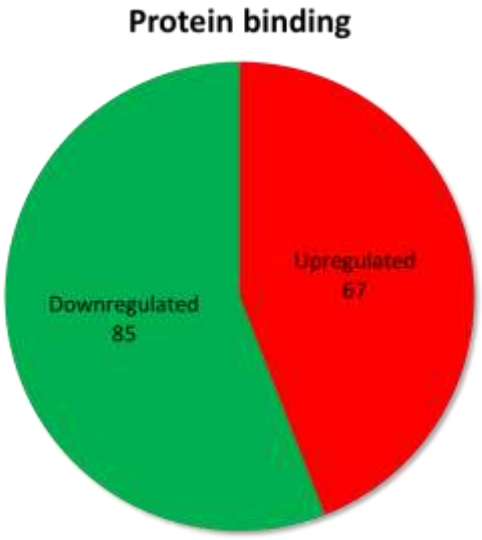

Figure 6.8: The number of up and downregulated genes involved protein transport. Gene ontology enrichment analysis revealed that the genes which showed altered expression upon ANRIL knock down were involved in one molecular function.

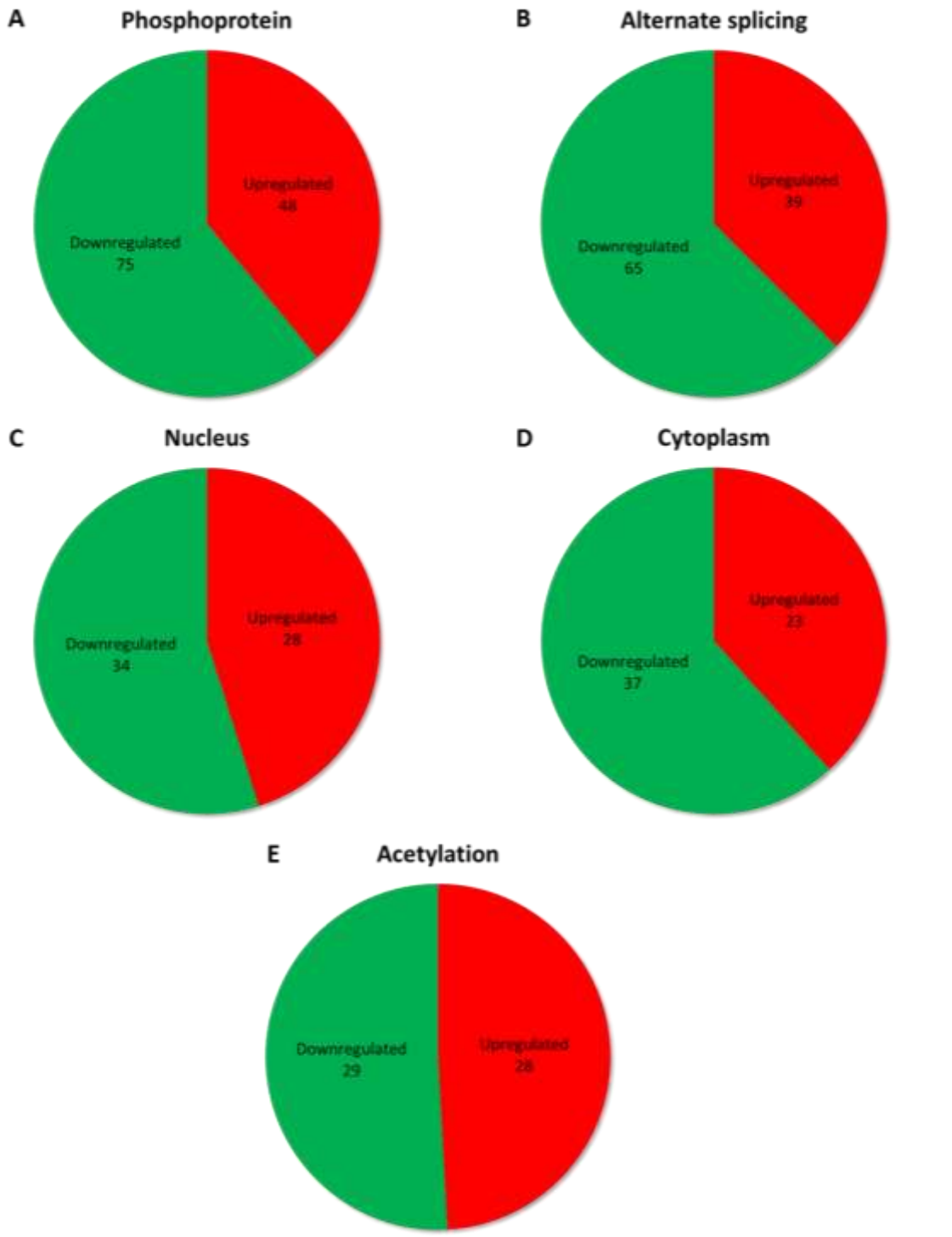

Figure 6.9: Top five enriched functional categories – (A) phosphoprotein, (B) alternate splicing, (C) nucleus, (D) cytoplasm and (E) acetylation. Gene ontology enrichment analysis revealed the top five functional categories that the genes which showed altered expression upon ANRIL knock down were involved in.

6.4 Discussion

To determine the mechanism by which a decrease in ANRIL expression affects primary osteoblast growth and differentiation, cells were treated with Congrains E1 siRNA against ANRIL and 'scrambled' control (n=5) as previously described, RNA was extracted and analysed by Illumina Human H12 Gene Expression array. Although treatment with both Congrains E1 and E19 siRNAs caused a decrease in ANRIL expression in primary osteoblasts and also caused changes in cell number and proliferation of primary human bone marrow stromal cells, only RNA from primary osteoblasts treated with Congrains E1 siRNA was sent off for gene expression analysis as it showed the most consistent results across each experiment.

Transfection of primary osteoblasts with a siRNA against exon 1 of ANRIL caused significant differential expression of 260 genes when compared to the 'scrambled' control. Of these genes 128 showed an increase in expression and 132 showed a decrease in expression when compared to control samples. Interestingly, the list of altered genes did not contain *CDKN2A* or *CDKN2B* from which $p16^{INK4A}$ and $p15^{INK4B}$ are transcribed and which ANRIL has been reported to negatively regulate in *cis*. This agrees with what was shown in the previous chapter by RT-qPCR, in that knock down of ANRIL expression did not cause any alteration in $p16^{INK4A}$ or $p15^{INK4B}$ expression. The array validated this previous finding using another platform and suggests that the decrease in cell proliferation and cell number is not dependent on $p16^{INK4A}$ or $p15^{INK4B}$ but is caused by an alternative mechanism.

The expression of six genes with known associations with osteogenesis and osteoblast differentiation, were chosen for RT-qPCR analysis to validate the results from the array. RT-qPCR analysis showed that ANRIL downregulation induced an increase in *HIF1A*, *IGF2* and *MAPK3* expression and caused a decrease in *ETS1*, *TWSG1* and *CYR61* expression, consistent with the findings from the array, although while IGF2, MAPK3 and ETS1 showed significant changes in expression between Congrains E1 siRNA treated cells and control cells, HIF1A and CYR61 showed a trend towards significance. These differences in the statistical significance is likely to reflect the different methodologies used but does suggest overall that the differences seen on the array are genuine.

As a number of the validation genes play roles in bone development and function, we also examined whether the siRNA directed against exon 19 of ANRIL also effected the expression of these genes. *HIF1A*, *IGF2* and *TWSG1* showed an increase in expression and *ETS1* and *CYR61* showed a significant decrease in expression. These differences in expression were in the same direction as what had been shown on the array for cells treated with Congrains E1 siRNA, apart from *TWSG1*, suggesting that in this case isoforms of ANRIL containing exon 19 may have different

effects on gene expression to those containing exon 1. Holdt *et al* have previously shown that overexpression of different isoforms of ANRIL containing different exons have different effects on cell adhesion and cell number in HEK293 cells, an embryonic kidney cell line (282).

In bone, HIF1α expression has been shown to have a role in promoting BMP9-induced osteogenic differentiation and suppressing the proliferation of osteoblasts (318,319). IGF2 has also been shown to potentiate the same BMP9-induced osteogenic differentiation pathway and bone formation and has been shown to promote osteogenic differentiation in murine embryonic stem cells (320,321). MAPK3 is a downstream signal transducer in the FGF signalling pathway and it has been demonstrated that inhibition of this kinase greatly decreases both osteoblast differentiation and matrix deposition (322). ETS1 has been shown to have a role in controlling the proliferation of osteoblasts (323,324), as has CYR61 (325). TWSG1 has been shown to regulate BMP2 dependent osteoblast differentiation, in that overexpression of TWSG1 has been shown to act as an antagonist for BMP2 signalling (326). This alteration in gene expression caused by a knock down in ANRIL expression seems to lead to a change in the pathways that regulate osteoblast differentiation, mineralisation and proliferation. This decrease in ANRIL expression leads to an upregulation of genes that cause differentiation and matrix mineralisation and a downregulation of genes that regulate cellular proliferation, such as ETS1 and CYR61. This decrease in ETS1 and CYR61 could explain the decrease in cell number and proliferation that was seen in the ANRIL knock down experiments in the previous chapter, thus suggesting that ANRIL regulates pathways other than those that involve *CDKN2A/B* transcripts.

The amplitude of the expression changes were not consistent across the two techniques used for analysis. This may be due to the different technologies used, as the probes used in the array may target different regions of the mRNA compared to the primer and probe sets used in the TaqMan RT-qPCR assays, thus explaining the differences seen in fold change. This could also explain why the changes in HIF1A, CYR61 and TWSG1 expression did not reach significance in osteoblasts treated with Congrains E1 siRNA against ANRIL.

Pathway analysis was carried out on the 260 significantly changed genes found upon treatment of cells with siRNA against exon1 of ANRIL using IPA. Pathways implicated in cellular development, cellular growth and proliferation, tissue development and skeletal and muscular system development and function were identified, with the highest number of genes changed in the molecular and cellular functions and physiological system development and function subcategories. Interestingly, each of these pathways contained genes that were directly linked to osteoblast proliferation, differentiation, migration, cell viability and adhesion as well as genes that were linked to pathways such as stem cell differentiation, development of bone marrow cells,

colony formation of cells and differentiation of bone cell lines. The tissue development pathways also showed altered genes that are involved in connective tissue generation, including those that regulate proliferation, growth and differentiation of connective tissue cells as well as genes that regulate the entry into S phase of fibroblasts, fibroblast senescence and deposition of fibrous tissue by fibroblasts. Along with cartilage and bone cells, fibroblasts make up the connective-tissue cell family, and are specialised for the secretion of extracellular matrix, and they can play an important role in bone repair and formation as they can act as a source of precursors for osteoblasts and osteoclasts (327).

The range of processes affected by ANRIL down regulation occurred in the absence of a change in the levels of $p16^{INK4A}$ and $p15^{INK4B}$ expression. Although ANRIL has not previously been shown to have any *trans*-functional effects in osteoblasts, Congrains *et al* have shown that knock down of ANRIL expression, using the same siRNA that has been used in these experiments, has effects on genes involved in atherogenesis in human VSMCs. When ANRIL expression was knocked down in VSMCs, HBEGF and CDH5 expression decreased and the expression of BCL2A1 and SERPINE increased, which are all key components in atherogenesis. One of the genes that was highlighted as having a positive effect on cell viability was IGF2. Upon knock down of ANRIL expression, IGF2 expression was shown to increase, which was predicted by IPA to activate cell viability pathways. This agrees with what was shown in the previous chapter using the CellTitre Glo 2.0 assay, where a knock down in ANRIL expression did not cause a decrease in cell viability, suggesting that the pathway involving IGF2 maybe become activated to prevent cell death in osteoblasts. Together, these results suggest that ANRIL potentially has *trans*-regulatory functions in osteoblast specific pathways and that a decrease in ANRIL expression can lead to the dysregulation of these pathways, which could lead to incorrect bone formation and remodelling.

Additional gene ontology enrichment analysis revealed that in cells that had been treated with Congrains E1 siRNA, there was an enrichment in processes other than cell cycle regulation. Genes that showed differential expression on the array had roles in protein transport and binding as well as other cellular processes, with the top five enriched functional categories were phosphoproteins, alternate splicing, nucleus, cytoplasm and acetylation. This demonstrates that ANRIL potentially regulates genes that are involved in a wide variety of cellular processes in osteoblasts. Sato *et al* have previously demonstrated in HeLa cells that an overexpression of ANRIL lead to an enrichment of genes that were involved in nuclear regulation, most of which were down regulated (36 downregulated vs 2 upregulated) (277). Other lncRNAs, such as MATAL1 and NEAT1, have been found to be enriched in the nucleus (328) and in osteoblasts, the lncRNA MATAL1 has been shown to act downstream of RANKL to inhibit cell proliferation and to

regulate the expression of osteoprotegerin (329). This suggests that although ANRIL has not been shown to have a specific role in nuclear regulation in osteoblasts, other lncRNAs have, suggesting that this may also be true for ANRIL. Another functional category that was enriched for genes with altered expression was those that have a role in acetylation. Although ANRIL has not previously been shown to influence acetylation mechanisms, it has been shown to bind with PRC2 and act as a scaffold to assist in histone methylation (283), another type of epigenetic regulatory mechanism. However, in osteoblasts, the lncRNA HIF1α-antisense 1, through the down regulation of HOXD10 interfered with histone acetylation and, subsequently, caused the inhibition of osteoblast differentiation (330), suggesting a possible role for ANRIL in regulating acetylation in osteoblasts.

The results in this chapter have demonstrated the potential for ANRIL to regulate other genes across the genome in *trans* in osteoblasts, with no change to the expression of genes that this lncRNA regulates in *cis*. However, it now needs to be determined whether the changes in gene expression seen is a direct effect of a decrease in ANRIL expression.

6.5 Summary

We sought to determine whether the knock down of ANRIL expression using a siRNA targeted against exon 1 of ANRIL (Congrains E1 siRNA) caused a change in gene expression in osteoblasts using the Illumina Human H12 Gene Expression Array. This showed that 260 genes had significantly altered expression between treated and control cells – 128 upregulated and 132 downregulated. Both *CDKN2A* and *CDKN2B* expression was unaltered on the array, confirming what had already been seen with RT-qPCR. *HIF1A*, *IGF2* and *MAPK3* showed increased expression on the array with ANRIL knock down, whereas *ETS1*, *CYR61* and *TWSG1* showed decreased expression on the array, with all of these genes having been linked to osteoblast specific pathways in the literature. Using RT-qPCR, only *IGF2*, *MAPK3* and *ETS1* expression changes reached significance, with HIF1A and CYR61 showing trends towards significance, all in the same directions as shown on the array. With Congrains E19 siRNA treated cells, *HIF1A*, *IGF2*, *ETS1*, *CYR61* and *TWSG1* expression was significantly altered when compared to control cells, suggesting that ANRIL may *trans*-regulate other genes beside *CDKN2A* and *CDKN2B*.

Using IPA and gene ontology enrichment analysis, it was determined that genes that showed significantly altered expression on the gene expression array were involved in osteoblast specific functions, such as differentiation, proliferation, cell viability and migration, as well as development of connective tissue specific pathways. Gene ontology analysis revealed that genes with significantly altered expression were enriched for protein transport, protein binding, nuclear

regulation and acetylation, as well as many of them being phosphoproteins. These results suggest that ANRIL may have a specific role in osteoblast regulation, and therefore bone formation, as well as roles other than the regulation of the cell cycle. In order to determine if ANRIL is actually binding to these genes to cause differential expression, further work needs to be done.

6.6 Future work

In order to determine whether ANRIL is directly binding to the promoters of the genes that demonstrated differential expression in the Ilumina Human H12 array, Chromatin Isolation by RNA Purification (ChIRP) assay can be used (331). This method allows for the determination of DNA regions that are associated with a specific lncRNA and would allow us to determine if ANRIL was directly binding to the promoters of these genes. Holdt *et al* have previously shown that genes which showed altered expression with ANRIL overexpression were enriched for Alu binding sequences (282), so we can use bioinformatic analyses of promoter regions to determine if any of the genes that displayed altered expression on the array also contain this motif.

As many of the pathways that were effected by knock down of ANRIL expression involved osteoblast differentiation and mineralisation, it would be interesting to see how gene expression changes when cells are differentiated from hBMSCs to osteoblasts, and whether this effects morphology and cell survival. As the differentiation and mineralisation processes take longer than the window for transient transfection, a stable transfection using lentivirus would have to be done into hBMSCs and then these cells directed down the osteogenic lineage. Differentiation and mineralisation could then be assessed to determine whether they have been affected.

A gene expression array using hBMSCs that had been treated with siRNAs against ANRIL could also be done to determine whether similar genes, or genes that are more specifically related with earlier stages of osteogenesis, such as SOX9, BMPs and β-catenin, are affected.

Chapter 7
The association between the methylation status of *CDKN2A*, *RXRA* and *NOS3* with bone outcomes at birth

7.1 Introduction

7.1.1 DNA methylation as a marker for later phenotype

Epidemiological studies measure DNA methylation within peripheral tissue in order to determine associations with future phenotype, as these are easily accessible tissues. However, as DNA methylation patterns are tissue specific, this would suggest that methylation in proxy tissues may not accurately reflect methylation in tissues such as bone and the functional significance of differential methylation in proxy tissue in the causal pathway is unknown. However, there are now studies that show that methylation patterns can be conserved across different tissue types (218,219). Lu *et al* have demonstrated that the methylation levels of five genes are stable across thirteen different tissues types that are derived from different germline layers (219).

Epidemiological studies have shown that there are associations between the methylation status of CpGs from umbilical cord tissue DNA and offspring anthropometric outcomes in childhood. Using both the PAH and SWS cohorts, Godfrey *et al* demonstrated that CpG methylation within the *RXRA* promoter is positively associated with childhood %FM and total fat mass at 6 and 9 years in two independent cohorts (220). The same paper also demonstrated that the methylation levels of a CpG within the *NOS3* promoter region also had similar positive associations with %FM, fat mass and ratio of trunk to limb fat but these associations were only seen in the PAH cohort. The methylation of these CpGs has also been investigated with regards to offspring bone outcomes, with the methylation of *RXRA* in cord tissue being negatively associated with bone outcomes (list) and methylation of *NOS3* in cord being positively associated with offspring bone outcomes at 4 years and 9 years respectively (205,234).

These studies have suggested that altered DNA methylation, even in proxy tissues, might provide useful biomarkers for disease risk, although whether they are simply markers or are causally significant is unknown. Therefore, methylation marks that could be used to predict offspring bone outcomes from as soon as they are born, and persist into later life, would allow for intervention and prevention of those with a higher risk of disease from birth.

7.1.2 Maternal vitamin D and offspring bone health

Vitamin D plays an important role in regulating calcium uptake and bone homeostasis, although there is conflicting evidence that maternal vitamin D status has an effect on offspring bone outcomes. Human studies by different groups across a variety of cohorts have shown that offspring born to mothers that have a lower serum vitamin D concentration have significantly lower bone mineral content, bone area and bone mineral density when compared to those born to mothers with higher levels of serum vitamin D (155–157). However, there are also conflicting reports: in an association study by Lawlor and colleagues using the ALSPAC cohort, where

mothers were split into three groups based on the serum vitamin D concentrations and comparisons made across the separate groups, did not find any associations between maternal vitamin D status and childhood bone outcomes (159).

Prior to the MAVIDOS study, there have been several, mainly small, intervention trials that have been carried out over the years examining whether vitamin D supplementation during pregnancy is beneficial for the mother and the infants; however, there has been only one that specifically looks at bone mass of the infant at birth. In these trials, mothers were either supplemented with daily oral doses of vitamin D, with doses ranging from 400-1,200 IU/day, or single/dual larger doses (5mg or 600,000 IU respectively) during the final trimester of pregnancy. Marya and colleagues found that biochemical parameters (calcium, inorganic phosphate and heat-labile alkaline phosphatase levels) in maternal serum were significantly improved in those mothers treated with two 600,000 IU vitamin D doses during the final trimester compared to those treated with daily doses throughout their third trimester, while levels did not change between the control and mothers that took a daily supplement of vitamin D (332). This latter observation agreed with what has been seen by other research groups (333,334). However, it has been shown that in infants of mothers that received daily doses of vitamin D, there are less cases of hypocalcaemia and that they have higher circulating concentrations of 25-hydroxyvitamin D_3 which is suggestive of improved calcium handling (333,335).

There is evidence from these studies that vitamin D supplementation can also have an effect on the size of the infant as results have shown that those infants born to mothers who are taking vitamin D supplements have higher birth weights than those born to unsupplemented mothers (332), whereas other groups have not seen a significant modification in birth weight across treatment and control groups (334). Congdon *et al* are the only group out of these earlier studies to specifically look at the effect of maternal vitamin D deficiency on infant skeletal mineralisation, which was assessed by measuring forearm BMC (336). In this study of 45 Asian women with vitamin D deficiency versus 19 Asian women supplemented with 1000 IU daily dose of vitamin D, there were a wide variety of serum 25-hydroxyvitamin D_3 concentrations across the groups, however there were no significant differences in the infant BMC, which would suggest that maternal vitamin D deficiency does not have an effect on fetal skeletal development.

A systematic review by Harvey *et al* which included 76 studies aimed to address the various questions regarding vitamin D deficiency, supplementation during pregnancy and how low maternal circulating 25-hydroxyvitamin D levels are associated with adverse neonatal and maternal health outcomes (337). This study revealed that there was insufficient evidence across all studies to reliably answer many of the questions being asked. Data from these 76 studies did

not provide sufficient evidence to determine whether maternal vitamin D supplementation during pregnancy leads to improvement in health outcome of the infant and/or the mother or evidence on the optimal dose or regimen to provide adequate levels of vitamin D throughout pregnancy. This was due to the heterogeneity across the studies and for most of the outcomes investigated there was conflicting evidence. However, they did provide some insight as to the associations between health outcomes and maternal 25-hydroxyvitamin D levels in that positive relationships were found between maternal 25-hydroxyvitamin D levels and infant birth weight, bone mass and post-natal calcium concentrations.

7.1.3 Maternal Vitamin D Osteoporosis Study (MAVIDOS)

The systematic review from Harvey and colleagues, coupled with the conflicting information across these smaller trials, revealed a need for a randomised controlled of vitamin D supplementation study using greater numbers of pregnant women and where there is a long term follow up of infants. It would allow for the determination of whether intervention and correction of vitamin D during pregnancy has a beneficial effect on the offspring and to determine the optimal concentration of maternal serum 25-hydroxyvitamin D_3 in order to promote ideal fetal development. Due to the role of vitamin D in bone development and homeostasis, there is also a need for a study that specifically examines whether maternal vitamin D status is associated with fetal bone outcomes.

The MAVIDOS trial was established to test the hypothesis that infants born to women with low vitamin D levels who have had vitamin D supplementation during pregnancy will have a greater BMC than those infants born to women who are supplemented with placebo. In this study, women in Southampton, Oxford and Sheffield had their serum 25-hydroxyvitamin D assessed during week 12 of pregnancy. Those that had a circulating concentration between 25-100nmol/l were randomised to either receive placebo or 1000 IU cholecalciferol/day from week 14 of pregnancy until the birth of the child (338) and were assessed at 14 and 34 weeks of pregnancy.

At the 14 weeks assessment, a urine sample was obtained as well as blood, which was stored for analysis of 25-hydroxyvitamin D, vitamin D binding protein, calcium, bone-specific alkaline phosphatase and albumin levels at the end of the study. A questionnaire was also completed that gathered information on parity, smoking status, alcohol intake, vitamin D dietary intake, exercise and sunlight exposure as well as anthropometric measurements, such as height and skinfold thickness. Medication was issued at the 14 week visit and pill counts were carried out at subsequent assessments to ensure that participants were compliant with the study medication.

The anthropometric measurements taken at the 14 week visit were repeated at the 34 week visit, as well as completing another questionnaire on maternal lifestyle and another blood sample was taken.

When the infants were born, cord blood samples were taken for analysis at the end of the study, as well as umbilical cord and placental tissue samples. The baby's anthropometric indices were also recorded and a DXA scan is arranged to obtain measurements of the baby's whole body and lumbar spine bone area, bone mineral density and bone mineral content. Follow up assessments are planned at 1, 2, 3 and 4 years of age to characterise diet, exercise, health and anthropometric measurements, with a DXA scan being repeated at 4 years of age to determine whole body, lumbar spine and hip bone mass. Currently, 2, 3 and 4 year assessments are ongoing, with 1 year follow ups recently completed. Through long term follow up of offspring, this should give a clearer idea of the effect of maternal vitamin D status on the bone outcomes of children over their lifetime.

Recently published results from the MAVIDOS study (339) have shown that daily supplementation of women with 1000 IU of cholecalciferol does not significantly change offspring total BMC at birth when compared to the placebo group. However, when offspring bone outcomes are stratified by season of birth, there is a significant difference between the two maternal treatment groups. Maternal cholecalciferol supplementation was shown to cause a significant increase in whole body BMC, BA and BMD in offspring born during the winter months. Results from this study have also shown that this dose of cholecalciferol is sufficient to ensure that most women are not vitamin D replete during pregnancy and that it is safe as no adverse events recorded during the study were due to the supplement of cholecalciferol.

7.2 Aims

The first aim of this chapter is to replicate the associations previously reported in the SWS cohort between the methylation of specific CpG loci in *CDKN2A*, *RXRA* and *NOS3* and offspring total BMC, total BA, total BMD, size corrected BMC (scBMC) at birth. The second aim in the MAVIDOS cohort was to use this as a randomised controlled trial to determine whether the supplementation of mothers with a daily 1000 IU dose of cholecalciferol affects the methylation levels of these CpG loci within *CDKN2A*, *RXRA* and *NOS3* and whether maternal supplementation affects offspring bone outcomes at birth.

7.3 Results

7.3.1 Is the methylation of *CDKN2A* associated with offspring bone outcomes at birth?

7.3.1.1 SWS umbilical cord

Previous results from Harvey *et al* have shown that there are associations between the methylation of two specific CpG loci within the *CDKN2A* gene at birth (CpGs -845 and -907) and offspring childhood bone outcomes at 4 and 6 years. These results showed that there is a significant negative association with both CpG -845 and -907 and offspring total bone area, total BMC and areal BMD at both 4 and 6 years of age in the SWS cohort (unpublished data).

However, as this work by Harvey *et al* compared methylation at birth with childhood bone outcomes, the associations between *CDKN2A* methylation in SWS umbilical cord tissue and offspring bone outcomes at birth was not determined. This will allow for direct comparisons to be made between the SWS cohort and the MAVIDOS samples, the latter only having DXA bone outcome data at birth available at present. Linear regression analysis explored the associations between methylation of each of the individual CpG sites in *CDKN2A* and offspring bone outcomes at birth in the SWS cohort revealed significant associations between the two after adjusting for sex, age at time of DXA and gestational age (Table 7.1).

There were significant negative associations between the methylation of CpGs -796, -845 and -907 and offspring total BMC at birth after adjusting for gestational age, sex and age at time of DXA ($p<0.041$ for all). The methylation of CpGs -852 and -887 showed a weak trend towards significance with total BMC, which was also in a negative direction ($p<0.089$ for both).

Linear regression analysis also determined significant associations between the methylation of CpGs -796 and -907 and offspring total BA at birth ($p<0.03$ for both), after adjusting for gestational age, sex and age at time of DXA. These associations were also in a negative direction. Trends towards significance were also seen between total BA and the methylation of CpGs -854, -852 and -887 ($p<0.091$ for all), which were also in a negative direction.

The methylation of CpG -845 was also significantly associated with total BMD at birth after adjusting for gestational age, sex and age at time of DXA ($p=0.035$), whilst a trend towards significance was seen between total BMD and the methylation of CpG -887 ($p=0.083$). Both of these associations were in a negative direction.

There were no significant associations between the methylation of any of the CpGs in the *CDKN2A* region of interest and scBMC. Figure 7.1 visually demonstrates some of the significant associations between specific *CDKN2A* CpG methylation in umbilical cord and offspring total BMC, total BA and total BMD at birth using scatter plots.

	Baby DXA: Total BMC (g), adjusted for gestational age, sex and age			Baby DXA: Total BA (cm sq), adjusted for gestational age, sex and age		
	n	b	p-value	n	b	p-value
***CDKN2A* CpG -769**	292	-0.0001022	0.225	292	-0.1653897	0.232
***CDKN2A* CpG -793**	290	-0.0001142	0.174	290	-0.1769149	0.198
***CDKN2A* CpG -796**	246	-0.000229	0.035	246	-0.3848732	0.029
***CDKN2A* CpG -836**	334	-0.0001204	0.114	334	-0.1980114	0.113
***CDKN2A* CpG -845**	330	-0.0001644	0.040	330	-0.250933	0.055
***CDKN2A* CpG -852**	330	-0.0001242	0.088	330	-0.2020511	0.090
***CDKN2A* CpG -861**	321	-0.0001167	0.162	321	-0.1653978	0.227
***CDKN2A* CpG -887**	312	-0.0001556	0.052	312	-0.2472543	0.059
***CDKN2A* CpG -907**	266	-0.0002086	0.030	266	-0.3470719	0.028
	Baby DXA: Total BMD (g/cm sq), adjusted for gestational age, sex and age			**Baby DXA: scBMC (g), adjusted for gestational age, sex and age**		
	n	b	p-value	n	b	p-value
***CDKN2A* CpG -769**	292	-0.0001437	0.315	291	-0.0000066	0.676
***CDKN2A* CpG -793**	290	-0.0001968	0.169	289	-0.0000167	0.289
***CDKN2A* CpG -796**	246	-0.0001885	0.309	245	-0.0000036	0.861
***CDKN2A* CpG -836**	334	-0.0001583	0.223	333	-0.0000091	0.529
***CDKN2A* CpG -845**	330	-0.0002875	0.035	329	-0.0000149	0.322
***CDKN2A* CpG -852**	330	-0.000149	0.232	329	-0.0000066	0.634
***CDKN2A* CpG -861**	321	-0.000209	0.151	320	-0.0000224	0.167
***CDKN2A* CpG -887**	312	-0.0002383	0.083	311	-0.000008	0.599
***CDKN2A* CpG -907**	266	-0.0002502	0.122	265	-0.0000045	0.787

Table 7.1: Associations between *CDKN2A* CpG methylation in umbilical cord tissue and offspring bone outcomes at birth in SWS cohort. There are significant negative associations between methylation of CpGs within *CDKN2A* and total BMC, total BA and total BMD ($p<0.05$; highlighted in orange), determined by linear regression and adjusting for gestational age, sex and age at time of DXA. There are also some negative trends towards significance ($p<0.1$) between CpGs within the *CDKN2A* region of interest and bone outcomes at birth ($p<0.1$; highlighted in blue). 'n' is number of subjects and 'b' is beta value. Linear regression analysis carried out by Phil Titcombe.

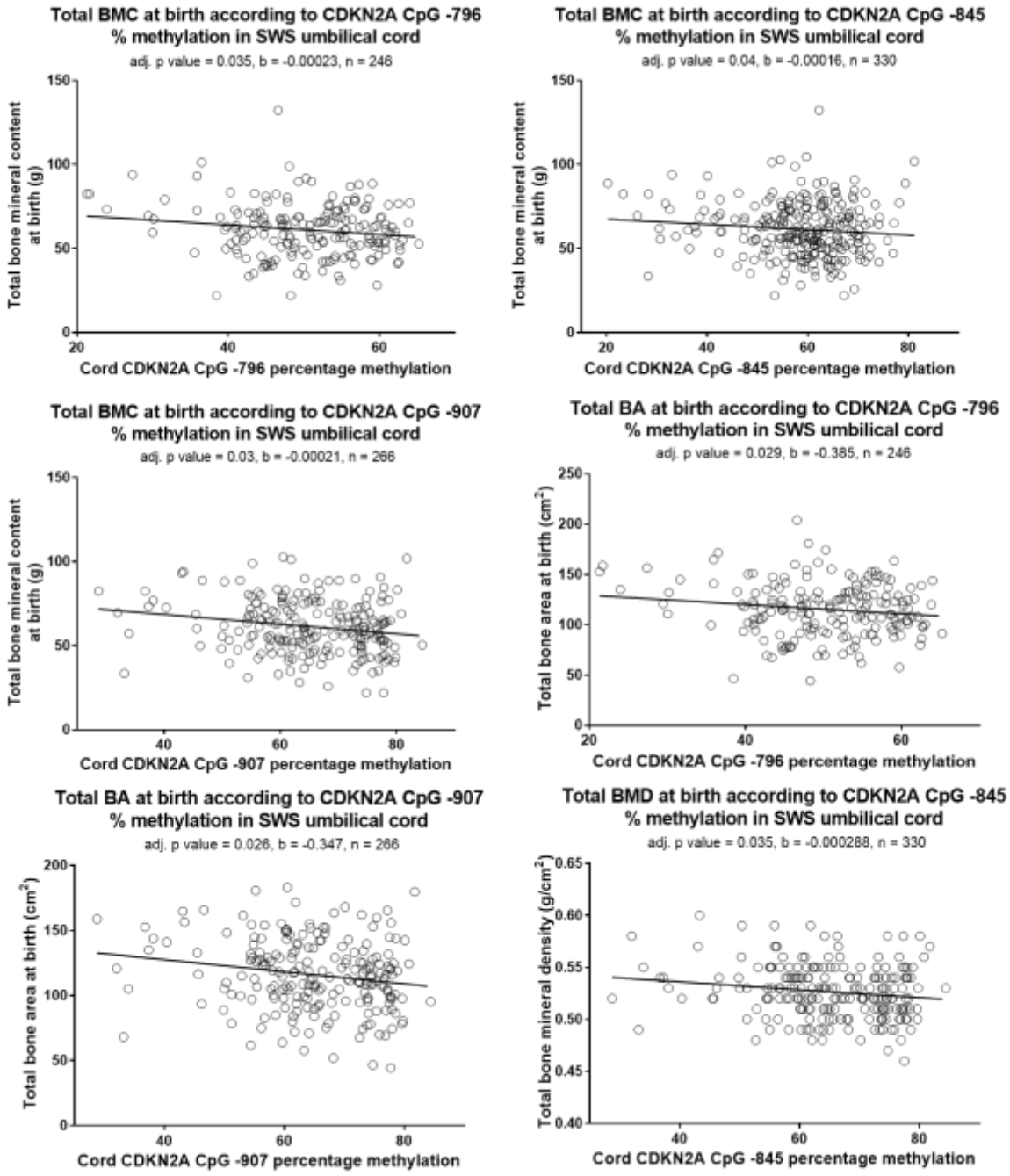

Figure 7.1: The methylation of CpGs -796, -845 and -907 in *CDKN2A* is shown plotted against total bone mineral content (BMC), total bone area (BA) and total bone mineral density (BMD)at birth. As the percentage methylation of each of these CpGs increases, total BMC, total BMD and total BA decreases at birth (adj. p<0.04). Linear regression analyses of methylation versus bone outcome produce a negative beta value, demonstrating a negative association between methylation of each of the CpGs and the bone outcome represented on the above graphs. p-values across all six graphs are adjusted for gestational age, sex and age at time of DXA in the linear regression model.

7.3.1.2 MAVIDOS umbilical cord

To see if the associations seen in the SWS cohort can be replicated, associations between methylation of CpGs within the CDKN2A locus and offspring bone outcomes at birth were investigated in the MAVIDOS cohort. In this cohort, the methylation of CpGs in *CDKN2A* in offspring umbilical cord was not significantly associated with total BMC, total BA, total BMD or size corrected BMC (scBMC) at birth in MAVIDOS samples when adjusted for sex, age at time of DXA and gestational age (Table 7.2). There were weak negative associations between the methylation of CpG -796, -887 and -907 and total BMC (p= 0.08, 0.083 and 0.099 respectively). CpG -796 also showed a weak negative association with total BMD ($p<0.1$) and CpG -887 a weak negative association with total BA (p=0.093). There were no associations between any of the CpGs and scBMC.

	Baby DXA: Total BMC (g), adjusted for gestational age, sex and age			Baby DXA: Total BA (cm sq), adjusted for gestational age, sex and age		
	n	**b**	**p-value**	**n**	**b**	**p-value**
***CDKN2A* CpG -769**	136	-0.074	0.376	136	-0.008	0.975
***CDKN2A* CpG -793**	119	-0.127	0.142	119	-0.364	0.195
***CDKN2A* CpG -796**	106	-0.304	0.08	106	-0.589	0.289
***CDKN2A* CpG -836**	147	-0.081	0.325	147	-0.116	0.669
***CDKN2A* CpG -845**	144	-0.046	0.633	144	0.000248	0.999
***CDKN2A* CpG -852**	142	-0.04	0.657	142	-0.024	0.935
***CDKN2A* CpG -861**	137	-0.017	0.87	137	-0.056	0.867
***CDKN2A* CpG -887**	146	-0.159	0.083	146	-0.505	0.093
***CDKN2A* CpG -907**	144	-0.155	0.099	144	-0.414	0.181
	Baby DXA: Total BMD (g/ cm sq), adjusted for gestational age, sex and age			**Baby DXA: scBMC (g), adjusted for gestational age, sex and age**		
	n	**b**	**p-value**	**n**	**b**	**p-value**
***CDKN2A* CpG -769**	136	-0.000235	0.13	136	-0.025	0.57
***CDKN2A* CpG -793**	119	-0.000175	0.272	119	0.008	0.857
***CDKN2A* CpG -796**	106	-0.001	0.099	106	-0.095	0.294
***CDKN2A* CpG -836**	147	-0.000195	0.204	147	-0.002	0.963
***CDKN2A* CpG -845**	144	-1.38E-04	0.436	144	0.017	0.728
***CDKN2A* CpG -852**	142	-1.12E-04	0.504	142	0.029	0.53
***CDKN2A* CpG -861**	137	-4.09E-06	0.983	137	0.036	0.479
***CDKN2A* CpG -887**	146	-0.000188	0.27	146	0.041	0.368
***CDKN2A* CpG -907**	144	-0.000229	0.189	144	0.027	0.574

Table 7.2: The association between methylation of *CDKN2A* in umbilical cord DNA and bone outcomes at birth in MAVIDOS cohort. There are no significant associations between methylation of any of the CpGs within the *CDKN2A* region of interest and bone outcomes at birth after correcting for gestational age, sex and age at time of DXA. There are some trends towards significance (p=0.051-0.1) in a negative direction between CpGs -796, -887 and -907 and total BMC, CpG -887 and total BA and CpG -796 and total BMD. 'n' denotes number of subjects and 'b' denotes beta value. Associations determined by linear regression model.

7.3.2 Is the methylation of *RXRA* associated with offspring bone outcomes at birth?

7.3.2.1 SWS umbilical cord

Previous analyses have determined association between methylation of these CpGs and offspring bone outcomes at 4 years of age (205), but no associations were investigated between *RXRA* methylation and offspring bone outcomes at birth. Methylation levels of CpGs within the *RXRA* promoter had previously been measured using the Sequenom MassARRAY platform in the SWS cohort umbilical cord samples. On this platform, CpGs -2686 and -2682 and CpGs -2649 and -2642 cannot be distinguished from each other and so are paired together for analysis.

Linear regression analysis determined that the methylation levels of CpGs -2686/-2682 and CpG -2673 are significantly associated with offspring total BMC at birth after adjusting for gestational age, sex and age at time of DXA ($p<0.023$ for both; Table 7.3). The methylation of CpG -2649/-2642 showed a weak trend towards significance with total BMC, which was also in a positive direction ($p=0.096$).

Significant associations were also seen between CpGs -2686/-2682 and -2673 methylation and offspring total BA at birth, after adjustments were made for gestational age, sex and age at time of DXA ($p<0.026$ for both). These associations were also in a positive direction, i.e. as percentage methylation increases, offspring total BA also increases. A trend towards significance is also seen between the methylation of CpG -2649/-2642 and off spring total BA ($p=0.093$).

CpG -2673 methylation was also significantly associated with total offspring BMD ($p=0.023$) in a positive direction, after adjusting for gestational age, sex and age at time of DXA. There were no significant associations or trends towards significance between the methylation of any of the other CpGs and offspring total BMD, nor were any significant associations or trends between the methylation levels of any of the CpGs and scBMC.

Figure 7.2 visually demonstrates some of the significant associations between specific *RXRA* CpG methylation in umbilical cord and offspring total BMC and total BA at birth using scatter plots.

	Baby DXA: Total BMC (g), adjusted for gestational age, sex and age			Baby DXA: Total BA (cm sq), adjusted for gestational age, sex and age		
	n	**b**	**p-value**	**n**	**b**	**p-value**
***RXRA* CpG -2686/-2682**	132	0.014	0.005	132	25.431	0.004
***RXRA* CpG -2673**	297	0.008	0.022	297	13.092	0.025
***RXRA* CpG -2649/-2642**	295	0.006	0.096	295	10.515	0.093
***RXRA* CpG -2554**	290	-0.003	0.374	290	-4.787	0.414
***RXRA* CpG -2406**	298	-0.002	0.532	298	-4.993	0.394
***RXRA* CpG -2357**	297	-0.003	0.35	297	-4.982	0.379
	Baby DXA: Total BMD (g/ cm sq), adjusted for gestational age, sex and age			**Baby DXA: scBMC (g), adjusted for gestational age, sex and age**		
	n	**b**	**p-value**	**n**	**b**	**p-value**
***RXRA* CpG -2686/-2682**	132	0.007	0.434	132	-0.001	0.466
***RXRA* CpG -2673**	297	0.011	0.081	297	-6.58E-05	0.93
***RXRA* CpG -2649/-2642**	295	0.006	0.363	295	-0.000171	0.832
***RXRA* CpG -2554**	290	-0.006	0.379	290	-0.000101	0.893
***RXRA* CpG -2406**	298	0.002	0.808	296	0.001	0.2
***RXRA* CpG -2357**	297	0.0	0.287	295	-0.000478	0.514

Table 7.3: Associations between *RXRA* CpG methylation in umbilical cord tissue and offspring bone outcomes at birth in SWS cohort. There are significant positive associations between methylation of both CpGs -2686/-2682 and -2673 and total BMC and total BA at birth ($p<0.026$; highlighted in orange), determined by linear regression and adjusting for gestational age, sex and age. There are also negative trends towards significance ($p<0.1$) between CpG -2649/-2642 within the *CDKN2A* region of interest and total BMC, total BA and total BMD at birth ($p<0.1$; highlighted in blue). 'n' is number of subjects and 'b' is beta value.

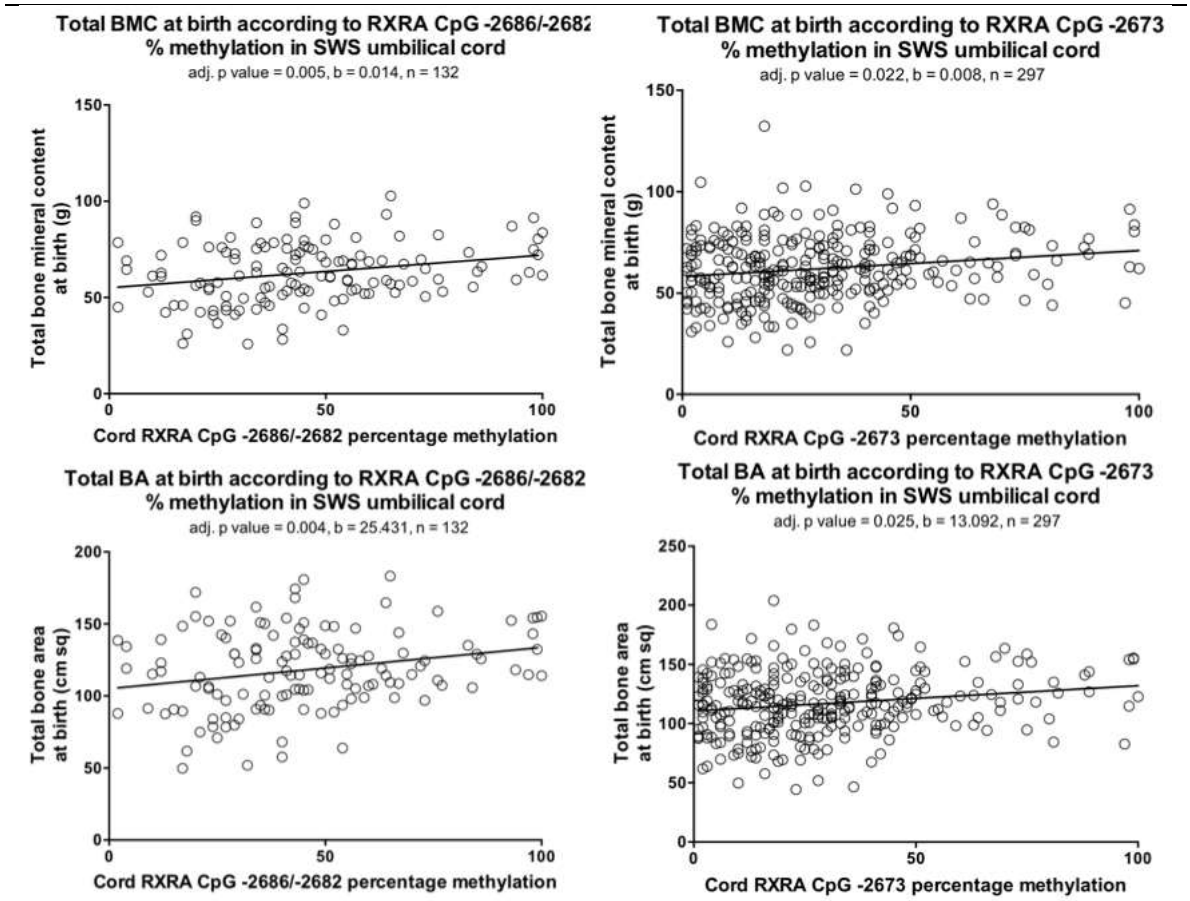

Figure 7.2: The methylation of CpGs -2686, -2673 and -2642 in *RXRA* is shown plotted against total bone mineral content (BMC) and total bone area (BA) at birth in the SWS cohort. Linear regression analyses of methylation versus bone outcome produce a positive beta value, demonstrating a positive association between methylation of each of the CpGs and the bone outcome represented on the above graphs. As the percentage methylation of each of these CpGs increases, total BMC and total BA also increases at birth. p-values across all four graphs are adjusted for gestational age, sex and age in the linear regression model.

7.3.2.2 MAVIDOS umbilical cord

To try and replicate the results seen in the SWS cohort between *RXRA* methylation in umbilical cord and offspring bone outcomes at birth, associations between methylation of these CpGs and bone outcomes of offspring in the MAVIDOS cohort were investigated. Methylation of CpGs -2686, -2682, -2673 and -2642 in *RXRA* in umbilical cord have a significant positive association with offspring total BMC at birth ($p<0.035$ in all cases), after adjusting for sex, age and gestational age (Table 7.4). Methylation of CpG -2649 also showed a weak trend towards significance with offspring total BMC, which was also in the positive direction ($p<0.072$). No other CpGs within the *RXRA* DMR were found to have any significant associations with offspring total BMC at birth ($p>0.05$).

Significant associations were also found between CpGs -2682, -2673 and -2642 methylation ($p<0.04$ in all cases) and offspring total BA after adjusting for sex, age and gestational age, which were in a positive direction. Associations trending towards significance were also found between the methylation of CpGs -2682 and -2649 ($p<0.06$) and total BA in a positive direction. There were no other significant associations measured between the remaining CpGs in the *RXRA* DMR and offspring total BA ($p>0.05$).

Only CpG -2686 showed a significance positive association between percentage methylation and offspring total BMD ($p=0.046$) and there were only weak associations between the methylation of CpGs -2406 and -2391 and prentice BMC ($p=0.064$ and $p=0.096$ respectively), after adjusting for sex, age and gestational age, though these associations were in a negative direction. No other CpGs within the *RXRA* DMR showed any significant associations between percentage methylation and these two offspring bone outcomes. Figure 7.3 visually demonstrates some of the significant associations between specific *RXRA* CpG methylation in umbilical cord and offspring total BMC, total BA and total BMD at birth using scatter plots.

	Baby DXA: Total BMC (g), adjusted for gestational age, sex and age			Baby DXA: Total BA (cm sq), adjusted for gestational age, sex and age		
	n	b	p-value	n	b	p-value
***RXRA* CpG -2686**	123	0.217	0.018	123	0.573	0.058
***RXRA* CpG -2682**	125	0.273	0.011	125	0.866	0.014
***RXRA* CpG -2673**	133	0.207	0.021	133	0.598	0.039
***RXRA* CpG -2649**	134	0.155	0.071	134	0.548	0.056
***RXRA* CpG -2642**	144	0.173	0.034	144	0.604	0.026
***RXRA* CpG -2406**	143	0.09	0.519	143	0.665	0.15
***RXRA* CpG -2391**	139	0.058	0.607	139	0.372	0.32
***RXRA* CpG -2387**	135	0.114	0.38	135	0.583	0.177
***RXRA* CpG -2385**	129	0.062	0.61	129	0.327	0.42
***RXRA* CpG -2357**	147	0.138	0.402	147	0.572	0.294
***RXRA* CpG -2346**	94	0.018	0.826	94	-0.008	0.977
	Baby DXA: Total BMD (g/ cm sq), adjusted for gestational age, sex and age			**Baby DXA: scBMC (g), adjusted for gestational age, sex and age**		
	n	**b**	**p-value**	**n**	**b**	**p-value**
***RXRA* CpG -2686**	123	0.000337	0.046	123	0.005	0.914
***RXRA* CpG -2682**	125	0.000312	0.12	125	-0.011	0.849
***RXRA* CpG -2673**	133	0.000271	0.117	133	-0.017	0.731
***RXRA* CpG -2649**	134	0.000117	0.466	134	-0.051	0.25
***RXRA* CpG -2642**	144	0.000145	0.341	144	-0.046	0.282
***RXRA* CpG -2406**	143	-0.000191	0.461	143	-0.135	0.064
***RXRA* CpG -2391**	139	-8.60E-05	0.681	139	-0.099	0.096
***RXRA* CpG -2387**	135	-5.94E-05	0.806	135	-0.101	0.141
***RXRA* CpG -2385**	129	-4.59E-05	0.839	129	-0.07	0.284
***RXRA* CpG -2357**	147	2.98E-05	0.922	147	-0.074	0.385
***RXRA* CpG -2346**	94	4.23E-05	0.775	94	0.012	0.758

Table 7.4: The associations between methylation of *RXRA* in MAVIDOS umbilical cord DNA and bone outcomes at birth, determined by linear regression. There were significant associations between methylation of CpGs -2686, -2682, -2673 and -2642 and total BMC, with a trend seen between CpG -2649 methylation and total BMC. Methylation of CpGs -2682, -2673 and -2642 also showed significant associations with offspring total BA, whereas there is a trend towards significance with CpGs -2686 and -2649. CpG -2686 methylation was significantly associated with offspring total BMD in a positive direction, whereas only trends towards significance were seen between CpG -2406 and -2391 methylation and total prentice BMC. Significant associations are highlighted in orange and trends towards significance are highlighted in blue. 'n' is number of subjects and 'b' is beta value.

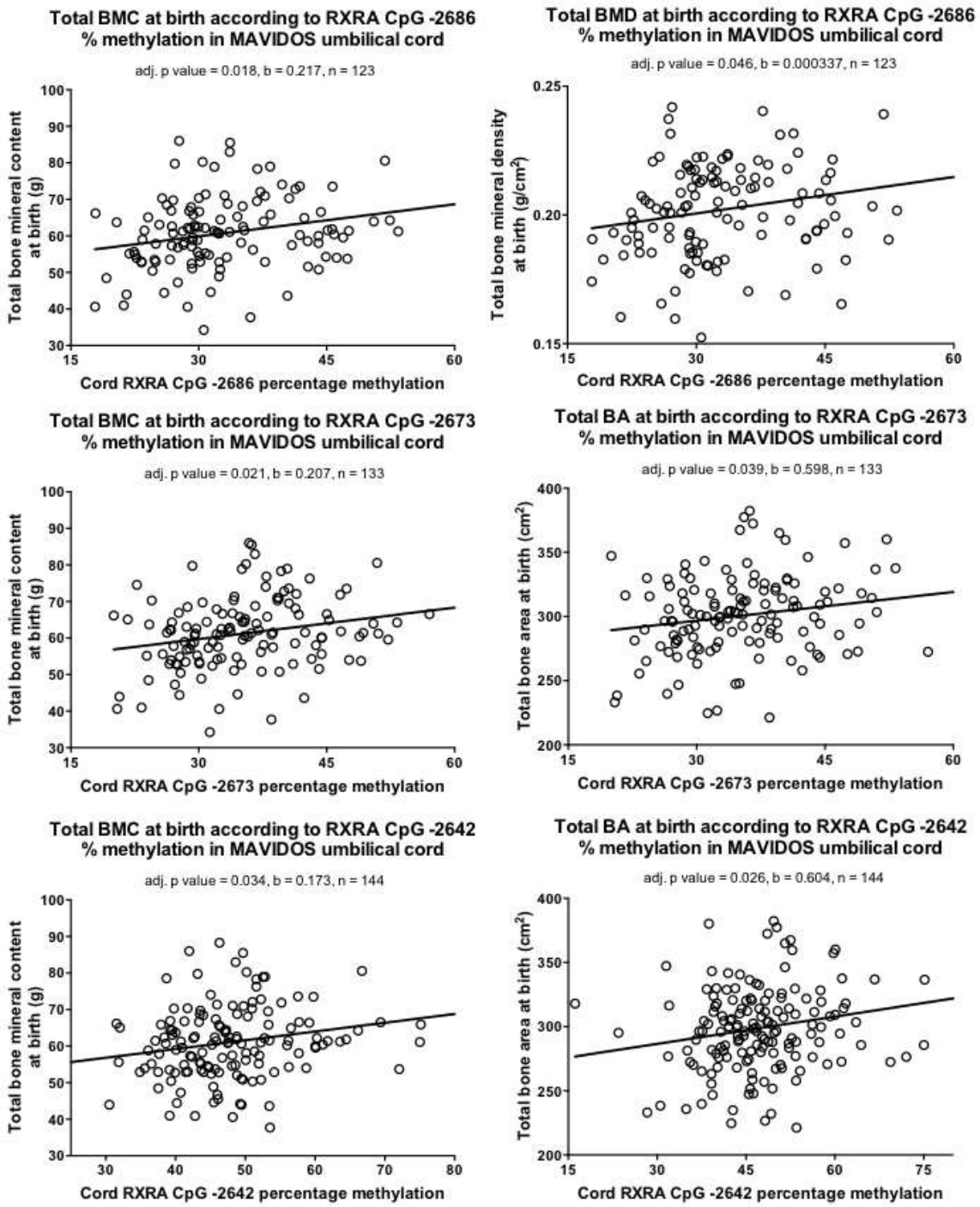

Figure 7.3: The methylation of CpGs -2686, -2673 and -2642 in *RXRA* is shown plotted against total bone mineral content (BMC), total bone mineral density (BMD) and total bone area (BA) at birth in the MAVIDOS cohort. As the percentage methylation of each of these CpGs increases, total BMC, total BMD and total BA increases at birth (adj. p<0.047). Linear regression analyses of methylation versus bone outcome produce a positive beta value, demonstrating a positive association between methylation of each of the CpGs and the bone outcome represented on the above graphs. p-values across all six graphs are adjusted for gestational age, sex and age in the linear regression model.

7.3.3 Is the methylation of *NOS3* associated with offspring bone outcomes at birth?

7.3.3.1 SWS umbilical cord

It has been shown that there are strong positive correlations between the methylation of a CpG within the *NOS3* promoter and offspring BA, BMC and aBMD at 9 years of age. Therefore, linear regression analysis was used to determine whether similar associations are present between methylation in umbilical cord and offspring bone outcomes at birth. These analyses revealed that there are no significant associations, nor trends towards significance, in SWS umbilical cord between the methylation of CpG -3526 in the *NOS3* promoter and offspring total BMC, total BA, total BMD or total prentice BMC after adjusting for gestational age, sex and age at time of DXA (Table 7.5).

	Baby DXA: Total BMC (g), adjusted for gestational age, sex and age			**Baby DXA: Total BA (cm sq), adjusted for gestational age, sex and age**		
	n	**b**	**p-value**	**n**	**b**	**p-value**
***NOS3* CpG -3526**	129	0.001	0.96	129	3.258	0.851
	Baby DXA: Total BMD (g/ cm sq), adjusted for gestational age, sex and age			**Baby DXA: scBMC (g), adjusted for gestational age, sex and age**		
	n	**b**	**p-value**	**n**	**b**	**p-value**
***NOS3* CpG -3526**	129	-0.011	0.547	129	-0.001	0.637
	Baby DXA: Percentage BMC (%), adjusted for gestational age, sex and age					
	n	**b**	**p-value**			
***NOS3* CpG -3526**	129	-0.034	0.856			

Table 7.5: The associations between methylation of *NOS3* in SWS umbilical cord DNA and bone outcomes at birth, determined by linear regression. There are no significant associations between the methylation of CpG -3526 and offspring total BMC, total BA, total BMD or total prentice BMC. 'n' is number of subjects and 'b' is beta value.

7.3.3.2 MAVIDOS umbilical cord

To replicate what was seen in the SWS cohort, linear regression analyses between methylation and offspring bone outcomes at birth were carried out using data from the MAVIDOS cohort. Methylation of CpG -3526 in the *NOS3* promoter in umbilical cord was associated with percentage BMC at birth after correcting for sex, age at time of DXA and gestational age (p=0.032; Table 7.6). This association is in the positive direction, with an increase in methylation leading to an increase in percentage BMC. There are no other significant associations between the methylation of CpG -3526 and the remaining offspring bone outcomes at birth (p>0.05).

	Baby DXA: Total BMC (g), adjusted for gestational age, sex and age			**Baby DXA: Total BA (cm sq), adjusted for gestational age, sex and age**		
	n	**b**	**p-value**	**n**	**b**	**p-value**
***NOS3* CpG -3526**	155	0.35	0.121	155	0.795	0.286
	Baby DXA: Total BMD (g/ cm sq), adjusted for gestational age, sex and age			**Baby DXA: scBMC (g), adjusted for gestational age, sex and age**		
	n	**b**	**p-value**	**n**	**b**	**p-value**
***NOS3* CpG -3526**	155	0.001	0.203	155	0.172	0.117
	Baby DXA: Percentage BMC (%), adjusted for gestational age, sex and age					
	n	**b**	**p-value**			
***NOS3* CpG -3526**	155	0.007	0.032			

Table 7.6: The associations between methylation of *NOS3* in MAVIDOS umbilical cord DNA and bone outcomes at birth. There is a significant association between the methylation levels of CpG -3526 in the *NOS3* promoter and offspring percentage BMC (highlighted in orange). There were no other significant associations, nor trends towards significance, between the methylation of this CpG and any other offspring bone outcomes. 'n' denotes number of subjects and 'b' is beta value.

7.3.4 Is the methylation of *CDKN2A*, *RXRA* and *NOS3* associated with birth weight?

7.3.4.1 *CDKN2A*

As birth weight has been shown to be associated with offspring bone outcomes at birth and in later life (118,340), analyses were run to see if the methylation of *CDKN2A*, *RXRA* and *NOS3* are affected by birth weight. Using linear regression analysis, the methylation of CpGs in the *CDKN2A* promoter in SWS umbilical cord was not significantly associated with birth weight, after adjusting for sex, age at time of DXA and gestational age (Table 7.7, left).

In the MAVIDOS cohort, the methylation of CpGs -887 and -907 in the *CDKN2A* promoter in umbilical cord was significantly associated with birth weight (p=0.014 and p=0.02 respectively), after adjusting for sex, age at time of DXA and gestational age, where the methylation was negatively associated with birth weight (Table 7.7, right). There were no significant associations between methylation and any of the remaining CpGs measured within the *CDKN2A* differentially methylated region of interest and birth weight in umbilical cord.

SWS	Birthweight (g), adjusted for sex, age and gestational age			MAVIDOS	Birthweight (g), adjusted for sex, age and gestational age		
	n	b	p-value		n	b	p-value
***CDKN2A*CpG -769**	443	-2.16	0.451	***CDKN2A*CpG -769**	136	-2.86	0.442
***CDKN2A*CpG -793**	435	-3.072	0.264	***CDKN2A*CpG -793**	119	-4.86	0.211
***CDKN2A*CpG -796**	370	-5.138	0.179	***CDKN2A*CpG -796**	106	-10.738	0.167
***CDKN2A*CpG -836**	499	-2.742	0.274	***CDKN2A*CpG -836**	147	-4.438	0.234
***CDKN2A*CpG -845**	495	-2.662	0.310	***CDKN2A*CpG -845**	144	-4.1	0.343
***CDKN2A*CpG -852**	495	-2.701	0.256	***CDKN2A*CpG -852**	142	-4.679	0.252
***CDKN2A*CpG -861**	493	-1.543	0.562	***CDKN2A*CpG -861**	137	-5.285	0.26
***CDKN2A*CpG -887**	479	-3.823	0.163	***CDKN2A*CpG -887**	146	-10.141	0.014
***CDKN2A*CpG -907**	421	-4.647	0.114	***CDKN2A*CpG -907**	144	-9.863	0.02

Table 7.7: The associations between *CDKN2A* CpG loci methylation in SWS (left) and MAVIDOS (right) umbilical cord tissue and birth weight. In the SWS cohort, methylation of the CpGs within the *CDKN2A* DMROI are not significantly associated with offspring birth weight, determined by a linear regression analysis and adjusting for sex, age at time of DXA and gestational age. In the MAVIDOS cohort, the methylation of CpGs -887 and -907 are significantly associated with offspring birth weight in a negative direction (p values highlighted in orange), determined by a linear regression analysis and adjusting for sex, age at time of DXA and gestational age. 'n' is number of subjects and 'b' is beta value.

7.3.4.2 *RXRA*

In the SWS cohort, the methylation of CpGs -2686/-2682 in *RXRA* in SWS umbilical cord has a significant positive association with birth weight after adjustments for sex, age at time of DXA and gestational age have been made (p=0.038), i.e. an increase in methylation is associated with an increase in birth weight (Table 7.8, left). The remaining CpGs do not show any significant associations between methylation and birth weight (p>0.05 in all cases).

In the MAVIDOS cohort, the methylation of CpGs -2686 to -2642 in *RXRA* in MAVIDOS umbilical cord has a significant positive association with birth weight after adjustments for sex, age and gestational age have been made (p<0.039 in all cases) (Table 7.8, right), i.e. an increase in methylation is associated with an increase in birth weight. The remaining CpGs do not show any significant associations between methylation and birth weight (p>0.05 in all cases).

SWS	**Birthweight (g), adjusted for sex, age and gestational age**			**MAVIDOS**	**Birthweight (g), adjusted for sex, age and gestational age**		
	n	**b**	**p-value**		**n**	**b**	**p-value**
***RXRA* CpG -2686/-2682**	306	165.2	0.038	***RXRA* CpG -2686**	123	8.184	0.049
***RXRA* CpG -2673**	563	120.43	0.287	***RXRA* CpG -2682**	125	10.859	0.026
***RXRA* CpG -2649/-2642**	561	119.81	0.459	***RXRA* CpG -2673**	133	8.425	0.037
***RXRA* CpG -2554**	556	113.85	0.557	***RXRA* CpG -2649**	134	9.728	0.026
***RXRA* CpG -2406**	564	112.43	0.904	***RXRA* CpG -2642**	144	8.94	0.019
***RXRA* CpG -2357**	564	108.21	0.21	***RXRA* CpG -2406**	143	5.083	0.441
				***RXRA* CpG -2391**	139	2.874	0.578
				***RXRA* CpG -2387**	135	3.82	0.518
				***RXRA* CpG -2385**	129	1.288	0.818
				***RXRA* CpG -2357**	147	3.708	0.623
				***RXRA* CpG -2346**	94	0.208	0.955

Table 7.8: The associations between specific *RXRA* CpG loci methylation in SWS (left) and MAVIDOS (right) umbilical cord tissue and birth weight. In the SWS cohort, the methylation of CpGs -2686/-2684 are significantly associated with offspring birth weight in a positive direction (p-values highlighted in orange), determined by a linear regression analysis and adjusting for sex, age and gestational age. In the MAVIDOS cohort, the methylation of CpGs -2686 to -2642 are significantly associated with offspring birth weight in a positive direction (p-values highlighted in orange), determined by a linear regression analysis and adjusting for sex, age and gestational age. 'n' is number of subjects and 'b' is beta value.

7.3.4.3 *NOS3*

In both the SWS and MAVIDOS cohorts, there were no significant associations, nor trends towards significance, between the methylation of CpG -3526 within the *NOS3* promoter and birth weight in umbilical cord samples (Table 7.9, left and right respectively).

SWS	**Birthweight (g), adjusted for sex, age and gestational age**			**MAVIDOS**	**Birthweight (g), adjusted for sex, age and gestational age**		
	n	**b**	**p-value**		**n**	**b**	**p-value**
***NOS3* CpG -3526**	292	13.32	0.967	***NOS3* CpG -3526**	155	7.327	0.478

Table 7.9: The associations between specific *NOS3* CpG loci methylation in SWS (left) and the MAVIDOS (right) umbilical cord tissue and birth weight. In both the SWS and MAVIDOS cohorts there are no significant associations between the methylation of CpG -3526 in the *NOS3* promoter and birth weight after adjusting for gestational age, sex and age at DXA, determined by linear regression. 'n' is number of subjects and 'b' is beta value.

7.3.4.4 The association between birth weight and offspring bone outcomes at birth

When previously significant associations between methylation of CpGs within the *CDKN2A* and *RXRA* regions of interest and offspring total BMC were adjusted for sex, age at time of DXA and birthweight, these associations are no longer significant in either cohort (Table 7.10). However, the association between *RXRA* CpG -2686 methylation and total BMC in the MAVIDOS cohort shows a trend towards significance (p=0.078). Linear regression revealed that there was a significant positive association between birth weight and offspring total BMC at birth in both the SWS and MAVIDOS cohorts (Figure 7.4).

SWS	Total BMC (g), adjusted for sex, age and birthweight			MAVIDOS	Total BMC (g), adjusted for sex, age and birth weight		
	n	b	p-value		n	b	p-value
***CDKN2A* CpG -796**	443	-5.38E-05	0.374	***CDKN2A* CpG -887**	146	0.012	0.816
***CDKN2A* CpG -845**	495	-6.62E-05	0.257	***CDKN2A* CpG -907**	144	0.008	0.881
***CDKN2A* CpG -907**	421	-0.000116	0.064	***RXRA* CpG -2686**	123	0.096	0.078
***RXRA* CpG -2686/-2682**	306	0.006	0.125	***RXRA* CpG -2682**	125	0.095	0.146
***RXRA* CpG -2673**	563	0.004	0.126	***RXRA* CpG -2673**	133	0.08	0.14
				***RXRA* CpG -2649**	134	0.064	0.197
				***RXRA* CpG -2642**	144	0.064	0.181

Table 7.10: The associations between *CDKN2A* and *RXRA* CpG methylation in umbilical cord and offspring total BMC at birth in the SWS (left) and MAVIDOS (right) cohorts. When associations between *CDKN2A* and *RXRA* CpG methylation and offspring total BMC at birth determined by linear regression are adjusted for sex, age at time of DXA and birth weight, all previous significant associations become non-significant. Association between methylation *RXRA* CpG -2686 and total BMC shows a trend towards significance (highlighted in blue). 'n' is number of subjects and 'b' is beta value.

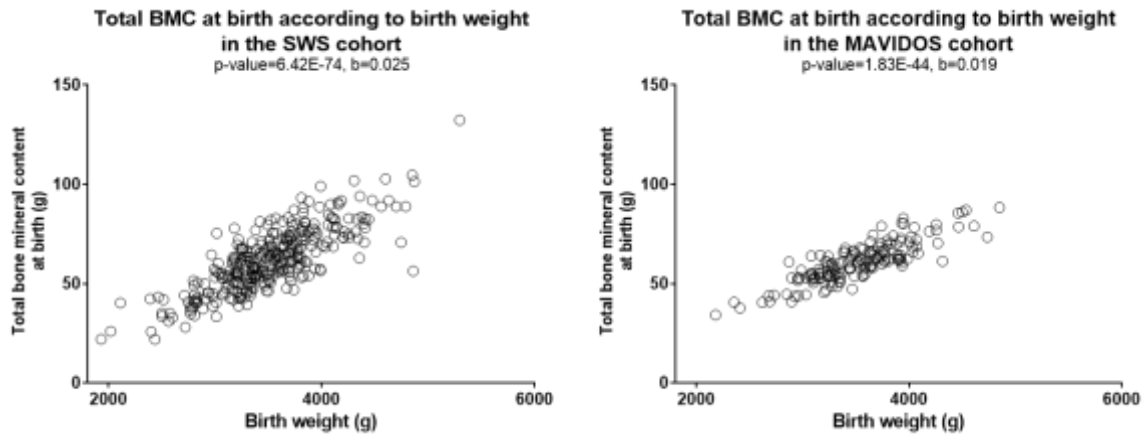

Figure 7.4: The association between birth weight and offspring total BMC at birth in the SWS cohort (left) and the MAVIDOS cohort (right). In both cohorts there is a significant positive association between birth weight and total BMC at birth determined by linear regression. 'b' is beta value.

When previously significant associations between methylation of CpG loci within *CDKN2A* and *RXRA* and offspring total BA were adjusted for sex, age at time of DXA and birth weight, these associations are no longer significant in either cohort (Table 7.11), with the exception of the methylation of CpGs -2686/-2682 and -2673 in the RXRA region of interest. In the SWS cohort, the associations of the methylation for these CpGs and total BA remained significant after adjusting for birth weight. Linear regression revealed that there was also a significant positive association between birth weight and offspring total BA at birth in both the SWS and MAVIDOS cohorts (Figure 7.5).

SWS	Total BA (cm sq), adjusted for sex, age and birthweight			MAVIDOS	Total BA (cm sq), adjusted for sex, age and birth weight		
	n	b	p-value		n	b	p-value
***CDKN2A* CpG -796**	443	-0.084	0.379	***CDKN2A* CpG -887**	146	0.09	0.598
***CDKN2A* CpG -907**	421	-0.185	0.062	***CDKN2A* CpG -907**	144	0.16	0.36
***RXRA* CpG -2686/-2682**	306	10.54	0.046	***RXRA* CpG -2686**	123	0.091	0.599
***RXRA* CpG -2673**	563	9.23	0.014	***RXRA* CpG -2682**	125	0.235	0.256
				***RXRA* CpG -2673**	133	0.117	0.491
				***RXRA* CpG -2649**	134	0.183	0.25
				***RXRA* CpG -2642**	144	0.186	0.222

Table 7.11: The associations between *CDKN2A* and *RXRA* CpG methylation in umbilical cord and offspring total BA at birth in the SWS (left) and MAVIDOS (right) cohorts. When associations between *CDKN2A* and *RXRA* CpG methylation and offspring total BA at birth determined by linear regression are adjusted for sex, age at time of DXA and birth weight, all previous significant associations become non-significant in both cohorts, with the exception of RXRA CpGs -2686/-2682 and -2673 in the SWS cohort, which remain significant (highlighted in orange). 'n' is number of subjects and 'b' is beta value.

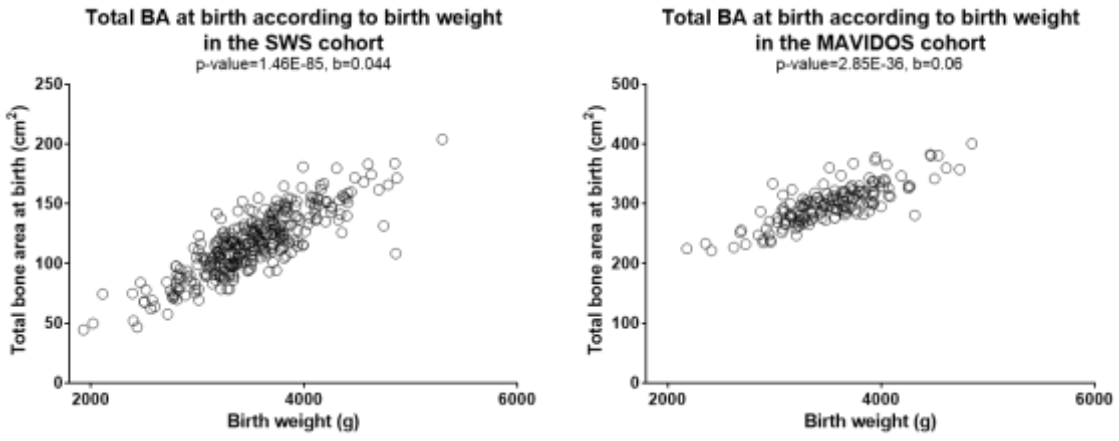

Figure 7.5: The association between birth weight and offspring total BA at birth in the SWS cohort (left) and the MAVIDOS cohort (right). In both cohorts there is a significant positive association between birth weight and total BMC at birth determined by linear regression. 'b' is beta value.

When previously significant associations between methylation of CpGs within the *CDKN2A* and *RXRA* regions of interest and total offspring BMD were adjusted for sex, age at time of DXA and birth weight, these associations are no longer significant in either cohort (Table 7.12). However, in the MAVIDOS cohort, the association between *RXRA* CpG -2686 methylation and total BMC shows a trend towards significance (p=0.086). Linear regression revealed that there was also a significant positive association between birth weight and offspring total BMD at birth in both the SWS and MAVIDOS cohorts (Figure 7.6).

SWS	Total BMD (g/cm sq), adjusted for sex, age and birth weight			MAVIDOS	Total BMD (g/cm sq), adjusted for sex, age and birth weight		
	n	b	p-value		n	b	p-value
***CDKN2A* CpG -845**	495	-0.000178	0.21	***CDKN2A* CpG -887**	146	-2.44E-05	0.874
				***CDKN2A* CpG -907**	144	-7.92E-05	0.615
				***RXRA* CpG -2686**	123	0.000261	0.086
				***RXRA* CpG -2682**	125	0.000144	0.43
				***RXRA* CpG -2673**	133	0.000175	0.263
				***RXRA* CpG -2649**	134	6.77E-05	0.638
				***RXRA* CpG -2642**	144	6.91E-05	0.616

Table 7.12: The associations between *CDKN2A* and *RXRA* CpG methylation in umbilical cord and offspring total BMD at birth in the SWS (left) and MAVIDOS (right) cohorts. When associations between *CDKN2A* and *RXRA* CpG methylation and offspring total BMD at birth determined by linear regression are adjusted for sex, age at time of DXA and birth weight, all previous significant associations become non-significant in both cohorts. The association between methylation *RXRA* CpG -2686 and total BMD shows a trend towards significance (highlighted in blue). 'n' is number of subjects and 'b' is beta value.

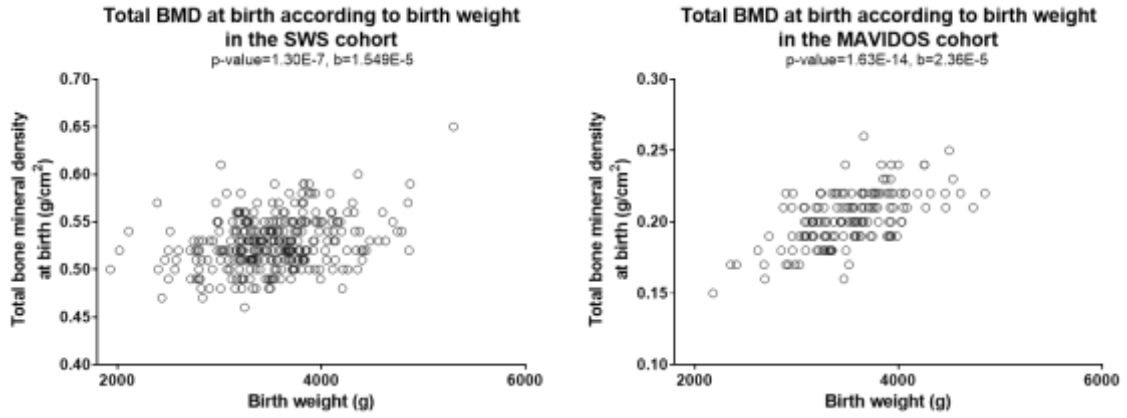

Figure 7.6: The association between birth weight and offspring total BMC at birth in the SWS cohort (left) and the MAVIDOS cohort (right). In both cohorts there is a significant positive association between birth weight and total BMD at birth determined by linear regression. 'b' is beta value.

7.3.5 Is the methylation of *CDKN2A*, *RXRA* and *NOS3* measured in MAVIDOS umbilical cord tissue affected by maternal vitamin D supplementation?

As the active metabolite of vitamin D_3 has been shown to induce the demethylation of DNA, we looked at whether there were any significant differences between CpG methylation in umbilical cord tissue across the three genes of interest between the mothers on placebo and the mothers supplemented daily with 1000 IU cholecalciferol.

This trial showed that there was a significant difference in maternal serum vitamin D concentrations between the placebo and cholecalciferol supplemented groups at 14 and 34 weeks gestation. There was no difference in the serum 25-hydroxyvitamin D concentrations between the two treatment groups at 14 weeks gestation, though this would be expected as this is when mothers began taking daily supplements of cholecalciferol (Figure 7.7A); however there was a significant difference in serum 25-hydroxyvitamin D concentrations between the placebo and cholecalciferol supplemented group at 34 weeks gestation (Figure 7.7B). At this time point there was a significant increase in maternal serum vitamin D concentrations when compared to the placebo group.

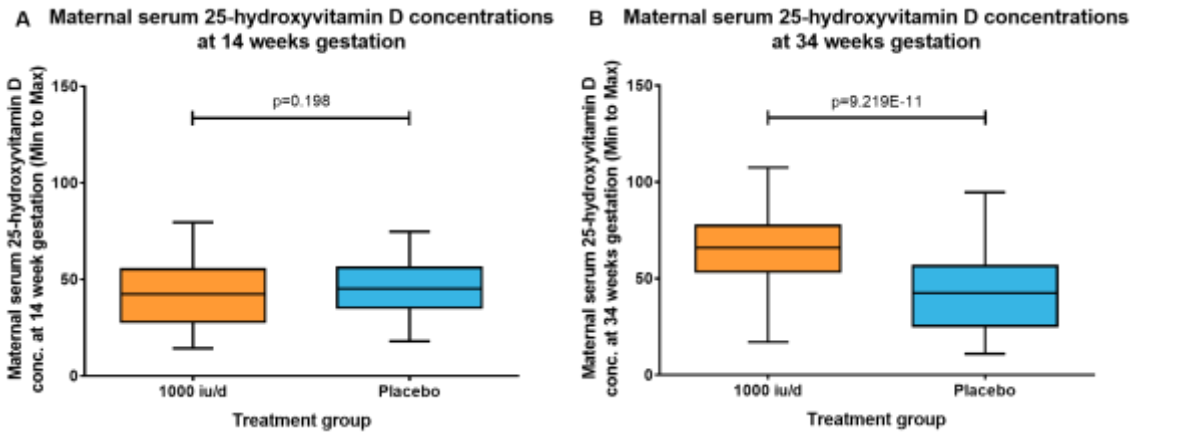

Figure 7.7: Comparison of maternal serum 25-hydroxyvitamin D concentrations between cholecalciferol supplemented and placebo groups at (A) 14 weeks and (B) 34 weeks gestation. At 14 weeks there was no significant difference in maternal serum vitamin D concentrations between the supplementation (n=77) and placebo (n=79) groups (A). At 34 weeks gestation there was a significant increase in serum vitamin D concentrations in mothers who were taking daily cholecalciferol supplements (n=75) when compared to the mothers taking placebo (n=78) ($p=9.219x10^{-11}$). Both p-values were determined by an unpaired *t*-test.

7.3.5.1 *CDKN2A*

Figure 7.8 shows that the methylation of CpGs within the *CDKN2A* region of interest in umbilical cord tissue from the offspring is not significantly different between the placebo and treatment groups, determined by a Mann-Whitney U test (p>0.05). When the analysis was stratified by season of birth, the methylation of CpG -836 was significantly different between the placebo and treatment groups for those babies born in the spring months. No other differences were seen for any other CpGs during any other season of birth.

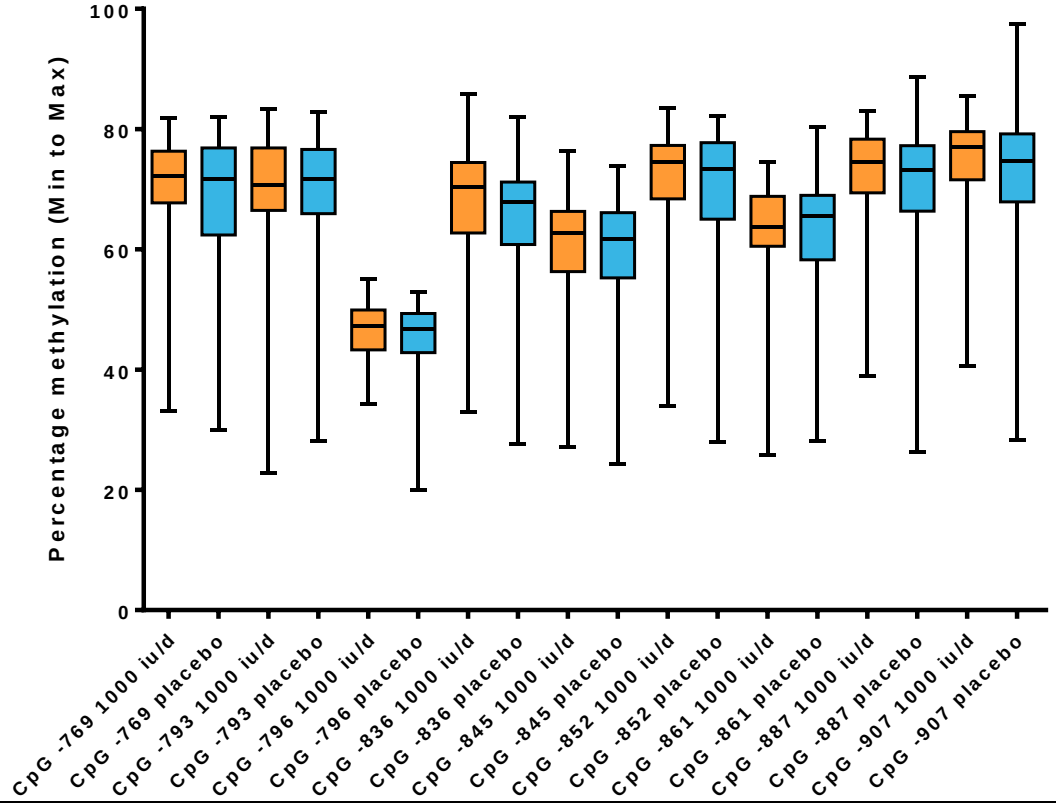

Figure 7.8: The methylation of *CDKN2A* in umbilical cord tissue of offspring of mothers on placebo or 1000 IU cholecalciferol/day. The methylation of the CpGs within the *CDKN2A* DMR was not significantly different in the umbilical cord tissue between mothers on 1000 IU cholecalciferol/day and mothers on placebo, determined by a Mann-Whitney U test (p>0.05).

7.3.5.2 *RXRA*

Methylation of CpGs -2673 to -2357 within the *RXRA* region of interest was significantly different between the placebo and treatment groups (Table 7.13), determined by an independent *t*-test. As the methylation levels of CpGs -2686, -2673, -2391, -2385 and -2335 were not normally distributed, the data had to be transformed before independent *t*-tests could be used. Data was log transformed, with the exception of CpG -2346, which was squared as the data was negatively skewed. CpGs -2673 to -2357 all showed a significant difference in methylation levels of umbilical cord tissue between the mothers taking placebo and the mothers treated with 1000 IU cholecalciferol/day ($p<0.043$ for all CpGs, highlighted in orange). The methylation of the remaining CpGs within the *RXRA* region of interest in offspring umbilical cord tissue was not found to be significantly different between the two treatment groups.

	n	p-value	Mean diff. % methylation	95% Confidence Intervals	
				Lower	Upper
***RXRA* CpG -2686 (log transformed)**	123	0.535	-0.0130	-0.0543	0.0283
***RXRA* CpG -2682**	125	0.148	-2.0703	-4.8847	0.7442
***RXRA* CpG -2673 (log transformed)**	133	0.042	-0.0371	-0.0728	-0.0013
***RXRA* CpG -2649**	134	0.037	-3.0375	-5.8832	-0.1919
***RXRA* CpG -2642**	144	0.019	-3.5889	-6.5680	-0.6099
***RXRA* CpG -2406**	143	0.005	-2.4872	-4.2106	-0.7638
***RXRA* CpG -2391 (log transformed)**	139	0.038	-0.0186	-0.0361	-0.0010
***RXRA* CpG -2387**	135	0.034	-2.0612	-3.9697	-0.1526
***RXRA* CpG -2385 (log transformed)**	129	0.027	-0.0172	-0.0324	-0.00198
***RXRA* CpG -2357**	147	0.011	-1.9506	-3.4544	-0.4469
***RXRA* CpG -2346 (squared)**	94	0.857	-46.7609	-561.24	467.72

Table 7.13: Independent *t*-test analysis of the *RXRA* CpG methylation in umbilical cord tissue between offspring of mothers supplemented with 1000 IU cholecalciferol/day and mothers taking placebo. The methylation of CpGs -2673 to -2357 is significantly different between the umbilical cord tissue of offspring from mothers supplemented with cholecalciferol and mothers taking placebo, determined by an independent *t*-test. The methylation of any of the other CpGs did not show significant differences across the two treatment groups. 'n' is the number of subjects and significant values, where $p<0.05$, are highlighted in orange.

Figure 7.9 visually demonstrates the significant differences in CpG methylation between the cholecalciferol supplemented group and the placebo group. Minimum to maximum box and whisker plots are shown for each of the CpGs determined to have a significant difference in methylation between the two treatment groups. For each CpG, the methylation levels were significantly lower in the umbilical cord tissue from offspring of mothers that have been supplemented with 1000 IU cholecalciferol per day than in the umbilical cord tissue from mothers in the placebo group.

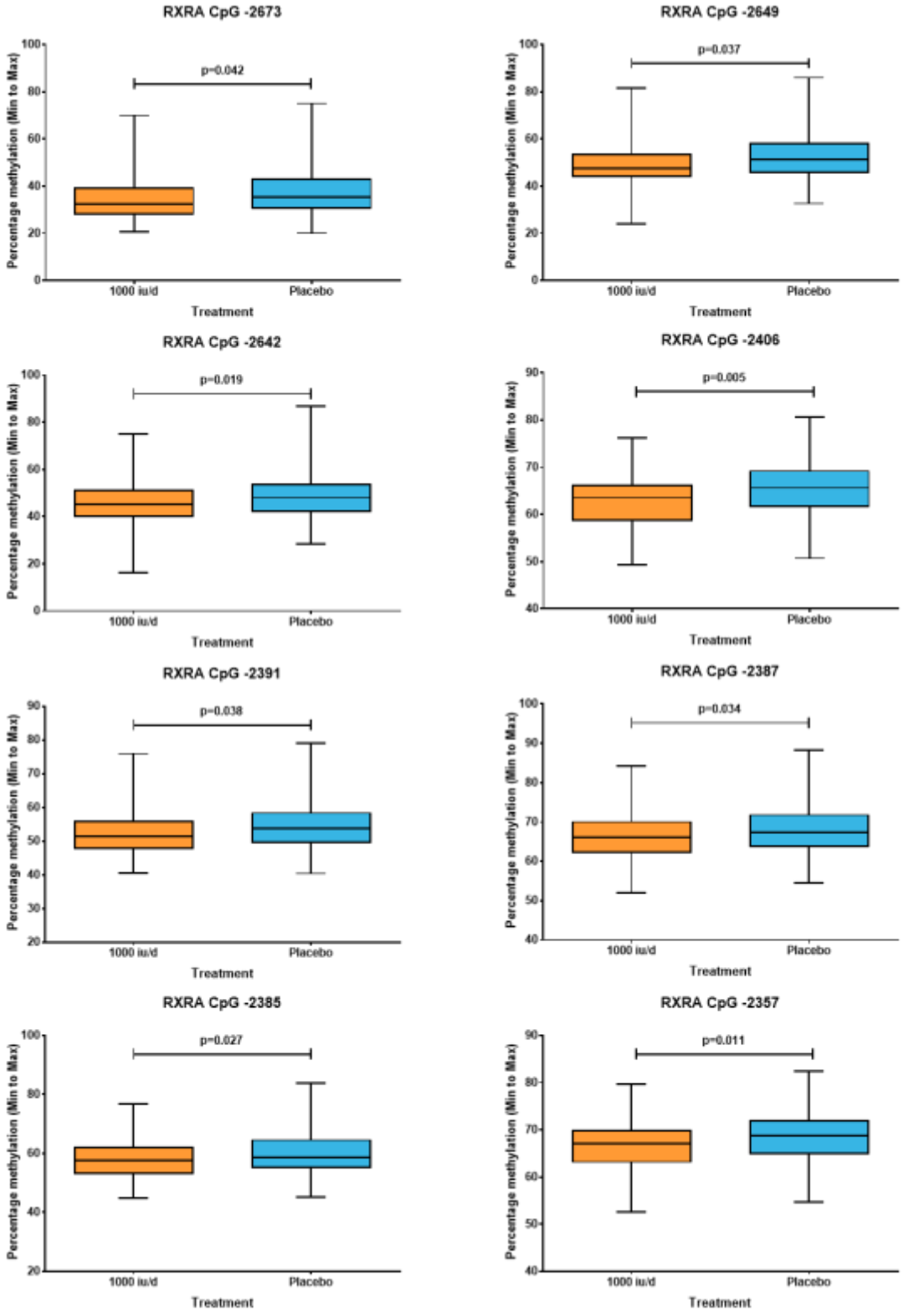

Figure 7.9: The methylation of *RXRA* in umbilical cord tissue of offspring of mothers on placebo or 1000 IU cholecalciferol/day. The methylation of *RXRA* CpGs -2673 to -2357 was significantly decreased in the umbilical cord tissue between mothers on placebo and mothers on 1000 IU cholecalciferol/day, determined by an independent *t*-test (p>0.043 for all).

The associations between *RXRA* CpG methylation and maternal treatment group were then stratified by season of birth to determine whether there were any seasonal effects on the methylation levels of CpG loci within the *RXRA* promoter. The results of an independent *t*-test show that methylation of specific CpG sites of the *RXRA* promoter in umbilical cord was significantly lower in the offspring of mothers supplemented with cholecalciferol for babies born during summer and autumn (Table 7.14).

CpGs -2682, -2649 to -2406, -2387 and -2357 show a significant change in methylation between the placebo and treatment groups for those babies born in the summer months, whereas CpGs -2673, -2391 and -2357 only show a trend towards a significant change in methylation between the two maternal treatment groups. There were no other significant differences in CpG methylation between the two treatment groups for babies born between June and August. For babies born in the autumn months, there was a significant difference in methylation of CpGs -2682 and -2673 in the umbilical cord of offspring that were born to mothers taking daily supplements of cholecalciferol when compared to mothers taking placebo. The methylation of CpGs -2642, -2391, -2385 and -2357 showed trends towards significance between the two treatment groups, whereas no other CpGs showed a significant change in methylation.

The methylation of the CpG sites within the *RXRA* promoter was not significantly different between the placebo and supplement groups in either spring or winter.

SPRING						SUMMER					
	n	p-value	Mean diff. % methylation	95% Confidence Intervals			n	p-value	Mean diff. % methylation	95% Confidence Intervals	
				Lower	Upper					Lower	Upper
RXRA CpG -2686 (log transformed)	30	0.39	0.0340	-0.0460	0.1140	RXRA CpG -2686 (log transformed)	40	0.187	-0.0424	-0.1063	0.0216
RXRA CpG -2682	30	0.153	4.0486	-1.6085	9.7057	RXRA CpG -2682	42	0.005	-5.6301	-9.4124	-1.8478
RXRA CpG -2673 (log transformed)	33	0.527	-0.0250	-0.1045	0.0546	RXRA CpG -2673 (log transformed)	44	0.089	-0.0422	-0.0912	0.0067
RXRA CpG -2649	37	0.443	1.9482	-3.1777	7.0741	RXRA CpG -2649	52	0.01	-6.0818	-10.6678	-1.4957
RXRA CpG -2642	37	0.861	-0.4972	-6.2492	5.2548	RXRA CpG -2642	52	0.012	-6.0950	-10.7567	-1.4333
RXRA CpG -2406	37	0.959	0.0884	-3.3413	3.5180	RXRA CpG -2406	53	0.014	-3.1216	-5.5704	-0.6727
RXRA CpG -2391 (log transformed)	37	0.952	0.0011	-0.0358	0.0380	RXRA CpG -2391 (log transformed)	53	0.053	-0.0268	-0.0541	0.0004
RXRA CpG -2387	37	0.811	0.4608	-3.4294	4.3510	RXRA CpG -2387	52	0.041	-2.9672	-5.8052	-0.1291
RXRA CpG -2385 (log transformed)	37	0.942	-0.0011	-0.0313	0.0291	RXRA CpG -2385 (log transformed)	51	0.074	-0.0228	-0.0479	0.0023
RXRA CpG -2357	36	0.726	-0.5017	-3.3866	2.3831	RXRA CpG -2357	52	0.033	-2.6807	-5.1408	-0.2205
RXRA CpG -2346 (squared)	21	0.877	55.4095	-682.6749	793.4939	RXRA CpG -2346 (squared)	32	0.812	-118.8375	-1136.5381	898.8630
AUTUMN						WINTER					
	n	p-value	Mean diff. % methylation	95% Confidence Intervals			n	p-value	Mean diff. % methylation	95% Confidence Intervals	
				Lower	Upper					Lower	Upper
RXRA CpG -2686 (log transformed)	32	0.82	-0.0779	-0.1666	0.0107	RXRA CpG -2686 (log transformed)	21	0.33	0.0632	-0.0690	0.1954
RXRA CpG -2682	32	0.034	-7.0212	-13.4509	-0.5915	RXRA CpG -2682	21	0.422	3.3723	-5.2481	11.9927
RXRA CpG -2673 (log transformed)	34	0.018	-0.0925	-0.1682	-0.0169	RXRA CpG -2673 (log transformed)	22	0.627	0.0268	-0.0864	0.1399
RXRA CpG -2649	40	0.51	-6.3205	-12.6642	0.0232	RXRA CpG -2649	26	0.865	0.7469	-8.2028	9.6967
RXRA CpG -2642	40	0.063	-6.6481	-13.6815	0.3855	RXRA CpG -2642	26	0.815	0.9962	-7.6841	9.6764
RXRA CpG -2406	40	0.67	-3.7737	-7.8184	0.2711	RXRA CpG -2406	26	0.341	-2.4862	-7.7575	2.7852
RXRA CpG -2391 (log transformed)	39	0.093	-0.0332	-0.0722	0.0058	RXRA CpG -2391 (log transformed)	26	0.805	-0.0065	-0.0601	0.0471
RXRA CpG -2387	39	0.105	-3.4722	-7.7112	0.7668	RXRA CpG -2387	26	0.601	-1.5469	-7.5893	4.4954
RXRA CpG -2385 (log transformed)	38	0.1	-0.0270	-0.0595	0.0055	RXRA CpG -2385 (log transformed)	25	0.553	-0.0139	-0.0615	0.0338
RXRA CpG -2357	39	0.072	-3.0561	-6.4007	0.2884	RXRA CpG -2357	26	0.764	-0.6623	-5.1740	3.8494
RXRA CpG -2346 (squared)	23	0.643	-312.0857	-1711.856	1087.6849	RXRA CpG -2346 (squared)	18	0.603	298.5476	-895.4320	1492.5272

Table 7.14: Associations between *RXRA* CpG methylation in MAVIDOS umbilical cord and maternal treatment group stratified by offspring season of birth. Independent *t*-test determined that there were significant differences in CpG -2682, -2649 to -2406, -2387 and -2357 methylation between maternal treatment groups for babies born in the summer months and significant differences in CpG -2682 and -2673 between the two groups for babies born in the autumn months. Significant p-values ($p<0.05$) highlighted in orange and p-values with a trend towards significance (0.051-0.1) highlighted in blue. 'n' denotes number of subjects.

7.3.5.3 *NOS3*

Unlike *RXRA*, there was no significant difference in the methylation levels of *NOS3* CpG -3526 in umbilical cord tissue between offspring of mothers in the placebo group and mothers in the 1000 IU cholecalciferol supplemented group (Table 7.15 and Figure 7.10). This suggests that maternal vitamin D_3 supplementation does not have an effect on the methylation status of CpG -3526 within *NOS3* in offspring umbilical cord tissue.

	n	p-value	Mean diff. % methylation	95% Confidence Intervals	
				Lower	Upper
***NOS3* CpG -3526**	123	0.469	0.3935	-1.465	0.678

Table 7.15: Independent *t*-test analysis of *NOS3* CpG -3526 methylation in umbilical cord tissue between placebo and daily 1000 IU cholecalciferol groups. There is no significance difference in the methylation levels of CpG -3526 in umbilical cord tissue of offspring between mothers supplemented with 1000 IU cholecalciferol/day and mothers on placebo. 'n' is the number of subjects.

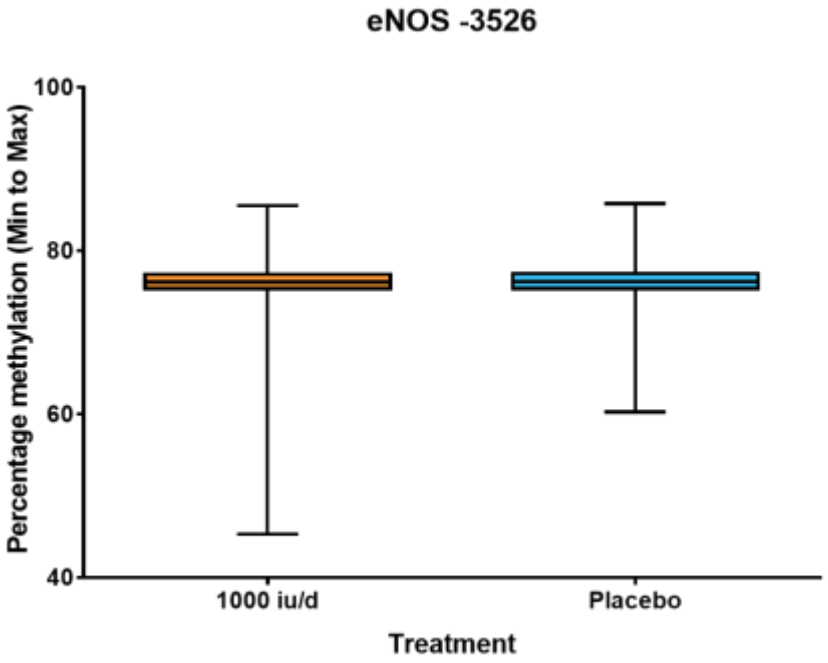

Figure 7.10: The methylation of *NOS3* CpG -3526 in umbilical cord tissue of offspring of mothers on 1000 IU cholecalciferol/day or placebo. The methylation of CpG -3526 within the *NOS3* region of interest was not significantly different in the offspring umbilical cord tissue between mothers on 1000 IU cholecalciferol/day and mothers on placebo, determined by an independent *t*-test ($p>0.05$).

7.4 Discussion

7.4.1 *CDKN2A* CpG methylation in umbilical cord and offspring bone outcomes

As with the associations at 4 and 6 years, there are significant negative associations between the methylation of CpG -907 in SWS umbilical cord and total BMC and total BA at birth. CpG -845 methylation is also significantly associated with total BMC and total BMD at birth, with a trend towards significance with total BA in a negative direction also seen. There are also associations between CpG methylation and bone outcomes at birth that are lost at 4 and 6 years. CpG -796 methylation shows a significant negative association with total BMC, total BA and total BMD at birth and there is a trend towards significance between methylation of CpG -887 and total BMC, total BA and total BMD at birth, all in a negative direction.

As none of the associations reached significance in the MAVIDOS cohort, the findings shown in the SWS cohort were not replicated. This could be because a smaller sample size from the MAVIDOS cohort was used for the regression analyses; therefore there is less power to detect a similar effect as there was less samples in the MAVIDOS cohort. However, as there were associations seen in the SWS cohort at 4 and 6 years, this may also be true of the MAVIDOS cohort, though this data is not yet available.

7.4.2 *RXRA* CpG methylation in umbilical cord and offspring bone outcomes

Previous results from Harvey and colleagues have shown that there are negative associations between the methylation of specific CpG loci in the promoter region of the *RXRA* gene and childhood bone outcomes (205). This paper revealed significant associations between the methylation levels of CpGs -2649/-2642, CpG -2554, CpG -2406 and CpG -2357 and scBMC at 4 years of age. However, there were no associations between these CpGs and BMC adjusted for total fat, total lean and height, nor where there any associations between any of the CpGs analysed and whole body BMC, BA or aBMD.

Linear regression analysis of CpG methylation in SWS umbilical cord and bone outcomes at birth revealed that, unlike at 4 years, there were no significant associations between methylation of any of the CpG sites and total prentice BMC. Whilst there were no significant associations between any of the CpGs and BMC, BA and aBMD at 4 years, total BMC and total BA showed significant positive associations with CpG -2686/-2682 and -2673 methylation at birth. The methylation of CpG -2649/-2642 showed a trend towards significance with both total BMC and total BA at birth, also in a positive direction. There was also a significant association between the methylation of CpGs -2673 and total BMD, once again in a positive direction, which were not seen at 4 years of age.

When comparing the associations between *RXRA* methylation and bone outcomes in the MAVIDOS cohort at birth to those seen in the SWS at birth, the results are a lot more consistent across the two cohorts. As the methylation analysis on the MAVIDOS cohort was done using pyrosequencing, the CpG sites that had previously been analysed together on the Sequenom MassARRAY platform (CpG -2686/-2682 and CpG -2649/-2642) could now be analysed individually and the methylation of previously unanalysed CpGs could now be examined. Unfortunately, due to sequence design, CpG -2554 could not be analysed on this platform due to sequence design constraints. Even though methylation levels have been assessed using two different platforms, it has been reported that methylation measurements are comparable across the two techniques (341).

Results from this chapter show that there are significant positive associations between methylation of CpGs -2686, -2682, -2673 and -2642 and total BMC at birth, with a trend towards significance with CpG -2649, also in a positive direction. This is also true of the SWS cohort to a certain extent as CpG -2649/-2642 came up as significant in the SWS cohort, whereas CpG -2649 only tended towards significance in MAVIDOS. The methylation of CpGs -2682, -2673 and -2642 are significantly associated with total BA in a positive direction across both cohorts, whereas the methylation of CpG -2686 only shows a significant association with total BMD in the MAVIDOS cohort, and the methylation of CpG -2673 shows a trend towards significance with BMD in the SWS cohort only.

This would suggest that, for at least some of the CpGs investigated, the associations seen in the SWS cohort between CpG methylation and offspring bone outcomes at birth have been replicated using samples from the MAVIDOS cohort. This gives us an indication that the results seen here for CpGs -2682, -2673 and -2642 are reproducible across independent cohorts and could be used as predictors of offspring bone outcomes at birth. As MAVIDOS data for childhood bone outcomes becomes available, it would be interesting to see whether these associations persist into childhood and whether they mimic what has already been seen in the SWS cohort.

7.4.3 *NOS3* CpG methylation in umbilical cord and offspring bone outcomes

Previous research has demonstrated that there are associations between the methylation of CpG -3526 within the *NOS3* promoter and offspring bone outcomes at 9 years of age (234). Methylation levels of this specific CpG site were widely varied across tested subjects and showed significant positive associations with whole-body BA, BMC and aBMD, after adjusting for sex and age. There was a trend towards a positive association between methylation and scBMD, which did not reach significance, nor did the negative association with percentage BMD.

The analysis between the methylation status of this CpG in SWS umbilical cord and offspring bone outcomes at birth, showed that there are no significant associations between methylation and total BMC, BA, and BMD. There are also no trends towards significance between CpG -3526 methylation and either scBMC or percentage BMC, which does not mimic what was seen at 9 years of age.

However, when compared to those seen in the MAVIDOS umbilical cord at birth, there are no associations between the methylation status of CpG -3526 and total BMC, BA or BMD at birth, which is consistent with what has been shown in the SWS cohort. Unfortunately scBMD was not calculated in the MAVIDOS cohort and so cannot be compared across the two. Where there is no association between methylation and percentage BMC at birth in the SWS cohort, there is a significant positive association between the two in the MAVIDOS cohort.

These findings show replication with the results seen in the SWS cohort between the methylation of CpG -3526 in the *NOS3* promoter and total BMC, BA and BMD using samples from the MAVIDOS cohort. However, as these associations did not reach significance they cannot be used as predictors of bone outcomes at birth.

7.4.4 *CDKN2A*, *RXRA* and *NOS3* methylation and birth weight

In the MAVIDOS cohort, the methylation of CpGs -887 and -907 in *CDKN2A* in umbilical cord was negatively associated with offspring birth weight, whereas there were no significant associations between *CDKN2A* CpG methylation and birth weight found in the SWS cohort through linear regression. With regards to *RXRA*, the methylation of CpG -2686/-2682 in the SWS cohort was positively associated with offspring birth weight, as was CpGs -2682 to -2642 in the MAVIDOS cohort. This could suggest that site-specific methylation of these two genes may be able to predict birth weight and other research groups have previously shown that the methylation status of CpGs in other genes, such as *CDK2* and *APOE*, has been associated with birth weight (342–344). However, in the case of *CDKN2A*, as the results were not replicated across the two cohorts this may not be the case. Instead this could be due to the difference in sample size tested, as the number of MAVIDOS samples tested was a lot smaller than those in the SWS cohort, therefore these significant associations may disappear when a greater number of MAVIDOS samples are investigated.

However, when our statistical model is adjusted for birth weight, the majority of associations seen previously between the methylation of these CpG loci in *CDKN2A* and *RXRA* and offspring bone outcomes at birth disappear, suggesting that birth weight is significantly associated with bone outcomes at birth. Linear regression showed significant positive associations between

birth weight and total BMC, BA and BMD in both the SWS and MAVIDOS cohorts, suggesting that birth weight highly influences bone outcomes at birth. A study by Beltrand *et al* has demonstrated that total BMC at birth is determined by birth weight (340) and there are various other studies to show that birth weight is associated with bone measurements in both childhood and later life (118,345,346).

As there are many components that contribute to birth weight, such as skeleton and fat mass, it cannot be said for certain that there is a direct link between a change in methylation leads to a change in birth weight and therefore a direct change in total BMC. Linear regression shows that birth weight and bone outcomes at birth are highly correlated with each other, i.e. as one increases so does the other, however we cannot elucidate which is the primary association as there are other factors to consider. The methylation of CDKN2A and RXRA may be having effects on downstream processes that could lead to an increase in birth weight by altering pathways that increase adiposity or regulate organ development. A longitudinal study by Simpkin *et al* showed that associations between methylation and developmental phenotypes, such as height, weight, fat mass and bone mass, can be influenced by birth weight (347). However by 7 years of age methylation levels have stabilised, suggesting a potential 'catch-up' period of methylation differences in the earlier years of childhood. This suggests that although site-specific CpG methylation may not be a good indicator of offspring bone outcomes at birth due to the influence of birth weight on the associations, it may still have a purpose in the prediction of offspring bone outcomes during childhood.

7.4.5 *CDKN2A*, *RXRA* and *NOS3* methylation and maternal vitamin D supplementation

There is now evidence to suggest that the active metabolite of vitamin D_3, 1α,25-dihydroxyvitamin D_3, can induce demethylation, though the exact mechanisms are not clear (196). Research groups have demonstrated that serum 25-hydroxyvitamin D_3 status, which is hydroxylated to 1α,25-dihydroxyvitamin D_3 in the kidney, was associated with lower levels of CpG methylation in the *APC*, *DKK1* and *WNT5A* genes in either cell line or primary cells (198,199). As fetuses receive vitamin D across the placenta from their mothers *in utero*, an increase in maternal 25-hydroxyvitamin D could lead to an increase in fetal 25-hydroxyvitamin D levels, and potentially a decrease in methylation of genes associated with offspring bone outcomes.

It has previously been demonstrated by Prof Harvey and colleagues (205) that an inverse relationship exists between maternal free 25-hydroxyvitamin D index (a ratio of serum 25-hydroxyvitamin D to vitamin D binding protein (VDBP) concentrations) and methylation of CpG -

2649/-2642 within the *RXRA* promoter. However, neither the maternal 34-week serum 25-hydroxyvitamin D nor VDBP relationships with methylation reached significance.

Similar to results seen in the SWS cohort, associations between 34-week serum 25-hydroxyvitamin D concentrations and *RXRA* CpG methylation levels did not reach significance (data not shown). VDBP concentrations for MAVIDOS are not available at present, therefore the association between VDBP, or the calculated maternal free 25-hydroxyvitamin D index, and methylation could not be examined. However, the MAVIDOS cohort is novel in that it allows us to directly compare changes in offspring outcomes between mothers taking placebo and mothers taking the cholecalciferol supplement. Statistical analysis revealed that there is a significant increase in maternal serum 25-hydroxyvitamin D at 34 weeks gestation in the treatment group when compared to the control group, suggesting that supplementation is increasing serum 25-hydroxyvitamin D levels in mothers during the later stages of pregnancy.

Results in this chapter suggest that maternal vitamin D supplementation with 1000 IU cholecalciferol/day has an effect on the methylation levels of specific CpG loci within the *RXRA* promoter region in offspring umbilical cord. The methylation of CpGs -2673 to -2357 in offspring umbilical cord was significantly lower in the maternal vitamin D supplemented group when compared to the placebo group, determined by independent *t*-test. No such effect was seen on the methylation of the remaining CpG loci within the *RXRA* promoter region of interest or those within the *CDKN2A* or *NOS3* regions of interest.

This could suggest that, in the neonates of the mothers supplemented with cholecalciferol, the increased vitamin D could be having an effect on the epigenetic regulation of the *RXRA* promoter. There are studies suggesting that vitamin D is associated with promoter demethylation (196,198,348) and it is well documented that a decrease in promoter methylation levels is associated with an increase in gene transcription (349–352). However, as *CDKN2A* and *NOS3* methylation levels are unaffected, this would suggest that the actions of maternal vitamin D supplementation are specific to *RXRA*.

Although a thorough literature search has not revealed any existing data demonstrating that these CpGs are important for *RXRA* expression, it has been demonstrated by Li and colleagues, through the use of a reporter construct containing the *RXRA* promoter, that when the area of the promoter region -2494 to -1500 upstream of the transcription start site is deleted from the construct, there is a significant decrease in luciferase activity (222) and that when this same region alone is ligated into luciferase reporter constructs, there is an increase in luciferase promoter activity when compared to control. This suggests that this region is important for promoter activity and that transcriptional enhancers may potentially bind to this 994bp region of

the promoter. Moreover, another reporter construct containing the region -2494 to -5114 from the TSS showed decreased luciferase activity when compared to control, suggesting that the region between these positions could contain potential binding sites for negative regulatory elements. Harvey and colleagues have also demonstrated using EMSAs, that methylation of CpG -2406 reduces transcription factor binding, suggesting that, at least for this CpG, methylation may have a functional role in *RXRA* expression (unpublished).

When the associations between RXRA methylation and supplement group were stratified by season, associations only remained significant in the summer and autumn months. The mothers of infants born in these seasons would have been exposed to more sunlight during the final months of their pregnancy than those mothers whose babies were born in the spring and winter months, which is when most placental 25-hydroxyvitamin D_3 transfer occurs due to infant bone mineralisation. This could lead to a natural increase in synthesis of maternal 25-hydroxyvitamin D_3 due to increased exposure to sunlight, which could have a cumulative effect in those mothers on the daily cholecalciferol supplement so that the amount of 25-hydroxyvitmain D_3 transferred to the fetus is increased further. This would lead to a larger decrease in methylation levels when compared to those mothers whose infants were born in the winter months.

However, as RXRα is a key mediator of the vitamin D signalling, as well as having an important role in the activation of other nuclear receptors that regulate bone homeostasis, such as PPARγ (353), the decrease in methylation seen in the *RXRA* CpG loci between the placebo and treatment groups could be caused as an indirect effect of increased levels of vitamin D, rather than vitamin D having an active role in the demethylation process, as an increase in vitamin D levels would cause a positive feedback loop, increasing the transcription of *RXRA*. When we also consider that the methylation of CpGs within *CDKN2A* and *NOS3* was unchanged, this would suggest a pathway specific incident rather than a genome-wide occurrence.

7.5 Summary

We sought to demonstrate that the associations found between methylation of *CDKN2A*, *RXRA* and *NOS3* in SWS umbilical cord and offspring bone outcomes at birth could be replicated in the MAVIDOS cohort. Results from this chapter show that both the associations seen between *RXRA* and *NOS3* in the SWS cohort were replicated in the MAVIDOS cohort. The associations between *CDKN2A* methylation and offspring bone outcomes at birth did not reach significance in the MAVIDOS cohort, though the trends were in the same direction as seen in the SWS samples. It was also shown that methylation of some of the CpG sites investigated within these genes were significantly associated with birth weight, which was shown to have significant positive

associations with total BMC, total BA and total BMD. As birth weight is a consequence of bone mass, fat mass, lean mass, etc., this suggests that methylation potentially causes a change in pathways that lead to a change in birth weight, which in turn could be driving the changes in offspring bone outcomes at birth in the MAVIDOS cohort.

We also sought to demonstrate whether maternal treatment group was having an effect on umbilical cord methylation and offspring bone outcomes. It was confirmed that a daily 1000 IU supplement of cholecalciferol caused an increase in maternal serum 25-hydroxyvitamin D at 34 weeks of pregnancy. For *RXRA*, it was demonstrated that methylation levels of CpGs -2673 to -2357 were significantly reduced in the umbilical cord of offspring from mothers that were supplemented daily with cholecalciferol when compared to mothers on placebo. Vitamin D supplementation did not have any effects on the methylation of CpGs within *CDKN2A* or *NOS3*, which suggests that vitamin D is potentially having a specific effect on *RXRA* promoter methylation. When these results were stratified by season of birth, it showed that the significant changes in methylation between the two groups were occurring in the umbilical cords of babies that had been born during the summer and autumn months, which is potentially due to increased sunlight in the final trimester leading to increased maternal 25-hydroxyvitamin D_3 synthesis. This would mean that there was more 25-hydroxyvitamin D_3 available for transfer to the fetus, thereby potentially causing the decrease in methylation that are seen in these months when compared to those seen in spring and winter months.

7.6 Further work

As some of the associations between umbilical cord methylation and offspring bone outcomes have been replicated across the SWS and MAVIDOS cohorts at birth, it would be interesting to see whether the associations between methylation and offspring bone outcomes during childhood seen in the SWS cohort can also be replicated in the MAVIDOS cohort. As the childhood data became available from the MAVIDOS cohort, linear regression analyses could be done between umbilical cord methylation and childhood bone outcomes to see if the associations seen at birth persist or change.

As well as fetal tissue, methylation levels of these CpGs within the *CDKN2A*, *RXRA* and *NOS3* genes could also be investigated in other peripheral tissues such as umbilical cord blood and venous blood samples taken throughout childhood. This would allow us to see if the methylation marks seen in umbilical cord tissue DNA are consistent across different tissue types or whether each tissue has a specific methylation pattern.

As vitamin D supplementation was shown to have a positive effect on the bone outcomes of offspring born in the winter months, it would be interesting to see if these effects persist into

childhood as childhood bone outcome data became available. As lifestyle and environmental factors after birth have been known to effect bone development (354), it would be interesting to see if these babies born to mothers who were supplemented with vitamin D still have a higher total BMC and total BA compared to those babies whose mothers were taking placebo or whether the environmental factors have a greater effect on the childhood development of the offspring. Though there is evidence to suggest that maternal vitamin D concentration may be an important determinant of skeletal growth trajectory during childhood (150). If maternal vitamin D supplementation during pregnancy does indeed allow for better bone development *in utero* and during childhood, this would allow for children to obtain a higher peak bone mass, and therefore put them at less of a risk of developing osteoporosis in later life.

As umbilical cord is a proxy tissue and as methylation profiles have been shown to be tissue specific in some cases, it is not known whether these CpGs investigated in the *RXRA* promoter region have a specific role in the regulation of *RXRA* expression in bone-related tissue. Therefore functional work in the form of dual luciferase assays, where plasmids containing the RXRA promoter region of interest with each of the CpGs mutated are transfected into SaOS-2 cells, can be used to determine whether these CpGs are important for the regulation of *RXRA* gene expression.

As maternal vitamin D treatment was shown to change to the methylation of CpGs within the RXRA promoter, if RNA can be extracted from umbilical cord, it could be determined whether this also caused a change in RXRA expression between the placebo and treatment group offspring. Primary osteoblasts could also be treated with vitamin D to determine if treatment causes any phenotypic changes to bone cells directly and whether it causes a change in the expression of markers associated with bone differentiation and mineralisation.

Chapter 8
Discussion

8. Discussion

As people live longer, diseases that are associated with age, such as osteoporosis, are becoming more frequent and are becoming a major burden on the healthcare system. The risk of developing osteoporosis in later life is determined by a number of factors, though epidemiological studies have suggested that childhood bone outcomes can be indicative of bone health in later life (151,153). Although CpG methylation within certain genes has been shown to potentially predict childhood bone outcomes, a future risk of fracture, and the mechanisms by which such methylation changes affect bone function is unknown or whether such methylation changes are simply markers of the disease process rather than causally involved. The aim of this study was to determine whether methylation of specific CpGs within the *CDKN2A* gene can be used as a biomarker for later risk of developing osteoporosis, and whether its gene products actually have a direct functional role in osteoblast regulation and bone formation.

8.1 Summary of main findings

Functional studies *in vitro* demonstrated that the *CDKN2A* CpGs associated with later bone outcomes may have an important role in the transcriptional regulation of ANRIL, a long non-coding RNA transcribed from the *CDKN2A* gene locus. These results have demonstrated that mutation of specific CpGs within CDKN2A alters ANRIL promoter activity in osteoblasts and that methylation of CpGs -887 and -907 decreased binding of transcription factors to this region. Of the transcription factor consensus sequences that were investigated, GAS and SMAD3/4 showed the strongest binding to this region, both of which play an important part in osteoblast differentiation and RUNX2 activity.

The results in chapter 4 show that ANRIL expression differs across cell types and that ANRIL expression is lower in cells that have undergone osteogenic differentiation. Transfection of an osteosarcoma cell line with siRNAs against ANRIL showed that a decrease ANRIL expression leads to a decrease in cell number that was not explained by upregulation of cell cycle arrest, but did show a significant increase in the expression of RUNX2 and ALP, two markers of osteogenic differentiation.

These knock down experiments were repeated in primary hBMSCs and osteoblasts, which also showed that ANRIL knock down induces a similar decrease in cell number as was seen in the osteosarcoma cell line. In addition, in the primary cells, there was a decrease in cell proliferation rate, though no change was seen regarding cell viability between the siRNA treated cells and controls. This suggests that the decrease in cell number is not due to differences in cell viability but due to a decrease in cell proliferation. Interestingly, RT-qPCR showed that the expression of

$p16^{INK4A}$ and $p15^{INK4B}$ were unchanged in primary osteoblasts, suggesting that ANRIL does not cause a decrease in proliferation rate and cell number through *cis*-regulatory mechanisms, but may have some *trans*-functional effects in these cells.

A gene expression array using RNA from cells that had been treated with a siRNA against exon 1 of ANRIL revealed significant differential expression of 260 genes that were altered upon ANRIL knock down, with 128 being upregulated and 132 being down regulated. Pathway analysis revealed genes that were involved in osteoblast specific pathways, such as differentiation, migration, cell viability and adhesion, as well as pathways that were involved in connective tissue deposition and development. Gene ontology enrichment analysis also revealed that the top five enriched functional categories were phosphoprotein, alternate splicing, nucleus, cytoplasm and acetylation, suggesting that ANRIL may affect other cellular processes as well as the cell cycle.

Finally, the associations between methylation of CpGs within the CDKN2A gene and bone outcomes at birth in the SWS cohort were not replicated in the MAVIDOS cohort. The methylation of CpGs within the *RXRA* and *NOS3* genes were shown to have a significant positive association with offspring total BMC, total BA, total BMD and percentage BMC at birth in both the SWS and MAVIDOS cohorts. It was also shown that the methylation of these CpGs were positively associated with offspring birth weight and when this was adjusted for in the statistical model, all significant associations between CpG methylation and offspring bone outcomes at birth were removed. When the MAVIDOS cohort samples were examined as a randomised control trial, methylation of CpGs within *RXRA* was shown to be significantly different between the placebo and cholecalciferol supplemented group, with significant decreases in CpG methylation shown between treatment groups for babies born in the summer and autumn months.

8.2 Discussion of main findings

Even though CDKN2A methylation at birth has been shown to be negatively associated with offspring bone outcomes at 4 and 6 years of age in the SWS cohort (Harvey *et al*, unpublished), it is not known whether these CpGs are functionally important in the regulation of *CDKN2A* and whether the products of this gene are important in regulating osteoblast function. Luciferase reporter assays revealed that CpGs within a 300bp region of *CDKN2A* influenced the level of ANRIL promoter activity. As CpGs -887 and -907 had been shown to have the strongest associations with offspring bone outcomes, the effect of differential methylation of these two CpGs loci was explored further using EMSA, to determine whether methylation affected transcription factor binding to the ANRIL promoter.

Methylation is generally associated with a reduction in transcription factor binding as the methyl group blocks the binding site, or recruits repressive complexes through methyl binding proteins which occupy the site (262). The results in chapter 3 have shown that the methylation of CpGs -887 and -907 decreases the binding affinity of transcription factors to this region. Two transcription factors were found to potentially bind to this region: IFN-gamma activation sequence (GAS) and SMAD3/4. In osteoblasts, these two transcription factors have been shown to regulate RUNX2, but in opposite directions, with IFNγ signalling causing an increase in function of RUNX2 (265) and SMAD3/4 binding causing a decrease in RUNX2 function (270), suggesting that these two signalling pathways work together to regulate appropriate bone differentiation. Although no direct interaction between STAT1 and SMAD3/4 has been observed, STAT1 has been shown to induce the transcription of SMAD7, an antagonist SMAD, which binds to SMAD3 and prevents its interaction with the TGF-β receptor (272). Chromatin immunoprecipitation assays could be used to determine whether GAS and SMAD3/4 bind *in vivo* to the ANRIL promoter and how binding is affected by osteoblast differentiation. Although methylation has been shown to inhibit the binding of STAT1 to the promoter of its target genes (355), this has not been investigated with regards to SMAD3/4. If methylation at these CpG sites caused a decrease in transcription factor binding affinity, this may lead to a decrease in ANRIL expression, leading to decreased cell proliferation and the onset of differentiation, potentially prior to the appropriate differentiation signals with consequences on bone structure and risk of fracture in later life by altering bone mineral content and bone mineral density.

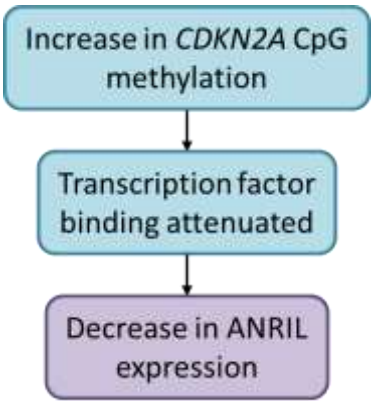

Figure 8.1: Methylation of specific CpG loci within the *CDKN2A* gene causes a decrease in ANRIL expression. CpG -887 in the *CDKN2A* 300bp differentially methylated region was shown to regulate the expression of ANRIL. EMSAs revealed that GAS and SMAD3/4 consensus sequences bound over this region and that methylation of the CpG attenuated transcription factor binding, which is often associated with a decrease in gene expression.

Because the CpGs within the *CDKN2A* locus were shown to alter the expression of ANRIL and as methylation was shown to reduce transcription factor binding, the effects of a knock down in ANRIL expression was examined firstly in an osteosarcoma cell line. SaOS-2 cells were transfected with three siRNAs against ANRIL, with two targeting exon 1 and the other targeting exon 19 of ANRIL. The results from chapter 4 demonstrated that in SaOS-2 cells, there was a decrease cell number, however neither $p16^{INK4A}$ nor $p15^{INK4B}$ expression increased, suggesting that the effect on cell proliferation may be independent of $p16^{INK4A}$ and $p15^{INK4B}$.

The mechanism by which ANRIL induces cell cycle arrest independently of a change in p16 expression is currently unknown, however ANRIL may directly affect $p16^{INK4A}$ protein activity, or the expression/activity of other members of this pathway. As the $p16^{INK4A}$ pathway is so important in preventing unregulated proliferation, it would seem logical to suggest that there would be other 'back up' mechanisms to regulate the expression of this cell cycle inhibitor. For Congrains E1 and Congrains E19 siRNAs, the decrease in cell number was seen along with an increase in cell death, suggesting a potential increase in pro-apoptotic pathways. This agrees with a previous study by Wan *et al*, where a decrease in ANRIL has previously been seen to cause apoptosis in cells (356).

These experiments were repeated in primary hBMSCs and osteoblasts using the Congrains E1 and E19 siRNAs. ANRIL knockdown with siRNA directed against exon 1 and exon 19 also induced a decrease in hBMSCs and osteoblast cell number. The finding of similar effects on cell growth in both SaOS-2 cells and primary cells strongly supports a role for ANRIL in osteoblast and mesenchymal cell growth. There were differences however between the cell line and primary cells, in SaOS-2 cells, ANRIL knock down led to a decrease in cell viability, while in primary cells this was not seen. SaOS-2 cells have, however, mutations within p53 and the p53 pathway which regulates apoptosis so this may explain the difference seen in apoptosis. However, the proliferation rate was decreased in both primary cell types upon ANRIL knock down, even though $p16^{INK4A}$ expression was unchanged in both primary cell types, suggesting that ANRIL may have a *trans*-functional effect in both hBMSCs and osteoblasts. As decrease in ANRIL expression induced by higher methylation may therefore cause a decrease in cell number and proliferation rate of both hBMSCs and osteoblast, this could cause a decrease in bone formation and mass, and therefore increase risk of fracture. Osteoblast number has been linked both directly and indirectly to bone formation and bone mass, in that a decrease in the number of osteoblasts present correlates with a decrease in both of these (64,68,101). This further supports a role for ANRIL in osteoblast regulation and bone formation, and its potential for a part in the pathogenesis of osteoporosis.

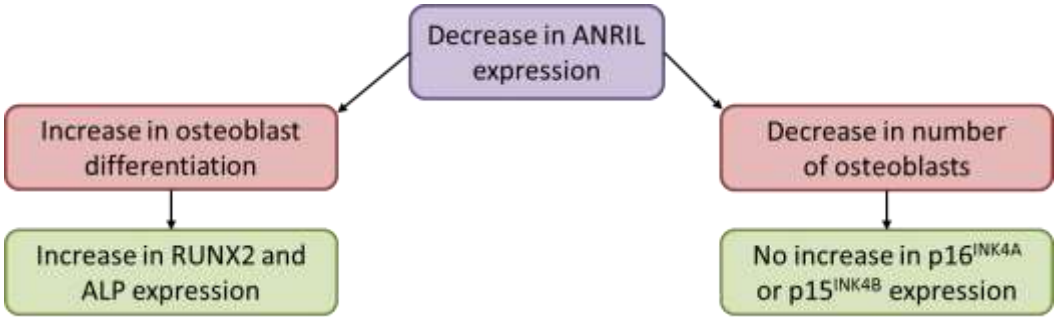

Figure 8.2: Decrease in ANRIL expression leads to an increase in differentiation markers and a decrease in cell number. In osteosarcoma cells, a knock down in ANRIL expression caused a significant increase in the differentiation markers RUNX2 and ALP. A decrease in cell number that was not explained by an increase in either $p16^{INK4A}$ or $p15^{INK4B}$ expression occurred in both the osteosarcoma cell line and the primary osteoblasts.

lncRNAs, such as HOTAIR, have been shown to have *trans*-functional effects, where they regulate genes that are 100,000 bps away from where they are transcribed. For example, HOTAIR is transcribed from the HOXC gene on chromosome 12 and regulates HOXD gene expression on chromosome 2 through the recruitment of the PRC2. lncRNAs have also been shown to have roles in regulating osteoblast function, such as lncRNA-ANCR. This lncRNA inhibits RUNX2 expression through the recruitment of EZH2 (214), which is a component of the PRC2. Although ANRIL to date has not been shown to have any specific functions in osteoblasts or osteoblast-specific pathways, it has been shown to have *trans*-functional effect in a variety of other cell lines and causes transcriptome wide change in gene expression (237,277). To this end, a gene expression array using RNA treated with a siRNA against exon 1 of ANRIL (Congrains E1) was carried out to determine what genes and pathways a decrease in ANRIL expression would affect in primary osteoblasts. The results presented in chapter 6 confirm that there is no change in $p16^{INK4A}$ and $p15^{INK4B}$ expression when ANRIL expression is knocked down in osteoblasts, but there were 260 genes that showed differential expression – 128 of these were upregulated and 132 of these were down regulated. Genes that have previously been shown to have roles in osteoblast function were shown to be altered on the array (*HIF3A*, *IGF2*, *MAPK3* and *TWSG1* expression was upregulated and *ETS1* and *CYR61* was down regulated) and the top pathways that contained the most altered genes were those relating to osteoblast differentiation, viability, adhesion and migration as well as those that related to the deposition of connective tissue and growth of connective tissue cells causing a dysregulation of these pathways. This further suggests that a down regulation in ANRIL expression could have adverse effects on bone formation and mass as key pathways that ensure correct bone development are altered. A knock down in ANRIL expression also had an effect on biological processes and functions. The expression of genes that

are involved in protein transport and binding processes, as well as those that encode for phosphoproteins, molecules involved in alternative splicing, nuclear regulation and acetylation, were significantly altered. Research has shown that ANRIL may implement its *trans*-regulatory effect through Alu elements (282), which are repeat sequences that have been shown to have a role in the regulation of gene expression, and in the paper by Holdt *et al*, they demonstrated that many of the genes that they found to be regulated by ANRIL contained Alu elements in their promoters or enhancers. It has been shown that many of the genes that are involved in alternative splicing and protein translation mechanisms contain Alu elements in their regulatory regions (357). This suggests a potential mechanism by which ANRIL regulates the expression of its target genes. The results shown in this chapter are the first step in elucidating a potential mechanism for ANRIL *trans*-regulation. The next step would be to determine where in the genome ANRIL binds in osteoblasts. To this end, a ChIRP assay could be used, where oligonucleotide probes would be used to tile the ANRIL RNA and regions of the chromosomes bound by ANRIL identified. This would allow for the discovery of primary ANRIL target genes.

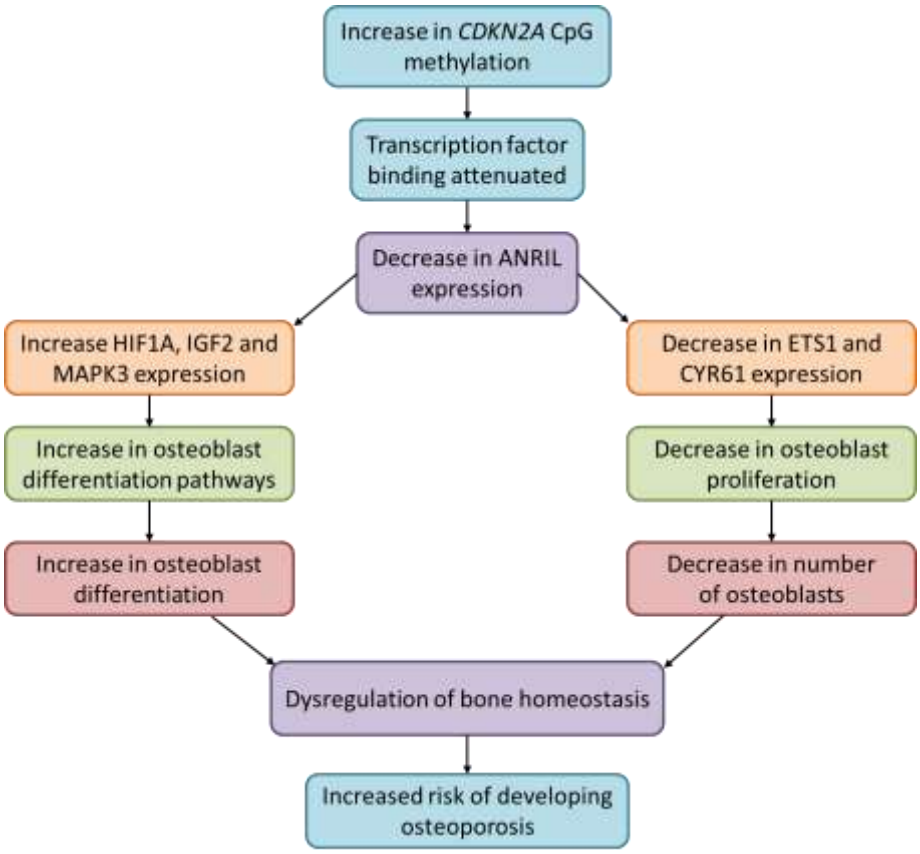

Figure 8.3: A potential mechanism by which *CDKN2A* methylation can cause dysregulation of bone homeostasis leading to an increased risk for osteoporosis. An increase in methylation of specific CpG loci within the *CDKN2A* gene can prevent transcription factor binding and thus cause a decrease in the expression of the lncRNA ANRIL. This would lead to altered expression of genes that cause an increase in osteoblast differentiation but at the same time inhibit pathways that cause osteoblast proliferation. This would cause an imbalance in bone homeostasis, which could lead to an increase risk of developing osteoporosis in later life as bone would not be forming and remodelling correctly.

Although the focus of this discussion has been bone forming osteoblasts and how the dysregulation of these cells could lead to adverse bone formation and potentially contribute to osteoporosis by preventing development of optimal peak bone mass, this is not the only mechanism involving osteoblasts that could contribute to the onset of osteoporosis. As the hallmarks of osteoporosis are increased osteoclast number, enhanced bone resorption activity and dysregulated bone remodelling, and due to the relationship between osteoblasts and osteoclasts, this is potentially another mechanism which may contribute to the regulation of the loss of bone mass seen with osteoporosis. It would also be interesting to see in ANRIL has a specific role in osteoclasts and their progenitors, therefore the experiments that have been carried out in this thesis could be repeated in osteoclasts to determine the role of ANRIL within these cells.

There is evidence to suggest that prenatal and early life environment can potentially induce differentially methylated loci, which, if associated with a particular disease or phenotype, has the potential to act as a biomarker for disease/phenotype risk. As CpG methylation with *CDKN2A* was shown to be associated with offspring bone outcomes in childhood, pyrosequencing and linear regression analysis was used on two separate cohorts to determine whether the same associations were seen between methylation and offspring bone outcomes at birth and whether the associations seen could be replicated across the SWS and MAVIDOS cohorts. The results from chapter 7 show that the methylation of CpG loci in *CDKN2A* was shown to be negatively associated with offspring bone outcomes at birth in the SWS cohort, independent of adjustments made for sex, age at time of DXA and gestational age, which agrees which what had previously been seen at 4 and 6 years of age, suggesting that methylation levels of this gene could potentially be used as a predictive mark from birth for bone health in later life. However, these results were not replicated in the MAVIDOS cohort, though this analysis used significantly reduced numbers than those used in the SWS analysis, which could explain the discrepancies between the two cohorts. It will be important to determine the robustness of such methylation marks predictive of later phenotype and replication is a key step in this process. However, to ensure studies are adequately powered, large numbers of subjects would need to be analysed and this is becoming more feasible with the advent of the 450k, and more latterly, the 850k array. Consortia are also being established to combine data sets to increase the number of subjects analysed. Genome wide approaches using the 450k/850k array would also allow for a more systematic approach to screening for biomarkers, as it would give us a better picture of the epigenome and whether specific CpG sites display altered methylation across numerous cohorts.

The results in chapter 7 also showed that methylation of CpG loci within *RXRA* at birth was positively associated with offspring total BMC, total BA and total BMD at birth in both the SWS and the MAVIDOS cohorts. The previous associations seen between *RXRA* methylation and scBMC at 4 years shown by Harvey *et al* (205) are not replicated at birth in the SWS cohort but associations between perinatal *RXRA* methylation and scBMC at birth show a weak negative association in the MAVIDOS cohort. However, the rest of the associations seen between *RXRA* methylation and offspring bone outcomes at birth were in a positive direction, whereas Harvey *et al* (205) did not find any associations between these bone outcomes and RXRA methylation at 4 years of age in the SWS cohort. Perinatal methylation of CpGs within *NOS3* at birth only showed significant associations with percentage BMC at birth in the MAVIDOS cohort, this was not observed in the SWS cohort.

Maternal diet is a potential factor that could alter the fetal methylation profile and maternal lifestyle has been shown to have influences of offspring bone health in childhood (150). Vitamin D is essential for the uptake of calcium and mineralisation of the skeleton *in utero* and through life. Studies have shown that maternal vitamin D status has an effect on skeletal development of the offspring (205,358), and could be a factor that determines peak bone mass of the child, and therefore future fracture risk. In the MAVIDOS trial, daily maternal supplement of cholecalciferol was shown to significantly increase the BMC, BA and BMD of babies born during the winter months (339). The results in chapter 7 demonstrate that an increase in maternal vitamin status causes a decrease in the methylation of CpGs within the *RXRA* gene, and that these associations are only significant for babies born during the summer and autumn months. Vitamin D has recently been shown to cause demethylation of CpGs (196); however, due to the interactions between *RXRA* and vitamin D, it's hard to elucidate whether this demethylation is caused by a direct or indirect interaction with vitamin D. However, the direction of association between vitamin D supplementation and *RXRA* methylation was not consistent with the direction of associations between *RXRA* methylation and BMC seen at birth. For instance, higher *RXRA* methylation was associated with higher BMC at birth, whereas maternal vitamin D supplementation caused a decrease in the methylation of *RXRA* and an increase in the BMC, BA and BMD of offspring at birth. However results in Chapter 7 showed that the relationships between offspring bone outcomes at birth and birth weight showed a strong positive correlation and it could be this that is driving the positive association between offspring bone outcomes and *RXRA* methylation. Harvey and colleagues did show that there was a trend towards significance between methylation of CpG -2649/-2642 and birth weight in the SWS cohort (205) and other studies have shown that birth weight can be associated with CpG methylation (220,347).

A limitation of this research is that methylation levels were measured in umbilical cord, a proxy tissue, and it is unknown how this relates to the methylation profile in bone tissue. This makes it difficult to potentially prove causality of these marks in influencing later bone health. Animal studies can be used to determine whether prenatal environment has an effect on the methylation status of these CpGs in bone tissue, as well as other tissues. In the future, CRISPR/Cas9 could be used to investigate the causality of this altered methylation. This technique allows for gene specific methylation by using zinc finger protein tags in DMNT1 or TET to direct the methylation machinery to the target site. This would allow us to see whether methylation of these CpGs in CDKN2A has a direct adverse effect on skeletal development. However, this technique still exhibits off-target methylation and so cannot be used at present.

Taken together, the results from this thesis demonstrate a novel role for ANRIL in osteoblast function as there is evidence to suggest that it potentially regulates genes that are involved in specific skeletal development and functional pathways. The CpG loci identified in *CDKN2A* having associations with offspring bone outcomes during childhood are important for the regulation of the lncRNA ANRIL, suggesting that this lncRNA may have some functional effects in human osteoblasts and that alterations to the expression of this lncRNA could have deleterious effects on bone development, assisting in the onset of osteoporosis in later life. This is a novel finding, as a direct function for this lncRNA in osteoblasts has never been suggested before and these results could suggest the discovery of a new regulator of bone cell differentiation and cell growth. The results in this thesis also suggest that the methylation of *CDKN2A* may not be able to predict childhood bone health at birth as in both the SWS and MAVIDOS cohorts the associations were highly influenced by birth weight. Further studies are needed to understand the relationship between birth weight and *CDKN2A* methylation, in order to elucidate what is the driver of the association. However, it may be possible to use these methylation marks to predict childhood bone outcomes, when birth weight may not have as much of an influence over bone health as the environment that the child is exposed to after birth, as these stimuli may have an effect on their epigenome. The influence of maternal vitamin D on the methylation levels of *RXRA* CpGs in the offspring umbilical cord DNA is interesting, especially as there seems to be a seasonal component that also influences the effects seen; however due to the interactions between vitamin D and *RXRA*, this relationship needs to be investigated further.

8.3 Implications for human health

It is well understood that prenatal and early life environment can alter the epigenetic regulation of genes, which can influence bone development and risk of osteoporosis in later life.

Results from this study have shown that altered expression of the lncRNA ANRIL can affect the regulation of genes involved in the differentiation and proliferation pathways of osteoblasts. A better understanding of the epigenetic regulation of these processes would help with identifying potential therapeutic targets and would potentially help identify those individuals as risk for developing a reduced peak bone mass and therefore at higher risk of developing osteoporosis in later life.

Chapter 9
Appendix

9.1 Appendix

9.1.1 Illumina Human H12 Gene Expression Array

Table 9.1: List of 260 genes that had significantly altered differential expression with ANRIL siRNA treatment on the Illumina Human H12 Gene Expression Array.

UPREGULATED GENES				DOWNREGULATED GENES			
Gene	**Fold Change**	**Raw p-value**	**False Discovery Rate**	**Gene**	**Fold Change**	**Raw p-value**	**False Discovery Rate**
BCYRN1	2.14	0.00083	0.0496	**ETS1**	-2.30	0.00037	0.0440
HS.570988	2.14	0.00043	0.0440	**CAV2**	-2.03	0.00008	0.0408
PTGES	2.05	0.00003	0.0395	**CPD**	-1.97	0.00080	0.0496
LOC100130516	1.94	0.00008	0.0408	**PLEKHB2**	-1.92	0.00027	0.0416
LSM14A	1.91	0.00041	0.0440	**GALC**	-1.78	0.00010	0.0408
OLFML3	1.89	0.00074	0.0496	**ATP2B1**	-1.74	0.00043	0.0440
HIF1A	1.81	0.00003	0.0395	**HOXA9**	-1.72	0.00038	0.0440
IL10RB	1.79	0.00078	0.0496	**HDDC2**	-1.71	0.00011	0.0408
NT5DC2	1.79	0.00027	0.0416	**NIN**	-1.67	0.00001	0.0395
TOP1MT	1.75	0.00014	0.0408	**GMFB**	-1.67	0.00001	0.0395
CHPF	1.74	0.00013	0.0408	**TFPI**	-1.66	0.00018	0.0408
LAMP2	1.73	0.00080	0.0496	**NQO1**	-1.63	0.00038	0.0440
ROD1	1.71	0.00005	0.0395	**EIF4EBP2**	-1.63	0.00085	0.0496
POLR3E	1.68	0.00015	0.0408	**C2ORF28**	-1.59	0.00065	0.0496
SCAMP1	1.67	0.00069	0.0496	**EAF1**	-1.57	0.00029	0.0425
GAMT	1.65	0.00070	0.0496	**ARL8B**	-1.57	0.00079	0.0496
ATP11C	1.64	0.00039	0.0440	**PIGA**	-1.54	0.00090	0.0496
MAPK3	1.62	0.00080	0.0496	**ZFYVE26**	-1.53	0.00014	0.0408
SAR1B	1.62	0.00061	0.0494	**C2CD2**	-1.51	0.00038	0.0440
IGF2	1.62	0.00047	0.0458	**TOMM20**	-1.51	0.00023	0.0408
IPO11	1.58	0.00025	0.0416	**TMEM9B**	-1.50	0.00069	0.0496
TLN1	1.58	0.00015	0.0408	**ANTXR1**	-1.49	0.00066	0.0496
DAP3	1.56	0.00071	0.0496	**TWSG1**	-1.49	0.00020	0.0408
LOC644879	1.51	0.00048	0.0461	**HS.348514**	-1.49	0.00041	0.0440
PLXNB2	1.51	0.00020	0.0408	**DNAJB4**	-1.49	0.00017	0.0408
GCNT1	1.49	0.00013	0.0408	**DCP2**	-1.47	0.00018	0.0408
FGFRL1	1.47	0.00012	0.0408	**CRIM1**	-1.47	0.00052	0.0485
SNRNP27	1.46	0.00081	0.0496	**CYR61**	-1.46	0.00061	0.0494
CMBL	1.45	0.00059	0.0494	**SEL1L3**	-1.45	0.00024	0.0415
IVNS1ABP	1.45	0.00011	0.0408	**FAM176A**	-1.45	0.00031	0.0434
GNB1	1.45	0.00010	0.0408	**ICK**	-1.44	0.00006	0.0395
UST	1.45	0.00070	0.0496	**DAB2**	-1.42	0.00039	0.0440
ICMT	1.44	0.00029	0.0425	**DPY19L1**	-1.42	0.00026	0.0416
SOCS4	1.44	0.00026	0.0416	**OKL38**	-1.41	0.00062	0.0494
TMEM158	1.42	0.00039	0.0440	**SLC30A7**	-1.41	0.00030	0.0431
CYB5R4	1.41	0.00055	0.0488	**BCL7B**	-1.40	0.00087	0.0496
RIT1	1.41	0.00063	0.0496	**LONRF1**	-1.40	0.00076	0.0496

CXCL16	1.40	0.00012	0.0408	**PGM2**	-1.39	0.00056	0.0488
PDCD2	1.39	0.00033	0.0440	**LOC729009**	-1.39	0.00088	0.0496
SDC4	1.38	0.00050	0.0473	**TDG**	-1.38	0.00069	0.0496
SEC24A	1.38	0.00080	0.0496	**KIAA1949**	-1.38	0.00074	0.0496
NICN1	1.38	0.00014	0.0408	**C9ORF80**	-1.38	0.00013	0.0408
SHISA5	1.37	0.00048	0.0461	**KHDRBS3**	-1.37	0.00020	0.0408
TMEM41A	1.37	0.00085	0.0496	**EFEMP1**	-1.37	0.00065	0.0496
PRMT2	1.36	0.00006	0.0408	**SENP2**	-1.37	0.00042	0.0440
GSTM2	1.35	0.00030	0.0434	**KIAA0494**	-1.37	0.00068	0.0496
LOC728969	1.34	0.00073	0.0496	**WIPI2**	-1.37	0.00084	0.0496
ATP1B1	1.34	0.00040	0.0440	**BNIP2**	-1.36	0.00037	0.0440
DTWD1	1.33	0.00072	0.0496	**FAM49B**	-1.36	0.00042	0.0440
SPATA18	1.33	0.00087	0.0496	**MTMR9**	-1.36	0.00002	0.0395
DSCR3	1.32	0.00058	0.0493	**KRAS**	-1.36	0.00021	0.0408
C2ORF24	1.32	0.00059	0.0494	**NEDD4**	-1.36	0.00040	0.0440
SLC22A18	1.32	0.00046	0.0454	**EXOC5**	-1.35	0.00023	0.0408
GOPC	1.32	0.00038	0.0440	**TRAM1**	-1.34	0.00055	0.0488
AKTIP	1.32	0.00026	0.0416	**AZIN1**	-1.34	0.00000	0.0320
CASK	1.31	0.00012	0.0408	**HS.535028**	-1.34	0.00029	0.0425
PCOLCE	1.31	0.00080	0.0496	**BDNF**	-1.34	0.00043	0.0440
TSKU	1.31	0.00044	0.0440	**ATRN**	-1.33	0.00069	0.0496
LGMN	1.29	0.00058	0.0493	**OTUD6B**	-1.32	0.00090	0.0496
ANO10	1.29	0.00036	0.0440	**DIXDC1**	-1.31	0.00091	0.0496
RPF2	1.28	0.00086	0.0496	**TUG1**	-1.31	0.00040	0.0440
ATP6V1G2	1.28	0.00080	0.0496	**TATDN3**	-1.30	0.00073	0.0496
C12ORF45	1.28	0.00001	0.0395	**NEK1**	-1.30	0.00019	0.0408
CTNNB1	1.28	0.00022	0.0408	**AHCTF1**	-1.29	0.00016	0.0408
LOC729926	1.28	0.00079	0.0496	**IFNAR1**	-1.29	0.00033	0.0440
PUS7	1.27	0.00082	0.0496	**KBTBD2**	-1.28	0.00021	0.0408
ERGIC1	1.27	0.00044	0.0440	**GAPVD1**	-1.28	0.00085	0.0496
TBC1D7	1.27	0.00040	0.0440	**RRAS2**	-1.28	0.00035	0.0440
ATP10A	1.27	0.00048	0.0461	**C21ORF7**	-1.28	0.00038	0.0440
THOC4	1.26	0.00057	0.0488	**NDUFB5**	-1.27	0.00005	0.0395
LAGE3	1.26	0.00086	0.0496	**CYP4V2**	-1.26	0.00061	0.0494
ASAP3	1.26	0.00020	0.0408	**PTTG1IP**	-1.26	0.00019	0.0408
TACC2	1.25	0.00006	0.0408	**LSM1**	-1.26	0.00010	0.0408
TTYH3	1.25	0.00080	0.0496	**USP46**	-1.26	0.00043	0.0440
ANKRD9	1.25	0.00082	0.0496	**AP4E1**	-1.26	0.00069	0.0496
CLPP	1.25	0.00044	0.0442	**KLC1**	-1.25	0.00018	0.0408
LOC100192378	1.25	0.00084	0.0496	**EXT2**	-1.24	0.00021	0.0408
CS	1.24	0.00007	0.0408	**OSBPL9**	-1.23	0.00040	0.0440
SLC25A4	1.24	0.00061	0.0494	**WNK1**	-1.23	0.00092	0.0498
LOC100129034	1.24	0.00036	0.0440	**MTMR14**	-1.23	0.00008	0.0408
DCUN1D1	1.24	0.00047	0.0458	**MAPKAP1**	-1.23	0.00031	0.0434
PHF21A	1.23	0.00056	0.0488	**SBF1**	-1.23	0.00041	0.0440
IAH1	1.23	0.00012	0.0408	**PHIP**	-1.22	0.00023	0.0408

HIST1H2BK	1.23	0.00068	0.0496	**PRKCD**	-1.22	0.00023	0.0408
NLGN2	1.22	0.00020	0.0408	**LOC647597**	-1.22	0.00082	0.0496
PHLDA3	1.22	0.00091	0.0496	**CRADD**	-1.21	0.00011	0.0408
CCT8	1.22	0.00075	0.0496	**NCK2**	-1.21	0.00048	0.0461
ZNF239	1.22	0.00090	0.0496	**CYTSA**	-1.20	0.00076	0.0496
NCL	1.21	0.00037	0.0440	**TM2D3**	-1.20	0.00005	0.0395
NSA2	1.20	0.00025	0.0416	**C4ORF41**	-1.20	0.00070	0.0496
C12ORF5	1.20	0.00037	0.0440	**ZNF275**	-1.20	0.00075	0.0496
THNSL1	1.19	0.00016	0.0408	**PSMC2**	-1.19	0.00041	0.0440
MGC39900	1.18	0.00004	0.0395	**NHLRC3**	-1.19	0.00027	0.0416
TAF10	1.18	0.00069	0.0496	**C20ORF24**	-1.19	0.00012	0.0408
TRIM33	1.18	0.00084	0.0496	**TFDP2**	-1.19	0.00088	0.0496
PSTPIP2	1.17	0.00074	0.0496	**LRRC57**	-1.19	0.00068	0.0496
ZNF558	1.17	0.00072	0.0496	**SSU72**	-1.19	0.00035	0.0440
C9ORF142	1.17	0.00090	0.0496	**ZNF322A**	-1.18	0.00083	0.0496
FAM125B	1.17	0.00089	0.0496	**CPSF2**	-1.18	0.00005	0.0395
C11ORF51	1.17	0.00055	0.0488	**MRLC2**	-1.18	0.00005	0.0395
TMEM5	1.17	0.00066	0.0496	**KIAA1715**	-1.18	0.00058	0.0493
ANKRA2	1.16	0.00081	0.0496	**HS.571502**	-1.17	0.00061	0.0494
STAG2	1.16	0.00004	0.0395	**DCK**	-1.17	0.00020	0.0408
LOC728139	1.16	0.00074	0.0496	**FBXO28**	-1.17	0.00017	0.0408
LOC728098	1.15	0.00023	0.0408	**RC3H2**	-1.17	0.00069	0.0496
HIST1H2BD	1.15	0.00064	0.0496	**CALR**	-1.17	0.00052	0.0482
DHX40	1.15	0.00023	0.0408	**ADAR**	-1.16	0.00029	0.0425
C7ORF55	1.14	0.00062	0.0494	**BCL2L12**	-1.16	0.00023	0.0408
DCUN1D4	1.14	0.00014	0.0408	**PPP1R12A**	-1.15	0.00018	0.0408
MRPL32	1.13	0.00079	0.0496	**GSTO1**	-1.15	0.00053	0.0485
ATP5G2	1.13	0.00001	0.0395	**MTMR3**	-1.15	0.00093	0.0498
RPAIN	1.13	0.00042	0.0440	**B4GALNT4**	-1.15	0.00023	0.0408
HS.534680	1.13	0.00009	0.0408	**CLDN15**	-1.15	0.00012	0.0408
PTDSS1	1.13	0.00092	0.0497	**ARHGAP21**	-1.14	0.00090	0.0496
ARD1A	1.12	0.00019	0.0408	**ASPH**	-1.14	0.00055	0.0488
ZNF627	1.12	0.00089	0.0496	**FLJ20254**	-1.14	0.00011	0.0408
CXXC5	1.11	0.00004	0.0395	**PSMA1**	-1.13	0.00054	0.0488
FICD	1.11	0.00026	0.0416	**LOC100133888**	-1.13	0.00055	0.0488
SLC16A2	1.11	0.00080	0.0496	**TP53BP2**	-1.13	0.00051	0.0477
MIR185	1.10	0.00005	0.0395	**RBM22**	-1.11	0.00066	0.0496
LOC646753	1.10	0.00037	0.0440	**KIAA1429**	-1.11	0.00008	0.0408
CYB5R1	1.09	0.00086	0.0496	**HS.582988**	-1.11	0.00080	0.0496
SREBF1	1.09	0.00010	0.0408	**CLEC11A**	-1.11	0.00027	0.0416
LRRC8E	1.08	0.00017	0.0408	**SNRNP40**	-1.10	0.00042	0.0440
NME5	1.08	0.00033	0.0440	**HS.436679**	-1.10	0.00057	0.0488
RBM4	1.08	0.00061	0.0494	**CHD9**	-1.09	0.00034	0.0440
C19ORF60	1.07	0.00008	0.0408	**CHEK2**	-1.09	0.00057	0.0492
RABL2B	1.05	0.00064	0.0496	**SON**	-1.09	0.00088	0.0496
				HIST2H2AA3	-1.08	0.00031	0.0434

	PRR13	-1.08	0.00024	0.0408
	SOD1	-1.06	0.00078	0.0496
	TFG	-1.05	0.00081	0.0496

9.1.2 Optimisation of primary cell siRNA transfection

hBMSCs were seeded at 30,000 and 50,000 cells per well in a 24-well plate and were transfected with 10nM 'scrambled' and 'cell death' using Lipofectamine RNAiMAX for 6, 24, 48 and 72hrs, with all cells being trypsinised and counted at 72hrs or fixed for FACS analysis. Cells transfected with 'scrambled' control were also counted at 24 and 48hr intervals to determine whether cells were still dividing over the 72hr period.

A seeding density of 30,000 cells per well with a 6hr siRNA treatment time was chosen for hBMSCs as cell numbers increased over the 72hr period (Figure 9.1A). Cell numbers did not increase after 48hrs with 24 and 48hr siRNA treatments; however, with 72hr siRNA treatment, cell number increased again at 72hrs after staying the same at 24 and 48hrs, though this was not to the same level as those cells treated with siRNA for 6hrs. FACS analysis revealed that there was an increase in the number of cells undergoing apoptosis in those cells treated with cell death siRNA for 6hrs compared to those treated with the 'scrambled' control siRNA, and that there was a decrease in the number of cells in the G_0/G_1 phase of the cell cycle (Figure 9.1B).

Using 6hr and 24hr treatment times as a starting point, the same optimisation was carried out on primary osteoblasts. A 6hr treatment time using a starting seeding density of 30,000 cells per well was found to be the most effective. For the 24hr treatment time at this seeding density there was no increase in cell numbers at 48hrs but they seemed to recover at 72hrs, however this number was still less that those seen at 72hrs with the 6hr siRNA treatment (Figure 9.2A). FACS analysis showed that there was not much different between the 'scrambled' siRNA treated wells at 6 and 24hrs, though there was a greater increase in the number of apoptotic cells when cells treated with cell death siRNA for 24hrs. However, as cells treated for 24hrs with siRNA did not grow as well as when they were treated with siRNA for 6hrs, this treatment time was not used for experiments.

Figure 9.1: Optimisation of hBMSCs for transfection with siRNAs against ANRIL using Lipofectamine RNAiMAX and a 30,000 cell seeding density. Wells seeded with 30,000 cells and transfected with 10nM 'scrambled' and 'cell death' siRNAs for 6, 24, 48 and 72hrs. (A) 'Scrambled' siRNA transfected cells were trypsinised and counted at 24, 48 and 72hr intervals to determine if cells continue to divide during this time frame. (B) Cells were trypsinised at 72hrs and fixed for FACS analysis to determine if the positive control 'cell death' siRNA is having an effect on the number of live cells after treatment for 6, 24, 48 and 72hrs.

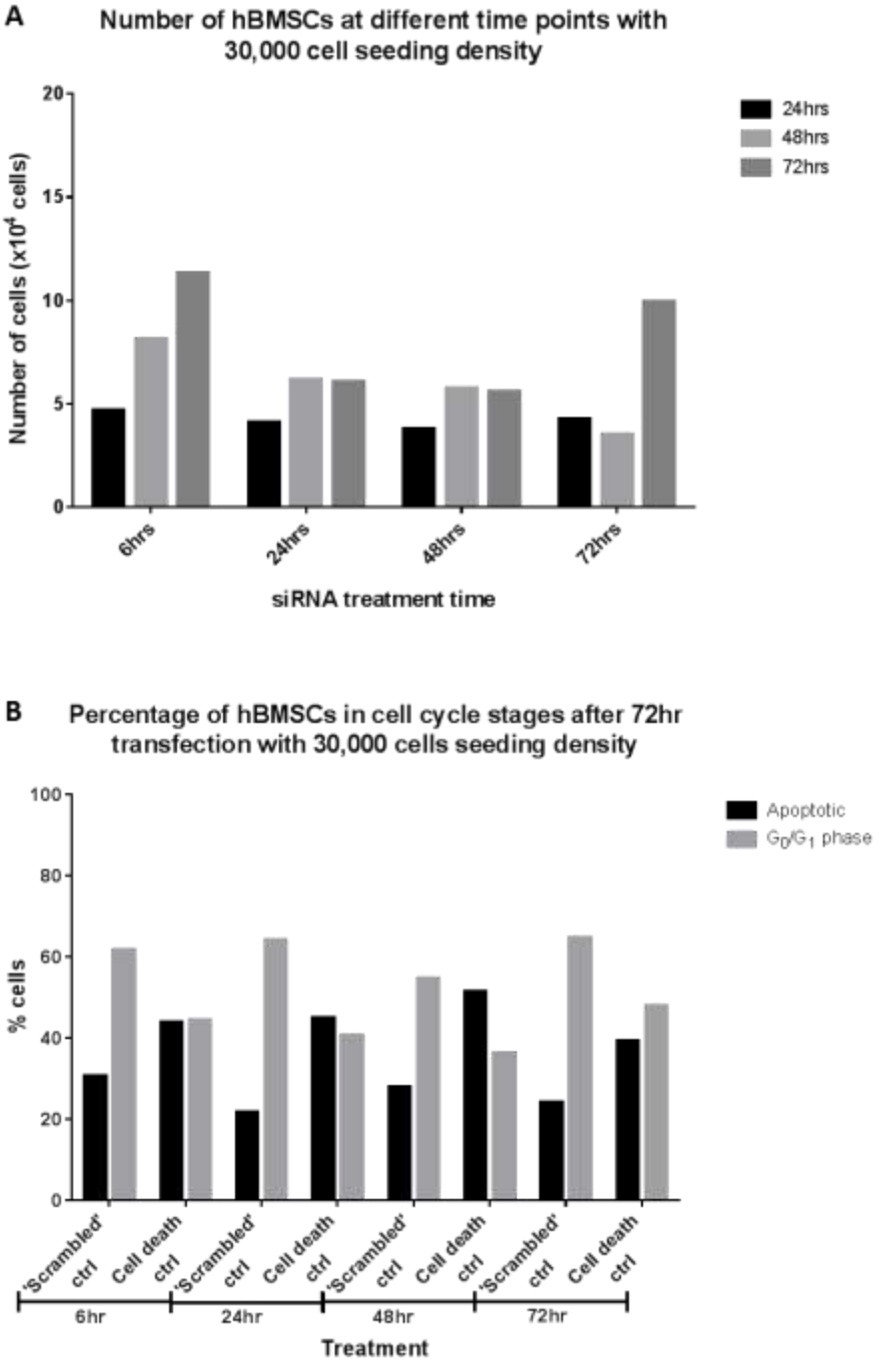

Figure 9.2: Optimisation of primary osteoblasts for transfection with siRNAs against ANRIL using Lipofectamine RNAiMAX and a 30,000 cell seeding density. Wells seeded with 30,000 cells and transfected with 10nM 'scrambled' and 'cell death' siRNAs for 6 and 24hrs. (A) 'Scrambled' siRNA transfected cells were trypsinised and counted at 24, 48 and 72hr intervals to determine if cells continue to divide during this time frame. (B) Cells were trypsinised at 72hrs and fixed for FACS analysis to determine if the positive control 'cell death' siRNA is having an effect on the number of live cells after treatment for 6 and 24hrs.

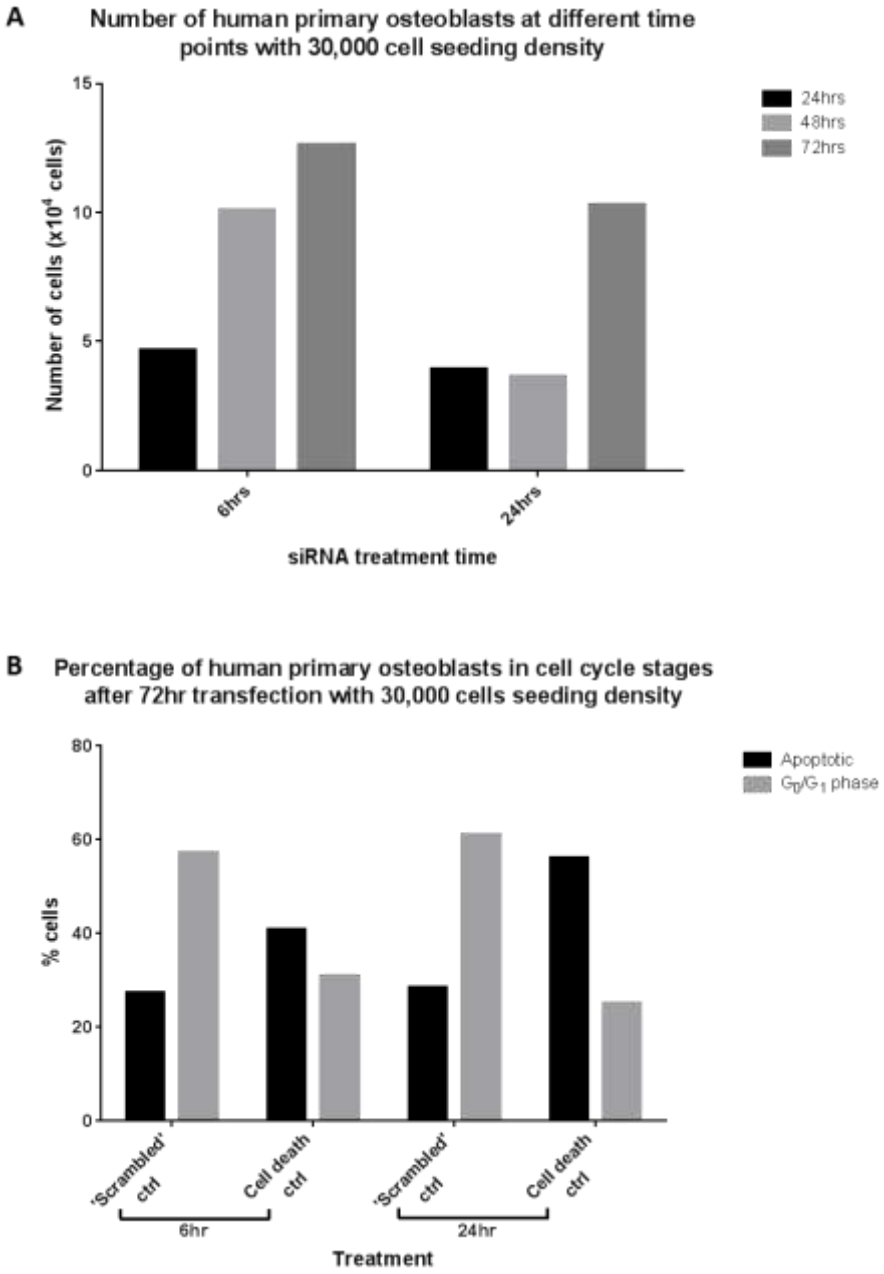

For comparison 50,000 seeding density optimisation experiment graphs are shown in Figure 9.3 for hBMSC graphs and Figure 9.4 for primary osteoblast graphs. A seeding density of 50,000 hBMSCs still showed continual growth with a 6hr treatment time (Figure 9.3A); however FACS analysis showed that the hBMSCs which had been treated with cell death control siRNA did not show as much of an increase in the number of apoptotic cells compared to their 30,000 cell seeding density counterpart (Figure 9.3B). In addition to this, when cells were observed down a microscope, the wells were close to confluency (data not shown), which could affect downstream results.

For primary osteoblasts, a 50,000 cell seeding density showed no increase in cell number at from 48hr to 72hrs with a 24hr siRNA treatment time (Figure 9.4A) and as the cell numbers and FACS analysis with a 6hr siRNA treatment were comparable to that seen with a 30,000 cell seeding density (Figure 9.4B), it was decided to use the same conditions as used for the hBMSCs.

Figure 9.3: Optimisation of hBMSCs for transfection with siRNAs against ANRIL using Lipofectamine RNAiMAX with 50,000 cell seeding density. Cells treated with 10nM 'scrambled' and 'cell death' siRNAs for 6, 24, 48 and 72hrs. After 72hrs, cells were trypsinised and counted (A) or fixed for FACS analysis (B).

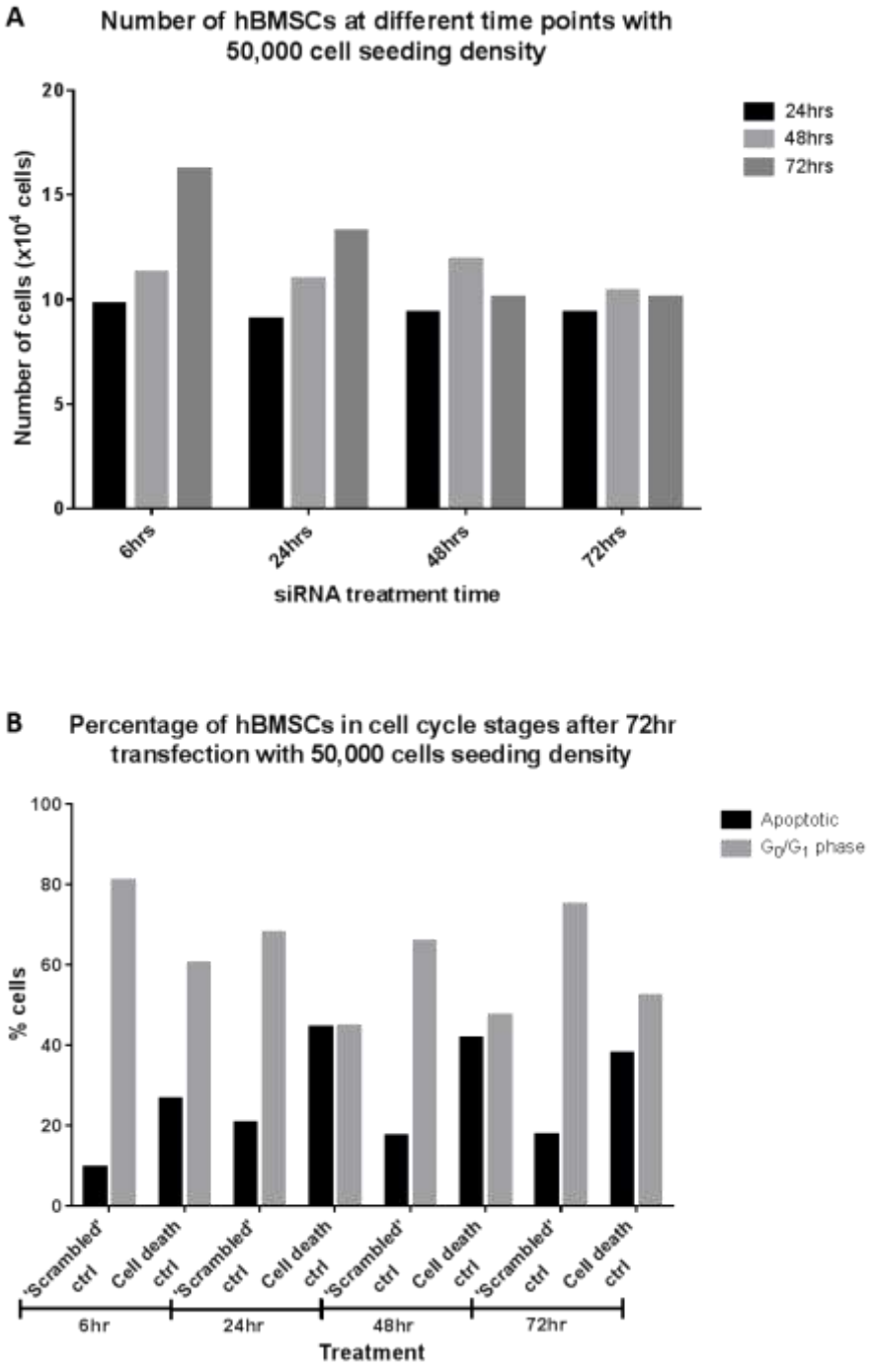

Figure 9.4: Optimisation of primary osteoblasts for transfection with siRNAs against ANRIL using Lipofectamine RNAiMAX with 50,000 cell seeding density. Cells treated with 10nM 'scrambled' and 'cell death' siRNAs for 6 and 24hrs. After 72hrs, cells were trypsinised and counted (A) or fixed for FACS analysis (B).

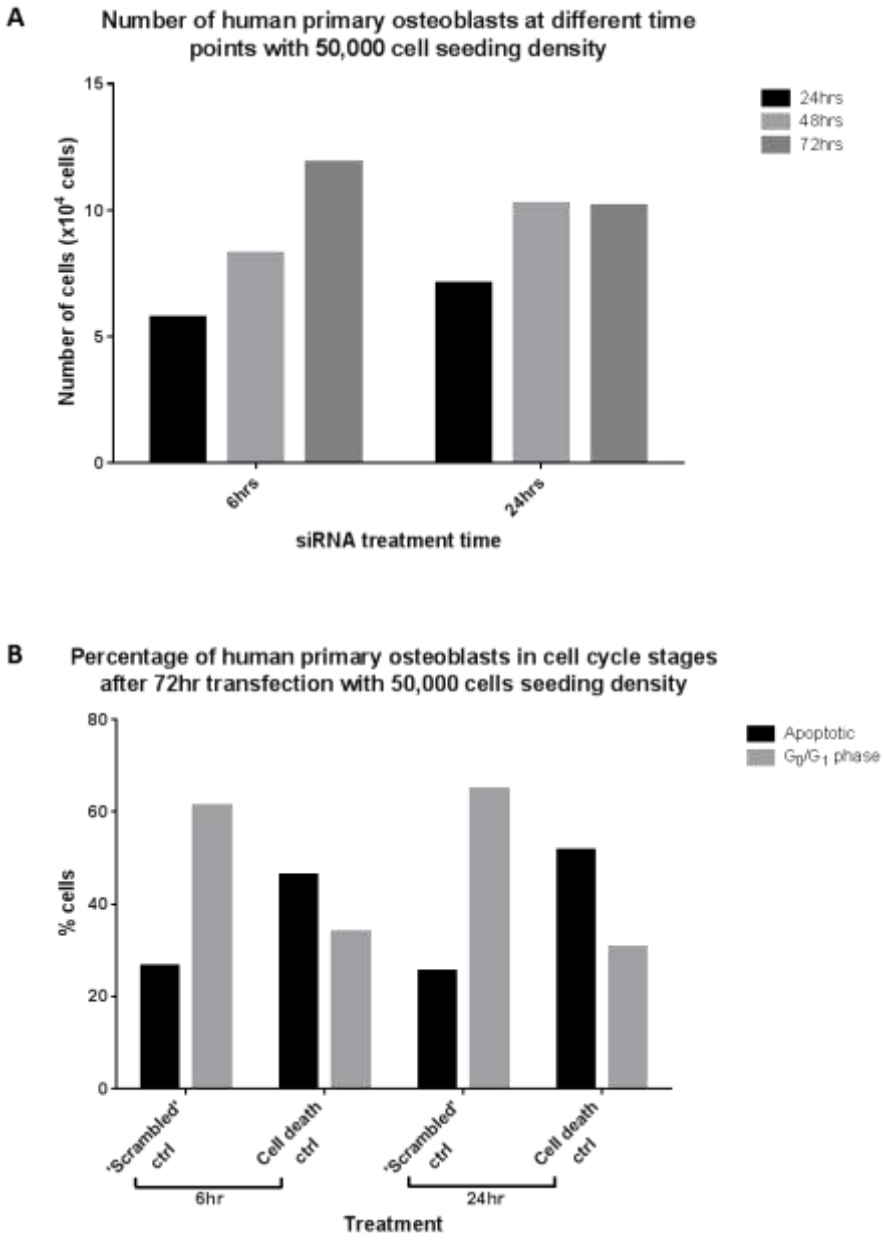

Chapter 10
References

1. Cummings SR, Melton LJ. Epidemiology and outcomes of osteoporotic fractures. Lancet [Internet]. 2002 May 18 [cited 2015 Jan 17];359(9319):1761–7. Available from: http://www.sciencedirect.com/science/article/pii/S0140673602086579

2. WHO. Assessment of fracture risk and its application to screening for postmenopausal osteoporosis. WHO, Geneva. 1994.

3. Sambrook P, Cooper C. Osteoporosis. Lancet [Internet]. 2006 Jun 17 [cited 2015 Feb 21];367(9527):2010–8. Available from: http://www.sciencedirect.com/science/article/pii/S0140673606688910

4. Harvey N, Dennison E, Cooper C. Osteoporosis: impact on health and economics. Nat Rev Rheumatol [Internet]. Nature Publishing Group; 2010 Feb;6(2):99–105. Available from: http://dx.doi.org/10.1038/nrrheum.2009.260

5. Cooper C. Epidemiology of Osteoporosis. Osteoporos Int [Internet]. 1999 Apr [cited 2015 Apr 20];9(S2):S2–8. Available from: http://link.springer.com/10.1007/PL00004156

6. Incidence of Vertebral Fracture in Europe: Results From the European Prospective Osteoporosis Study (EPOS). J Bone Miner Res [Internet]. John Wiley and Sons and The American Society for Bone and Mineral Research (ASBMR); 2002 Apr 1;17(4):716–24. Available from: http://dx.doi.org/10.1359/jbmr.2002.17.4.716

7. Ensrud KE. Epidemiology of Fracture Risk With Advancing Age. Journals Gerontol Ser A Biol Sci Med Sci [Internet]. 2013 Oct 1;68 (10):1236–42. Available from: http://biomedgerontology.oxfordjournals.org/content/68/10/1236.abstract

8. Johnell O, Kanis J. Epidemiology of osteoporotic fractures. Osteoporos Int [Internet]. 2005 Mar [cited 2015 May 11];16 Suppl 2:S3–7. Available from: http://www.ncbi.nlm.nih.gov/pubmed/15365697

9. Parkkari J, Kannus P, Palvanen M, Natri A, Vainio J, Aho H, et al. Majority of Hip Fractures Occur as a Result of a Fall and Impact on the Greater Trochanter of the Femur: A Prospective Controlled Hip Fracture Study with 206 Consecutive Patients. Calcif Tissue Int [Internet]. Springer-Verlag; 1999;65(3):183–7. Available from: http://dx.doi.org/10.1007/s002239900679

10. Holroyd C, Cooper C, Dennison E. Epidemiology of osteoporosis. Best Pract Res Clin Endocrinol Metab [Internet]. 2008 Oct [cited 2015 Jun 19];22(5):671–85. Available from: http://www.sciencedirect.com/science/article/pii/S1521690X08000766

11. Johnell O, Gullberg B, Kanis JA, Allander E, Elffors L, Dequeker J, et al. Risk factors for hip fracture in European women: the MEDOS Study. J Bone Miner Res [Internet]. 1995 Nov [cited 2015 Jun 19];10(11):1802–15. Available from: http://www.ncbi.nlm.nih.gov/pubmed/8592959

12. Chang KP, Center JR, Nguyen T V, Eisman JA. Incidence of hip and other osteoporotic fractures in elderly men and women: Dubbo Osteoporosis Epidemiology Study. J Bone Miner Res [Internet]. 2004 Apr [cited 2015 Jun 19];19(4):532–6. Available from: http://www.ncbi.nlm.nih.gov/pubmed/15005838

13. Cooper C, Atkinson EJ, O'Fallon WM, Melton LJ. Incidence of clinically diagnosed vertebral fractures: a population-based study in Rochester, Minnesota, 1985-1989. J Bone Miner Res [Internet]. 1992 Feb [cited 2015 Jun 20];7(2):221–7. Available from: http://www.ncbi.nlm.nih.gov/pubmed/1570766

14. Sernbo I, Johnell O. Consequences of a hip fracture: a prospective study over 1 year. Osteoporos Int [Internet]. 1993 May [cited 2015 Jun 21];3(3):148–53. Available from: http://www.ncbi.nlm.nih.gov/pubmed/8481591

15. Miller CW. Survival and ambulation following hip fracture. J Bone Jt Surgery [Internet]. The Journal of Bone and Joint Surgery, Inc.; 1978 Oct 1 [cited 2015 May 7];60(7):930–4. Available from: http://jbjs.org/content/60/7/930.abstract

16. Miyakoshi N, Itoi E, Kobayashi M, Kodama H. Impact of postural deformities and spinal mobility on quality of life in postmenopausal osteoporosis. Osteoporos Int [Internet]. 2003 Dec [cited 2015 Jun 21];14(12):1007–12. Available from: http://www.ncbi.nlm.nih.gov/pubmed/14557854

17. Cooper C, Atkinson EJ, Jacobsen SJ, O'Fallon WM, Melton LJ. Population-Based Study of Survival after Osteoporotic Fractures. Am J Epidemiol [Internet]. 1993 May 1;137(9):1001–5. Available from: http://aje.oxfordjournals.org/content/137/9/1001.abstract

18. Johnell O, Kanis JA, Odén A, Sernbo I, Redlund-Johnell I, Petterson C, et al. Mortality after osteoporotic fractures. Osteoporos Int [Internet]. 2004 Jan [cited 2015 Jun 12];15(1):38–42. Available from: http://www.ncbi.nlm.nih.gov/pubmed/14593451

19. Burge R, Dawson-Hughes B, Solomon DH, Wong JB, King A, Tosteson A. Incidence and economic burden of osteoporosis-related fractures in the United States, 2005-2025. J Bone Miner Res [Internet]. 2007 Mar [cited 2015 Jun 22];22(3):465–75. Available from: http://www.ncbi.nlm.nih.gov/pubmed/17144789

20. Gilbert SF. Osteogenesis: The Development of Bones. Developmental Biology 6th edition [Internet]. Sinauer Associates; 2000 [cited 2015 Jul 13]. Available from: http://www.ncbi.nlm.nih.gov/books/NBK10056/

21. Erlebacher A, Filvaroff EH, Gitelman SE, Derynck R. Toward a molecular understanding of skeletal development. Cell [Internet]. 1995 Feb [cited 2015 Jul 8];80(3):371–8. Available from: http://www.sciencedirect.com/science/article/pii/0092867495904875

22. Hall BK, Miyake T. The membranous skeleton: the role of cell condensations in vertebrate skeletogenesis. Anat Embryol (Berl) [Internet]. 1992 Jul [cited 2015 Jul 13];186(2):107–24. Available from: http://www.ncbi.nlm.nih.gov/pubmed/1510240

23. Bruder SP, Caplan AI. Cellular and molecular events during embryonic bone development. Connect Tissue Res [Internet]. 1989 Jan [cited 2015 Jul 13];20(1-4):65–71. Available from: http://www.ncbi.nlm.nih.gov/pubmed/2692958

24. Olsen BR, Reginato AM, Wang W. Bone development. Annu Rev Cell Dev Biol [Internet]. 16:191–220. Available from: http://ovidsp.ovid.com/ovidweb.cgi?T=JS&CSC=Y&NEWS=N&PAGE=fulltext&D=med4&AN=11031235

25. Kronenberg HM. Developmental regulation of the growth plate. Nature [Internet]. 2003;423(6937):332–6. Available from: http://www.ncbi.nlm.nih.gov/pubmed/12748651

26. Crockett JC, Rogers MJ, Coxon FP, Hocking LJ, Helfrich MH. Bone remodelling at a glance. J Cell Sci [Internet]. 2011 Apr 1 [cited 2015 Jan 25];124(Pt 7):991–8. Available from: http://jcs.biologists.org/content/124/7/991.full

27. Akiyama H, Kim J-E, Nakashima K, Balmes G, Iwai N, Deng JM, et al. Osteo-chondroprogenitor cells are derived from Sox9 expressing precursors. Proc Natl Acad Sci U S A [Internet]. 2005 Oct 11 [cited 2015 Jul 1];102(41):14665–70. Available from: http://www.pubmedcentral.nih.gov/articlerender.fcgi?artid=1239942&tool=pmcentrez&rendertype=abstract

28. Akiyama H, Chaboissier M-C, Martin JF, Schedl A, de Crombrugghe B. The transcription factor Sox9 has essential roles in successive steps of the chondrocyte differentiation pathway and is required for expression of Sox5 and Sox6. Genes Dev [Internet]. 2002 Nov 1 [cited 2015 Apr 24];16(21):2813–28. Available from:

http://genesdev.cshlp.org/content/16/21/2813.short

29. Komori T, Yagi H, Nomura S, Yamaguchi A, Sasaki K, Deguchi K, et al. Targeted disruption of Cbfa1 results in a complete lack of bone formation owing to maturational arrest of osteoblasts. Cell [Internet]. 1997 May 30 [cited 2015 Jun 17];89(5):755–64. Available from: http://www.ncbi.nlm.nih.gov/pubmed/9182763

30. Otto F, Thornell AP, Crompton T, Denzel A, Gilmour KC, Rosewell IR, et al. Cbfa1, a Candidate Gene for Cleidocranial Dysplasia Syndrome, Is Essential for Osteoblast Differentiation and Bone Development. Cell [Internet]. 1997 May [cited 2015 May 21];89(5):765–71. Available from: http://www.sciencedirect.com/science/article/pii/S0092867400802597

31. Ducy P, Starbuck M, Priemel M, Shen J, Pinero G, Geoffroy V, et al. A Cbfa1-dependent genetic pathway controls bone formation beyond embryonic development. Genes Dev [Internet]. 1999 Apr 15 [cited 2015 Jul 2];13(8):1025–36. Available from: http://genesdev.cshlp.org/content/13/8/1025.short

32. Nakashima K, Zhou X, Kunkel G, Zhang Z, Deng JM, Behringer RR, et al. The Novel Zinc Finger-Containing Transcription Factor Osterix Is Required for Osteoblast Differentiation and Bone Formation. Cell [Internet]. 2002 Jan [cited 2015 Jul 2];108(1):17–29. Available from: http://www.sciencedirect.com/science/article/pii/S0092867401006225

33. Wang X, Kua H-Y, Hu Y, Guo K, Zeng Q, Wu Q, et al. p53 functions as a negative regulator of osteoblastogenesis, osteoblast-dependent osteoclastogenesis, and bone remodeling. J Cell Biol [Internet]. 2006 Jan 2 [cited 2015 May 22];172(1):115–25. Available from: http://www.pubmedcentral.nih.gov/articlerender.fcgi?artid=2063539&tool=pmcentrez&rendertype=abstract

34. Day TF, Guo X, Garrett-Beal L, Yang Y. Wnt/β-Catenin Signaling in Mesenchymal Progenitors Controls Osteoblast and Chondrocyte Differentiation during Vertebrate Skeletogenesis. Dev Cell [Internet]. 2005 May [cited 2015 Jul 2];8(5):739–50. Available from: http://www.ncbi.nlm.nih.gov/pubmed/15866164

35. Hill TP, Später D, Taketo MM, Birchmeier W, Hartmann C. Canonical Wnt/beta-catenin signaling prevents osteoblasts from differentiating into chondrocytes. Dev Cell [Internet]. 2005 May [cited 2015 Jul 2];8(5):727–38. Available from: http://www.ncbi.nlm.nih.gov/pubmed/15866163

36. Hu H, Hilton MJ, Tu X, Yu K, Ornitz DM, Long F. Sequential roles of Hedgehog and Wnt signaling in osteoblast development. Development [Internet]. 2005 Jan [cited 2015 Jul 2];132(1):49–60. Available from: http://www.ncbi.nlm.nih.gov/pubmed/15576404

37. Gaur T, Lengner CJ, Hovhannisyan H, Bhat RA, Bodine PVN, Komm BS, et al. Canonical WNT signaling promotes osteogenesis by directly stimulating Runx2 gene expression. J Biol Chem [Internet]. 2005 Sep 30 [cited 2015 Jun 14];280(39):33132–40. Available from: http://www.ncbi.nlm.nih.gov/pubmed/16043491

38. Eferl R, Hoebertz A, Schilling AF, Rath M, Karreth F, Kenner L, et al. The Fos-related antigen Fra-1 is an activator of bone matrix formation. EMBO J [Internet]. 2004 Jul 21 [cited 2015 Jul 2];23(14):2789–99. Available from: http://www.pubmedcentral.nih.gov/articlerender.fcgi?artid=514946&tool=pmcentrez&rendertype=abstract

39. Jochum W, David JP, Elliott C, Wutz A, Plenk H, Matsuo K, et al. Increased bone formation and osteosclerosis in mice overexpressing the transcription factor Fra-1. Nat Med [Internet]. 2000 Sep [cited 2015 Jul 2];6(9):980–4. Available from: http://www.ncbi.nlm.nih.gov/pubmed/10973316

40. Yang X, Matsuda K, Bialek P, Jacquot S, Masuoka HC, Schinke T, et al. ATF4 is a substrate of RSK2 and an essential regulator of osteoblast biology; implication for Coffin-Lowry Syndrome. Cell [Internet]. 2004 Apr 30 [cited 2015 Jul 2];117(3):387–98. Available from: http://www.ncbi.nlm.nih.gov/pubmed/15109498

41. Bandyopadhyay A, Tsuji K, Cox K, Harfe BD, Rosen V, Tabin CJ. Genetic analysis of the roles of BMP2, BMP4, and BMP7 in limb patterning and skeletogenesis. PLoS Genet [Internet]. Public Library of Science; 2006 Dec 22 [cited 2015 Jun 24];2(12):e216. Available from: http://journals.plos.org/plosgenetics/article?id=10.1371/journal.pgen.0020216

42. Tsuji K, Bandyopadhyay A, Harfe BD, Cox K, Kakar S, Gerstenfeld L, et al. BMP2 activity, although dispensable for bone formation, is required for the initiation of fracture healing. Nat Genet [Internet]. 2006 Dec [cited 2015 Jul 8];38(12):1424–9. Available from: http://www.ncbi.nlm.nih.gov/pubmed/17099713

43. Devlin RD, Du Z, Pereira RC, Kimble RB, Economides AN, Jorgetti V, et al. Skeletal overexpression of noggin results in osteopenia and reduced bone formation. Endocrinology [Internet]. 2003 May [cited 2015 Jul 8];144(5):1972–8. Available from: http://www.ncbi.nlm.nih.gov/pubmed/12697704

44. Tan X, Weng T, Zhang J, Wang J, Li W, Wan H, et al. Smad4 is required for maintaining normal murine postnatal bone homeostasis. J Cell Sci [Internet]. 2007 Jul 1 [cited 2015 Jul 8];120(Pt 13):2162–70. Available from: http://www.pubmedcentral.nih.gov/articlerender.fcgi?artid=2692485&tool=pmcentrez&rendertype=abstract

45. Long F. Building strong bones: molecular regulation of the osteoblast lineage. Nat Rev Mol Cell Biol [Internet]. Nature Publishing Group, a division of Macmillan Publishers Limited. All Rights Reserved.; 2012;13(1):27–38. Available from: http://dx.doi.org/10.1038/nrm3254

46. Gong Y, Slee RB, Fukai N, Rawadi G, Roman-Roman S, Reginato AM, et al. LDL receptor-related protein 5 (LRP5) affects bone accrual and eye development. Cell [Internet]. 2001 Nov 16 [cited 2015 Jul 9];107(4):513–23. Available from: http://www.ncbi.nlm.nih.gov/pubmed/11719191

47. Kato M, Patel MS, Levasseur R, Lobov I, Chang BH-J, Glass DA, et al. Cbfa1-independent decrease in osteoblast proliferation, osteopenia, and persistent embryonic eye vascularization in mice deficient in Lrp5, a Wnt coreceptor. J Cell Biol [Internet]. 2002 Apr 15 [cited 2015 Jun 12];157(2):303–14. Available from: http://www.pubmedcentral.nih.gov/articlerender.fcgi?artid=2199263&tool=pmcentrez&rendertype=abstract

48. Rodda SJ, McMahon AP. Distinct roles for Hedgehog and canonical Wnt signaling in specification, differentiation and maintenance of osteoblast progenitors. Development [Internet]. 2006;133(16):3231–44. Available from: http://dev.biologists.org/content/133/16/3231.abstract

49. Tu X, Joeng KS, Nakayama KI, Nakayama K, Rajagopal J, Carroll TJ, et al. Noncanonical Wnt signaling through G protein-linked PKCdelta activation promotes bone formation. Dev Cell [Internet]. 2007 Jan [cited 2015 Jun 25];12(1):113–27. Available from: http://www.pubmedcentral.nih.gov/articlerender.fcgi?artid=1861818&tool=pmcentrez&rendertype=abstract

50. Takada I, Mihara M, Suzawa M, Ohtake F, Kobayashi S, Igarashi M, et al. A histone lysine methyltransferase activated by non-canonical Wnt signalling suppresses PPAR-gamma transactivation. Nat Cell Biol [Internet]. 2007 Nov [cited 2015 Jun 25];9(11):1273–85. Available from: http://www.ncbi.nlm.nih.gov/pubmed/17952062

51. Hilton MJ, Tu X, Cook J, Hu H, Long F. Ihh controls cartilage development by antagonizing Gli3, but requires additional effectors to regulate osteoblast and vascular development. Development [Internet]. 2005 Oct [cited 2015 Jul 9];132(19):4339–51. Available from: http://www.ncbi.nlm.nih.gov/pubmed/16141219

52. Joeng KS, Long F. The Gli2 transcriptional activator is a crucial effector for Ihh signaling in osteoblast development and cartilage vascularization. Development [Internet]. 2009 Dec [cited 2015 Jul 9];136(24):4177–85. Available from: http://www.pubmedcentral.nih.gov/articlerender.fcgi?artid=2781053&tool=pmcentrez&rendertype=abstract

53. St-Jacques B, Hammerschmidt M, McMahon AP. Indian hedgehog signaling regulates proliferation and differentiation of chondrocytes and is essential for bone formation. Genes Dev [Internet]. 1999 Aug 15 [cited 2015 Jul 9];13(16):2072–86. Available from: http://www.pubmedcentral.nih.gov/articlerender.fcgi?artid=316949&tool=pmcentrez&rendertype=abstract

54. Long F, Chung U, Ohba S, McMahon J, Kronenberg HM, McMahon AP. Ihh signaling is directly required for the osteoblast lineage in the endochondral skeleton. Development [Internet]. 2004 Mar 15 [cited 2015 Jul 9];131(6):1309–18. Available from: http://dev.biologists.org/content/131/6/1309.long

55. Honjo T. The shortest path from the surface to the nucleus: RBP-Jkappa/Su(H) transcription factor. Genes to Cells [Internet]. 1996 Jan [cited 2015 Jul 9];1(1):1–9. Available from: http://doi.wiley.com/10.1046/j.1365-2443.1996.10010.x

56. Hilton MJ, Tu X, Wu X, Bai S, Zhao H, Kobayashi T, et al. Notch signaling maintains bone marrow mesenchymal progenitors by suppressing osteoblast differentiation. Nat Med [Internet]. Nature Publishing Group; 2008 Feb 24 [cited 2015 Jul 2];14(3):306–14. Available from: http://dx.doi.org/10.1038/nm1716

57. Montero A, Okada Y, Tomita M, Ito M, Tsurukami H, Nakamura T, et al. Disruption of the fibroblast growth factor-2 gene results in decreased bone mass and bone formation. J Clin Invest [Internet]. 2000 Apr [cited 2015 Jul 9];105(8):1085–93. Available from: http://www.pubmedcentral.nih.gov/articlerender.fcgi?artid=300831&tool=pmcentrez&rendertype=abstract

58. Jacob AL, Smith C, Partanen J, Ornitz DM. Fibroblast growth factor receptor 1 signaling in the osteo-chondrogenic cell lineage regulates sequential steps of osteoblast maturation. Dev Biol [Internet]. 2006 Aug 15 [cited 2015 Jul 9];296(2):315–28. Available from: http://www.pubmedcentral.nih.gov/articlerender.fcgi?artid=2077084&tool=pmcentrez&rendertype=abstract

59. Yu K, Xu J, Liu Z, Sosic D, Shao J, Olson EN, et al. Conditional inactivation of FGF receptor 2 reveals an essential role for FGF signaling in the regulation of osteoblast function and bone growth. Development [Internet]. 2003 Jul [cited 2015 Jul 9];130(13):3063–74. Available from: http://www.ncbi.nlm.nih.gov/pubmed/12756187

60. Tam CS, Heersche JN, Murray TM, Parsons JA. Parathyroid hormone stimulates the bone apposition rate independently of its resorptive action: differential effects of intermittent and continuous administration. Endocrinology [Internet]. 1982 Feb [cited 2015 Jul 10];110(2):506–12. Available from: http://www.ncbi.nlm.nih.gov/pubmed/7056211

61. Isogai Y, Akatsu T, Ishizuya T, Yamaguchi A, Hori M, Takahashi N, et al. Parathyroid hormone regulates osteoblast differentiation positively or negatively depending on the differentiation stages. J Bone Miner Res [Internet]. 1996 Oct [cited 2015 Jul 10];11(10):1384–93. Available from: http://www.ncbi.nlm.nih.gov/pubmed/8889836

62. Yang D, Guo J, Divieti P, Bringhurst FR. Parathyroid hormone activates PKC-delta and regulates osteoblastic differentiation via a PLC-independent pathway. Bone [Internet]. Elsevier; 2006 Apr 4 [cited 2015 Jul 10];38(4):485–96. Available from: http://www.thebonejournal.com/article/S8756328205004151/fulltext

63. McCauley LK, Koh AJ, Beecher CA, Rosol TJ. Proto-oncogene c-fos is transcriptionally regulated by parathyroid hormone (PTH) and PTH-related protein in a cyclic adenosine monophosphate-dependent manner in osteoblastic cells. Endocrinology [Internet]. 1997 Dec [cited 2015 Jul 10];138(12):5427–33. Available from: http://www.ncbi.nlm.nih.gov/pubmed/9389528

64. Jilka RL, Weinstein RS, Bellido T, Roberson P, Parfitt AM, Manolagas SC. Increased bone formation by prevention of osteoblast apoptosis with parathyroid hormone. J Clin Invest [Internet]. 1999 Aug [cited 2015 Mar 16];104(4):439–46. Available from: http://www.pubmedcentral.nih.gov/articlerender.fcgi?artid=408524&tool=pmcentrez&rendertype=abstract

65. Yakar S, Bouxsein ML, Canalis E, Sun H, Glatt V, Gundberg C, et al. The ternary IGF complex influences postnatal bone acquisition and the skeletal response to intermittent parathyroid hormone. J Endocrinol [Internet]. 2006 May [cited 2015 Jul 10];189(2):289–99. Available from: http://www.ncbi.nlm.nih.gov/pubmed/16648296

66. Sabbieti MG, Agas D, Xiao L, Marchetti L, Coffin JD, Doetschman T, et al. Endogenous FGF-2 is critically important in PTH anabolic effects on bone. J Cell Physiol [Internet]. 2009 Apr [cited 2015 Jul 10];219(1):143–51. Available from: http://www.pubmedcentral.nih.gov/articlerender.fcgi?artid=2763338&tool=pmcentrez&rendertype=abstract

67. Xian L, Wu X, Pang L, Lou M, Rosen CJ, Qiu T, et al. Matrix IGF-1 maintains bone mass by activation of mTOR in mesenchymal stem cells. Nat Med [Internet]. 2012 Jul [cited 2015 Jul 10];18(7):1095–101. Available from: http://www.pubmedcentral.nih.gov/articlerender.fcgi?artid=3438316&tool=pmcentrez&rendertype=abstract

68. Zhang M, Xuan S, Bouxsein ML, von Stechow D, Akeno N, Faugere MC, et al. Osteoblast-specific knockout of the insulin-like growth factor (IGF) receptor gene reveals an essential role of IGF signaling in bone matrix mineralization. J Biol Chem [Internet]. 2002 Nov 15 [cited 2015 Jul 10];277(46):44005–12. Available from: http://www.jbc.org/content/277/46/44005.full

69. Nefussi JR, Baron R. PGE2 stimulates both resorption and formation of bone in vitro: differential responses of the periosteum and the endosteum in fetal rat long bone cultures. Anat Rec [Internet]. 1985 Jan [cited 2015 Jul 10];211(1):9–16. Available from: http://www.ncbi.nlm.nih.gov/pubmed/3985383

70. Yoshida K, Oida H, Kobayashi T, Maruyama T, Tanaka M, Katayama T, et al. Stimulation of bone formation and prevention of bone loss by prostaglandin E EP4 receptor activation. Proc Natl Acad Sci U S A [Internet]. 2002 Apr 2 [cited 2015 Jul 10];99(7):4580–5. Available from: http://www.pubmedcentral.nih.gov/articlerender.fcgi?artid=123690&tool=pmcentrez&rendertype=abstract

71. Conconi MT, Tommasini M, Baiguera S, De Coppi P, Parnigotto PP, Nussdorfer GG. Effects of prostaglandins E1 and E2 on the growth and differentiation of osteoblast-like cells cultured in vitro. Int J Mol Med [Internet]. 2002 Oct [cited 2015 Jul 10];10(4):451–6. Available from: http://www.ncbi.nlm.nih.gov/pubmed/12239592

72. Baylink D, Stauffer M, Wergedal J, Rich C. Formation, mineralization, and resorption of

bone in vitamin D-deficient rats. J Clin Invest [Internet]. 1970 Jun [cited 2015 Jul 10];49(6):1122–34. Available from: http://www.pubmedcentral.nih.gov/articlerender.fcgi?artid=322580&tool=pmcentrez&rendertype=abstract

73. Brenza HL, Kimmel-Jehan C, Jehan F, Shinki T, Wakino S, Anazawa H, et al. Parathyroid hormone activation of the 25-hydroxyvitamin D3-1alpha-hydroxylase gene promoter. Proc Natl Acad Sci U S A [Internet]. 1998 Feb 17 [cited 2015 Jul 10];95(4):1387–91. Available from: http://www.pubmedcentral.nih.gov/articlerender.fcgi?artid=19012&tool=pmcentrez&rendertype=abstract

74. Brenza HL, DeLuca HF. Regulation of 25-hydroxyvitamin D3 1alpha-hydroxylase gene expression by parathyroid hormone and 1,25-dihydroxyvitamin D3. Arch Biochem Biophys [Internet]. 2000 Sep 1 [cited 2015 Jul 10];381(1):143–52. Available from: http://www.ncbi.nlm.nih.gov/pubmed/11019830

75. Haussler MR, Haussler CA, Jurutka PW, Thompson PD, Hsieh JC, Remus LS, et al. The vitamin D hormone and its nuclear receptor: molecular actions and disease states. J Endocrinol [Internet]. 1997 Sep [cited 2015 Jul 10];154 Suppl:S57–73. Available from: http://www.ncbi.nlm.nih.gov/pubmed/9379138

76. Lips P. Vitamin D physiology. Prog Biophys Mol Biol [Internet]. 2006 Sep [cited 2014 Dec 11];92(1):4–8. Available from: http://www.sciencedirect.com/science/article/pii/S0079610706000083

77. Sierra J, Villagra A, Paredes R, Cruzat F, Gutierrez S, Javed A, et al. Regulation of the Bone-Specific Osteocalcin Gene by p300 Requires Runx2/Cbfa1 and the Vitamin D3 Receptor but Not p300 Intrinsic Histone Acetyltransferase Activity. Mol Cell Biol [Internet]. 2003 May 1 [cited 2015 Mar 2];23(9):3339–51. Available from: http://mcb.asm.org/content/23/9/3339.long

78. Noda M, Vogel RL, Craig AM, Prahl J, DeLuca HF, Denhardt DT. Identification of a DNA sequence responsible for binding of the 1,25-dihydroxyvitamin D3 receptor and 1,25-dihydroxyvitamin D3 enhancement of mouse secreted phosphoprotein 1 (SPP-1 or osteopontin) gene expression. Proc Natl Acad Sci [Internet]. 1990 Dec 1 [cited 2015 Jul 10];87(24):9995–9. Available from: http://www.pnas.org/content/87/24/9995.short

79. Gardiner EM, Baldock PA, Thomas GP, Sims NA, Henderson NK, Hollis B, et al. Increased formation and decreased resorption of bone in mice with elevated vitamin D receptor in mature cells of the osteoblastic lineage. FASEB J [Internet]. 2000 Oct [cited 2015 Jul 12];14(13):1908–16. Available from: http://www.ncbi.nlm.nih.gov/pubmed/11023975

80. Baldock PA, Thomas GP, Hodge JM, Baker SU, Dressel U, O'Loughlin PD, et al. Vitamin D action and regulation of bone remodeling: suppression of osteoclastogenesis by the mature osteoblast. J Bone Miner Res [Internet]. 2006 Oct [cited 2015 Jul 12];21(10):1618–26. Available from: http://www.ncbi.nlm.nih.gov/pubmed/16995817

81. Erben RG, Scutt AM, Miao D, Kollenkirchen U, Haberey M. Short-term treatment of rats with high dose 1,25-dihydroxyvitamin D3 stimulates bone formation and increases the number of osteoblast precursor cells in bone marrow. Endocrinology [Internet]. Endocrine Society; 1997 Nov 1 [cited 2015 Jul 12];138(11):4629–35. Available from: http://press.endocrine.org/doi/abs/10.1210/endo.138.11.5511

82. Crockett JC, Mellis DJ, Scott DI, Helfrich MH. New knowledge on critical osteoclast formation and activation pathways from study of rare genetic diseases of osteoclasts: focus on the RANK/RANKL axis. Osteoporos Int [Internet]. Springer-Verlag; 2011 Jan 11 [cited 2016 Aug 3];22(1):1–20. Available from: http://link.springer.com/10.1007/s00198-

010-1272-8

83. Weitzmann MN, Pacifici R. T cells: unexpected players in the bone loss induced by estrogen deficiency and in basal bone homeostasis. Ann N Y Acad Sci [Internet]. 2007 Nov [cited 2016 Aug 2];1116:360–75. Available from: http://www.ncbi.nlm.nih.gov/pubmed/18083938

84. Miller SC, de Saint-Georges L, Bowman BM, Jee WS. Bone lining cells: structure and function. Scanning Microsc [Internet]. 1989 Sep [cited 2016 Aug 15];3(3):953–60; discussion 960–1. Available from: http://www.ncbi.nlm.nih.gov/pubmed/2694361

85. Andersen TL, Sondergaard TE, Skorzynska KE, Dagnaes-Hansen F, Plesner TL, Hauge EM, et al. A Physical Mechanism for Coupling Bone Resorption and Formation in Adult Human Bone. Am J Pathol. 2009;174(1):239–47.

86. Mulari M, Vääräniemi J, Väänänen HK. Intracellular membrane trafficking in bone resorbing osteoclasts. Microsc Res Tech [Internet]. Wiley Subscription Services, Inc., A Wiley Company; 2003 Aug 15 [cited 2016 Aug 3];61(6):496–503. Available from: http://doi.wiley.com/10.1002/jemt.10371

87. Salo J, Lehenkari P, Mulari M, Metsikkö K, Väänänen HK, Frost HM, et al. Removal of osteoclast bone resorption products by transcytosis. Science [Internet]. American Association for the Advancement of Science; 1997 Apr 11 [cited 2016 Aug 3];276(5310):270–3. Available from: http://www.ncbi.nlm.nih.gov/pubmed/9092479

88. Smith DM, Nance WE, Kang KW, Christian JC, Johnston CC. Genetic factors in determining bone mass. J Cinical Investig [Internet]. American Society for Clinical Investigation; 1973 Nov 1 [cited 2015 Apr 20];52(11):2800–8. Available from: http://www.jci.org/articles/view/107476

89. Arden NK, Baker J, Hogg C, Baan K, Spector TD. The heritability of bone mineral density, ultrasound of the calcaneus and hip axis length: a study of postmenopausal twins. J Bone Miner Res [Internet]. 1996 Apr [cited 2015 Apr 20];11(4):530–4. Available from: http://www.ncbi.nlm.nih.gov/pubmed/8992884

90. Richards JB, Zheng H-F, Spector TD. Genetics of osteoporosis from genome-wide association studies: advances and challenges. Nat Rev Genet [Internet]. Nature Publishing Group, a division of Macmillan Publishers Limited. All Rights Reserved.; 2012 Aug [cited 2015 Apr 10];13(8):576–88. Available from: http://dx.doi.org/10.1038/nrg3228

91. Richards JB, Rivadeneira F, Inouye M, Pastinen TM, Soranzo N, Wilson SG, et al. Bone mineral density, osteoporosis, and osteoporotic fractures: a genome-wide association study. Lancet [Internet]. 2008 May 3 [cited 2015 Mar 31];371(9623):1505–12. Available from: http://www.sciencedirect.com/science/article/pii/S0140673608605991

92. Rivadeneira F, Styrkársdottir U, Estrada K, Halldórsson B V, Hsu Y-H, Richards JB, et al. Twenty bone-mineral-density loci identified by large-scale meta-analysis of genome-wide association studies. Nat Genet [Internet]. Nature Publishing Group; 2009 Nov [cited 2015 Apr 10];41(11):1199–206. Available from: http://dx.doi.org/10.1038/ng.446

93. Ralston SH, Uitterlinden AG. Genetics of osteoporosis. Endocr Rev [Internet]. Endocrine Society; 2010 Oct 1 [cited 2015 Apr 24];31(5):629–62. Available from: http://press.endocrine.org/doi/full/10.1210/er.2009-0044

94. Estrada K, Styrkarsdottir U, Evangelou E, Hsu Y-H, Duncan EL, Ntzani EE, et al. Genome-wide meta-analysis identifies 56 bone mineral density loci and reveals 14 loci associated with risk of fracture. Nat Genet [Internet]. Nature Publishing Group, a division of Macmillan Publishers Limited. All Rights Reserved.; 2012 May [cited 2015 Mar 5];44(5):491–501. Available from: http://dx.doi.org/10.1038/ng.2249

95. Styrkarsdottir U, Halldorsson B V, Gretarsdottir S, Gudbjartsson DF, Walters GB, Ingvarsson T, et al. Multiple Genetic Loci for Bone Mineral Density and Fractures. N Engl J Med [Internet]. Massachusetts Medical Society; 2008 May 29;358(22):2355–65. Available from: http://dx.doi.org/10.1056/NEJMoa0801197

96. Styrkarsdottir U, Halldorsson B V, Gretarsdottir S, Gudbjartsson DF, Walters GB, Ingvarsson T, et al. New sequence variants associated with bone mineral density. Nat Genet [Internet]. Nature Publishing Group; 2009 Jan [cited 2015 Apr 27];41(1):15–7. Available from: http://dx.doi.org/10.1038/ng.284

97. Duncan EL, Danoy P, Kemp JP, Leo PJ, McCloskey E, Nicholson GC, et al. Genome-wide association study using extreme truncate selection identifies novel genes affecting bone mineral density and fracture risk. PLoS Genet [Internet]. 2011 Apr 21 [cited 2015 Apr 27];7(4):e1001372. Available from: http://journals.plos.org/plosgenetics/article?id=10.1371/journal.pgen.1001372

98. Manolagas SC. Birth and death of bone cells: basic regulatory mechanisms and implications for the pathogenesis and treatment of osteoporosis. Endocr Rev [Internet]. 2000 Apr [cited 2015 Jul 7];21(2):115–37. Available from: http://www.ncbi.nlm.nih.gov/pubmed/10782361

99. Lips P, Courpron P, Meunier PJ. Mean wall thickness of trabecular bone packets in the human iliac crest: changes with age. Calcif Tissue Res [Internet]. 1978 Nov 10 [cited 2015 Jul 11];26(1):13–7. Available from: http://www.ncbi.nlm.nih.gov/pubmed/737547

100. Parfitt AM, Han ZH, Palnitkar S, Rao DS, Shih MS, Nelson D. Effects of ethnicity and age or menopause on osteoblast function, bone mineralization, and osteoid accumulation in iliac bone. J Bone Miner Res [Internet]. 1997 Nov [cited 2015 Jul 11];12(11):1864–73. Available from: http://www.ncbi.nlm.nih.gov/pubmed/9383691

101. Jilka RL, Weinstein RS, Takahashi K, Parfitt AM, Manolagas SC. Linkage of decreased bone mass with impaired osteoblastogenesis in a murine model of accelerated senescence. J Clin Invest [Internet]. 1996 Apr 1 [cited 2015 Jul 11];97(7):1732–40. Available from: http://www.pubmedcentral.nih.gov/articlerender.fcgi?artid=507238&tool=pmcentrez&rendertype=abstract

102. Mueller SM, Glowacki J. Age-related decline in the osteogenic potential of human bone marrow cells cultured in three-dimensional collagen sponges. J Cell Biochem [Internet]. 2001 Jan [cited 2015 May 29];82(4):583–90. Available from: http://www.ncbi.nlm.nih.gov/pubmed/11500936

103. Garnero P, Sornay-Rendu E, Chapuy MC, Delmas PD. Increased bone turnover in late postmenopausal women is a major determinant of osteoporosis. J Bone Miner Res [Internet]. 1996 Mar [cited 2015 Jul 11];11(3):337–49. Available from: http://www.ncbi.nlm.nih.gov/pubmed/8852944

104. Raisz LG. Pathogenesis of osteoporosis: concepts, conflicts, and prospects. J Clin Invest [Internet]. 2005 Dec [cited 2015 Jan 26];115(12):3318–25. Available from: http://www.pubmedcentral.nih.gov/articlerender.fcgi?artid=1297264&tool=pmcentrez&rendertype=abstract

105. Cauley JA. Estrogen and bone health in men and women. Steroids [Internet]. 2014 Dec [cited 2015 Mar 30];99(Pt A):11–5. Available from: http://www.ncbi.nlm.nih.gov/pubmed/25555470

106. Lee K, Jessop H, Suswillo R, Zaman G, Lanyon L. Endocrinology: bone adaptation requires oestrogen receptor-alpha. Nature [Internet]. 2003 Jul 24 [cited 2015 Jul 11];424(6947):389. Available from: http://dx.doi.org/10.1038/424389a

107. Prestwood KM, Pilbeam CC, Burleson JA, Woodiel FN, Delmas PD, Deftos LJ, et al. The short-term effects of conjugated estrogen on bone turnover in older women. J Clin Endocrinol Metab [Internet]. 1994 Aug [cited 2015 Jul 11];79(2):366–71. Available from: http://www.ncbi.nlm.nih.gov/pubmed/8045949

108. Prestwood KM, Kenny AM, Kleppinger A, Kulldorff M. Ultralow-dose micronized 17beta-estradiol and bone density and bone metabolism in older women: a randomized controlled trial. JAMA [Internet]. 2003 Aug 27 [cited 2015 Jul 11];290(8):1042–8. Available from: http://www.ncbi.nlm.nih.gov/pubmed/12941676

109. Lane NE. Epidemiology, etiology, and diagnosis of osteoporosis. Am J Obstet Gynecol [Internet]. 2006 Feb [cited 2015 May 4];194(2 Suppl):S3–11. Available from: http://www.sciencedirect.com/science/article/pii/S0002937805013700

110. Bischoff-Ferrari HA, Dawson-Hughes B, Willett WC, Staehelin HB, Bazemore MG, Zee RY, et al. Effect of Vitamin D on falls: a meta-analysis. JAMA [Internet]. 2004 Apr 28 [cited 2015 Mar 20];291(16):1999–2006. Available from: http://www.ncbi.nlm.nih.gov/pubmed/15113819

111. Sambrook PN, Chen JS, March LM, Cameron ID, Cumming RG, Lord SR, et al. Serum parathyroid hormone predicts time to fall independent of vitamin D status in a frail elderly population. J Clin Endocrinol Metab [Internet]. 2004 Apr [cited 2015 Jul 1];89(4):1572–6. Available from: http://www.ncbi.nlm.nih.gov/pubmed/15070914

112. Patten BM, Bilezikian JP, Mallette LE, Prince A, Engel WK, Aurbach GD. Neuromuscular disease in primary hyperparathyroidism. Ann Intern Med [Internet]. 1974 Feb [cited 2016 Jun 1];80(2):182–93. Available from: http://www.ncbi.nlm.nih.gov/pubmed/4811792

113. Lips P. Vitamin D Deficiency and Secondary Hyperparathyroidism in the Elderly: Consequences for Bone Loss and Fractures and Therapeutic Implications. Endocr Rev [Internet]. 2001 Aug [cited 2015 Jul 1];22(4):477–501. Available from: http://www.ncbi.nlm.nih.gov/pubmed/11493580

114. Hansen MA, Overgaard K, Riis BJ, Christiansen C. Role of peak bone mass and bone loss in postmenopausal osteoporosis: 12 year study. BMJ [Internet]. 1991 Oct 19 [cited 2015 Apr 8];303(6808):961–4. Available from: http://www.bmj.com/content/303/6808/961.full.pdf+html

115. Barker DJ, Osmond C. Infant mortality, childhood nutrition, and ischaemic heart disease in England and Wales. Lancet (London, England) [Internet]. 1986 May 10 [cited 2016 Jun 1];1(8489):1077–81. Available from: http://www.ncbi.nlm.nih.gov/pubmed/2871345

116. Barker DJ. The developmental origins of adult disease. J Am Coll Nutr [Internet]. 2004;23(6 Suppl):588S – 595S. Available from: http://www.ncbi.nlm.nih.gov/pubmed/15640511

117. Inskip HM, Godfrey KM, Robinson SM, Law CM, Barker DJP, Cooper C, et al. Cohort profile: The Southampton Women's Survey. Int J Epidemiol [Internet]. 2006;35(1):42–8. Available from: http://ije.oxfordjournals.org/content/35/1/42.short

118. Dennison EM, Syddall HE, Sayer AA, Gilbody HJ, Cooper C. Birth weight and weight at 1 year are independent determinants of bone mass in the seventh decade: the Hertfordshire cohort study. Pediatr Res [Internet]. International Pediatrics Research Foundation, Inc.; 2005 Apr [cited 2015 Apr 28];57(4):582–6. Available from: http://dx.doi.org/10.1203/01.PDR.0000155754.67821.CA

119. Roseboom TJ, van der Meulen JH, Ravelli AC, Osmond C, Barker DJ, Bleker OP. Effects of prenatal exposure to the Dutch famine on adult disease in later life: an overview. Mol Cell Endocrinol [Internet]. 2001 Dec 20 [cited 2016 May 17];185(1-2):93–8. Available from: http://www.ncbi.nlm.nih.gov/pubmed/11738798

120. Martyn CN, Barker DJ, Osmond C. Mothers' pelvic size, fetal growth, and death from stroke and coronary heart disease in men in the UK. Lancet (London, England) [Internet]. 1996 Nov 9 [cited 2016 Jun 2];348(9037):1264–8. Available from: http://www.ncbi.nlm.nih.gov/pubmed/8909378

121. Barker DJ, Bull AR, Osmond C, Simmonds SJ. Fetal and placental size and risk of hypertension in adult life. BMJ [Internet]. 1990 Aug 4 [cited 2016 Jun 2];301(6746):259–62. Available from: http://www.pubmedcentral.nih.gov/articlerender.fcgi?artid=1663477&tool=pmcentrez&rendertype=abstract

122. Lumey LH, Stein AD, Kahn HS, van der Pal-de Bruin KM, Blauw GJ, Zybert PA, et al. Cohort Profile: The Dutch Hunger Winter Families Study. Int J Epidemiol [Internet]. 2007;36(6):1196–204. Available from: http://ije.oxfordjournals.org/content/36/6/1196.short

123. Roseboom TJ, van der Meulen JH, Osmond C, Barker DJ, Ravelli AC, Schroeder-Tanka JM, et al. Coronary heart disease after prenatal exposure to the Dutch famine, 1944-45. Heart [Internet]. 2000 Dec [cited 2016 Mar 1];84(6):595–8. Available from: http://www.pubmedcentral.nih.gov/articlerender.fcgi?artid=1729504&tool=pmcentrez&rendertype=abstract

124. Ravelli AC, van Der Meulen JH, Osmond C, Barker DJ, Bleker OP. Obesity at the age of 50 y in men and women exposed to famine prenatally. Am J Clin Nutr [Internet]. 1999 Nov [cited 2016 Jun 2];70(5):811–6. Available from: http://www.ncbi.nlm.nih.gov/pubmed/10539740

125. Cooper C, Fall C, Egger P, Hobbs R, Eastell R, Barker D. Growth in infancy and bone mass in later life. Ann Rheum Dis [Internet]. 1997 Jan 1 [cited 2015 Apr 28];56(1):17–21. Available from: http://ard.bmj.com/content/56/1/17

126. Fall CH, Osmond C, Barker DJ, Clark PM, Hales CN, Stirling Y, et al. Fetal and infant growth and cardiovascular risk factors in women. BMJ [Internet]. 1995;310(6977):428–32. Available from: http://www.ncbi.nlm.nih.gov/pubmed/7873947

127. Lucas JS, Inskip HM, Godfrey KM, Foreman CT, Warner JO, Gregson RK, et al. Small size at birth and greater postnatal weight gain: relationships to diminished infant lung function. Am J Respir Crit Care Med [Internet]. 2004 Sep 1 [cited 2016 Jun 2];170(5):534–40. Available from: http://www.ncbi.nlm.nih.gov/pubmed/15172897

128. Javaid MK, Crozier SR, Harvey NC, Taylor P, Inskip HM, Godfrey KM, et al. Maternal and seasonal predictors of change in calcaneal quantitative ultrasound during pregnancy. J Clin Endocrinol Metab [Internet]. 2005 Sep [cited 2016 Jun 2];90(9):5182–7. Available from: http://www.ncbi.nlm.nih.gov/pubmed/15985491

129. McKnight CM, Newnham JP, Stanley FJ, Mountain JA, Landau LI, Beilin LJ, et al. Birth of a cohort--the first 20 years of the Raine study. Med J Aust [Internet]. 2012 Dec 10 [cited 2016 Jun 2];197(11):608–10. Available from: http://www.ncbi.nlm.nih.gov/pubmed/23230915

130. Oken E, Levitan EB, Gillman MW. Maternal smoking during pregnancy and child overweight: systematic review and meta-analysis. Int J Obes (Lond) [Internet]. 2008 Feb [cited 2016 Mar 19];32(2):201–10. Available from: http://www.pubmedcentral.nih.gov/articlerender.fcgi?artid=2586944&tool=pmcentrez&rendertype=abstract

131. Whitehouse AJO, Zubrick SR, Blair E, Newnham JP, Hickey M. Fetal head circumference growth in children with specific language impairment. Arch Dis Child [Internet]. 2012 Jan

[cited 2016 Jun 2];97(1):49–51. Available from: http://www.pubmedcentral.nih.gov/articlerender.fcgi?artid=3704335&tool=pmcentrez&rendertype=abstract

132. Langley-Evans SC, Phillips GJ, Jackson AA. In utero exposure to maternal low protein diets induces hypertension in weanling rats, independently of maternal blood pressure changes. Clin Nutr [Internet]. 1994 Oct [cited 2016 Jun 2];13(5):319–24. Available from: http://www.ncbi.nlm.nih.gov/pubmed/16843406

133. Langley-Evans SC, Gardner DS, Welham SJ. Intrauterine programming of cardiovascular disease by maternal nutritional status. Nutrition [Internet]. 1998 Jan [cited 2016 Jun 2];14(1):39–47. Available from: http://www.ncbi.nlm.nih.gov/pubmed/9437680

134. Desai M, Byrne CD, Meeran K, Martenz ND, Bloom SR, Hales CN. Regulation of hepatic enzymes and insulin levels in offspring of rat dams fed a reduced-protein diet. Am J Physiol [Internet]. 1997 Oct [cited 2016 Jun 2];273(4 Pt 1):G899–904. Available from: http://www.ncbi.nlm.nih.gov/pubmed/9357833

135. Ozanne SE, Hales CN. The long-term consequences of intra-uterine protein malnutrition for glucose metabolism. Proc Nutr Soc [Internet]. 1999 Aug [cited 2016 Jun 2];58(3):615–9. Available from: http://www.ncbi.nlm.nih.gov/pubmed/10604194

136. Guberman C, Jellyman JK, Han G, Ross MG, Desai M. Maternal high-fat diet programs rat offspring hypertension and activates the adipose renin-angiotensin system. Am J Obstet Gynecol [Internet]. 2013 Sep 3 [cited 2016 Jun 2];209(3):262.e1–8. Available from: https://www.researchgate.net/publication/237069597_Maternal_high-fat_diet_programs_rat_offspring_hypertension_and_activates_the_adipose_renin-angiotensin_system

137. Elahi MM, Cagampang FR, Mukhtar D, Anthony FW, Ohri SK, Hanson MA. Long-term maternal high-fat feeding from weaning through pregnancy and lactation predisposes offspring to hypertension, raised plasma lipids and fatty liver in mice. Br J Nutr [Internet]. Cambridge University Press; 2009 Aug 1 [cited 2016 Jun 2];102(4):514–9. Available from: http://journals.cambridge.org/abstract_S000711450820749X

138. Williams L, Seki Y, Vuguin PM, Charron MJ. Animal models of in utero exposure to a high fat diet: a review. Biochim Biophys Acta [Internet]. 2014 Mar [cited 2016 Jun 2];1842(3):507–19. Available from: http://www.sciencedirect.com/science/article/pii/S0925443913002469

139. Cooper C, Westlake S, Harvey N, Javaid K, Dennison E, Hanson M. Review: developmental origins of osteoporotic fracture. Osteoporos Int [Internet]. 2006 Jan [cited 2015 Apr 10];17(3):337–47. Available from: http://www.ncbi.nlm.nih.gov/pubmed/16331359

140. Cooper C, Cawley M, Bhalla A, Egger P, Ring F, Morton L, et al. Childhood growth, physical activity, and peak bone mass in women. J Bone Miner Res [Internet]. 1995 Jun [cited 2015 Apr 28];10(6):940–7. Available from: http://www.ncbi.nlm.nih.gov/pubmed/7572318

141. Dennison EM, Arden NK, Keen RW, Syddall H, Day INM, Spector TD, et al. Birthweight, vitamin D receptor genotype and the programming of osteoporosis. Paediatr Perinat Epidemiol [Internet]. 2001 Jul [cited 2015 Apr 28];15(3):211–9. Available from: http://doi.wiley.com/10.1046/j.1365-3016.2001.00350.x

142. Pocock NA, Eisman JA, Hopper JL, Yeates MG, Sambrook PN, Eberl S. Genetic determinants of bone mass in adults. A twin study. J Cinical Investig [Internet]. 1987 Sep [cited 2015 Jun 23];80(3):706–10. Available from: http://www.pubmedcentral.nih.gov/articlerender.fcgi?artid=442294&tool=pmcentrez&rendertype=abstract

143. Fall C, Hindmarsh P, Dennison E, Kellingray S, Barker D, Cooper C. Programming of growth hormone secretion and bone mineral density in elderly men: a hypothesis. J Clin Endocrinol Metab [Internet]. Endocrine Society; 1998 Jan 1 [cited 2015 Apr 28];83(1):135–9. Available from: http://press.endocrine.org/doi/abs/10.1210/jcem.83.1.4487?url_ver=Z39.88-2003&rfr_id=ori:rid:crossref.org&rfr_dat=cr_pub%3dpubmed

144. Dennison E, Hindmarsh P, Fall C, Kellingray S, Barker D, Phillips D, et al. Profiles of Endogenous Circulating Cortisol and Bone Mineral Density in Healthy Elderly Men 1. J Clin Endocrinol Metab [Internet]. Endocrine Society; 1999 Sep 1 [cited 2015 Apr 28];84(9):3058–63. Available from: http://press.endocrine.org/doi/abs/10.1210/jcem.84.9.5964

145. Dennison EM, Syddall HE, Rodriguez S, Voropanov A, Day INM, Cooper C. Polymorphism in the growth hormone gene, weight in infancy, and adult bone mass. J Clin Endocrinol Metab [Internet]. Endocrine Society; 2004 Oct 2 [cited 2015 Apr 28];89(10):4898–903. Available from: http://press.endocrine.org/doi/abs/10.1210/jc.2004-0151?url_ver=Z39.88-2003&rfr_id=ori:rid:crossref.org&rfr_dat=cr_pub%3dpubmed

146. Fleeman TL, Cappon GD, Chapin RE, Hurtt ME. The effects of feed restriction during organogenesis on embryo-fetal development in the rat. Birth Defects Res Part B Dev Reprod Toxicol [Internet]. 2005 Oct [cited 2015 Apr 10];74(5):442–9. Available from: http://www.ncbi.nlm.nih.gov/pubmed/16193501

147. Lanham S, DuPriest E, Kupfer P, Roberts C, Cooper C, Bagby S, et al. Alteration of fetal bone structure by a maternal low protein diet. J Dev Orig Health Dis. 2009;1(Supplement S1):S285.

148. Lanham SA, Roberts C, Hollingworth T, Sreekumar R, Elahi MM, Cagampang FR, et al. Maternal high-fat diet: effects on offspring bone structure. Osteoporos Int [Internet]. 2010 Oct 21 [cited 2015 Apr 10];21(10):1703–14. Available from: http://link.springer.com/10.1007/s00198-009-1118-4

149. Godfrey K, Walker-Bone K, Robinson S, Taylor P, Shore S, Wheeler T, et al. Neonatal bone mass: influence of parental birthweight, maternal smoking, body composition, and activity during pregnancy. J Bone Miner Res [Internet]. 2001 Sep [cited 2015 Apr 28];16(9):1694–703. Available from: http://www.ncbi.nlm.nih.gov/pubmed/11547840

150. Javaid MK, Crozier SR, Harvey NC, Gale CR, Dennison EM, Boucher BJ, et al. Maternal vitamin D status during pregnancy and childhood bone mass at age 9 years: a longitudinal study. Lancet [Internet]. 2006;367(9504):36–43. Available from: http://www.ncbi.nlm.nih.gov/pubmed/16399151

151. Javaid MK, Eriksson JG, Kajantie E, Forsén T, Osmond C, Barker DJP, et al. Growth in childhood predicts hip fracture risk in later life. Osteoporos Int [Internet]. 2011 Jan [cited 2014 Nov 10];22(1):69–73. Available from: http://www.ncbi.nlm.nih.gov/pubmed/20379699

152. Baird J, Kurshid MA, Kim M, Harvey N, Dennison E, Cooper C. Does birthweight predict bone mass in adulthood? A systematic review and meta-analysis. Osteoporos Int [Internet]. 2011 May [cited 2015 Feb 13];22(5):1323–34. Available from: http://www.ncbi.nlm.nih.gov/pubmed/20683711

153. Cooper C, Eriksson JG, Forsén T, Osmond C, Tuomilehto J, Barker DJ. Maternal height, childhood growth and risk of hip fracture in later life: a longitudinal study. Osteoporos Int [Internet]. 2001 Jan [cited 2014 Nov 10];12(8):623–9. Available from: http://www.ncbi.nlm.nih.gov/pubmed/11580075

154. MacDonald PN, Dowd DR, Nakajima S, Galligan MA, Reeder MC, Haussler CA, et al. Retinoid X receptors stimulate and 9-cis retinoic acid inhibits 1,25-dihydroxyvitamin D3-activated expression of the rat osteocalcin gene. Mol Cell Biol [Internet]. 1993 Sep [cited 2016 Jan 5];13(9):5907–17. Available from: http://www.pubmedcentral.nih.gov/articlerender.fcgi?artid=360339&tool=pmcentrez&rendertype=abstract

155. Harvey NC, Javaid MK, Poole JR, Taylor P, Robinson SM, Inskip HM, et al. Paternal skeletal size predicts intrauterine bone mineral accrual. J Clin Endocrinol Metab [Internet]. 2008 May [cited 2015 Dec 11];93(5):1676–81. Available from: http://www.ncbi.nlm.nih.gov/pubmed/18285416

156. Hart PH, Lucas RM, Walsh JP, Zosky GR, Whitehouse AJO, Zhu K, et al. Vitamin D in fetal development: findings from a birth cohort study. Pediatrics [Internet]. 2015 Jan [cited 2015 Dec 14];135(1):e167–73. Available from: http://www.ncbi.nlm.nih.gov/pubmed/25511121

157. Zhu K, Whitehouse AJO, Hart PH, Kusel M, Mountain J, Lye S, et al. Maternal vitamin D status during pregnancy and bone mass in offspring at 20 years of age: a prospective cohort study. J Bone Miner Res [Internet]. 2014 Jan [cited 2015 Nov 8];29(5):1088–95. Available from: http://www.ncbi.nlm.nih.gov/pubmed/24189972

158. Sayers A, Tobias JH. Estimated maternal ultraviolet B exposure levels in pregnancy influence skeletal development of the child. J Clin Endocrinol Metab [Internet]. 2009 Mar [cited 2015 Dec 14];94(3):765–71. Available from: http://www.pubmedcentral.nih.gov/articlerender.fcgi?artid=2742727&tool=pmcentrez&rendertype=abstract

159. Lawlor DA, Wills AK, Fraser A, Sayers A, Fraser WD, Tobias JH. Association of maternal vitamin D status during pregnancy with bone-mineral content in offspring: a prospective cohort study. Lancet (London, England) [Internet]. 2013 Jun 22 [cited 2015 Dec 14];381(9884):2176–83. Available from: http://www.pubmedcentral.nih.gov/articlerender.fcgi?artid=3691477&tool=pmcentrez&rendertype=abstract

160. Sayers A, Fraser WD, Lawlor DA, Tobias JH. 25-Hydroxyvitamin-D3 levels are positively related to subsequent cortical bone development in childhood: findings from a large prospective cohort study. Osteoporos Int [Internet]. 2012 Aug [cited 2016 Jun 15];23(8):2117–28. Available from: http://www.ncbi.nlm.nih.gov/pubmed/22080378

161. Bocheva G, Boyadjieva N. Epigenetic regulation of fetal bone development and placental transfer of nutrients: progress for osteoporosis. Interdiscip Toxicol [Internet]. 2011;4(4):167–72. Available from: http://www.ncbi.nlm.nih.gov/pubmed/22319250

162. Barter MJ, Bui C, Young DA. Epigenetic mechanisms in cartilage and osteoarthritis: DNA methylation, histone modifications and microRNAs. Osteoarthr Cartil [Internet]. 2012;20(5):339–49. Available from: http://www.ncbi.nlm.nih.gov/pubmed/22281264

163. Kim JK, Samaranayake M, Pradhan S. Epigenetic mechanisms in mammals. Cell Mol Life Sci [Internet]. 2009;66(4):596–612. Available from: http://www.ncbi.nlm.nih.gov/pubmed/18985277

164. Adcock I, Ford P, Ito K, Barnes P. Epigenetics and airways disease. Respir Res [Internet]. 2006;7(1):21. Available from: http://respiratory-research.com/content/7/1/21

165. Takai D, Jones PA. Comprehensive analysis of CpG islands in human chromosomes 21 and 22. Proc Natl Acad Sci U S A [Internet]. 2002;99(6):3740–5. Available from: http://www.ncbi.nlm.nih.gov/pubmed/11891299

166. Miranda TB, Jones PA. DNA methylation: the nuts and bolts of repression. J Cell Physiol [Internet]. 2007;213(2):384–90. Available from: http://www.ncbi.nlm.nih.gov/pubmed/17708532

167. Jaenisch R, Bird A. Epigenetic regulation of gene expression: how the genome integrates intrinsic and environmental signals. Nat Genet [Internet]. 2003;33 Suppl:245–54. Available from: http://www.ncbi.nlm.nih.gov/pubmed/12610534

168. Metivier R, Gallais R, Tiffoche C, Le Peron C, Jurkowska RZ, Carmouche RP, et al. Cyclical DNA methylation of a transcriptionally active promoter. Nature [Internet]. 2008;452(7183):45–50. Available from: http://www.ncbi.nlm.nih.gov/pubmed/18322525

169. Zardo G, Fazi F, Travaglini L, Nervi C. Dynamic and reversibility of heterochromatic gene silencing in human disease. Cell Res [Internet]. 2005;15(9):679–90. Available from: http://www.ncbi.nlm.nih.gov/pubmed/16212874

170. Williams K, Christensen J, Pedersen MT, Johansen J V, Cloos PAC, Rappsilber J, et al. TET1 and hydroxymethylcytosine in transcription and DNA methylation fidelity. Nature [Internet]. Nature Publishing Group, a division of Macmillan Publishers Limited. All Rights Reserved.; 2011;473(7347):343–8. Available from: http://dx.doi.org/10.1038/nature10066

171. Li B, Carey M, Workman JL. The role of chromatin during transcription. Cell [Internet]. 2007 Feb 23 [cited 2014 Jul 10];128(4):707–19. Available from: http://www.ncbi.nlm.nih.gov/pubmed/17320508

172. Urnov FD, Wolffe AP. Chromatin remodeling and transcriptional activation: the cast (in order of appearance). Oncogene [Internet]. 2001;20(24):2991–3006. Available from: http://www.ncbi.nlm.nih.gov/pubmed/11420714

173. Peterson CL. HDAC's at Work: Everyone Doing Their Part. Mol Cell [Internet]. 2002;9(5):921–2. Available from: http://www.sciencedirect.com/science/article/pii/S1097276502005348

174. Bartel D. MicroRNAs: Genomics, Biogenesis, Mechanism, and Function. Cell [Internet]. 2004 Jan [cited 2014 Jul 22];116(2):281–97. Available from: http://www.sciencedirect.com/science/article/pii/S0092867404000455

175. Chien C-H, Sun Y-M, Chang W-C, Chiang-Hsieh P-Y, Lee T-Y, Tsai W-C, et al. Identifying transcriptional start sites of human microRNAs based on high-throughput sequencing data. Nucleic Acids Res [Internet]. 2011 Nov [cited 2015 Mar 29];39(21):9345–56. Available from: http://nar.oxfordjournals.org/content/early/2011/08/05/nar.gkr604.abstract

176. Shomron N, Levy C. MicroRNA-biogenesis and pre-mRNA splicing crosstalk. J Biomed Biotechnol [Internet]. 2009 Jan [cited 2015 Apr 12];2009:594678. Available from: http://www.scopus.com/inward/record.url?eid=2-s2.0-68949144764&partnerID=tZOtx3y1

177. Yi R, Qin Y, Macara IG, Cullen BR. Exportin-5 mediates the nuclear export of pre-microRNAs and short hairpin RNAs. Genes Dev [Internet]. 2003 Dec 15 [cited 2014 Dec 6];17(24):3011–6. Available from: http://genesdev.cshlp.org/content/17/24/3011.abstract

178. Basyuk E. Human let-7 stem-loop precursors harbor features of RNase III cleavage products. Nucleic Acids Res [Internet]. 2003 Nov 15 [cited 2015 Apr 29];31(22):6593–7. Available from: http://nar.oxfordjournals.org/content/31/22/6593.abstract

179. Schanen BC, Li X. Transcriptional regulation of mammalian miRNA genes. Genomics [Internet]. 2011 Jan [cited 2015 Apr 29];97(1):1–6. Available from: http://www.sciencedirect.com/science/article/pii/S088875431000220X

180. Kusenda B, Mraz M, Mayer J, Pospisilova S. MicroRNA biogenesis, functionality and cancer relevance. Biomed Pap [Internet]. Biomedical Papers; 2006 Dec 1 [cited 2015 Apr

29];150(2):205–15. Available from: http://biomed.papers.upol.cz/doi/10.5507/bp.2006.029.html

181. Ravasi T, Suzuki H, Pang KC, Katayama S, Furuno M, Okunishi R, et al. Experimental validation of the regulated expression of large numbers of non-coding RNAs from the mouse genome. Genome Res [Internet]. 2006 Jan 1 [cited 2015 Jan 12];16(1):11–9. Available from: http://genome.cshlp.org/content/16/1/11.abstract?ijkey=cd7d2e6e4acf2014ff9f99b01a814faede57dd6a&keytype2=tf_ipsecsha

182. Wilusz JE, Sunwoo H, Spector DL. Long noncoding RNAs: functional surprises from the RNA world. Genes Dev [Internet]. 2009 Jul 1 [cited 2014 Jul 10];23(13):1494–504. Available from: http://genesdev.cshlp.org/content/23/13/1494.long

183. Squires JE, Patel HR, Nousch M, Sibbritt T, Humphreys DT, Parker BJ, et al. Widespread occurrence of 5-methylcytosine in human coding and non-coding RNA. Nucleic Acids Res [Internet]. 2012 Jun 1 [cited 2014 Dec 3];40(11):5023–33. Available from: http://nar.oxfordjournals.org/content/40/11/5023.long

184. Zhang X, Rice K, Wang Y, Chen W, Zhong Y, Nakayama Y, et al. Maternally expressed gene 3 (MEG3) noncoding ribonucleic acid: isoform structure, expression, and functions. Endocrinology [Internet]. Endocrine Society; 2010 Mar 1 [cited 2014 Dec 18];151(3):939–47. Available from: http://press.endocrine.org/doi/full/10.1210/en.2009-0657

185. Carrieri C, Cimatti L, Biagioli M, Beugnet A, Zucchelli S, Fedele S, et al. Long non-coding antisense RNA controls Uchl1 translation through an embedded SINEB2 repeat. Nature [Internet]. Nature Publishing Group, a division of Macmillan Publishers Limited. All Rights Reserved.; 2012 Nov 15 [cited 2014 Jul 16];491(7424):454–7. Available from: http://dx.doi.org/10.1038/nature11508

186. Hogan DJ, Riordan DP, Gerber AP, Herschlag D, Brown PO. Diverse RNA-binding proteins interact with functionally related sets of RNAs, suggesting an extensive regulatory system. PLoS Biol [Internet]. Public Library of Science; 2008 Oct 28 [cited 2014 Oct 16];6(10):e255. Available from: http://dx.plos.org/10.1371/journal.pbio.0060255

187. Chu C, Qu K, Zhong FL, Artandi SE, Chang HY. Genomic maps of long noncoding RNA occupancy reveal principles of RNA-chromatin interactions. Mol Cell [Internet]. 2011 Nov 18 [cited 2014 Jul 9];44(4):667–78. Available from: http://www.pubmedcentral.nih.gov/articlerender.fcgi?artid=3249421&tool=pmcentrez&rendertype=abstract

188. Rinn JL, Chang HY. Genome regulation by long noncoding RNAs. Annu Rev Biochem [Internet]. Annual Reviews; 2012 Jan 4 [cited 2014 Jul 9];81:145–66. Available from: http://www.annualreviews.org/doi/abs/10.1146/annurev-biochem-051410-092902

189. Spitale RC, Tsai M-C, Chang HY. RNA templating the epigenome: Long noncoding RNAs as molecular scaffolds. Epigenetics [Internet]. Taylor & Francis; 2014 Oct 27 [cited 2015 Jan 5];6(5):539–43. Available from: http://www.tandfonline.com/doi/full/10.4161/epi.6.5.15221#tabModule

190. Rinn JL, Kertesz M, Wang JK, Squazzo SL, Xu X, Brugmann SA, et al. Functional demarcation of active and silent chromatin domains in human HOX loci by noncoding RNAs. Cell [Internet]. Elsevier; 2007 Jun 29 [cited 2014 Jul 16];129(7):1311–23. Available from: http://www.cell.com/article/S0092867407006599/fulltext

191. Li W, Notani D, Ma Q, Tanasa B, Nunez E, Chen AY, et al. Functional roles of enhancer RNAs for oestrogen-dependent transcriptional activation. Nature [Internet]. Nature Publishing Group, a division of Macmillan Publishers Limited. All Rights Reserved.; 2013 Jun 27 [cited

2014 Jul 9];498(7455):516–20. Available from: http://dx.doi.org/10.1038/nature12210

192. Gluckman PD, Hanson MA, Buklijas T, Low FM, Beedle AS. Epigenetic mechanisms that underpin metabolic and cardiovascular diseases. Nat Rev Endocrinol [Internet]. 2009;5(7):401–8. Available from: http://www.ncbi.nlm.nih.gov/pubmed/19488075

193. Waterland RA, Jirtle RL. Early nutrition, epigenetic changes at transposons and imprinted genes, and enhanced susceptibility to adult chronic diseases. Nutrition [Internet]. 2004;20(1):63–8. Available from: http://www.sciencedirect.com/science/article/pii/S0899900703002156

194. Lillycrop KA, Phillips ES, Jackson AA, Hanson MA, Burdge GC. Dietary protein restriction of pregnant rats induces and folic acid supplementation prevents epigenetic modification of hepatic gene expression in the offspring. J Nutr [Internet]. 2005;135(6):1382–6. Available from: http://www.ncbi.nlm.nih.gov/pubmed/15930441

195. Weaver ICG, Cervoni N, Champagne FA, D'Alessio AC, Sharma S, Seckl JR, et al. Epigenetic programming by maternal behavior. Nat Neurosci [Internet]. 2004;7(8):847–54. Available from: http://dx.doi.org/10.1038/nn1276

196. Fetahu IS, Höbaus J, Kállay E. Vitamin D and the epigenome. Front Physiol [Internet]. 2014 Jan [cited 2015 Jun 4];5:164. Available from: http://www.pubmedcentral.nih.gov/articlerender.fcgi?artid=4010791&tool=pmcentrez&rendertype=abstract

197. Doig CL, Singh PK, Dhiman VK, Thorne JL, Battaglia S, Sobolewski M, et al. Recruitment of NCOR1 to VDR target genes is enhanced in prostate cancer cells and associates with altered DNA methylation patterns. Carcinogenesis [Internet]. 2013 Feb [cited 2016 Jan 11];34(2):248–56. Available from: http://www.pubmedcentral.nih.gov/articlerender.fcgi?artid=3564435&tool=pmcentrez&rendertype=abstract

198. Tapp HS, Commane DM, Bradburn DM, Arasaradnam R, Mathers JC, Johnson IT, et al. Nutritional factors and gender influence age-related DNA methylation in the human rectal mucosa. Aging Cell [Internet]. 2013 Feb 6 [cited 2016 Jan 11];12(1):148–55. Available from: http://www.pubmedcentral.nih.gov/articlerender.fcgi?artid=3572581&tool=pmcentrez&rendertype=abstract

199. Rawson JB, Sun Z, Dicks E, Daftary D, Parfrey PS, Green RC, et al. Vitamin D intake is negatively associated with promoter methylation of the Wnt antagonist gene DKK1 in a large group of colorectal cancer patients. Nutr Cancer [Internet]. NIH Public Access; 2012 Jan [cited 2016 Jan 11];64(7):919–28. Available from: /pmc/articles/PMC4323165/?report=abstract

200. Zhu H, Wang X, Shi H, Su S, Harshfield GA, Gutin B, et al. A Genome-Wide Methylation Study of Severe Vitamin D Deficiency in African American Adolescents. J Pediatr [Internet]. NIH Public Access; 2013 May 1 [cited 2016 Jan 11];162(5):1004–9.e1. Available from: /pmc/articles/PMC3935318/?report=abstract

201. Kim S, Shevde NK, Pike JW. 1,25-Dihydroxyvitamin D3 stimulates cyclic vitamin D receptor/retinoid X receptor DNA-binding, co-activator recruitment, and histone acetylation in intact osteoblasts. J Bone Miner Res [Internet]. 2005 Feb [cited 2016 Jan 11];20(2):305–17. Available from: http://www.ncbi.nlm.nih.gov/pubmed/15647825

202. Kim M-S, Fujiki R, Kitagawa H, Kato S. 1alpha,25(OH)2D3-induced DNA methylation suppresses the human CYP27B1 gene. Mol Cell Endocrinol [Internet]. 2007 Feb [cited 2016 Jan 11];265-266:168–73. Available from: http://www.sciencedirect.com/science/article/pii/S0303720706005697

203. Watkins AJ, Ursell E, Panton R, Papenbrock T, Hollis L, Cunningham C, et al. Adaptive responses by mouse early embryos to maternal diet protect fetal growth but predispose to adult onset disease. Biol Reprod [Internet]. 2008;78(2):299–306. Available from: http://www.ncbi.nlm.nih.gov/pubmed/17989357

204. Heijmans BT, Tobi EW, Stein AD, Putter H, Blauw GJ, Susser ES, et al. Persistent epigenetic differences associated with prenatal exposure to famine in humans. Proc Natl Acad Sci U S A [Internet]. 2008 Nov 4 [cited 2014 Dec 29];105(44):17046–9. Available from: http://www.pnas.org/content/early/2008/10/24/0806560105

205. Harvey NC, Sheppard A, Godfrey KM, McLean C, Garratt E, Ntani G, et al. Childhood Bone Mineral Content Is Associated With Methylation Status of the RXRA Promoter at Birth. J Bone Miner Res [Internet]. 2014;29(3):600–7. Available from: http://dx.doi.org/10.1002/jbmr.2056

206. Huang S, Wang S, Bian C, Yang Z, Zhou H, Zeng Y, et al. Upregulation of miR-22 promotes osteogenic differentiation and inhibits adipogenic differentiation of human adipose tissue-derived mesenchymal stem cells by repressing HDAC6 protein expression. Stem Cells Dev [Internet]. 2012 Sep 1 [cited 2016 Jun 3];21(13):2531–40. Available from: http://www.pubmedcentral.nih.gov/articlerender.fcgi?artid=3424982&tool=pmcentrez&rendertype=abstract

207. Li H, Li T, Wang S, Wei J, Fan J, Li J, et al. miR-17-5p and miR-106a are involved in the balance between osteogenic and adipogenic differentiation of adipose-derived mesenchymal stem cells. Stem Cell Res [Internet]. 2013 May [cited 2016 May 30];10(3):313–24. Available from: http://www.ncbi.nlm.nih.gov/pubmed/23399447

208. Hassan MQ, Tare R, Lee SH, Mandeville M, Weiner B, Montecino M, et al. HOXA10 controls osteoblastogenesis by directly activating bone regulatory and phenotypic genes. Mol Cell Biol [Internet]. 2007 May [cited 2016 Jun 3];27(9):3337–52. Available from: http://www.pubmedcentral.nih.gov/articlerender.fcgi?artid=1899966&tool=pmcentrez&rendertype=abstract

209. Hemming S, Cakouros D, Isenmann S, Cooper L, Menicanin D, Zannettino A, et al. EZH2 and KDM6A act as an epigenetic switch to regulate mesenchymal stem cell lineage specification. Stem Cells [Internet]. 2014 Mar [cited 2016 Jun 3];32(3):802–15. Available from: http://www.ncbi.nlm.nih.gov/pubmed/24123378

210. Villagra A, Gutiérrez J, Paredes R, Sierra J, Puchi M, Imschenetzky M, et al. Reduced CpG methylation is associated with transcriptional activation of the bone-specific rat osteocalcin gene in osteoblasts. J Cell Biochem [Internet]. 2002 Jan [cited 2016 Jun 3];85(1):112–22. Available from: http://www.ncbi.nlm.nih.gov/pubmed/11891855

211. Delgado-Calle J, Sañudo C, Sánchez-Verde L, García-Renedo RJ, Arozamena J, Riancho JA. Epigenetic regulation of alkaline phosphatase in human cells of the osteoblastic lineage. Bone [Internet]. 2011 Oct [cited 2016 Jun 3];49(4):830–8. Available from: http://www.sciencedirect.com/science/article/pii/S8756328211010477

212. Delgado-Calle J, Sanudo C, Fernandez AF, Garcia-Renedo R, Fraga MF, Riancho JA. Role of DNA methylation in the regulation of the RANKL-OPG system in human bone. Epigenetics [Internet]. 2012;7(1):83–91. Available from: http://www.ncbi.nlm.nih.gov/pubmed/22207352

213. Zuo C, Wang Z, Lu H, Dai Z, Liu X, Cui L. Expression profiling of lncRNAs in C3H10T1/2 mesenchymal stem cells undergoing early osteoblast differentiation. Mol Med Rep [Internet]. Spandidos Publications; 2013 Aug 1 [cited 2015 Apr 8];8(2):463–7. Available from: http://www.spandidos-publications.com/mmr/8/2/463/abstract

214. Zhu L, Xu P-C. Downregulated LncRNA-ANCR promotes osteoblast differentiation by targeting EZH2 and regulating Runx2 expression. Biochem Biophys Res Commun [Internet]. 2013 Mar 22 [cited 2015 Apr 8];432(4):612–7. Available from: http://www.sciencedirect.com/science/article/pii/S0006291X13002969

215. de PJ van, Drabek K, Eijken M, Strini T, van der EB, van LH. Long non-coding RNA H19 positively stimulates osteogenic human mesenchymal stem cells differentiation and mineralisation. BioScientifica; 2015 Apr 8 [cited 2015 Nov 10]; Available from: http://abstracts.ects-ibms2015.org/ectsibms/0001/ectsibms0001P158.htm

216. Jain KK. The Handbook of Biomarkers [Internet]. New York: Springer; 2010. p. 1 p. Available from: http://books.google.co.uk/books?id=Tr6JEXqSWk0C&lpg=PR5&ots=BPpc4NJswP&dq=methylation biomarker osteoporosis&lr&pg=PA1#v=onepage&q&f=false

217. Burdge GC, Hanson MA, Slater-Jefferies JL, Lillycrop KA. Epigenetic regulation of transcription: a mechanism for inducing variations in phenotype (fetal programming) by differences in nutrition during early life? Br J Nutr [Internet]. 2007;97(6):1036–46. Available from: http://www.ncbi.nlm.nih.gov/pubmed/17381976

218. Woodfine K, Huddleston JE, Murrell A. Quantitative analysis of DNA methylation at all human imprinted regions reveals preservation of epigenetic stability in adult somatic tissue. Epigenetics Chromatin [Internet]. 2011 Jan [cited 2015 May 12];4(1):1. Available from: http://www.epigeneticsandchromatin.com/content/4/1/1

219. Lu T-P, Chen KT, Tsai M-H, Kuo K-T, Hsiao CK, Lai L-C, et al. Identification of genes with consistent methylation levels across different human tissues. Sci Rep [Internet]. Nature Publishing Group; 2014 Jan 12 [cited 2015 May 12];4:4351. Available from: http://www.nature.com/srep/2014/140312/srep04351/full/srep04351.html

220. Godfrey KM, Sheppard A, Gluckman PD, Lillycrop KA, Burdge GC, McLean C, et al. Epigenetic gene promoter methylation at birth is associated with child's later adiposity. Diabetes [Internet]. 2011;60(5):1528–34. Available from: http://www.ncbi.nlm.nih.gov/pubmed/21471513

221. Clarke-Harris R, Wilkin TJ, Hosking J, Pinkney J, Jeffery AN, Metcalf BS, et al. PGC1α promoter methylation in blood at 5-7 years predicts adiposity from 9 to 14 years (EarlyBird 50). Diabetes [Internet]. 2014 Jul 1 [cited 2015 Jan 19];63(7):2528–37. Available from: http://diabetes.diabetesjournals.org/content/63/7/2528.long

222. Li G, Yin W, Chamberlain R, Hewett-Emmett D, Roberts JN, Yang X, et al. Identification and characterization of the human retinoid X receptor alpha gene promoter. Gene [Internet]. 2006 May 10 [cited 2015 Mar 3];372:118–27. Available from: http://www.sciencedirect.com/science/article/pii/S0378111906000217

223. Kliewer SA, Umesono K, Mangelsdorf DJ, Evans RM. Retinoid X receptor interacts with nuclear receptors in retinoic acid, thyroid hormone and vitamin D3 signalling. Nature [Internet]. 1992 Jan 30 [cited 2016 Jan 12];355(6359):446–9. Available from: http://dx.doi.org/10.1038/355446a0

224. Kliewer SA, Umesono K, Noonan DJ, Heyman RA, Evans RM. Convergence of 9-cis retinoic acid and peroxisome proliferator signalling pathways through heterodimer formation of their receptors. Nature [Internet]. 1992 Aug 27 [cited 2015 Nov 14];358(6389):771–4. Available from: http://www.ncbi.nlm.nih.gov/pubmed/1324435

225. Menéndez-Gutiérrez MP, Rőszer T, Fuentes L, Núñez V, Escolano A, Redondo JM, et al. Retinoid X receptors orchestrate osteoclast differentiation and postnatal bone remodeling. J Clin Invest [Internet]. 2015 Feb [cited 2016 Jan 12];125(2):809–23. Available from:

http://www.pubmedcentral.nih.gov/articlerender.fcgi?artid=4319420&tool=pmcentrez&rendertype=abstract

226. MacDonald PN, Dowd DR, Nakajima S, Galligan MA, Reeder MC, Haussler CA, et al. Retinoid X receptors stimulate and 9-cis retinoic acid inhibits 1,25-dihydroxyvitamin D3-activated expression of the rat osteocalcin gene. Mol Cell Biol [Internet]. 1993 Sep 1 [cited 2016 Jan 12];13(9):5907–17. Available from: http://mcb.asm.org/content/13/9/5907.short

227. Driel van M, Pols H, van Leeuwen JP. Osteoblast Differentiation and Control by Vitamin D and Vitamin D Metabolites. Curr Pharm Des [Internet]. Bentham Science Publishers; 2004 Aug 1 [cited 2016 Jan 12];10(21):2535–55. Available from: http://www.ingentaconnect.com/content/ben/cpd/2004/00000010/00000021/art00002

228. Villanueva C, Giulivi C. Subcellular and cellular locations of nitric oxide synthase isoforms as determinants of health and disease. Free Radic Biol Med [Internet]. 2010 Aug 1 [cited 2016 Jan 12];49(3):307–16. Available from: http://www.pubmedcentral.nih.gov/articlerender.fcgi?artid=2900489&tool=pmcentrez&rendertype=abstract

229. Denninger JW, Marletta MA. Guanylate cyclase and the .NO/cGMP signaling pathway. Biochim Biophys Acta [Internet]. 1999 May 5 [cited 2016 Jan 12];1411(2-3):334–50. Available from: http://www.ncbi.nlm.nih.gov/pubmed/10320667

230. Cockcroft J. Exploring Vascular Benefits of Endothelium-Derived Nitric Oxide. Am J Hypertens [Internet]. 2005 Dec [cited 2016 Jan 12];18(12):177–83. Available from: http://www.ncbi.nlm.nih.gov/pubmed/16373196

231. Nilforoushan D, Gramoun A, Glogauer M, Manolson MF. Nitric oxide enhances osteoclastogenesis possibly by mediating cell fusion. Nitric Oxide [Internet]. 2009 Aug [cited 2016 Jan 12];21(1):27–36. Available from: http://www.ncbi.nlm.nih.gov/pubmed/19389479

232. Sabanai K, Tsutsui M, Sakai A, Hirasawa H, Tanaka S, Nakamura E, et al. Genetic Disruption of All NO Synthase Isoforms Enhances BMD and Bone Turnover in Mice In Vivo: Involvement of the Renin-Angiotensin System. J Bone Miner Res [Internet]. 2008 Feb 4 [cited 2016 Jan 12];23(5):633–43. Available from: http://www.ncbi.nlm.nih.gov/pubmed/18433298

233. Zaman G, Pitsillides AA, Rawlinson SCF, Suswillo RFL, Mosley JR, Cheng MZ, et al. Mechanical Strain Stimulates Nitric Oxide Production by Rapid Activation of Endothelial Nitric Oxide Synthase in Osteocytes. J Bone Miner Res [Internet]. 1999 Jul 1 [cited 2016 Jan 12];14(7):1123–31. Available from: http://www.ncbi.nlm.nih.gov/pubmed/10404012

234. Harvey NC, Lillycrop KA, Garratt E, Sheppard A, McLean C, Burdge G, et al. Evaluation of methylation status of the eNOS promoter at birth in relation to childhood bone mineral content. Calcif Tissue Int [Internet]. 2012;90(2):120–7. Available from: http://www.ncbi.nlm.nih.gov/pubmed/22159788

235. Sharpless NE, DePinho RA. The INK4A/ARF locus and its two gene products. Curr Opin Genet Dev [Internet]. 1999 Feb [cited 2014 Sep 7];9(1):22–30. Available from: http://www.sciencedirect.com/science/article/pii/S0959437X99800045

236. Cooper C, Fall C, Egger P, Hobbs R, Eastell R, Barker D. Growth in infancy and bone mass in later life. Ann Rheum Dis [Internet]. 1997;56(1):17–21. Available from: http://www.ncbi.nlm.nih.gov/pubmed/9059135

237. Congrains A, Kamide K, Katsuya T, Yasuda O, Oguro R, Yamamoto K, et al. CVD-associated non-coding RNA, ANRIL, modulates expression of atherogenic pathways in VSMC. Biochem Biophys Res Commun [Internet]. 2012 Mar 23 [cited 2014 Sep 8];419(4):612–6. Available

from: http://www.sciencedirect.com/science/article/pii/S0006291X12002835

238. Burd CE, Jeck WR, Liu Y, Sanoff HK, Wang Z, Sharpless NE. Expression of linear and novel circular forms of an INK4/ARF-associated non-coding RNA correlates with atherosclerosis risk. PLoS Genet [Internet]. 2010;6(12):e1001233. Available from: http://www.ncbi.nlm.nih.gov/pubmed/21151960

239. Krishnamurthy J, Torrice C, Ramsey MR, Kovalev GI, Al-Regaiey K, Su L, et al. Ink4a/Arf expression is a biomarker of aging. J Clin Invest [Internet]. The American Society for Clinical Investigation; 2004;114(9):1299–307. Available from: http://www.jci.org/articles/view/22475

240. Popov N, Gil J. Epigenetic regulation of the INK4b-ARF-INK4a locus: In sickness and in health. epigenetics [Internet]. Landes Bioscience Inc.; 2010 Nov 1;5(8):685–90. Available from: http://www.landesbioscience.com/journals/epigenetics/article/12996/

241. Lowe SW, Sherr CJ. Tumor suppression by Ink4a–Arf: progress and puzzles. Curr Opin Genet Dev [Internet]. 2003;13(1):77–83. Available from: http://www.sciencedirect.com/science/article/pii/S0959437X02000138

242. Yap KL, Li S, Muñoz-Cabello AM, Raguz S, Zeng L, Mujtaba S, et al. Molecular interplay of the noncoding RNA ANRIL and methylated histone H3 lysine 27 by polycomb CBX7 in transcriptional silencing of INK4a. Mol Cell [Internet]. 2010 Jun 11 [cited 2014 Jul 16];38(5):662–74. Available from: http://www.sciencedirect.com/science/article/pii/S1097276510003357

243. Kotake Y, Nakagawa T, Kitagawa K, Suzuki S, Liu N, Kitagawa M, et al. Long non-coding RNA ANRIL is required for the PRC2 recruitment to and silencing of p15(INK4B) tumor suppressor gene. Oncogene [Internet]. Macmillan Publishers Limited; 2011 Apr 21 [cited 2014 Aug 28];30(16):1956–62. Available from: http://dx.doi.org/10.1038/onc.2010.568

244. Kim WY, Sharpless NE. The regulation of INK4/ARF in cancer and aging. Cell [Internet]. 2006;127(2):265–75. Available from: http://www.ncbi.nlm.nih.gov/pubmed/17055429

245. Zindy F, Quelle DE, Roussel MF, Sherr CJ. Expression of the p16INK4a tumor suppressor versus other INK4 family members during mouse development and aging. Oncogene [Internet]. 1997;15(2):203–11. Available from: http://www.ncbi.nlm.nih.gov/pubmed/9244355

246. Molofsky A V, Slutsky SG, Joseph NM, He S, Pardal R, Krishnamurthy J, et al. Increasing p16INK4a expression decreases forebrain progenitors and neurogenesis during ageing. Nature [Internet]. 2006;443(7110):448–52. Available from: http://www.ncbi.nlm.nih.gov/pubmed/16957738

247. Baker DJ, Wijshake T, Tchkonia T, LeBrasseur NK, Childs BG, van de Sluis B, et al. Clearance of p16Ink4a-positive senescent cells delays ageing-associated disorders. Nature [Internet]. 2011 Nov 10 [cited 2014 Jul 11];479(7372):232–6. Available from: http://www.pubmedcentral.nih.gov/articlerender.fcgi?artid=3468323&tool=pmcentrez&rendertype=abstract

248. Janzen V, Forkert R, Fleming HE, Saito Y, Waring MT, Dombkowski DM, et al. Stem-cell ageing modified by the cyclin-dependent kinase inhibitor p16INK4a. Nature [Internet]. 2006;443(7110):421–6. Available from: http://www.ncbi.nlm.nih.gov/pubmed/16957735

249. Krishnamurthy J, Ramsey MR, Ligon KL, Torrice C, Koh A, Bonner-Weir S, et al. p16INK4a induces an age-dependent decline in islet regenerative potential. Nature [Internet]. 2006;443(7110):453–7. Available from: http://dx.doi.org/10.1038/nature05092

250. Melzer D, Frayling TM, Murray A, Hurst AJ, Harries LW, Song H, et al. A common variant of the p16INK4a genetic region is associated with physical function in older people. Mech

Ageing Dev [Internet]. 2007;128(5–6):370–7. Available from: http://www.sciencedirect.com/science/article/pii/S0047637407000401

251. Broadbent HM, Peden JF, Lorkowski S, Goel A, Ongen H, Green F, et al. Susceptibility to coronary artery disease and diabetes is encoded by distinct, tightly linked SNPs in the ANRIL locus on chromosome 9p. Hum Mol Genet [Internet]. 2008;17(6):806–14. Available from: http://hmg.oxfordjournals.org/content/17/6/806.abstract

252. Emanuele E, Lista S, Ghidoni R, Binetti G, Cereda C, Benussi L, et al. Chromosome 9p21.3 genotype is associated with vascular dementia and Alzheimer's disease. Neurobiol Aging [Internet]. 2011;32(7):1231–5. Available from: http://www.ncbi.nlm.nih.gov/pubmed/19664850

253. Smith AJP, Humphries SE. Characterization of DNA-binding proteins using multiplexed competitor EMSA. J Mol Biol [Internet]. 2009 Jan 23 [cited 2016 Mar 12];385(3):714–7. Available from: http://www.ncbi.nlm.nih.gov/pubmed/19059416

254. Lu Q, Richardson B. Methods for Analyzing the Role of DNA Methylation and Chromatin Structure in Regulating T Lymphocyte Gene Expression. Biol Proced Online [Internet]. BioMed Central; 2004 [cited 2016 Jul 25];6:189–203. Available from: http://www.ncbi.nlm.nih.gov/pubmed/15448721

255. DiNardo DNM, Butcher DT, Robinson DP, Archer TK, Rodenhiser DI. Functional analysis of CpG methylation in the BRCA1 promoter region. Oncogene [Internet]. Nature Publishing Group; 2001 Aug 30 [cited 2016 Jul 25];20(38):5331–40. Available from: http://www.nature.com/doifinder/10.1038/sj.onc.1204697

256. Levine JJ, Stimson-Crider KM, Vertino PM. Effects of methylation on expression of TMS1/ASC in human breast cancer cells. Oncogene [Internet]. Nature Publishing Group; 2003 May 29 [cited 2016 Jul 25];22(22):3475–88. Available from: http://www.nature.com/doifinder/10.1038/sj.onc.1206430

257. McGowan PO, Sasaki A, D'Alessio AC, Dymov S, Labonté B, Szyf M, et al. Epigenetic regulation of the glucocorticoid receptor in human brain associates with childhood abuse. Nat Neurosci [Internet]. Nature Publishing Group; 2009 Feb 22 [cited 2016 Jul 25];12(3):342–8. Available from: http://www.nature.com/doifinder/10.1038/nn.2270

258. Han W, Shi M, Spivack SD. Site-specific methylated reporter constructs for functional analysis of DNA methylation. Epigenetics [Internet]. 2013 Nov [cited 2016 Mar 12];8(11):1176–87. Available from: http://www.ncbi.nlm.nih.gov/pubmed/24004978

259. Brun RP, Spiegelman BM. PPAR gamma and the molecular control of adipogenesis. J Endocrinol [Internet]. 1997 Nov 1;155 (2):217–8. Available from: http://joe.endocrinology-journals.org/content/155/2/217.short

260. Farmer SR. Regulation of PPARgamma activity during adipogenesis. Int J Obes (Lond) [Internet]. 2005 Mar [cited 2015 Feb 1];29 Suppl 1(S1):S13–6. Available from: http://dx.doi.org/10.1038/sj.ijo.0802907

261. Spiegelman BM, Hu E, Kim JB, Brun R. PPARγ and the control of adipogenesis. Biochimie [Internet]. 1997 Feb [cited 2015 Mar 2];79(2-3):111–2. Available from: http://www.sciencedirect.com/science/article/pii/S0300908497815003

262. Gaston K, Fried M. CpG methylation has differential effects on the binding of YY1 and ETS proteins to the bi-directional promoter of the Surf-1 and Surf-2 genes. Nucleic Acids Res [Internet]. 1995 Mar 25;23 (6):901–9. Available from: http://nar.oxfordjournals.org/content/23/6/901.abstract

263. Decker T, Kovarik P, Meinke A. GAS elements: a few nucleotides with a major impact on cytokine-induced gene expression. J Interferon Cytokine Res [Internet]. 1997 Mar [cited

2016 Mar 20];17(3):121–34. Available from: http://www.ncbi.nlm.nih.gov/pubmed/9085936

264. Duque G, Huang DC, Macoritto M, Rivas D, Yang XF, Ste-Marie LG, et al. Autocrine regulation of interferon gamma in mesenchymal stem cells plays a role in early osteoblastogenesis. Stem Cells [Internet]. 2009 Mar [cited 2016 Mar 21];27(3):550–8. Available from: http://www.ncbi.nlm.nih.gov/pubmed/19096039

265. Duque G, Huang DC, Dion N, Macoritto M, Rivas D, Li W, et al. Interferon-γ plays a role in bone formation in vivo and rescues osteoporosis in ovariectomized mice. J Bone Miner Res [Internet]. 2011 Jul [cited 2016 Mar 21];26(7):1472–83. Available from: http://www.ncbi.nlm.nih.gov/pubmed/21308779

266. Takayanagi H, Ogasawara K, Hida S, Chiba T, Murata S, Sato K, et al. T-cell-mediated regulation of osteoclastogenesis by signalling cross-talk between RANKL and IFN-gamma. Nature [Internet]. 2000 Nov 30 [cited 2016 Mar 21];408(6812):600–5. Available from: http://www.ncbi.nlm.nih.gov/pubmed/11117749

267. Gao Y, Grassi F, Ryan MR, Terauchi M, Page K, Yang X, et al. IFN-gamma stimulates osteoclast formation and bone loss in vivo via antigen-driven T cell activation. J Clin Invest [Internet]. 2007 Jan [cited 2016 Mar 4];117(1):122–32. Available from: http://www.pubmedcentral.nih.gov/articlerender.fcgi?artid=1697800&tool=pmcentrez&rendertype=abstract

268. Chen W, Fu X, Sheng Z. Review of current progress in the structure and function of Smad proteins. Chin Med J (Engl) [Internet]. 2002 Mar [cited 2015 Nov 9];115(3):446–50. Available from: http://www.ncbi.nlm.nih.gov/pubmed/11940386

269. Feng XH, Lin X, Derynck R. Smad2, Smad3 and Smad4 cooperate with Sp1 to induce p15(Ink4B) transcription in response to TGF-beta. EMBO J [Internet]. EMBO Press; 2000 Oct 2 [cited 2015 Mar 4];19(19):5178–93. Available from: http://emboj.embopress.org/content/19/19/5178.abstract

270. Kang JS, Alliston T, Delston R, Derynck R. Repression of Runx2 function by TGF-beta through recruitment of class II histone deacetylases by Smad3. EMBO J [Internet]. 2005 Jul 20 [cited 2015 Nov 9];24(14):2543–55. Available from: http://www.pubmedcentral.nih.gov/articlerender.fcgi?artid=1176457&tool=pmcentrez&rendertype=abstract

271. Alliston T, Choy L, Ducy P, Karsenty G, Derynck R. TGF-beta-induced repression of CBFA1 by Smad3 decreases cbfa1 and osteocalcin expression and inhibits osteoblast differentiation. EMBO J [Internet]. 2001 May 1 [cited 2015 Nov 9];20(9):2254–72. Available from: http://www.pubmedcentral.nih.gov/articlerender.fcgi?artid=125448&tool=pmcentrez&rendertype=abstract

272. Ulloa L, Doody J, Massagué J. Inhibition of transforming growth factor-beta/SMAD signalling by the interferon-gamma/STAT pathway. Nature [Internet]. 1999 Feb 25 [cited 2016 Jun 14];397(6721):710–3. Available from: http://www.ncbi.nlm.nih.gov/pubmed/10067896

273. Illingworth R, Kerr A, Desousa D, Jørgensen H, Ellis P, Stalker J, et al. A novel CpG island set identifies tissue-specific methylation at developmental gene loci. PLoS Biol [Internet]. Public Library of Science; 2008 Jan 29 [cited 2016 Mar 12];6(1):e22. Available from: http://journals.plos.org/plosbiology/article?id=10.1371/journal.pbio.0060022

274. Byun H-M, Siegmund KD, Pan F, Weisenberger DJ, Kanel G, Laird PW, et al. Epigenetic profiling of somatic tissues from human autopsy specimens identifies tissue- and individual-specific DNA methylation patterns. Hum Mol Genet [Internet]. 2009 Dec 15

[cited 2016 May 6];18(24):4808–17. Available from: http://www.pubmedcentral.nih.gov/articlerender.fcgi?artid=4481584&tool=pmcentrez&rendertype=abstract

275. Lokk K, Modhukur V, Rajashekar B, Märtens K, Mägi R, Kolde R, et al. DNA methylome profiling of human tissues identifies global and tissue-specific methylation patterns. Genome Biol [Internet]. 2014 Jan [cited 2015 May 12];15(4):r54. Available from: http://genomebiology.com/2014/15/4/R54

276. Congrains A, Kamide K, Oguro R, Yasuda O, Miyata K, Yamamoto E, et al. Genetic variants at the 9p21 locus contribute to atherosclerosis through modulation of ANRIL and CDKN2A/B. Atherosclerosis [Internet]. 2012;220(2):449–55. Available from: http://www.sciencedirect.com/science/article/pii/S0021915011010860

277. Sato K, Nakagawa H, Tajima A, Yoshida K, Inoue I. ANRIL is implicated in the regulation of nucleus and potential transcriptional target of E2F1. Oncol Rep. 2010;24(3).

278. Mattick JS. The Genetic Signatures of Noncoding RNAs. PLoS Genet [Internet]. Public Library of Science; 2009;5(4):e1000459. Available from: http://dx.doi.org/10.1371/journal.pgen.1000459

279. Tsai M-C, Manor O, Wan Y, Mosammaparast N, Wang JK, Lan F, et al. Long noncoding RNA as modular scaffold of histone modification complexes. Science (80-) [Internet]. 2010 Aug 6 [cited 2014 Jul 15];329(5992):689–93. Available from: http://www.sciencemag.org/content/329/5992/689.long

280. Wang KC, Chang HY. Molecular mechanisms of long noncoding RNAs. Mol Cell [Internet]. 2011 Sep 16 [cited 2015 Sep 27];43(6):904–14. Available from: http://www.pubmedcentral.nih.gov/articlerender.fcgi?artid=3199020&tool=pmcentrez&rendertype=abstract

281. Pasmant E, Laurendeau I, Héron D, Vidaud M, Vidaud D, Bièche I. Characterization of a germ-line deletion, including the entire INK4/ARF locus, in a melanoma-neural system tumor family: identification of ANRIL, an antisense noncoding RNA whose expression coclusters with ARF. Cancer Res [Internet]. 2007 Apr 15 [cited 2015 Mar 26];67(8):3963–9. Available from: http://cancerres.aacrjournals.org/content/67/8/3963.abstract

282. Holdt LM, Hoffmann S, Sass K, Langenberger D, Scholz M, Krohn K, et al. Alu Elements in ANRIL Non-Coding RNA at Chromosome 9p21 Modulate Atherogenic Cell Functions through Trans-Regulation of Gene Networks. PLoS Genet [Internet]. Public Library of Science; 2013;9(7):e1003588. Available from: http://www.plosgenetics.org/article/fetchObject.action?uri=info:doi/10.1371/journal.pgen.1003588&representation=PDF

283. Yap KL, Li S, Munoz-Cabello AM, Raguz S, Zeng L, Mujtaba S, et al. Molecular interplay of the noncoding RNA ANRIL and methylated histone H3 lysine 27 by polycomb CBX7 in transcriptional silencing of INK4a. Mol Cell [Internet]. 2010;38(5):662–74. Available from: http://www.ncbi.nlm.nih.gov/pubmed/20541999

284. Folkersen L, Kyriakou T, Goel A, Peden J, Malarstig A, Paulsson-Berne G, et al. Relationship between CAD risk genotype in the chromosome 9p21 locus and gene expression. Identification of eight new ANRIL splice variants. PLoS One [Internet]. 2009;4(11):e7677. Available from: http://www.ncbi.nlm.nih.gov/pubmed/19888323

285. Congrains A, Kamide K, Ohishi M, Rakugi H. ANRIL: Molecular Mechanisms and Implications in Human Health. Int J Mol Sci [Internet]. 2013;14(1):1278–92. Available from: http://www.mdpi.com/1422-0067/14/1/1278

286. Lee JT. Epigenetic Regulation by Long Noncoding RNAs. Science (80-) [Internet].

2012;338(6113):1435–9. Available from: http://www.sciencemag.org/content/338/6113/1435.abstract

287. Pasmant E, Sabbagh A, Vidaud M, Bièche I. ANRIL, a long, noncoding RNA, is an unexpected major hotspot in GWAS. FASEB J [Internet]. 2011;25(2):444–8. Available from: http://www.fasebj.org/content/25/2/444.abstract

288. Yu W, Gius D, Onyango P, Muldoon-Jacobs K, Karp J, Feinberg AP, et al. Epigenetic silencing of tumour suppressor gene p15 by its antisense RNA. Nature [Internet]. 2008 Jan 10 [cited 2014 Dec 5];451(7175):202–6. Available from: http://www.pubmedcentral.nih.gov/articlerender.fcgi?artid=2743558&tool=pmcentrez&rendertype=abstract

289. Chen D, Zhang Z, Mao C, Zhou Y, Yu L, Yin Y, et al. ANRIL inhibits p15(INK4b) through the TGFβ1 signaling pathway in human esophageal squamous cell carcinoma. Cell Immunol [Internet]. 2014 Jan [cited 2015 Feb 6];289(1-2):91–6. Available from: http://www.sciencedirect.com/science/article/pii/S0008874914000604

290. Pautke C, Schieker M, Tischer T, Kolk A, Neth P, Mutschler W, et al. Characterization of Osteosarcoma Cell Lines MG-63, Saos-2 and U-2 OS in Comparison to Human Osteoblasts. Anticancer Res [Internet]. 2004 Nov 1 [cited 2015 Aug 12];24(6):3743–8. Available from: http://ar.iiarjournals.org/content/24/6/3743.abstract

291. Buttitta LA, Edgar BA. Mechanisms controlling cell cycle exit upon terminal differentiation. Curr Opin Cell Biol [Internet]. 2007 Dec [cited 2016 Feb 29];19(6):697–704. Available from: http://www.pubmedcentral.nih.gov/articlerender.fcgi?artid=2700000&tool=pmcentrez&rendertype=abstract

292. Cunnington MS, Santibanez Koref M, Mayosi BM, Burn J, Keavney B. Chromosome 9p21 SNPs Associated with Multiple Disease Phenotypes Correlate with ANRIL Expression. PLoS Genet [Internet]. Public Library of Science; 2010;6(4):e1000899. Available from: http://dx.doi.org/10.1371/journal.pgen.1000899

293. Bochenek G, Häsler R, El Mokhtari N-E, König IR, Loos BG, Jepsen S, et al. The large non-coding RNA ANRIL, which is associated with atherosclerosis, periodontitis and several forms of cancer, regulates ADIPOR1, VAMP3 and C11ORF10. Hum Mol Genet [Internet]. 2013 Nov 15 [cited 2014 Aug 25];22(22):4516–27. Available from: http://hmg.oxfordjournals.org/content/early/2013/07/30/hmg.ddt299.short

294. Bialek P, Kern B, Yang X, Schrock M, Sosic D, Hong N, et al. A Twist Code Determines the Onset of Osteoblast Differentiation. Dev Cell [Internet]. 2004 Mar [cited 2015 Apr 8];6(3):423–35. Available from: http://www.sciencedirect.com/science/article/pii/S1534580704000589

295. Chai PC, Liu Z, Chia W, Cai Y. Hedgehog signaling acts with the temporal cascade to promote neuroblast cell cycle exit. PLoS Biol [Internet]. 2013 Jan 26 [cited 2015 Apr 7];11(2):e1001494. Available from: http://journals.plos.org/plosbiology/article?id=10.1371/journal.pbio.1001494

296. López-Otín C, Blasco MA, Partridge L, Serrano M, Kroemer G. The hallmarks of aging. Cell [Internet]. 2013 Jun 6 [cited 2014 Jul 10];153(6):1194–217. Available from: http://www.sciencedirect.com/science/article/pii/S0092867413006454

297. Kawaguchi H, Manabe N, Miyaura C, Chikuda H, Nakamura K, Kuro-o M. Independent impairment of osteoblast and osteoclast differentiation in klotho mouse exhibiting low-turnover osteopenia. J Cinical Investig [Internet]. American Society for Clinical Investigation; 1999 Aug 1 [cited 2015 Apr 8];104(3):229–37. Available from: http://www.jci.org/articles/view/5705

298. Pignolo RJ, Suda RK, McMillan EA, Shen J, Lee S-H, Choi Y, et al. Defects in telomere maintenance molecules impair osteoblast differentiation and promote osteoporosis. Aging Cell [Internet]. 2008 Feb [cited 2015 Apr 8];7(1):23–31. Available from: http://doi.wiley.com/10.1111/j.1474-9726.2007.00350.x

299. Egermann M, Heil P, Tami A, Ito K, Janicki P, Von Rechenberg B, et al. Influence of defective bone marrow osteogenesis on fracture repair in an experimental model of senile osteoporosis. J Orthop Res [Internet]. 2010 Jun [cited 2015 Apr 8];28(6):798–804. Available from: http://www.ncbi.nlm.nih.gov/pubmed/20014309

300. Weinstein RS, Jilka RL, Parfitt AM, Manolagas SC. Inhibition of osteoblastogenesis and promotion of apoptosis of osteoblasts and osteocytes by glucocorticoids. Potential mechanisms of their deleterious effects on bone. J Clin Invest [Internet]. 1998 Jul 15 [cited 2015 Mar 16];102(2):274–82. Available from: http://www.pubmedcentral.nih.gov/articlerender.fcgi?artid=508885&tool=pmcentrez&rendertype=abstract

301. O'Brien CA, Jia D, Plotkin LI, Bellido T, Powers CC, Stewart SA, et al. Glucocorticoids act directly on osteoblasts and osteocytes to induce their apoptosis and reduce bone formation and strength. Endocrinology [Internet]. Endocrine Society; 2004 Apr 1 [cited 2015 Mar 15];145(4):1835–41. Available from: http://press.endocrine.org/doi/full/10.1210/en.2003-0990

302. Zhang Y, Xiong Y, Yarbrough WG. ARF promotes MDM2 degradation and stabilizes p53: ARF-INK4a locus deletion impairs both the Rb and p53 tumor suppression pathways. Cell [Internet]. 1998 Mar 20 [cited 2016 Feb 22];92(6):725–34. Available from: http://www.ncbi.nlm.nih.gov/pubmed/9529249

303. Irwin M, Marin MC, Phillips AC, Seelan RS, Smith DI, Liu W, et al. Role for the p53 homologue p73 in E2F-1-induced apoptosis. Nature [Internet]. 2000 Oct 5 [cited 2016 Feb 25];407(6804):645–8. Available from: http://dx.doi.org/10.1038/35036614

304. De Laurenzi V, Costanzo A, Barcaroli D, Terrinoni A, Falco M, Annicchiarico-Petruzzelli M, et al. Two New p73 Splice Variants, γ and δ, with Different Transcriptional Activity. J Exp Med [Internet]. 1998 Nov 2 [cited 2016 Mar 1];188(9):1763–8. Available from: http://jem.rupress.org/content/188/9/1763.abstract

305. Pratap J, Galindo M, Zaidi SK, Vradii D, Bhat BM, Robinson JA, et al. Cell Growth Regulatory Role of Runx2 during Proliferative Expansion of Preosteoblasts. Cancer Res [Internet]. 2003 Sep 1 [cited 2015 Dec 1];63(17):5357–62. Available from: http://cancerres.aacrjournals.org/content/63/17/5357.short

306. Galindo M, Pratap J, Young DW, Hovhannisyan H, Im H-J, Choi J-Y, et al. The bone-specific expression of Runx2 oscillates during the cell cycle to support a G1-related antiproliferative function in osteoblasts. J Biol Chem [Internet]. 2005 May 27 [cited 2015 Dec 1];280(21):20274–85. Available from: http://www.jbc.org/content/280/21/20274.short

307. Teplyuk NM, Galindo M, Teplyuk VI, Pratap J, Young DW, Lapointe D, et al. Runx2 regulates G protein-coupled signaling pathways to control growth of osteoblast progenitors. J Biol Chem [Internet]. 2008 Oct 10 [cited 2015 Dec 2];283(41):27585–97. Available from: http://www.pubmedcentral.nih.gov/articlerender.fcgi?artid=2562077&tool=pmcentrez&rendertype=abstract

308. Chau JFL, Leong WF, Li B. Signaling pathways governing osteoblast proliferation, differentiation and function. Histol Histopathol [Internet]. 2009 Dec [cited 2015 Dec 2];24(12):1593–606. Available from: http://www.ncbi.nlm.nih.gov/pubmed/19795357

309. Banfi A, Muraglia A, Dozin B, Mastrogiacomo M, Cancedda R, Quarto R. Proliferation

kinetics and differentiation potential of ex vivo expanded human bone marrow stromal cells: Implications for their use in cell therapy. Exp Hematol [Internet]. 2000 Jun [cited 2015 Oct 20];28(6):707–15. Available from: http://www.ncbi.nlm.nih.gov/pubmed/10880757

310. Kretlow JD, Jin Y-Q, Liu W, Zhang WJ, Hong T-H, Zhou G, et al. Donor age and cell passage affects differentiation potential of murine bone marrow-derived stem cells. BMC Cell Biol [Internet]. BioMed Central Ltd; 2008 Jan 28 [cited 2015 Nov 20];9(1):60. Available from: http://www.biomedcentral.com/1471-2121/9/60

311. Jia L, Young MF, Powell J, Yang L, Ho NC, Hotchkiss R, et al. Gene expression profile of human bone marrow stromal cells: high-throughput expressed sequence tag sequencing analysis. Genomics [Internet]. 2002 Jan [cited 2015 Dec 2];79(1):7–17. Available from: http://www.sciencedirect.com/science/article/pii/S0888754301966832

312. Zhang Y, Wen G, Shao G, Wang C, Lin C, Fang H, et al. TGFBI deficiency predisposes mice to spontaneous tumor development. Cancer Res [Internet]. 2009 Jan 1 [cited 2015 Dec 2];69(1):37–44. Available from: http://cancerres.aacrjournals.org/content/69/1/37.full

313. Adams JC, Watt FM. Fibronectin inhibits the terminal differentiation of human keratinocytes. Nature [Internet]. 1989 Jul 27 [cited 2015 Dec 2];340(6231):307–9. Available from: http://www.ncbi.nlm.nih.gov/pubmed/2473404

314. Basu S, Liu Q, Qiu Y, Dong F. Gfi-1 represses CDKN2B encoding p15INK4B through interaction with Miz-1. Proc Natl Acad Sci U S A [Internet]. 2009 Feb 3 [cited 2015 Dec 1];106(5):1433–8. Available from: http://www.pnas.org/content/106/5/1433.short

315. Staller P, Peukert K, Kiermaier A, Seoane J, Lukas J, Karsunky H, et al. Repression of p15INK4b expression by Myc through association with Miz-1. Nat Cell Biol [Internet]. 2001 Apr [cited 2015 Dec 1];3(4):392–9. Available from: http://www.ncbi.nlm.nih.gov/pubmed/11283613

316. Gilad Y, Rifkin SA, Pritchard JK. Revealing the architecture of gene regulation: the promise of eQTL studies. Trends Genet [Internet]. 2008 Aug [cited 2016 May 2];24(8):408–15. Available from: http://www.pubmedcentral.nih.gov/articlerender.fcgi?artid=2583071&tool=pmcentrez&rendertype=abstract

317. Maston GA, Evans SK, Green MR. Transcriptional Regulatory Elements in the Human Genome. Annual Reviews; 2006 Sep 1 [cited 2016 May 31]; Available from: http://www.annualreviews.org/doi/full/10.1146/annurev.genom.7.080505.115623

318. Beederman M, Lamplot JD, Nan G, Wang J, Liu X, Yin L, et al. BMP signaling in mesenchymal stem cell differentiation and bone formation. J Biomed Sci Eng [Internet]. 2013 Aug [cited 2016 Jun 9];6(8A):32–52. Available from: http://www.ncbi.nlm.nih.gov/pubmed/26819651

319. Lechler P, Klein SM, Prantl L, Englert C, Renkawitz T, Grifka J. Hypoxic downregulation of cellular proliferation and loss of phenotype stability in human osteoblasts is mediated by HIF-1α. Clin Hemorheol Microcirc [Internet]. 2011 [cited 2016 Jun 9];49(1-4):279–86. Available from: http://www.ncbi.nlm.nih.gov/pubmed/22214699

320. Chen L, Jiang W, Huang J, He B-C, Zuo G-W, Zhang W, et al. Insulin-like growth factor 2 (IGF-2) potentiates BMP-9-induced osteogenic differentiation and bone formation. J Bone Miner Res [Internet]. Wiley Subscription Services, Inc., A Wiley Company; 2010 Nov [cited 2016 Jun 9];25(11):2447–59. Available from: http://doi.wiley.com/10.1002/jbmr.133

321. Kang H, Sung J, Jung H-M, Woo KM, Hong S-D, Roh S. Insulin-like growth factor 2 promotes osteogenic cell differentiation in the parthenogenetic murine embryonic stem cells. Tissue

Eng Part A [Internet]. 2012 Feb [cited 2016 Jun 9];18(3-4):331–41. Available from: http://www.ncbi.nlm.nih.gov/pubmed/21902466

322. Lai C-F, Chaudhary L, Fausto A, Halstead LR, Ory DS, Avioli L V., et al. Erk Is Essential for Growth, Differentiation, Integrin Expression, and Cell Function in Human Osteoblastic Cells. J Biol Chem. 2001;276(17):14443–50.

323. Vary CPH, Li V, Raouf A, Kitching R, Kola I, Franceschi C, et al. Involvement of Ets Transcription Factors and Targets in Osteoblast Differentiation and Matrix Mineralization. Exp Cell Res [Internet]. Academic Press; 2000 May [cited 2016 Jun 12];257(1):213–22. Available from: http://linkinghub.elsevier.com/retrieve/pii/S0014482700948791

324. Raouf A, Seth A. Ets transcription factors and targets in osteogenesis. Oncogene [Internet]. Nature Publishing Group; 2000 Dec 18 [cited 2015 Mar 3];19(55):6455–63. Available from: http://www.nature.com/onc/journal/v19/n55/full/1204037a.html

325. Su J-L, Chiou J, Tang C-H, Zhao M, Tsai C-H, Chen P-S, et al. CYR61 regulates BMP-2-dependent osteoblast differentiation through the {alpha}v{beta}3 integrin/integrin-linked kinase/ERK pathway. J Biol Chem [Internet]. 2010 Oct 8 [cited 2016 Jun 12];285(41):31325–36. Available from: http://www.ncbi.nlm.nih.gov/pubmed/20675382

326. Chang C, Holtzman DA, Chau S, Chickering T, Woolf EA, Holmgren LM, et al. Twisted gastrulation can function as a BMP antagonist. Nature [Internet]. 2001 Mar 22 [cited 2016 Jun 12];410(6827):483–7. Available from: http://www.ncbi.nlm.nih.gov/pubmed/11260717

327. Ferretti C, Mattioli-Belmonte M. Periosteum derived stem cells for regenerative medicine proposals: Boosting current knowledge. World J Stem Cells [Internet]. 2014 Jul 26 [cited 2016 Jun 10];6(3):266–77. Available from: http://www.ncbi.nlm.nih.gov/pubmed/25126377

328. van Heesch S, van Iterson M, Jacobi J, Boymans S, Essers PB, de Bruijn E, et al. Extensive localization of long noncoding RNAs to the cytosol and mono- and polyribosomal complexes. Genome Biol [Internet]. BioMed Central; 2014 [cited 2016 Jun 12];15(1):R6. Available from: http://genomebiology.biomedcentral.com/articles/10.1186/gb-2014-15-1-r6

329. Che W, Dong Y, Quan H-B. RANKL inhibits cell proliferation by regulating MALAT1 expression in a human osteoblastic cell line hFOB 1.19. Cell Mol Biol (Noisy-le-grand) [Internet]. 2015 [cited 2016 Jun 12];61(1):7–14. Available from: http://www.ncbi.nlm.nih.gov/pubmed/25817340

330. Xu Y, Wang S, Tang C, Chen W. Upregulation of long non-coding RNA HIF 1α-anti-sense 1 induced by transforming growth factor-β-mediated targeting of sirtuin 1 promotes osteoblastic differentiation of human bone marrow stromal cells. Mol Med Rep [Internet]. 2015 Nov [cited 2016 Jun 12];12(5):7233–8. Available from: http://www.ncbi.nlm.nih.gov/pubmed/26460121

331. Chu C, Quinn J, Chang HY. Chromatin isolation by RNA purification (ChIRP). J Vis Exp [Internet]. 2012 [cited 2016 Jun 12];(61). Available from: http://www.ncbi.nlm.nih.gov/pubmed/22472705

332. Marya RK, Rathee S, Lata V, Mudgil S. Effects of vitamin D supplementation in pregnancy. Gynecol Obstet Invest [Internet]. 1981 Jan [cited 2015 Dec 14];12(3):155–61. Available from: http://www.ncbi.nlm.nih.gov/pubmed/7239350

333. Delvin EE, Salle BL, Glorieux FH, Adeleine P, David LS. Vitamin D supplementation during pregnancy: effect on neonatal calcium homeostasis. J Pediatr [Internet]. 1986 Aug [cited 2015 Dec 14];109(2):328–34. Available from:

http://www.ncbi.nlm.nih.gov/pubmed/3488384

334. Mallet E, Gügi B, Brunelle P, Hénocq A, Basuyau JP, Lemeur H. Vitamin D supplementation in pregnancy: a controlled trial of two methods. Obstet Gynecol [Internet]. 1986 Sep [cited 2015 Dec 15];68(3):300–4. Available from: http://www.ncbi.nlm.nih.gov/pubmed/3755517

335. Cockburn F, Belton NR, Purvis RJ, Giles MM, Brown JK, Turner TL, et al. Maternal vitamin D intake and mineral metabolism in mothers and their newborn infants. Br Med J [Internet]. 1980 Jul 5 [cited 2015 Dec 15];281(6232):11–4. Available from: http://www.pubmedcentral.nih.gov/articlerender.fcgi?artid=1713762&tool=pmcentrez&rendertype=abstract

336. Congdon P, Horsman A, Kirby PA, Dibble J, Bashir T. Mineral content of the forearms of babies born to Asian and white mothers. Br Med J (Clin Res Ed) [Internet]. 1983 Apr 16 [cited 2015 Dec 15];286(6373):1233–5. Available from: http://www.pubmedcentral.nih.gov/articlerender.fcgi?artid=1547285&tool=pmcentrez&rendertype=abstract

337. Harvey NC, Holroyd C, Ntani G, Javaid K, Cooper P, Moon R, et al. Vitamin D supplementation in pregnancy: a systematic review. Health Technol Assess (Rockv) [Internet]. 2014 Jul [cited 2015 Nov 19];18(45):1–190. Available from: http://www.pubmedcentral.nih.gov/articlerender.fcgi?artid=4124722&tool=pmcentrez&rendertype=abstract

338. Harvey NC, Javaid K, Bishop N, Kennedy S, Papageorghiou AT, Fraser R, et al. MAVIDOS Maternal Vitamin D Osteoporosis Study: study protocol for a randomized controlled trial. The MAVIDOS Study Group. Trials [Internet]. 2012 Jan [cited 2015 Oct 6];13(1):13. Available from: http://www.pubmedcentral.nih.gov/articlerender.fcgi?artid=3395865&tool=pmcentrez&rendertype=abstract

339. Cooper C, Harvey NC, Bishop NJ, Kennedy S, Papageorghiou AT, Schoenmakers I, et al. Maternal gestational vitamin D supplementation and offspring bone health (MAVIDOS): a multicentre, double-blind, randomised placebo-controlled trial. Lancet Diabetes Endocrinol [Internet]. Elsevier; 2016 Mar 1 [cited 2016 Mar 2];4(5):393–402. Available from: http://www.thelancet.com/article/S2213858716000449/fulltext

340. Beltrand J, Alison M, Nicolescu R, Verkauskiene R, Deghmoun S, Sibony O, et al. Bone mineral content at birth is determined both by birth weight and fetal growth pattern. Pediatr Res [Internet]. 2008 Jul [cited 2016 Feb 11];64(1):86–90. Available from: http://www.ncbi.nlm.nih.gov/pubmed/18391851

341. Claus R, Wilop S, Hielscher T, Sonnet M, Dahl E, Galm O, et al. A systematic comparison of quantitative high-resolution DNA methylation analysis and methylation-specific PCR. Epigenetics [Internet]. 2012 Jul [cited 2016 Feb 10];7(7):772–80. Available from: http://www.pubmedcentral.nih.gov/articlerender.fcgi?artid=3414395&tool=pmcentrez&rendertype=abstract

342. Turan N, Ghalwash MF, Katari S, Coutifaris C, Obradovic Z, Sapienza C. DNA methylation differences at growth related genes correlate with birth weight: a molecular signature linked to developmental origins of adult disease? BMC Med Genomics [Internet]. BioMed Central; 2012 Jan 12 [cited 2016 Feb 11];5(1):10. Available from: http://bmcmedgenomics.biomedcentral.com/articles/10.1186/1755-8794-5-10

343. Fryer AA, Emes RD, Ismail KMK, Haworth KE, Mein C, Carroll WD, et al. Quantitative, high-resolution epigenetic profiling of CpG loci identifies associations with cord blood plasma homocysteine and birth weight in humans. Epigenetics [Internet]. Taylor & Francis; 2011 Jan 1 [cited 2016 Jan 26];6(1):86–94. Available from:

http://www.tandfonline.com/doi/abs/10.4161/epi.6.1.13392

344. Engel SM, Joubert BR, Wu MC, Olshan AF, Håberg SE, Ueland PM, et al. Neonatal genome-wide methylation patterns in relation to birth weight in the Norwegian Mother and Child Cohort. Am J Epidemiol [Internet]. 2014 Apr 1 [cited 2016 Feb 11];179(7):834–42. Available from: http://aje.oxfordjournals.org/content/179/7/834.long

345. Yarbrough DE, Barrett-Connor E, Morton DJ. Birth weight as a predictor of adult bone mass in postmenopausal women: the Rancho Bernardo Study. Osteoporos Int [Internet]. 2000 Jan [cited 2016 Feb 11];11(7):626–30. Available from: http://www.ncbi.nlm.nih.gov/pubmed/11069198

346. Jones G, Dwyer T. Birth weight, birth length, and bone density in prepubertal children: evidence for an association that may be mediated by genetic factors. Calcif Tissue Int [Internet]. 2000 Oct [cited 2016 Feb 11];67(4):304–8. Available from: http://www.ncbi.nlm.nih.gov/pubmed/11000344

347. Simpkin AJ, Suderman M, Gaunt TR, Lyttleton O, McArdle WL, Ring SM, et al. Longitudinal analysis of DNA methylation associated with birth weight and gestational age. Hum Mol Genet [Internet]. 2015 Jul 1 [cited 2016 Feb 9];24(13):3752–63. Available from: http://www.pubmedcentral.nih.gov/articlerender.fcgi?artid=4459393&tool=pmcentrez&rendertype=abstract

348. Haslberger A, Varga F, Karlic H. Recursive causality in evolution: a model for epigenetic mechanisms in cancer development. Med Hypotheses [Internet]. 2006 Jan [cited 2016 Feb 9];67(6):1448–54. Available from: http://www.ncbi.nlm.nih.gov/pubmed/16844314

349. Lillycrop KA, Slater-Jefferies JL, Hanson MA, Godfrey KM, Jackson AA, Burdge GC. Induction of altered epigenetic regulation of the hepatic glucocorticoid receptor in the offspring of rats fed a protein-restricted diet during pregnancy suggests that reduced DNA methyltransferase-1 expression is involved in impaired DNA methylation and . Br J Nutr [Internet]. 2007;97(6):1064–73. Available from: http://www.ncbi.nlm.nih.gov/pubmed/17433129

350. De Smet C, Lurquin C, Lethé B, Martelange V, Boon T. DNA methylation is the primary silencing mechanism for a set of germ line- and tumor-specific genes with a CpG-rich promoter. Mol Cell Biol [Internet]. 1999 Nov [cited 2016 Feb 9];19(11):7327–35. Available from: http://www.pubmedcentral.nih.gov/articlerender.fcgi?artid=84726&tool=pmcentrez&rendertype=abstract

351. Oda M, Yamagiwa A, Yamamoto S, Nakayama T, Tsumura A, Sasaki H, et al. DNA methylation regulates long-range gene silencing of an X-linked homeobox gene cluster in a lineage-specific manner. Genes Dev [Internet]. 2006 Dec 15 [cited 2016 Feb 9];20(24):3382–94. Available from: http://www.pubmedcentral.nih.gov/articlerender.fcgi?artid=1698446&tool=pmcentrez&rendertype=abstract

352. Fouse SD, Shen Y, Pellegrini M, Cole S, Meissner A, Van Neste L, et al. Promoter CpG methylation contributes to ES cell gene regulation in parallel with Oct4/Nanog, PcG complex, and histone H3 K4/K27 trimethylation. Cell Stem Cell [Internet]. 2008 Feb 7 [cited 2016 Jan 5];2(2):160–9. Available from: http://www.pubmedcentral.nih.gov/articlerender.fcgi?artid=3070208&tool=pmcentrez&rendertype=abstract

353. Chandra V, Huang P, Hamuro Y, Raghuram S, Wang Y, Burris TP, et al. Structure of the intact PPAR-gamma-RXR- nuclear receptor complex on DNA. Nature [Internet]. 2008 Nov 20 [cited 2016 May 21];456(7220):350–6. Available from:

http://www.pubmedcentral.nih.gov/articlerender.fcgi?artid=2743566&tool=pmcentrez&rendertype=abstract

354. Bachrach LK. Acquisition of optimal bone mass in childhood and adolescence. Trends Endocrinol Metab [Internet]. 2001 Jan [cited 2016 May 30];12(1):22–8. Available from: http://www.sciencedirect.com/science/article/pii/S1043276000003362

355. Chen B, He L, Savell VH, Jenkins JJ, Parham DM. Inhibition of the interferon-gamma/signal transducers and activators of transcription (STAT) pathway by hypermethylation at a STAT-binding site in the p21WAF1 promoter region. Cancer Res [Internet]. 2000 Jun 15 [cited 2016 Jun 17];60(12):3290–8. Available from: http://www.ncbi.nlm.nih.gov/pubmed/10866323

356. Wan G, Mathur R, Hu X, Liu Y, Zhang X, Peng G, et al. Long non-coding RNA ANRIL (CDKN2B-AS) is induced by the ATM-E2F1 signaling pathway. Cell Signal [Internet]. 2013 May [cited 2014 Sep 8];25(5):1086–95. Available from: http://www.sciencedirect.com/science/article/pii/S0898656813000466

357. Häsler J, Strub K. Alu elements as regulators of gene expression. Nucleic Acids Res [Internet]. 2006 [cited 2016 Jun 14];34(19):5491–7. Available from: http://www.ncbi.nlm.nih.gov/pubmed/17020921

358. Cooper C, Javaid K, Westlake S, Harvey N, Dennison E. Developmental Origins of Osteoporotic Fracture: the Role of Maternal Vitamin D Insufficiency. J Nutr [Internet]. 2005 Nov 1 [cited 2015 Apr 10];135(11):2728S – 2734. Available from: http://jn.nutrition.org/content/135/11/2728S.full